

The University of Nottingham
Department of Chemical and Environmental
Engineering



**UTILISATION OF HIGH CARBON
PULVERISED FUEL ASH**

Maythem N. Mahmud

Thesis submitted to the University of Nottingham for the degree of
Doctor of Philosophy

October 2010

Abstract

Coal combustion by-products generated from coal-fired power plant and cause enormous problems for disposal unless a way can be found to utilize these by-products through resource recovery programs. The implementation of air act regulations to reduce NO_x emission have resulted millions of tonnes of pulverised fuel ash (PFA) accumulated with high percentage of unburned carbon made it un-saleable for the cement industry. Moreover, alternative fuels such as biomass and import coals were suggested to reduce gas emissions but on the other hand PFA marketability was reduced. The main objective of this study was thus to utilise high carbon PFA into value added products. Through this work, the relationships beside the factors that could influence the carbon content in the PFA and reduce it in terms of producing raw material useful for different applications were explored. These factors were extensively investigated through thermogravimetric analyses, surface area measurements, microscopy and optical studies, and particle size distribution analyses.

Five high unburned carbon PFAs were selected as feedstocks for PFA beneficiation, cement tests, and carbon activation. In order to beneficiate a high carbon PFA, incipient fluidisation was selected as the preferred route being a dry separation method which does not expose the carbon to potential contaminants that may alter its reactivity or physical properties. Enriched PFAs (*i.e.* depleted carbon) were separated and then cement tests were conducted in different mixture ratios (PFA/cement) throughout different time scales. These tests were demonstrated by using samples derived from biomass co-firing and

import coals. The PFA/cement mixtures achieved good strength and workability via standard values.

Unburned carbon (*i.e.* enriched carbon) streams were activated using steam at temperature 850 °C and time from 60-300 minutes. For all unburned carbons investigated in this project, the surface areas of their activated counterparts increased to reach maximum level after three hours and four hours compared with other works. But this increase dropped back according to the reduction of the pore widening. Consequently, the surface area exhibited a high level of low carbon burn-out for the carbon sourced from biomass co-firing (1435 m²/g and 38 wt.%, respectively). This was revealed due to the carbon gasification and pore widening level. In addition, optical studies showed that the carbon types changed in a different manner during the activation.

Publications and Conferences

- **Mahmud, M., Maroto-Valer, M.M., and Brandwood, R. (2007).**
Utilisation of Coal Combustion by-Products. WARMNET conference, Jubilee Campus-University of Nottingham on 4th -5th July 2007, Nottingham UK.
- **Mahmud, M., Maroto-Valer, M.M., and Brandwood, R. (2007).**
Applications for High Carbon Pulverised Fuel Ash (PFA). International Conference on Coal Science and Technology, 28th-30th September 2007, p. 141, Paper 2P28, Nottingham University, East Midland Conference Centre, Nottingham, UK.
- **Mahmud, M., Maroto-Valer, M.M., and Brandwood, R. (2007).**
Impact of Increasing Use of Alternative Fuels on Emissions and Marketability of Combustion by-Products. The Future Energy: Chemical Solutions in September 2007, Jubilee Campus-University of Nottingham, Nottingham UK.
- **Mahmud, M., Maroto-Valer, M.M., and Brandwood, R. (2008).**
“Utilisation of Pulverised Fuel Ash Derived from Import Coals into Value Added Products”. 7th European Conference on Coal Research and its Applications, Cardiff University from 3rd-5th September 2008, p.165, Cardiff UK.
- **Mahmud, M., Maroto-Valer, M.M., and Brandwood, R. (2009).**
“Characterisation of pulverised fuel ash derived from co-firing biomass and their utilisation for value added products”. The World of Coal Ash, Science, Applications, and Sustainability, May 4-7

2009, Lexington, Kentucky. Organised by the American Coal Ash Association and the University of Kentucky Centre for Applied Energy Research.

- **Mahmud, M., Maroto-Valer, M.M., and Brandwood, R. (2010).** “Utilisation high carbon pulverised fuel ash”. The Coal Research Forum, 21st Annual Meeting of The Combustion and Environmental Divisions. Ratcliffe-On-Soar, Nottinghamshire, 14th April 2010.

Proposed Journals Publication

- Mahmud, M., Maroto-Valer, M.M., and Brandwood, R. Characterisations Pulverised Fuel Ash from Co-firing Different Biomass Fuels, Fuel.
- Mahmud, M., Maroto-Valer, M.M., and Brandwood, R. Characterising Series of High Carbon Fly Ashes Collected From Different Systems, Fuel.

Acknowledgements

I would like to express great thanks to my supervisor *Prof. M. Mercedes Maroto-Valer* for her supervision and great support throughout my PhD, thank you *Prof. Mercedes* for everything. Many thanks also go to *Roger Brandwood* from E-ON Engineering Ltd. for his help, and guidance throughout this project work. I would like to thank my internal assessors *Prof. Nick Miles and Dr Ng Yuen*.

I also would like to thank *E-ON Engineering Ltd.* for financial support and for providing the samples and *EPSRC (CNA-CASE award)* for supporting this work.

I would like to thank *Prof. John Patrick, Dr Mick Cooper, Dr Miguel Castro,* and *Ron Perry* for all their supports and guidance during the work. Also, I would like to thank all lab technicians in L3 and L4 for their help. I would like also to thank all my friends in L3 and L4, and I wish them the best in their research work.

Finally, I would like to thank my wife “*Alaa*” for all her efforts consumed in the last four years for supporting me to work hard in terms of developing good work and all her care put into our sons when I am at work “*Ali & Mohammed Hussein*”, thank you *Alaa*. I would like also to thank my parents, and *Alaa’s* parents for all their support and Doea.

TABLE OF CONTENTS

Abstract.....	ii
Publications and conferences.....	iv
Acknowledgements.....	vi
Table of contents.....	vii
List of figures.....	xii
List of tables.....	xv
CHAPTER ONE–INTRODUCTION.....	1
1.1 Introduction.....	1
1.2 Aim and objectives.....	4
1.3 Methodology.....	4
CHAPTER TWO-LITERATURE REVIEW.....	7
2.1 Mineral matter transformation during coal combustion.....	7
2.1.1 Coal formation.....	7
2.1.2 Mineral matter transformation.....	10
2.1.3 Coal combustion by-products.....	14
2.2 Pulverised fuel ash.....	18
2.2.1 The status of ash utilisation Worldwide.....	20
2.2.2 Legislation.....	22
2.2.3 Classification and specifications of PFA.....	25
2.3 PFA characterisation.....	29
2.3.1 Physical and chemical properties of PFA.....	29

TABLE OF CONTENTS

2.3.2 Mineralogy and morphology.....	32
2.3.3 Leachable compounds in PFA.....	33
2.3.4 Carbon forms.....	34
2.4 Co-firing of biomass with coal.....	36
2.4.1 Biomass co-firing PFA characteristics.....	38
2.4.2 Biomass co-firing PFA utilisation.....	42
2.4.3 Co-firing methods.....	44
2.4.3.1 Direct co-firing.....	44
2.4.3.2 Parallel co-firing.....	44
2.4.3.3 Indirect co-firing.....	45
2.4.4 Implications of biomass co-firing.....	45
2.5 PFA beneficiation.....	48
2.5.1 Residual carbon in PFA.....	48
2.5.2 High unburned carbon PFA.....	49
2.5.3 PFA beneficiation processes.....	49
2.5.3.1 Carbon burn out.....	51
2.5.3.2 Combined processes.....	51
2.6 Carbon activation.....	53
2.6.1 Carbon activation methods.....	55
 CHAPTER THREE-EXPERIMENTAL PROCEDURES.....	 58
3.1 Introduction.....	58
3.2 Samples procurement.....	58
3.3 Samples characterisation.....	60
3.3.1 Thermogravimetric analyses.....	60

TABLE OF CONTENTS

3.3.1.1 LOI analyses.....	60
3.3.1.2 Proximate analyses.....	61
3.3.2 Ultimate analyses.....	61
3.3.3 Porosity studies.....	62
3.3.4 Particle size distribution.....	63
3.3.5 Microscopy and X-ray studies.....	64
3.3.5.1 Scanning electron microscopy and Energy dispersive X-Ray.....	64
3.3.5.2 X-Ray diffraction.....	65
3.4 PFA beneficiation.....	65
3.4.1 Microwave treatment.....	66
3.4.2 Incipient fluidisation.....	66
3.5 Cement tests.....	69
3.6 Carbon activation.....	70
3.6.1 Calorific value.....	72
3.6.2 Optical microscopy-automated analyses.....	73
3.6.3 Methylene blue measurements.....	74
3.7 Inductively Coupled Plasma-Atomic Emission Spectrometry.....	77
 CHAPTER FOUR-RESULTS & DISCUSSION.....	 80
4.1 Thermogravimetric analyses.....	80
4.1.1 LOI analyses.....	80
4.1.2 Proximate analyses.....	83
4.2. Ultimate analyses.....	86

TABLE OF CONTENTS

4.3 Porosity studies.....	88
4.4 Particle size distribution.....	92
4.4.1 Particle size distribution using water as a dispersant.....	93
4.4.2 Particle size distribution using Isopropanol as a dispersant.....	97
4.5 Microscopy and X-ray studies.....	99
4.5.1 Scanning electron microscopy studies.....	99
4.5.2 Energy dispersive X-Ray.....	103
4.5.3 X-Ray diffraction.....	107
4.6 High carbon PFA beneficiation.....	110
4.6.1 Microwave treatment.....	111
4.6.2 Incipient fluidisation.....	113
4.7 Cement tests.....	116
4.8 Carbon activation.....	119
4.8.1 Calorific value.....	120
4.8.2 Adsorption-desorption isotherms.....	120
4.8.3 Carbon burn-out, porosity development, and solid yield.....	126
4.8.4 Optical microscopy-automated analyses.....	133
4.8.5 Optical microscopy comparison of the biomass co-firing char and coal char samples.....	138
4.9 Methylene blue studies.....	140
4.10 Inductively Coupled Plasma-Atomic Emission Spectrometry.....	146

CHAPTER FIVE CONCLUSIONS & FUTURE WORK.....	149
5.1 Overview.....	149
5.2 The resulting impacts from using alternative fuels.....	149
5.3 The main factors are affecting the surface area of the activated carbon produced from PFA beneficiation.....	151
5.4 PFA applications developed from alternative fuels	152
5.5 Final conclusion.....	153
5.6 Future work.....	154
 REFERENCES.....	 155
 Appendix A- Particle size distribution graphs.....	 182
Appendix B- SEM images for all the samples.....	188
Appendix C- EDX graphs for all the samples.....	209
Appendix D- XRD graphs for all the samples.....	217
Appendix E- Adsorption isotherms for the enriched and activated carbons.....	225
Appendix F- Optical microscopy images for the enriched and activated carbons.....	229
Appendix G- Porosity development and isotherm types.....	235

List of figures

Figure 1.1: Project plan.....	6
Figure 2.1: Schematic diagram of the interactions of different inorganic components during combustion.....	12
Figure 2.2: Coal-fired power plant.....	16
Figure 2.3: Hungry Horse Dam, Montana.....	19
Figure 2.4: World wide of PFA production at year 2000.....	20
Figure 2.5: Tax-related costs of landfilling non-hazardous waste in selected countries.....	23
Figure 2.6: Costs of landfilling non-hazardous waste in selected countries...	24
Figure 2.7: PFA particles under SEM.....	30
Figure 2.8: Biomass configurations in direct co-firing.....	37
Figure 2.9: Carbon burn-out unit at Wateree station in South Carolina.....	51
Figure 2.10: Separation schematic for PFA beneficiation process.....	52
Figure 3.1: Incipient fluidisation apparatus used for PFA beneficiation.....	67
Figure 3.2: GD-10 compression strength tester.....	70
Figure 3.3: Photo of steam activation system.....	70
Figure 3.4: Calibration curve to calculate the constants (a & b).....	76
Figure 4.1: Proximate analyses for all PFA samples received presented in columns.....	84
Figure 4.2: LOI results and the total contents of moisture, volatile matter and fixed carbon.....	86
Figure 4.3: Adsorption isotherms.....	89
Figure 4.4: cont. adsorption isotherms.....	91

LIST OF FIGURES

Figure 4.5: The total surface area and LOI % (db) for all PFAs received.....	92
Figure 4.6: Particle size distribution with volume % in size.....	94
Figure 4.7: cont. particle size distribution with volume % in size.....	94
Figure 4.8: Particle size distribution with % passing.....	96
Figure 4.9: cont. particle size distribution with % passing.....	96
Figure 4.10: Particle size distribution with volume % in size.....	98
Figure 4.11: cont. particle size distribution with volume % in size.....	98
Figure 4.12: Particle size distribution with % passing.....	99
Figure 4.13: SEM image of C1 sample.....	100
Figure 4.14: SEM image of sample B1.....	101
Figure 4.15: SEM image of sample C6.....	102
Figure 4.16: SEM image of sample B5.....	103
Figure 4.17: EDX graph for C2 sample.....	104
Figure 4.18: EDX graph for B1 sample.....	104
Figure 4.19: EDX graph for C5 sample.....	106
Figure 4.20: EDX graph for B5 sample.....	106
Figure 4.21: XRD graph for C2 sample.....	108
Figure 4.22: XRD graph for B1 sample.....	108
Figure 4.23: XRD graph for C6 sample.....	109
Figure 4.24: XRD graph for B5 sample.....	110
Figure 4.25: Photo of B1 after vitrification.....	112
Figure 4.26: Photo of B3 after vitrification.....	112
Figure 4.27: Isotherms of carbon rich samples prior activation.....	121
Figure 4.28: Isotherms of B5e sample before and after activation.....	122

xiv

List of tables

Table 2.1: Coal inorganic matter transformation during combustion process.....	14
Table 2.2: PFA utilisation in main countries at year 2002.....	21
Table 2.3: The chemical requirements to be specified for PFA under EN- 450, and ASTM C618.....	28
Table 2.4: The physical requirements to be specified for PFA under EN- 450, and ASTM C618.....	28
Table 2.5: Other physical properties of the PFA.....	30
Table 2.6: Typical ranges of oxides can be found with PFA in different coal types.....	31
Table 2.7: Typical elemental compositions for UK PFA.....	32
Table 2.8: Raw materials characterisation properties as a precursor for activated carbon.....	57
Table 3.1: PFA samples and characterisation works.....	59
Table 3.2: Mix details of each cube for 5% and 10% Cement/PFA.....	69
Table 3.3: Twelve mixtures of methylene blue & water.....	75
Table 4.1: LOI values for all PFAs samples received.....	82
Table 4.2: LOI values and ultimate analyses for all PFAs received (asr).....	87
Table 4.3: Incipient data analyses for the PFA samples selected.....	115
Table 4.4: The test results of concrete mixes after 7 days.....	118
Table 4.5: The test results of concrete mixes after 28 days.....	119
Table 4.6: Calorific values for the carbon rich streams (asr).....	120
Table 4.7: The solid yield and surface area for all the samples at 60 and 120 minutes activation.....	131

LIST OF TABLES

Table 4.8: The surface areas for the selected samples.....	140
Table 4.9 Methylene blue measurements after seven days for samples C2a and C4a.....	142
Table 4.10 cont. methylene blue measurements after seven days for samples B5a and Fisher-DC.....	143
Table 4.11: ICP-AES data for the PFA (asr) and resulted streams.....	148

CHAPTER ONE

1.1 Introduction

Coal combustion is the predominant energy source (*i.e.* electricity) for many industrialized countries. Unfortunately, these combustion processes also produce large quantities of by products, mainly pulverised fuel ash (PFA). PFA had been marketed for a long time as a cement extender, when its residual carbon or loss-on-ignition (LOI) content is consistently below 7%. However, implementation of increasing stringent Clean Air Act Regulations by the coal utility industry (NO_x control devices), has resulted in an increase in the concentration of unburned carbon in the PFA [Maroto-Valer *et al.*, 2001]. However, the marketability of PFA is further complicated by the increasing use of alternative fuels, such as biomass and imported coals in the power industry. Consequently, the complications of PFA marketability were illustrated in the environmental regulations of NO_x reductions, and PFA quality (*i.e.* high LOI value > 7%). From using alternative fuels, main minerals oxides (silicates, alumina, and ferrous) in the resultant PFA which changed in compositions compared with ASTM C618, and physico-chemical properties of PFA different, for example hardness, fineness, and particle shape.

These alternative fuels were approved NO_x emissions reduction, yet changed PFA quality. This has restricted the principal use of ash in the cement industry, since the unburned carbon (*i.e.* residual carbon) tends to adsorb the air-entrainment agents, which are added to prevent crack formation and propagation [Maroto-Valer *et al.*, 1998]. Consequently, the high carbon ash is disposed in landfill as a cheaper option, but the UK government is trying to

raise the landfill tax in a way to reduce or prevent any landfills option [UKQAA, 2007]. Therefore, high carbon PFA beneficiation will result in a good impact to resolve the economical and environmental issues. It will also achieve a good return to the energy companies. Moreover, power plants are continuously increasing their dependence on foreign coals. Thus, the impact of these secondary fuels, such as biomass, and imported fuels on properties of PFA and its marketability of combustion by-products, mainly PFA, is not well understood. PFA as a by-product is currently not utilised in a full scale (*i.e.* <40%) and recently there has been a decline in this industry.

The environmental regulations are getting tougher due to increase in gas emissions that resulted from burning more coal to substitute high energy demand, which lead the disposal of these by-products into landfill without any utilisation. Moreover, it has been shown in previous studies that unburned carbon resulted with PFA can be considered as a potential precursor for the production of adsorbent material and re-feed it as a fuel [Maroto-Valer *et al.*, 1998 and Li *et al.*, 1999]. Consequently, previous works have illustrated in steam activation that the porous properties of the resultant activated unburned carbons, such as BET surface area and pore volume, achieve the maximum within two hours. Furthermore, the microscopy analyses only described the unburned carbons before activation [Rodri *et al.*, 1991].

However, to the best of the author's knowledge, previous studies have not included the unburned carbon resourced from biomass co-firing. Microscopy studies were conducted before and after activation for these unburned carbons. It is still to be learned about the reasons why not all unburned carbons are

equally suitable for activation, and why some unburned carbons showed differently in terms of the porous properties of their corresponding activated carbons, as observed by Zhang works [Zhang *et al.*, 2003].

It is important to select only the suitable unburned carbon, which will generate activated carbon with desired porous structures for commercial applications. Therefore, the goal of the present project was to achieve through first understanding the scientific literature in order to acquire an enhanced understanding of high carbon PFA, its properties (for example physical and chemical), and the suitable method to remove the carbon material from PFA without any reaction taking place. Thus, one could ascertain which treatment could help to improve the separation or adding multi-stage process in order to increase the efficiency. In addition, the depleted carbon PFA that derived from alternative fuels was approved to be used with cement. Furthermore, this will persuade the construction companies to use this type in the cement industry in terms of increasing the PFA marketability and reducing landfill waste.

Accordingly, this project aims to give a better understanding of the factors that may affect the behaviour of unburned carbon in terms of using steam activation. The porous properties of the resultant activated carbons were suspected to consist of PFA (*i.e.* minerals impurities) and the precursor unburned carbons as well as the activation conditions. Consequently, a characterisation of the physical and chemical properties of high unburned PFAs and the resultant unburned carbons, will help to lead to the above mentioned goal.

1.2 Aim and objectives

The aim of the project is to understand the impact of using of alternative fuels, such as biomass and imported coals, on the physico-chemical properties of PFA particularly on their marketability.

The objectives of the research project are as follows:

- Identify high carbon PFA samples produced from alternative fuels (imported coals and biomass).
- Beneficiate high carbon PFA samples to produce a high quality depleted carbon PFA stream and an enriched carbon stream.
- Study the impacts of using depleted carbon PFA that are produced from alternative fuels with cement (*i.e.* improving the PFA marketability).
- Investigate applications for carbon-rich material produced by PFA beneficiation and to establish the separation purities required for these applications.

1.3 Methodology

The project work is divided into four tasks as presented in Figure 1.1. The description of each task is discussed in more detail in chapter three. Figure 1.1 summarises the techniques used in each task as follows:

Task 1: Sample procurement and characterisation:

The study samples with LOI value between 5-40% were provided by three power plants. The suite included samples generated from co-firing of biomass with coal and burning only coal. The samples were characterised using a

battery of tests listed in Figure 1.1. Accordingly, the properties of these samples (*i.e.* as received) were investigated.

Task 2: High carbon PFA beneficiation:

The samples identified with high carbon contents from task 1 were beneficiated using physical and chemical processes, namely incipient fluidisation and thermal treatment (microwave), respectively. Incipient fluidisation has been previously shown to efficiently remove unburned carbon from PFA, while microwave process has only been used to vitrify waste (*i.e.* toxic) ashes [Zhang *et al.*, 2003 and Pierre *et al.*, 2007]. Incipient fluidisation generated two streams depleted carbon PFA and enriched carbon PFA, while the thermal method (*i.e.* microwave) produced only one stream that was depleted carbon PFA.

Task 3: Enriched carbon PFA streams characterisation and activation:

The enriched carbon PFA streams were activated physically using steam at temperature at 850 °C for periods of time between 1-5 hrs. Characterisation tests were conducted before and after activation to determine the physical and chemical properties of the resulted precursor. Finally, the adsorption capacity for the activated carbons after two hours activation were analysed by methylene blue measurements (Figure 1.1).

Task 4: Depleted carbon PFA marketability investigation:

Depleted carbon PFAs were characterised through thermal-gravimetric analysis, particle size distribution studies, and Inductively Coupled Plasma

Atomic Emission Spectrometry (ICP-AES) analysis. In addition, the resulted impacts from using alternative fuels on PFA properties as regards to marketability were investigated through concrete tests.

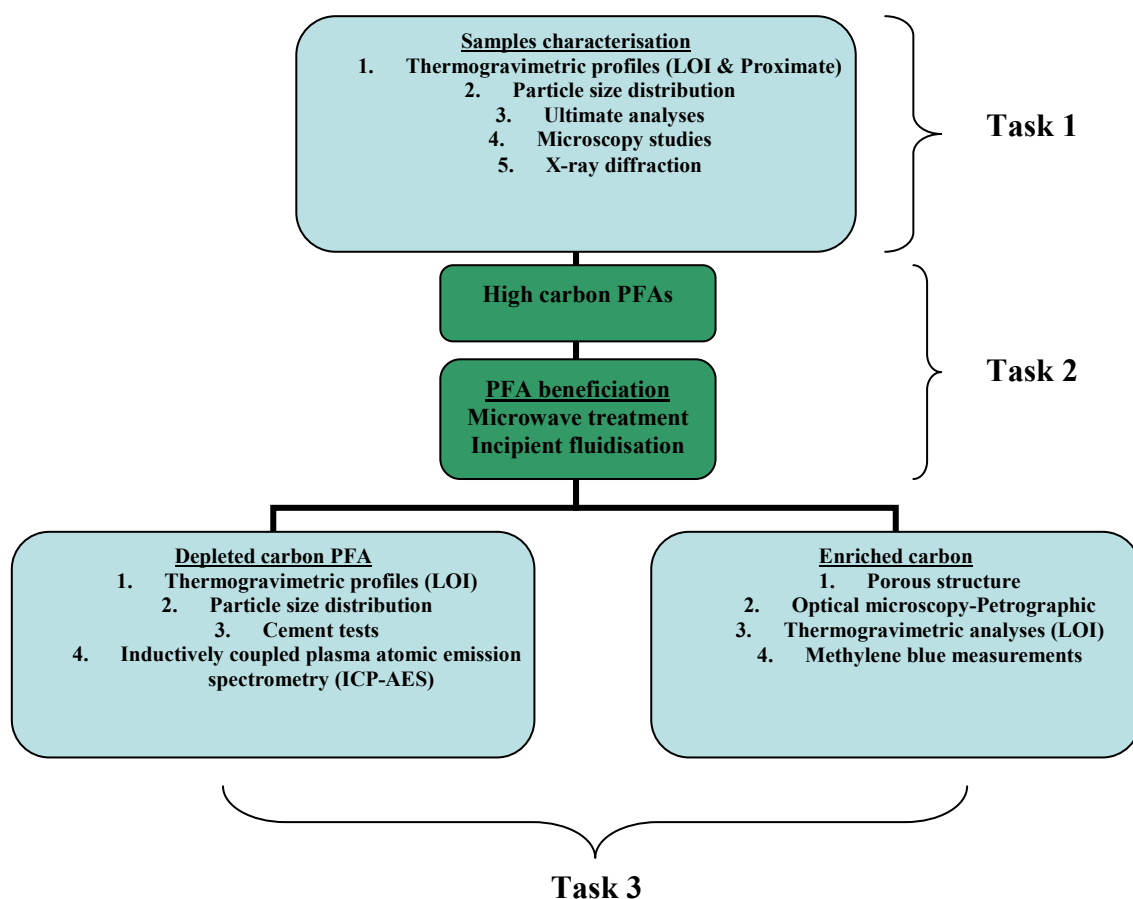


Figure 1.1: Project plan

CHAPTER TWO

LITERATURE REVIEW

2.1 Mineral matter transformation during coal combustion

2.1.1 Coal formation

Coal is a fossil fuel that was formed from the remains of vegetation that grew as long as 400 million years ago. Plants which formed coal captured energy from the sun and through photosynthesis created the compounds that make up plant tissues. The most important element in the plant material was carbon, which gave coal most of its energy sourced today [WCI, 2010].

Over long periods of time, the makeup of the earth's surface changed, and seas and great rivers caused deposits of sand, clay and other mineral matter to accumulate, burying the peat. Sandstone and other sedimentary rocks were formed, and the pressure caused by their weight squeezed water from the peat. Increasingly deeper burial and the heat associated with it gradually changed the material to coal [WCI, 2010].

Coal is a naturally occurring combustible material consisting primarily of three categories: organic carbonaceous matter termed macerals, inorganic (mainly crystalline) minerals, and fluids. The fluids prior to mining are mainly moisture and methane. The mineral matter of coal refers to the mineralogical phases containing inorganic elements which are found in coal and are associated in

various ways to the organic (C, H, O, N, and S) components. The mineral content consists mainly of quartz, mullite, pheldspates, and pyrite [Kenneth *et al.*, 1987].

Mineral matter in coal occurs as discrete grains, flakes or aggregates in one of five physical modes [Harvey *et al.*, 1986 and Kenneth *et al.*, 1987], 1) microscopically disseminated can be found within macerals (distinct organic designations such as vitrinite, liptinite, and inertinite), 2) layers of partings wherein predominated by fine-grained clay minerals, 3) nodules including lenticular and spherical concentrations, 4) fissures including cleat and other fracture or void fillings, and 5) rock fragments can be found within coal bed due to faulting, slumping or otherwise related disturbances (*i.e.* temperature, moisture, pressure, origin of the sediment, *etc.*). Mineral matter is formed by three different mechanisms, namely detrital deposition, syngenesist, or epigenesist as described below.

Detrital grains were introduced into a coal formation basin (*i.e.* swamp land) by rivers, tidal waves, and wind. Flakes of clays and microscopic grains of quartz, feldspars, apatite and others were deposited as discrete grains, which became inter-bedded with peat and then later with the resultant coal. Most wind deposited minerals are recognized as such by the presence of high temperature phases. These minerals consisted of dust particles derived from distant volcanoes [Harvey *et al.*, 1986]. Syngenetic minerals were formed during the peat stage of coalification and include minerals formed by crystallization of inorganic elements in plants (*i.e.* intrinsic mineral matter). This appeared

before the peat was deeply buried by other sediments, probably by not more than 50 feet. Accordingly, disseminated pyrite is thought to have formed in sulfate bearing peat by bacterial reduction of sulfur, and much of this type shows spherical form. Nodules of peat accompanied with various carbonates are comprised of microcrystalline quartz and/or hematite which occurred in early coal development. It was thought by Strehlow and Wert [Strehlow *et al.*, 1979 and Wert *et al.*, 1981] that these forms were crystallized from inorganic matter inherited from the original plant material. Epigenetic mineral exist as filling of fissures and voids after the peat was formed [Harvey *et al.*, 1986 and Kenneth *et al.*, 1987]. This type of minerals represents the calcite, part of pyrite and kaolinite in coals. They were formed long after the peat was consolidated and cooled enough to allow joints to develop (*i.e.* minerals precipitation). For example, this happened during the late lignite or early subbtuminous stages of coalification [Cecil *et al.*, 1981].

Palmer and Filby [Palmer *et al.*, 1984] determined the particle size of the main minerals (*i.e.* pyrite, clays, and quartz) for Ohio coal. Pyrite was concentrated in the range of 5-20 and >20 micron, clays were ranged of 0.2-2 and 2-5 micro, while quartz was in the range of 0.2-2 micron. Moreover, it was reported by Straszheim [Straszheim *et al.*, 1986] that mineral analyses versus mineral particle size for coals had been tested. For example Illinois no.6 and Pittsburgh no.8, and among this, the minerals consisted differently in concentration with Illinois coal which contains more than 90 wt.% of pyrite, kaolinite, and quartz.

Furthermore, coal contains to a greater or lesser extent heavy metals (Cd, Co, Cu, Hg, Ni, Pb, Sb, and Zn). The actual concentration of each in a coal depends on its origin. Coal is usually classified into the sub-groups known as anthracite, bituminous, sub-bituminous and lignite. The physical and chemical properties of coals vary considerably between sources [Rock Talk, 2005]. However, most coals are not composed of the same compounds, as different types of coals are characterized by their unique properties resulting in different combustion behavior. Accordingly, anthracite is physically the hardest, having been subjected to more extreme pressure and temperatures during its formation, and has the highest carbon content, giving it a higher heating calorific value. Lignite is the softest coal and contains the least amount of carbon when compared with other groups of coal on a dry basis [Karayigit, 2001].

2.1.2 Mineral matter transformation

Mineral matter particulates present in coal are transferred into ash when the coal is burned inside the combustor. Within the flame there is a rapid heat release as the organic volatile materials released from pulverized fuel (PF) coal particles burn very quickly in just a few milliseconds [Huffman *et al.*, 1978] (Figure 2.1). Residual carbon char particles within the main body of the flame and burn out more slowly in a few hundreds of milliseconds as the particles progress to the hottest part of the boiler which with current technology approaches 1650 °C. Prior to modifying power plants with the aim of reducing NO_x emissions, the peak temperatures for burning PF were at least 100 °C higher than used to be the case [Unsworth *et al.*, 1991 and Livingston, 2007].

However, biomass fuel particles co-fired with coal (*i.e.* at 1-7%) are very rapidly combusted in a few milliseconds and the most ash content accumulated from coal relatively to biomass ash content [Demirbas *et al.*, 2004]. On the other hand, the average residence time of a particle of pulverized fuel in the boiler is approximately 3-4 seconds, by which time the combustion process is completed with very high efficiency. Each stage in the combustion process has an effect in determining what type of PFA is formed. Three types of PFA precursors can be identified according to the composition of fragmented particles as follows [Karner *et al.*, 1994] (Figure 2.1):

- 1) Excluded mineral particles which break free of coal fragments during crushing are relatively large. These particles may be fragmented during combustion and partly or wholly fused depending on temperature, composition and volatile content (Figure 2.1-A). Furthermore, it was shown accordingly that pyrite particles are fused at temperature 1100 °C, clays at 1300 °C and quartz at 1550 °C [Karner *et al.*, 1994]. It can be seen that these mineral particles observed bigger sizes, for example, bedded particles with carbon.
- 2) Included are mineral particles which are retained in coal fragments and tend to be smaller. These particles are affected by coal swelling, char fragmentation and combustion, and take part in several reactions including fragmentation, volatile migration, coalescence and fusion, as shown in (Figure 2.1-B).
- 3) Organically associated inorganic elements are distributed within the coal macerals. These elements are freed during combustion to form vapour and fine particles that typically adhere to and coat larger particles (Figure 2.1-B).

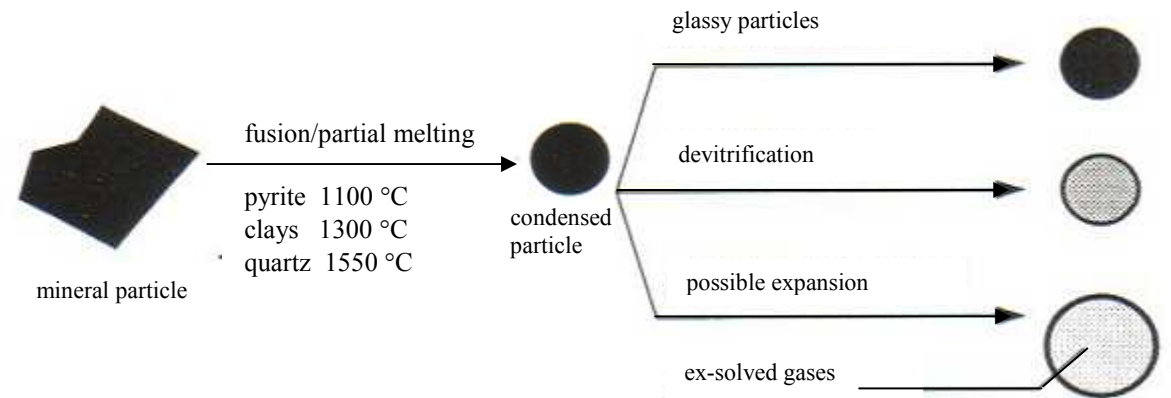
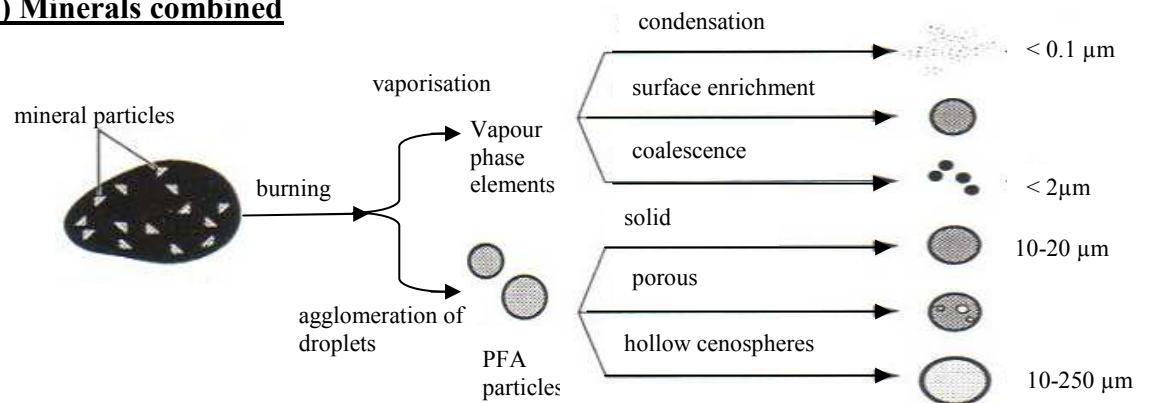
A) Discrete mineral particles**B) Minerals combined**

Figure 2.1: Schematic diagram of the interactions of different inorganic components during combustion [Clark *et al.*, 1993b].

Figure 2.1 shows the forms of pulverized fuel coal particles associated with mineral and organic compositions which take place inside the boiler. The particles developed inside the boiler are in different forms depending on their composition, shape, temperature and volatile content. This figure shows how pulverized particles contain minerals when entering the boiler. These minerals

will fuse and condense according to their properties (*i.e.* discrete minerals). Usually pyrite goes first, followed by clays, and quartz (Figure 2.1-A). Following this there are more stages such as vaporisation, condensation, and agglomeration due to type, shape, size, reactivity, and porosity (*i.e.* combined particles) (Figure 2.1-B). The differences between both types are illustrated as the first type (Figure 2.1-A) which shows the particle size is larger than the second one (Figure 2.1-B). The first type observed high temperatures compared to the second kind. The first type took place in later stages, while the second type appeared in the early stages of the combustion process. Finally the second kind obtained different forms of particles compared to the first.

Moreover, in the flame zone where the burners are located, the mineral matter in the coal particles decomposes to form domains of ash within coal char particles. The particles continue to lose carbon as they move from the flame and the ash begins to form into new materials. Some of the changes which occur during this process are listed in Table 2.1. It can be seen that minerals in coal decompose in different stages according to the conditions applied and the properties of each mineral. Consequently PFA had formed from the minerals transformed and this varies according to the origin of the coal (Table 2.1). In addition, the aluminosilicates in the coal melt to form a glass and the inherent ash in the coal melts to produce a sticky mixture of alkali-metal oxides [Huffman *et al.*, 1978 and Graham, 1992]. When the carbon has largely burned away, the ash may be released either as individual ash particles or as aggregates. Organic and inorganic compositions of PFA will be discussed in more detail in sections 4.7.1 and 4.11.

Table 2.1: Coal inorganic matter transformation during combustion process [Unsworth *et al.*, 1991 and Lesley *et al.*, 1996].

Minerals in coal	Minerals in PFA
Phyllosilicates	Mullite $\text{Al}_6\text{Si}_2\text{O}_{13}$, Quartz SiO_2
Quartz	Glass, Quartz SiO_2
Pyrite FeS_2 , siderite FeCO_3 , iron sulphates	Hematite Fe_2O_3 , magnetite Fe_3O_4
Calcite CaCO_3	Lime CaO
Dolomite $\text{CaMg}(\text{CO}_3)_2$	Lime CaO , Periclase MgO
Gypsum $\text{CaSO}_4 \cdot 2\text{H}_2\text{O}$	Anhydrite CaSO_4
Ankerite $\text{CaMg}_x\text{Fe}_{(1-x)}(\text{CO}_3)_2$	Calcium Ferrite CaFe_2O_4 , periclase MgO

2.1.3 Coal Combustion by-products (CCBs)

Coal has long been considered a major source of energy. It has been used for about a century to generate electricity throughout the world. When coal is burned to create electricity, coal combustion by-products (CCBs) are also generated. Modern thermal power plants burning coal produce large amounts of these solid by-products. As this derives from burning pulverised fuel, it is usually referred to as pulverised fuel ash (PFA) in the UK, but the term fly ash is widely used throughout the rest of the world for coal fired power station ash in all European Standards. Coal combustion by-products (CCBs) include:

- 1) Coal ash (*i.e.* PFA) that exits from the combustion chamber in the flue gas and is captured by air pollution control equipment such as electrostatic

precipitators (Figure 2.2), baghouses, and wet scrubbers. This by-product represents the greatest proportion of total CCBs, accounting for more than 58% [Rustu, 2001].

2) Bottom ash is agglomerated ash particles formed through the combustion process inside the boiler. These particles are too large to be carried in the flue gases and falls to the bottom of the boiler (Figure 2.2), without fusing. Bottom ash has a similar chemical composition to PFA but is produced in a different range of particle size ranging from fine sand to small aggregate from 37.5-150 mm [Scotash, 2006]. The percentage of this by-product is about 16% of the total CCBs.

3) Boiler slag is molten ash and only represents 2% of the total by-products. This substance is collected from the slag tap at the bottom of cyclone boilers. Since, the slag has been fused; it possesses very little chemical activity and cannot normally contaminate or leach out into the soil.

4) Flue gas desulphurisation (FGD) materials are derived from a variety of processes used to control sulphur emissions from boiler stacks. These systems include wet scrubbers, spray dry scrubbers, sorbent injector and a combined sulphur oxide (SO_x) and nitrogen oxide (NO_x) process (Figure 2.2). Sorbents include lime, limestone, sodium-based compounds and high-calcium PFA. The physical nature of these materials varies from a wet, thixotropic sludge (the sulphite sludge settles and filters poorly) or a dry, powder material, depending on the process used [Rustu, 2001].

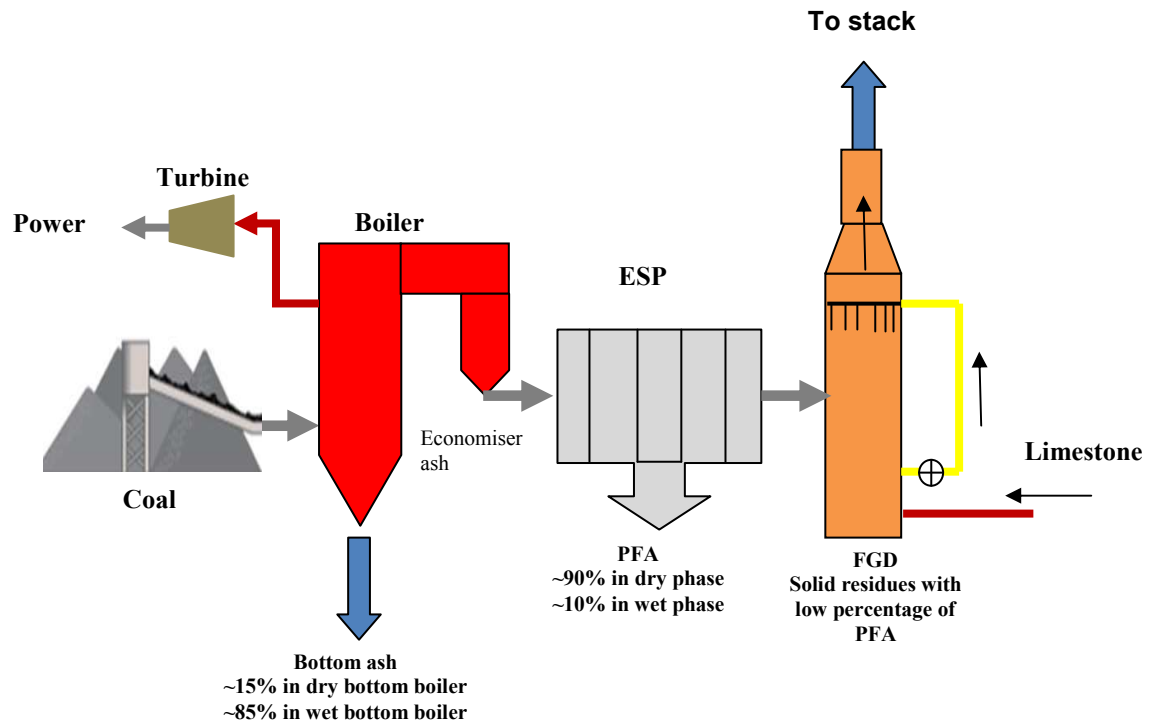


Figure 2.2: Coal-fired power plant.

CCBs utilisation is considered an important task in regards to reduce landfill wastes in terms of reducing landfill option. The benefits can return from the sale of these products. Moreover the re-use of these materials also contributes to improved environmental quality and sustainable development. Based on the ECOBA document ‘‘Production and Utilisation of Coal Combustion Products (CCPs) in Europe (EU 15) in 2004’’ about 64 million tonnes of CCPs were produced in this year. Around 89% of the CCPs were utilised in the building industry, underground coal mining as well as for recultivation and restoration purposes in open cast mining [ECOBA, 2004]. This percentage varies for each

country depending on coal burning equipment and environmental regulations in that country.

As mentioned previously, the solid coal combustion by-products resulting from the coal combustion process are mainly PFA, bottom ash and boiler slag. Figure 2.2 shows also where the different ashes are formed in a typical coal-fired power station. Some ashes are received in a dry and wet state from the boiler unit. Economizer has also a share of the flue gas particles collected either from top tray or bottom tray. The main PFA residue can be collected by the ESP unit and mostly in dry phase, as shown in Figure 2.2. The last part has very little portion of PFA depends on the efficiency of the FGD unit.

The proportion of residues collected as PFA varies with different types of boiler. This illustrated by a ‘dry-bottom ‘ pulverized coal-fired boiler, so called because the bottom ash is removed from the base of the boiler as discrete, non-molten particles or clinkers. This produces 80-90% of the residues in the form of gas-borne PFA. In a ‘wet-bottom’ boiler most of the residues are collected as gas-borne PFA, due to the finer coal ash particle size fraction suspended in the flue gases [Joshi *et al.*, 1995]. Particulate emission standards in most countries require the separation of PFA from flue gases. For more details see [Soud, 1991 and Giulio, 2000]. This may be achieved by different techniques such as electrostatic precipitators (ESP), fabric filters (baghouses), cyclones and wet scrubbers.

2.2 Pulverised fuel ash

PFA is a term used for the fine ash carried over in the gases from a furnace. It can refer to the ash from any furnace, but for furnaces other than those at coal fired power stations it is normal to prefix the words with the type of process which generates it e.g. incinerator ash, paper sludge fly ash, etc. [UKQAA, 2007].

PFA's are generally finer than cement and consist mainly of glassy-spherical particles as well as residues of hematite and magnetite, char and some crystalline phases formed during cooling. PFA is the main and most valuable by-product from a coal fired power station. As stated previously, under more stringent environmental regulations for reducing NO_x emissions, the unburned carbon content has increased in PFA. This results from a lowering of the boiler temperature from 1300 °C to 1100 °C to reduce NO_x emissions. Hence, the efficiency decreases, and thus, the unburned carbon content of PFA increases. This has disadvantages on ash sales, especially to the cement industry [Lesley *et al.*, 1996, Giulio, 2000, and UKQAA, 2007]. This will be discussed in more detail when considering PFA beneficiation section 2.5.

PFA has not been considered as hazardous waste, [EPRI, 2009] except those generated with heavy metals, and therefore it can be utilised under environmental regulations. PFA is nowadays commonly used as a secondary raw material in the production of blended cements and concrete mixtures [Giulio, 2000]. In these construction products, PFA work as pozzolanic additive and micronic filler, improving mechanical properties and the cements durability to aggression from environmental agent aggression. Nevertheless,

close quality control of PFA is required in terms of the consistent value as possible for industrial product.

Use of PFA in concrete started in the United States in the early 1930's. The first comprehensive study was described in 1937, by Davis at the University of California [Mccarthy, 1990]. The major breakthrough in using PFA in concrete was the construction of Hungry Horse Dam in 1948, utilising 120,000 tonnes of PFA (Figure 2.3) [Rustu, 2006]. This decision by the USA Bureau of Reclamation paved the way for using PFA in concrete constructions. In addition to economic and ecological benefits, the PFA in the cement mixture can improve workability, reduce segregation, bleeding and heat evolution. Moreover, it inhibits alkali-aggregate reaction, and enhances sulphate resistance [Joshi, 1992].



Figure 2.3: Hungry Horse Dam, Montana [Joshi, 1992].

2.2.1 The status of ash utilisation Worldwide

It has been estimated that in 2000, worldwide PFA production was approximately 480 M tonnes (Figure 2.4) with the majority of ash arising originating from seven countries. This number is rising year by year because of increasing energy demand of approximately 10% [Vom Berg, 2000].

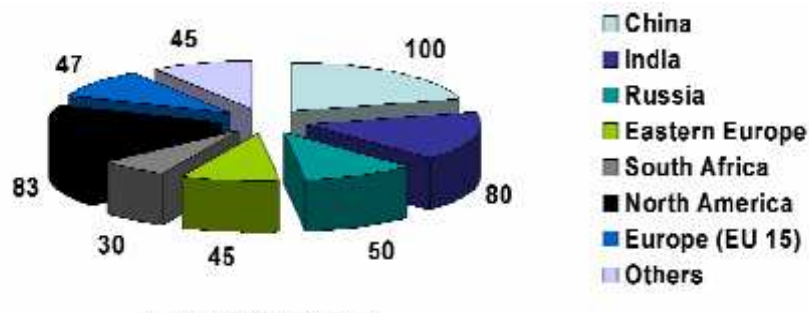


Figure 2.4: World wide of PFA production at year 2000 [Vom Berg, 2000].

In recent years coal-fired power generation and hence ash production has grown sharply. Utilisation rate of the latter around the world remained low, but in 2002 the total ash utilisation increased rapidly (Table 2.2), according to the adoption of more stringent environmental regulations applied to this industry. This table shows that the PFA utilisation is different from country to country e.g. Japan utilises a high percentage (78%) while Canada only 8%. This is because of landfill size in this country, regulated to dump PFA, most the energy supply come from burning coal compared with other sources of energy. There are environmental regulations in this industry, and public awareness, together with conditions of PFA produced according to the rules applied in England. South Africa generates PFA with very low LOI and has not yet installed any low-NO_x burners.

The application of modern ESP systems to flue gas cleanup has increased and has therefore improved the quality and consistency of ash, thus enhancing prospects for its use [Barns, 2004].

Table 2.2: PFA utilisation in main countries at 2002 [Barns, 2004].

Country-region	Total percentage
Japan	78%
Poland	70%
China	66%
India	50%
EU-15	46%
USA	35.4%
Russian (including commonwealth of independent states)	11%
Canada	8%
South Africa	No Low NO _x Burners installed yet, LOI <1%

A US study identified institutional barriers to increase ash utilisation. These barriers are related to technical, economic, institutional and legal issues [Pflughoeft *et al.*, 2001]. It considered a lack of data on environmental and health effects, PFA beneficiation frustrated by the restrictive regulation implemented by the environmental agencies, and PFA in most states considered as a solid waste.

However, these acquired problems according to many countries are being addressed by respective trade organisations representing ash producers and users, with each national association actively promoting PFA use and potential. Many of these associations interact on an international level, such as ECOBA “European coal combustion products association”, UKQAA “United Kingdom quality ash association”, and ACAA “American coal ash association”. These

organisations work regularly to discuss the use of by-products of coal-fired power stations and can interact with other organisations.

Currently, there is much confusion throughout Europe about the definition of ‘waste’ and the implementation of the EU Waste Directive and how it applies to CCPs. ECOBA has encouraged ash to be categorised as a ‘product’. The problems are arising from the official classification of many long-established ash products as waste. This is particularly acute in the UK where it is the subject of an intense dialogue between the ash producers and users and the main regulatory body, the Environment Agency. The issues with the implementation of the EU Waste Directive are not restricted to coal ash. They also impact on the recycling of other recovered materials. These classifications appear to run counter to the concept of sustainability which is increasingly at the heart of European development strategy [Barns, 2004]. This by-product was beneficiated through this project according to increase the marketability and understanding the behaviour of organic material through different constraints.

2.2.2 Legislation

Legislation impacts on ash utilisation prospects at the national, international, and local level and they include, EU-wide, country-specific, US National and State legislation.

Legislation can encourage or impede ash utilisation. Examples of the former include an Indian government directive on PFA use, and Chinese subsidies on ash transportation costs plus tax breaks for ash use in construction. Legislation

impeding ash use includes limits to levels of heavy elements introduced into the environment (Germany) and the use of ash as mine backfill (USA) [ERTD, 2007]. This is dependent on the original coal from where the ash has derived, the leachability of the ash together with the utilisation cost with heavy metals. Consideration has also to be given to the disposal cost which is restricted to the local authorities in each country, as well as environmental conditions and the economy issue.

However, local legislation will determine elements of the disposal costs of ash, particularly the taxes levied on materials sent to landfill. Taxation levels can vary between countries and even location. These impacts affected significantly on economics of utilisation (Figure 2.5). Sweden and Netherlands have the highest tax-related costs of landfilling non-hazardous waste, while in Belgium, Denmark, and Norway landfill taxes are low for such materials.

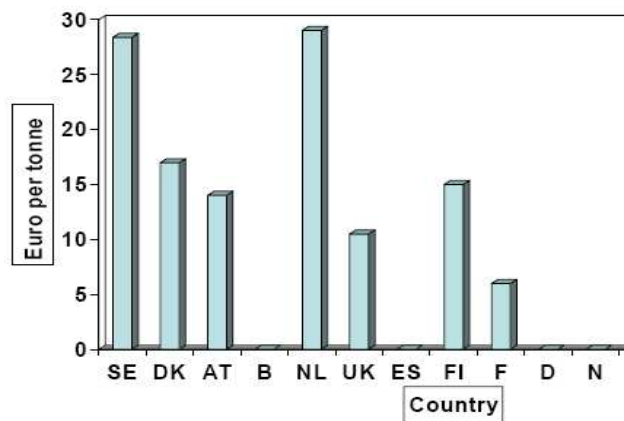


Figure 2.5: Tax-related costs of landfilling non-hazardous waste in selected countries [ERTD, 2007].

Thus, an economically viable process in one location may not be viable elsewhere, due to the differences in costs resulting in ash disposal. This could be illustrated to benefit PFA in useful applications. Therefore in that location to avoid high disposal costs, compared with different locations or countries, applying low disposal costs in unlimited landfill areas. The importance of these differences can be demonstrated by OECD (Organisation for Economic Co-Operation and Development) data on tax-related and landfilling costs for several countries (Figures 2.5 and 2.6) [ERTD, 2007].

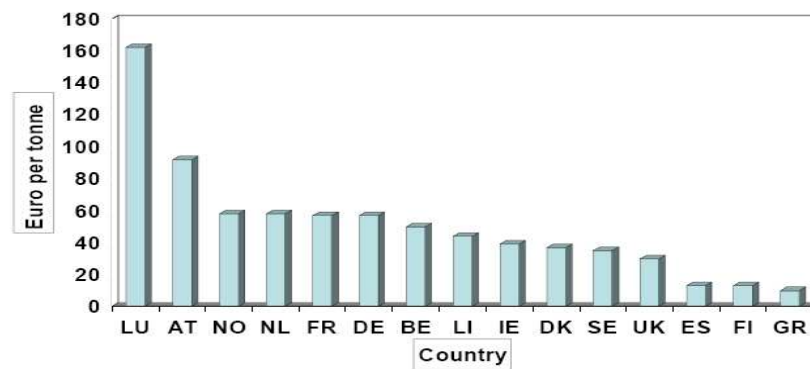


Figure 2.6: Costs of landfilling non-hazardous waste in selected countries
[ERTD, 2007].

It can be seen that Luxembourg has the highest level of cost for landfilling non-hazardous waste. Each country applies its own national specifications and the suitability of ash residues for different applications, as it will be revealed in PFA classifications in the next section. The suitability of ash for a particular purpose is determined primarily by its meeting the requirements of specific tests set out in relevant standards or specifications. However, it is not universally accepted that all such tests are appropriate, and practical experience has shown that some ashes which fail to meet certain test requirements still produce technically acceptable final products.

Many current specifications focus solely on use of PFA from coal and exclude those from co-combustion, thus restricting its scope for utilisation. Similar problems can also occur with residues from advanced coal use technologies, such as fluidised bed combustor (FBC) and integrated gas coal combustor (IGCC). For instance, in some US states, combined fluidised bed combustor (CFBC) residues are utilised widely, whereas in others, specifications automatically exclude their use. In reality few of the common tests for additives in cement are appropriate and new more appropriate criteria based on final performance need to be developed [ECOBA, 2002].

It would be preferable for specifications to be based on the advice from technical standards committees and customer user groups can be instrumental in leading to such change. For acceptance of novel products, the situation may be no better, as relevant standards may not be applicable, or even exist. Where new standards need developing to assist such products enter the marketplace, the increasing drive to EU-wide standards requires a pan-European approach [Barns, 2004].

2.2.3 Classification and specifications of PFA

As previously described in section 2.2, PFA is an important commodity to industries such as those producing cement and concrete. However, PFA has different and variable characteristics and the buyers need to determine which PFA is suitable for a particular application. Thus, classification and specifications schemes are required to find proper and predictable performances of PFA where it is needed. Classification schemes use intrinsic

properties to categorise the PFA itself, regardless of end use. Specification schemes are used to define PFA properties in terms of its use in different applications. There is an inevitable overlap between classification and specification. Classification schemes depend mostly on PFA properties which determine the applicability of the PFA as an admixture in cement. When PFA is used as a filler in cement and concrete only a few basic specifications are required to be met [Lesley *et al.*, 1996]. For more advanced uses in cement and concrete, PFA has to be of a higher standard that is, for example, finer, with lower carbon content.

Specification schemes are necessary in order to ensure proper and predictable performances of PFA for each required use. They define properties of PFA which need to be met for its use in different applications. Each country has different system for PFA classification and specification, and each one has a way to classify and to specify ash under particular physical and chemical properties. For example, the USA uses ASTM C618 for cement and concrete, ASTM-C-33 [ASTM, 2006] for concrete aggregates. In the ASTM system the suitability of PFA as pozzolanic and cementitious materials is considered. PFA composition varies depending on the parent coal and the furnace operating conditions. From mineralogy of PFA as described below, the most important components are quartz (SiO_2), mullite ($3\text{Al}_2\text{O}_3 \cdot 2\text{SiO}_2$), hematite (Fe_2O_3), magnetite (Fe_3O_4), lime (CaO), and gypsum ($\text{CaSO}_4 \cdot 2\text{H}_2\text{O}$) [Tazaki, 1989].

The more important systems to be considered are the US ASTM C618 and the new European EN450. PFA is classified under ASTM C618 as class F and class C [Philadelphia, 1993 and ASTM, 2006].

- Class F, pozzolanic, $\text{SiO}_2 + \text{Al}_2\text{O}_3 + \text{Fe}_2\text{O}_3 = 70$ wt.% minimum;
- Class C, cementitious, $\text{SiO}_2 + \text{Al}_2\text{O}_3 + \text{Fe}_2\text{O}_3 = 50$ wt.% minimum.

Class F ashes emanate from anthracite or bituminous coals, while class C ashes arise from lignite or sub-bituminous coals. However, this is not always the case; for example, class F PFA can be produced from sub-bituminous Alberta coals. Similarly, bituminous coals can produce ash which is not class F. The ASTM classification itself does not require that the PFA is produced from any particular coal type [Joshi *et al.*, 1995].

The new European standard governing the use of PFA in concrete is EN-450 [BS EN 450, 1995], and mainly considers hard coal (anthracite or bituminous), because brown coal is only of limited regional significance in Europe. The PFA originating from lignite may be accepted if its CaO content is below 10% by mass, and it complies with other requirements of the standard. In UK, BS 3892 Part I was the standard used to specify PFA for Portland cement (cementitious component) [BS 3892 Part 1, 1982], while BS-3892 Part II applies as additional to Part I [BS3892 Part II, 1996]. Germany, Italy and Denmark use EN-450 and now in the UK, it has replaced BS 3892 since 1st January 2007 [BS EN 450, 2008].

Tables 2.3 and 2.4 present the physical and chemical requirements for PFA according to ASTM C618 and EN-450 standards [Vom Berg, 1993]. All the requirements in these tables are recommended when the PFA is used as an additive in cement, and they are characteristic values. To get a consistent quality of PFA requires carrying out continuous statistical quality control at

every generating facility. It can be seen from the details in Table 2.3 the maximum chemical limits for PFA when it is used in the cement industry in the US and Europe, whilst Table 2.4 shows the physical test requirements.

Table 2.3: The chemical requirements to be specified for PFA under EN-450, and ASTM C618 [Vom Berg, 1993].

Parameter	Requirement	
	EN-450	ASTM C618 Class F
$\text{SiO}_2 + \text{Al}_2\text{O}_3 + \text{Fe}_2\text{O}_3$, min %	-	70.0
Loss on ignition, max %	5.0	6.0
Chloride, max %	0.10	-
Free calcium oxide (CaO), max %	2.5	-
Moisture content, max %	-	3.0
Available alkalies as Na_2O , max %	-	1.5

Table 2.4: The physical requirements to be specified for PFA under EN-450, and ASTM C618 [Vom Berg, 1993].

Parameter	Requirement	
	EN-450	ASTM C618 Class F
Amount retained when wet sieved on 45 μm sieve, max %	40	34
Activity index at 7 days, min, percentage of control	-	75
Activity index at 28 days, min, percentage of control	75	75
Activity index at 90 days, min, percentage of control	85	-
Activity index with lime at 7 days, min, kPa	-	5500
Water requirement, max, percentage of control	-	105
Autoclave expansion or contraction, max %	-	0.8
Le Chatelier expansion, max, mm	10	-
Uniformity requirements:		
Percent retained on 45 μm , max, percentage points from average	10	5
Specific gravity, max, variation from average %	-	5
Specific gravity, max, variation from average kg/m^3	150	-

Other test methods are used depending on the ultimate of PFA use and include measurements of pozzolanicity, fineness, strength, autoclave expansion, permeability, and LOI value [Vom Berg, 1993].

2.3 PFA characterisation

2.3.1 Physical and chemical properties of PFA

PFA is the fine particulate mineral residue produced from the firing process in coal-burning thermo-electric power stations. The temperature of combustion is around 1400 °C which is above the melting point of most minerals present in the coal. PFA is formed when molten minerals solidify as glassy spheres around a bubble of gas. PFA is composed of three main elements, silicon, aluminium and iron, the oxides of which account for 75-85% [Hall, 2005] of the material. Physically it consists predominantly of finely divided spherical and non-spherical particles of between 10 and 100 microns (Figure 2.7). These small spherical particles are called cenospheres. Approximately 20% of PFA fuses and agglomerates into large particles. Their very size separates them off as furnace bottom ash or as coarser PFA which are rejected leaving a uniform PFA complying with the fineness requirement in BS EN 450.

PFA is tested routinely in the laboratories of the cement companies in order to confirm its compliance with all requirements of BS EN 450 [Castle Cement, 2006].

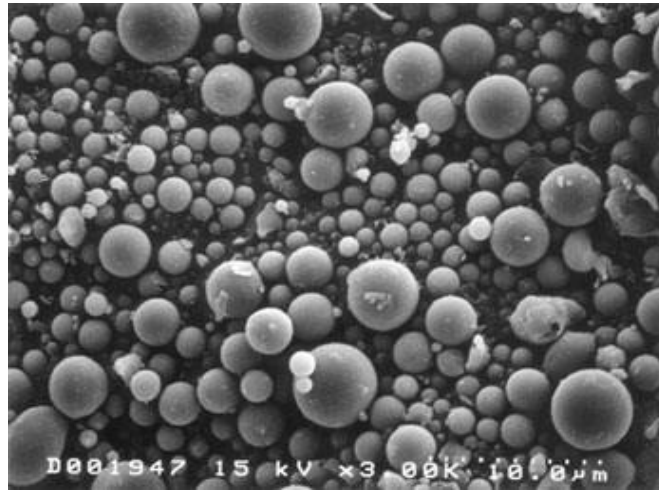


Figure 2.7: PFA particles under SEM [Castle Cement, 2006].

The colour of the PFA can be tan to dark gray, depending on its chemical and mineral constituents. Tan and light colours are typically associated with high lime content. A brownish colour is typically associated with iron content. A dark grey to black is typically attributed to an elevated unburned carbon content. PFA colour is usually very consistent for each power plant and coal source [Castle Cement, 2006]. Table 2.5 presented some physical properties are needed to specify the PFA for cement requirements.

Table 2.5: Other physical properties of PFA [Scotash, 2006].

Property	Typical value(s)
Compacted bulk density	1300-1500 kg/m ³
Relative density (oven dry)	2-2.4
Specific heat gravity	0.8-0.7 J/kg/°C
Water permeability-compacted PFA	1×10^{-6} - 7×10^{-7}
Electrical conductivity	0.09 W/mK
LOI	6-10%

The chemical properties of PFA are influenced to a great extent by the coal burned and the techniques used for handling and storage. As mentioned earlier, there are four main types of coal (anthracite, bituminous, sub-bituminous, and lignite) [Krevelen *et al.*, 1993]. Each varies in terms of its heating value, its

chemical composition, ash content, and geological origin [Amanda, 2003]. The principal components of bituminous coal PFA are SiO_2 , Al_2O_3 , Fe_2O_3 , and CaO , with varying amounts of carbon, as measured by loss on ignition (LOI). The typical ranges for these minerals in PFA are shown in Table 2.6 [Adriano, 2001]. The compositions of these minerals within PFA are different depending on the original coal. The main elemental oxides which exist in PFA are (SiO_2 , Al_2O_3 , Fe_2O_3 , CaO). Lignite and sub-bituminous coal PFAs are characterized by higher concentration of calcium and magnesium oxide and reduced percentages of silica and iron oxide. There is a lower carbon content, compared with bituminous coal PFA. Very little anthracite coal (*i.e.* hard coal) is burned in utility boilers, so there are only small amounts of anthracite coal PFA to be dealt with.

Table 2.6: Typical ranges of oxides can be found with PFA in different coal types [Adriano, 2001].

Component	Bituminous	Subbituminous	Lignite
SiO_2	20-60	40-60	15-45
Al_2O_3	5-35	20-30	10-25
Fe_2O_3	10-40	4-10	4-15
CaO	1-12	5-30	15-40
MgO	0-5	1-6	3-10
SO_3	0-4	0-2	0-10
Na_2O	0-4	0-2	0-6
K_2O	0-3	0-4	0-4
LOI	0-15	0-3	0-5

The average trace elemental compositions for PFA are shown in Table 2.7 [Lindon, 2000]. Certain elements are characteristically enriched in PFA particles, especially As, B, Mo, S, and Se. It has been noticed that As, Cd, Cu, Mo, Pb, S, Se, Ti, and Zn concentrations generally increase with decreasing particle size. The main mechanism suggested to be responsible for this phenomenon involves the volatilization of elements during combustion,

followed by condensation on the surface of PFA particles as temperature decreases along the flue-gas path.

Table 2.7: Typical elemental compositions of UK PFA [Lindon, 2000].

Element	Typical range of results mg.kg ⁻¹	Element	Typical range of results mg.kg ⁻¹
Arsenic, As	4-128	Nickel, Ni	35-583
Boron, B	5-310	Phosphorus, P	372-2,818
Barium, Ba	0-36,000	Lead, Pb	<1-976
Cadmium, Cd	<1.0-4	Antimony, Sb	1-325
Chloride, Cl	0-2,990	Selenium, Se	<1-162
Cobalt, Co	2-115	Tin, Sn	<10-1,847
Chromium, Cr	33-192	Vanadium, V	96-1,339
Copper, Cu	33-474	Zinc, Zn	49-918
Fluoride, F	0-200		
Mercury, Hg	<0.01-0.61		
Manganese, Mn	103-1,555		
Molybdenum, Mo	2-81		

2.3.2 Mineralogy and Morphology

PFA chemical compositions are obviously dependant on the coal and inorganic impurities from which it is formed. Minerals dominate the inorganic components of high-rank coals, while organically bound inorganic elements are most abundant in low-rank coal and often exert a strong influence on ash deposition behaviour [Karner *et al.*, 1994]. Generally, PFA is predominantly amorphous glass or carbon but can contain about 11-48% crystalline matter, as shown in (Figure 2.7). The most common crystalline phases are mullite, quartz, hematite, magnetite, anhydrite, tri-calcium aluminate, melilite, merwinite, perclase and lime [McCarthy *et al.*, 1990]. Usually glass and mullite have the largest fractions, 70-90% and 6-15% respectively, of the total ash content [Joshi, 1992].

Morphology describes the micrometer-scale size and shape, chemical data that are necessary to characterise fine grained coal constituents, intermediate combustion products and the resultant by-products. A previous study has used Computer Controlled Scanning Electron Microscopy (CCSEM) as well as inductively-coupled plasma (ICP-MS) for identifying the mineralogy of PFA and the compositions [Georgakopoulos, 1994].

2.3.3 Leachable compounds in PFA

The pH of PFA can vary from 4.5 to 12 depending on the sulphur content of the parent coal. Eastern USA coals that include anthracite are generally high in sulphur and produce acidic ashes while those originating from the western USA that include lignites, tend to be lower in sulphur, higher in Ca and generally produce alkaline ash. Likewise Greece and Poland have high lignite coal. Turkey also follows these countries, as they produce lignite coals and the PFA resulted with high Ca. Moreover, PFAs from western USA coals tend to be with high B content, but are lower in some trace elements (e.g. As, Cd, Co, Pb, Sb, and Zn) than those from eastern coals [Adriano, 2001]. However in Europe countries, the heavy metals concentration in coal are low. The leaching characteristics of PFA are determined by measuring the solubility of the compounds within. Usually PFA is reported as having very low solubility. This is because most of the solid elemental inventory is held within the largely insoluble ‘glassy’ alumino silicate matrix [Adriano, 2001 and Lindon, 2000].

In general, approximately 2% of PFA is soluble and the leachates are dominated by calcium sulphate (Gypsum), which is a naturally occurring

compound found in many soils, with lesser contributions from sodium, potassium and chloride ions. Most of the metals and metalloids present in the ash are either retained in the glass beads or firmly adhered to them, resulting in a very low leaching potential. Alkaline PFA with a pH of typically 9-12 assists in retaining metals.

PFA particles have only a small fraction of the constituents mentioned above present on the surface and they are leachable in water. The major water-soluble constituents are calcium and sulphur (usually present as sulphate). There are small amounts of sodium and potassium, and traces of chloride, magnesium, aluminium and silicon. Most of these constituents are present in small concentrations as soluble species within PFA, so their leachability into water is low (below the data of NRA (National River Authority) extraction test). PFA has no biodegradable organic material and produces no gas as a product of such degradation. When mixed with process water, as in an ash slurry system, the pick-up of trace elements is substantially less than values obtained in a standard leaching test [Lindon, 2000].

2.3.4 Carbon forms

Optical microscopy identifies forms of carbon and includes inertinite, isotropic coke and an isotropic coke [Zhang *et al.*, 2003]. The last two forms are extensively reacted particles, which appear to have passed through a molten stage [McMahan *et al.*, 2002]. Both coke forms are derived from vitrinite macerals and are artifacts of incomplete combustion, while inertinite particles appear not fused. Isotropic coke is considered as graphitisable carbon particles,

while anisotropic coke consists of more highly aligned carbon particles. Both types can be differentiated by the optical activity. Most of the carbon precursors used for activated carbon comes from isotropic, and thus it could be proposed that a high degree of orientation of the carbonaceous lamellae could confer low reactivity of the unburned carbon sample to the activation agent [Zhang *et al.*, 2003]. The surface area is increasing linearly with growing particle density. Carbon forms are expected to have different adsorption behaviour to air-entrainment admixtures (AEAs) on the distinctive physical and chemical properties (density, oxygen and nitrogen concentrations as well as surface area and mesopore volume) [Maroto-Valer *et al.*, 2001].

The LOI restriction is due to the fact that the unburned carbon tends to absorb the AEAs that are added to the cement to prevent crack formation and propagation. However, the ASTM LOI specification is not sufficient to identify the suitability of PFA for the cement industry. This criterion only presents approximately carbon content in PFA, and in many instances, especially for low carbon content in PFAs and flue gas desulphurisation (FGD) residues will provide a poor correlation for the capacity to absorb AEAs [Freeman *et al.*, 1997 and Hill *et al.*, 1997]. It was reported in previous studies that the adsorption behaviour of carbon forms appear differently to AEAs [Maroto-Valer *et al.*, 1999b].

PFA suitability as a pozzolanic additive to concrete depends upon several factors related to its carbon content. However, the utilisation of PFA is determined by properties such as fineness, specific surface area, particle shape, density, hardness, freeze-thaw resistance *etc.* The surface area of carbon is

important for estimating the capacity to absorb AEAs [Linsay *et al.*, 1997]. The adsorption of this chemical agent reduces concrete freeze-thaw resistance specially in winter time, and which dictates the rejection of large amounts of commercial utility ash. The ability of the carbon to absorb AEAs depends upon not only its surface area, but also the accessibility of that area and its polarity. These factors are well-known in activated carbon design *i.e.* the ozonation process [Kulaots *et al.*, 1998]. Consequently, this has led to the identification of a tool to utilise high carbon PFA through this principal, and thus of lower AEAs adsorption capacity [Guo *et al.*, 1997].

2.4 Co-firing of Biomass with Coal

The increasing concentration of CO₂ in the atmosphere is regarded as one of the main man-made causes of global warming. However, there are a few strategies to reduce green house gases which have been suggested, such as improving the efficiency of coal-fired power plants and the substitution of low-carbon fuels for high-carbon fuels. Greater dependence on renewable and nuclear energy sources can offset CO₂ emissions from traditional fossil-fuel fired power plant [Heinzel *et al.*, 1998].

There has been increasing interest in the use of biomass for power generation in recent years. Biomass-coal co-firing represents a more sustainable and green form of energy production as long as the biomass is consumed at less than the rate it grows. The principal reason is that the use of biomass can significantly reduce net CO₂ emissions. However, there are some disadvantages of the use of biomass which relate to its supply, transportation and composition, although

these can be reduced if the biomass is co-fired with coal. Many countries have initiated incentives in recent years to encourage the utilisation of biomass for electricity production, as shown in Figure 2.8. This figure shows the biomass share in electricity production in 2001. Finland had the biggest share (over 10%) of co-firing biomass with coal, followed by Austria, Portugal, and Sweden [Fernando, 2005].

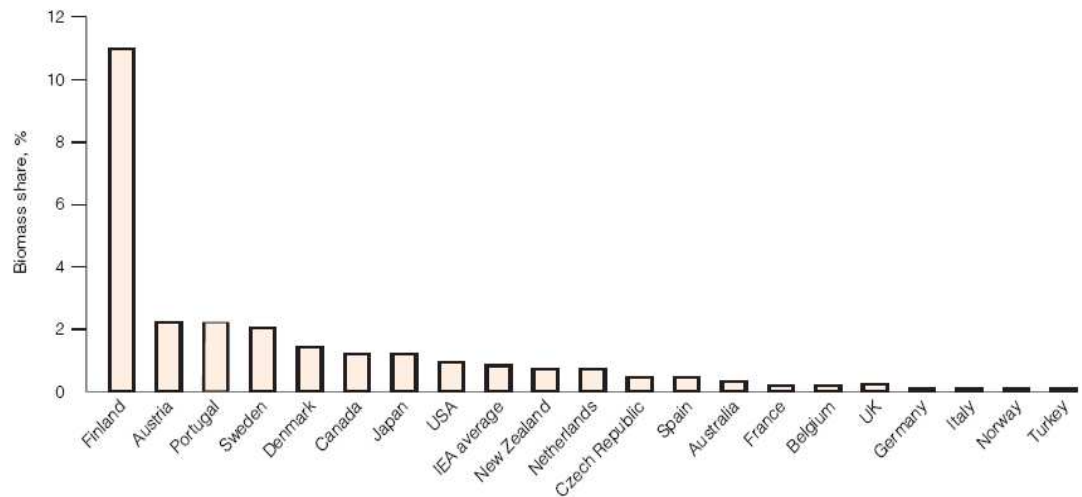


Figure 2.8: Biomass share in electricity production [DTI, 2005].

The biomass share for the UK market was small, but it is expected that it could reach 10% in the near future. Moreover, biomass co-firing provides a relatively low-cost means of increasing renewables capacity and an effective way of taking advantage of the high thermal efficiency of large coal-fired boilers. The use of biomass as a renewable energy source is beneficial to the environment and can make a real contribution to the UK Government's renewable targets and obligation. However, without economic and political incentives it would be difficult to commercially justify the ongoing utilisation of biomass in the UK.

This is because biofuels are generally much more expensive than conventional fuels and have significantly different properties with respect to storage, bulk handling, volume flow, milling, combustion, slagging, corrosion and gaseous emissions [DTI, 2005].

Biomass fuels can be used to generate power from renewable organic sources, including non-recyclable paper, wood scraps, straw, nut hulls, fruit pits and other agricultural wastes. The CO₂ produced by the combustion of biomass fuels is recycled in the process of growing more fuel. Thus, a negligible net amount of greenhouse emissions is produced from biomass combustion. Biomass is also a useful fuel source, because it reuses wastes that would otherwise be uselessly burned or placed in landfill. One of the largest impediments to the widespread use of biomass is its tendency to form unmanageable ash deposits on boiler surfaces. This can cause poor operating performances or boiler shutdown [Heinzel *et al.*, 1998].

2.4.1 Biomass co-firing PFA characteristics

Biomass is a renewable energy source, and is biological material derived from living or recently living organisms, such as wood, plant waste and alcohol fuels. The characteristics of biomass are very different from that of coal. The volatile matter content in wood-based biomass is around 80 wt.%, whereas in coal it is around 30 wt.%. The carbon content (*i.e.* organic matter) as associated with (H, O, N, and S) is showing less than coal. Furthermore, ash content is considerably low (approximately < 10 wt.%) in most biomass fuel. This ash is typically considered the inorganic contents, which mainly includes (Ca, Mg,

Na, Fe, Si, P, Al, K, and Cl) [Veijonen *et al.*, 2003 and Biedermann *et al.*, 2005]. These elements vary between biomass fuels, for example, wood usually shows low in contents, while significantly higher contents are typically found in bark, straw, grasses and grains [Biedermann *et al.*, 2005]. Some of these elements are presented in soluble form (*i.e.* simple inorganic salts) such as S, P, and Cl. Silicon presents as a silica on a precipitated form, whereas the alkaline earth metals are more complex forms [Livington, 2007]. Therefore, biomass materials tend to be associated inorganic species with the organic structure to behave essentially as inherent component of the fuel.

Inorganic constituents can play major issues for biomass combustion especially for aerosols emissions and ash deposition. Aerosols are very small sized particles with diameter $<1\ \mu\text{m}$ and are mainly consisted of alkali and heavy metal salts [Biedermann *et al.*, 2005].

It has been reported that the inorganic content in biomass transforms from the soil into the plant. As a result soil has its rocks originated which lie below the Earth's surface and consequently, the rain washes minerals into it. These washed minerals are evolved from consolidated rocks, sediments, glacial tills and volcanic ash [Birkeland, 1999]. Since, the soil is a complex mixture of minerals and organic material; these contents are built up over billions of years.

Moreover, the dead plants can add a little more organic and inorganic materials to the ground. Thus, all these materials (*i.e.* organic and inorganic) first dissolved in the water and existed in the soil. Later they are absorbed by the plant roots which are essentially for the plant growth life. It also can be found

that these materials (organic and inorganic) are accounted differently between plants due to many factors like soil type, environment, weather conditions and fertilizer [Romero *et al.*, 1996 and Birkeland, 1999].

Accordingly, the inorganic materials were transferred into ash during biomass combustion with some of organic content due incomplete combustion identically similar to coal behavior. Consequently, the determination of the coal ash content is conducted with heating at a temperature of 815 °C, while biomass ash is involved with most of it volatile matter and is carried out at a temperature of 550 °C to avoid the loss of inorganic components [Livingston, 2007].

The behaviour of biomass fuels during combustion regime is working differently. This behaviour is illustrated in their fusion activity. According to Bryers who has described three types of biomass ash under their chemical compositions [Bryers, 1996]. First type contains high silica, high potassium, and low calcium ashes. This type shows low fusion temperatures and could be presented by many agricultural residues. The second type contains low silica, low potassium, and high calcium ashes. This type has presented high fusion temperatures included in most woody materials. The third one has high calcium and high phosphorus ashes and presented low fusion temperatures included in animal wastes and poultry litters [Bryers, 1996].

Ash fusion is related to the biomass fuels behaviour and some types depend on thermal processer. For example, stoker-fired combustors show the sintering and fusion of ash particles on the grates and fluidised bed-fired combustors show sintering, fusion and agglomeration. Moreover, it can be added that the

fusion behaviour plays an important factor in the propensity analyses of the fuels or partly-fused slag deposits on wall surfaces of the combustor [Backman *et al.*, 2005]. Furthermore, it could influence the nature of the fouling deposits that can occur on the heat exchange on the grates and other surfaces.

Consequently, the potential slagging behaviour of biomass-coal ashes are driving differently due to the alkali and alkaline earth metals which are powerful fluxes for alumina-silicate oxides [Miles *et al.*, 1995]. As a result, this will make a reduction in the fusion temperatures, and hence an increase in the slagging activity. This will, of course, relate to the level of flux agents in the coal and on the co-firing ratio [Freeman *et al.*, 1997].

Biomass particle shape districts the fuel conversion in as an easy way like coal particles. Biomass devolatilises in a higher fraction than coal, for example, biomass produces a typical heating rate (dry and inorganic free mass) of 90-95% whereas coal presents 55-60% [Robinson *et al.*, 1997 and 1998]. Biomass fuels and their resultant PFA exhibit more variation in both organic and inorganic (mineral) compositions compared to coal. PFA biomass varies more than coal ash because it originates from woody to herbaceous and other sources.

For a given type of biomass co-fired, the properties of PFA will depend on biomass growth and production factors including weather, season, purity, type, storage and geographical origin [Fouad *et al.*, 1998, Biricik *et al.*, 1999 and Villar-Cocina *et al.*, 2002]. Moreover, it also depends on the biomass waste quality. This applies if it contains heavy metals and the characteristics of the biomass particles [Baxter, 2005]. It can be considered according to different

studies that biomass ashes have more alkali and high LOI than coal ashes [Turn, 2003 and Thy, 2006]. Also, the mineral compositions of biomass ashes with cement mixture are different to coal ashes [Pietersen, 1993 and Ollila, 2004]. High alkali content could result into in concrete cancer (*i.e.* alkali silica reaction ASR) and high LOI ashes have the same effect as that from coal PFAs (*i.e.* insufficient air amount in concrete specimen) and present poor durability.

2.4.2 Biomass co-firing PFA utilisation

Recently, PFA was produced in some coal-fired plants from biomass co-firing with coal, and this PFA is a mixture of biomass and coal ash. It has been mentioned previously that PFA is derived from coal-fired power plant and has been utilised in the concrete industry, to reduce landfill waste and gas emissions. However, the ASTM C618 and EN-450 publications specify the requirements for the PFA used in concrete. Coal PFA is an artificial pozzolan and reacts with calcium hydroxide, in the cement mixture, to produce similar products to cement hydration (Ca-Si gel), which account for the main strength in concrete [Mindness *et al.*, 2002]. The reactions between PFA and calcium hydroxide are called pozzolanic reactions.

Calcium hydroxide contributes only a small portion to the concrete strength, and that is typically the reason why PFA addition can impart more strength to the concrete [Baxter, 2005]. ASTM C618 has excluded the use of co-firing ashes in concrete applications. Alkali and chlorine existing in PFA are often the problematic components. There are components present in certain PFAs (e.g. phosphates), that have a negative effect on the quality of the concrete when biomass PFA is used as a substitute for coal PFA [Jan *et al.*, 2005]. For

example, there are few types of biomass fuel including rice husk, wheat straw, sugar cane bagasse and wood. Their PFAs potentially qualify as mineral admixture according to similar pozzolanic activity to coal PFA [Fouad *et al.* 1998 and Villar-Cocina *et al.*, 2002]. Under these strict rules, PFA is in rapid decline for use in concrete because of issues such as co-firing.

Power plants are currently co-firing biomass with coal up to 5% [Fouad *et al.*, 1998 and Jan *et al.*, 2005]. Thus, the accumulated minerals in the resulted PFA are fairly similar to PFA coal when combusting coal only. Usually, biomass co-firing results in reduced ash deposition relative to coal fuel ash. Relatively, biomass ash accounts for less than coal ash. Therefore, the European Committee has through EN 450 approved the inclusion of PFA from up to 25% straw co-firing with coal in concrete. However, because of the wide range of biomass sources and combustion conditions, the upper weight limit of alkali content, chloride and unburned carbon is restricted to 5%, 0.1% and 5% respectively [Cen, 2005]. It is known from the literature that 1) alkali can react with silica to produce alkali silica reaction (ASR) expansion, which is called “cancer of concrete”, 2) unburned carbon interferes with the air content of concrete, reducing its resistance to freezing and thawing through cracking; and 3) chloride can enhance severe corrosion for steel bars inside the concrete [Swamy, 1994 and Shuangzhen *et al.*, 2007].

Furthermore, some types of biomass ash need more water to mix with cement not like normal coal ash. For example, wood and oat which have been proved in the cement tests and will be regarded in the chapter 4 [Shuangzhen *et al.*,

2008a]. Also, there are some types of biomass ash which do not qualify for concrete applications due to their physical and chemical properties. Therefore, those types could be useful in soil stabiliser, and road surfacing. This could be noted that these types are biomass waste with heavy metals and some other types. Their silica, alumina, and ferrite contents are very low or do not exist and this can fail the concrete structure [Jan *et al.*, 2005].

2.4.3 Co-firing methods

There are three main methods used to co-fire biomass in the power plant. The description of each method as follows:

2.4.3.1 Direct co-firing

In this method, either biomass (secondary fuel) is blended with coal (primary fuel) and then enters the boiler together, or biomass is prepared separately from the coal and then injected with coal in same boiler. This is the cheapest and most straightforward option. However, the differences in the characteristics of two mixed fuels caused problems during milling and in combustion equipment. Furthermore, some types of biomass cannot be processed by this method (for example, herbaceous) [Livingston, 2005], but it can be applied to biomass such as olive/palm kernels or cocoa shells as well as saw dust. It has been considered that direct co-firing is the most popular option for biomass co-firing with coal, practised mainly in Europe [Livingston, 2005].

2.4.3.2 Parallel co-firing

This method is also called parallel co-combustion or co-firing in a hybrid system. In this method biomass is combusted in a separate boiler from coal and

suppliers steam to a common header. There is no possibility of supplying the biomass-combusting boilers with coal, because the fuel preparation and feeding of the two fuels are physically independent [Zuwala *et al.*, 2005]. In a parallel co-combustion configuration the biomass and coal ashes are kept separate. The investment in unit installation and running cost in parallel co-firing is significantly higher than for the direct co-firing method. However, there is a greater possibility of success using this option by keeping separate the firing and ash handling of relatively difficult fuels with high alkali and chlorine contents, as both ashes remain separated. This is an important advantage of this type of installation [Jensen *et al.*, 2001]. Parallel co-firing units are used mostly at power plants operated within the pulp and paper industry.

2.4.3.3 Indirect co-firing

In indirect co-firing the biomass material is either gasified or combusted separately from the coal and the produced gas is injected and burned in the coal boiler. This technique keeps the biomass ashes separated from the coal ashes, while allowing very high co-firing ratios. Furthermore, the investment required for indirect co-firing is lower relative to the parallel option [Zuwala *et al.*, 2005 and IEA, 2000]. The latter two options for co-firing are currently considered to be too expensive for European markets; this was proved by the co-firing experience in the UK [Livingston, 2005].

2.4.4 Implications of biomass co-firing

Biomass co-firing may face many challenges, which include fuel preparation, handling, storage issues, milling and feeding. There is also the behaviour of

fuel combustion to consider and conditions, combustion efficiency, slagging and fouling. Other challenges include ash agglomeration and sintering, pipes corrosion and erosion. There is also the equipment maintenance and working life time, ash utilisation and total economic issues. The carbonaceous material in biomass is considerably lower than coal resulting in a lower calorific value ($< 20000 \text{ J/g}$, compared to coal $> 25000 \text{ J/g}$), but this varies depending on the source of the biomass. Furthermore, biomass fuels are generally accounted with higher moisture compared to coal, and lower contents of nitrogen and sulfur [Khan *et al.*, 2009].

Biomass milling is considered a problematic issue in direct co-firing systems. There are a number of reasons, for example, the coal mill unit has limited capacity while the biomass calorific values are average half to the coal. This can limit the amount of biomass co-milled with coal, and consequently the proportion of biomass co-fired. Moreover, coal mills cannot process certain types of biomass in terms of its fibrous nature [Kiel, 2005].

Generally, these problems are not often faced in indirect or parallel co-firing. Biomass milled independently and delivered by a separate route to the boiler (such as dedicated line could also be fitted to a direct co-firing system). These implications are the result of direct and indirect co-firing systems [Zuwala *et al.*, 2005 and Kiel, 2005]. Mixtures of blended wood with straw cannot be combusted or gasified together in certain equipment, for example in a grate furnace, whereas fluidised bed combustion systems are more fuel flexible, but may face different problems such as bed agglomeration. Biomass from herbaceous biomass is difficult to mill, because of the chlorine and alkali

contents. Potentially these contents can cause corrosion problems and deposit formation. Also, alkali contents can reduce the catalyst deactivation at the selective catalytic reduction (SCR) unit due to the side reactions [Kiel, 2005].

However, wood biomass contains less chlorine and alkali components, which makes this type of fuel preferable as a feedstock. Biomass fuels incur high transportation costs, due to low energy density, and at the biomass delivery point can create problems such as storage, handling, milling and feeding. During co-firing process there could be slagging, fouling, etc. and dealing with ash utilisation issues. Moreover, there are non-technical constraints related to biomass co-firing such as legislative aspects or negative public perception, but these vary from place to place.

Additionally, biomass has three main undesirable properties relative to coal. It is bulkier than coal, contains more volatiles and has higher moisture content. Biomass degrades more quickly than coal, meaning that it cannot be stored on-site for a long period of time [DTI, 2005]. This requires that a co-milled mixture of biomass and coal must be prepared shortly before the fuel is to be fired or else the quality of the feedstock will be affected by the degradation of the biomass. The calorific value of the biomass is also an important factor in maintaining plant output. The lower density biomass may require a greater volume to be milled in terms of producing the fuel input. It is also important that the moisture content of the biomass is as low as possible. Biomass with higher moisture content can cause an adverse effect on the fuel combustion performance inside the boiler, and may require greater treatment prior to

combustion. Corrosion impact is higher due to the high chlorine and alkali content of biomass fuels [NREL, 1998]. This problem can be reduced by selection of low chlorine biomass fuels and by reaction of the alkali chlorides with sulphur contained in the fuel to form less corrosive alkali sulphates and hydrochloric acid.

2.5. PFA beneficiation

2.5.1 Residual carbon in PFA

The residual carbon was increased in PFA for the last few years under the stringent Clean Air Act Regulations and using alternative fuel like biomass. These regulations were implemented in order to reduce NO_x emissions. This excessive carbon in PFA is a serious issue in terms of being unsuitable for cement industry. There are environmental impacts from keeping this unsalable PFA into landfill and it also reduces market opportunities. Variable or unacceptable carbon contents adversely affect ash utilisation. Consequently, there is a need to remove this unburned carbon from PFA streams, ideally completely or at least to the acceptable level suitable to other industries (*i.e.* cement). Carbon removal from PFA stays an issue in UK and worldwide according to the accumulation of large amounts of this by-product. Therefore, there is a possibility of increasing landfill tax in future to overcome this problem from using more land to store it [Hamley *et al.*, 2001 and Maroto-Valer *et al.*, 2002a]. Moreover, the increasingly severe regulations on disposal may demand the utility industry to begin offsetting coal combustion with natural gas, or utilising the unburned carbon in PFA into value added products.

2.5.2 High unburned carbon PFA

High unburned carbon PFA could be utilised into PFA with low percentage of unburned carbon (<5 wt.%) as a cement admixture and high enriched unburned carbon either recycle as a fuel or as adsorbent material. The physico-chemical properties of the carbon play an important role in each of these applications. Previously, it was reported that this unburned carbon was used as a carbon precursor which had been activated [Yangkyu *et al.*, 1998 and Maroto-Valer *et al.*, 2002a].

The activated carbons have been used as adsorbent materials in a broad range of increasing household, medical, industrial, military and scientific applications, such as household air conditioning equipment, industrial emissions control, water treatment and even gold recovery. The commercial activated carbons were manufactured from different sources such as hard coal and biomass (*e.g.* nutshells) [Patrick, 1995]. The conventional production of activated carbons consists of a two-step process, which includes a devolatilization of the raw materials, followed by an activation step. In contrast, unburned carbon (*i.e.* sourced PFA) requires only a one-step activation process, since it has already gone through a devolatilization process while in the combustor [Bansal *et al.*, 1988 and Maroto-Valer *et al.*, 1999a]. These applications will be discussed in details in sections (2.5.3 and 2.6).

2.5.3 PFA beneficiation processes

Beneficiation processes could add benefits such as emissions reduction and converting PFA with high carbon content into value-added products. However, the utilising of high carbon PFA can significantly enhance the marketability of

PFA and add more revenue from selling carbonaceous products [Derbyshire *et al.*, 1995 and Maroto-Valer *et al.*, 1999a]. As stated in previous sections, the carbon concentration in PFA was increased over 7% (*i.e.* acceptable value) according to the LOI measurement and made it unsaleable product. The possibility of utilising this PFA by separating the unburned carbon from PFA and make it suitable for the cement industry. PFA beneficiation aims to separate the unburned carbon from PFA and produce PFA with Low LOI value (*i.e.* <7%) and high enriched carbon. There are different processes for separation, such as separation technologies Inc. (STI's), wet separation (froth floatation), air flotation, thermal treatment (carbon burn-out), and combined processes. The main processes applied commercially like STI's, froth floatation, and carbon burn-out.

The efficiency varies depending on the conditions applied and many other factors. There are equipment design, the consistency of the input and the output after the separation, speed of separation, the physical and chemical of the PFA, and finally the residual carbon in the PFA [John *et al.*, 1999, James *et al.*, 2001 and McMahan *et al.*, 2002]. Basically, each process is fed with high carbon PFA and then two streams are produced: one is depleted carbon PFA (LOI<7%) suitable for cement application, and the second is enriched carbon (LOI >90%) with very a low percent in ash except thermal treatment as it produces depleted carbon PFA.

Furthermore, the above processes can be classified as methods which not expose the carbon from PFA such as electrostatic separator-STI, wet separation and air flotation and other methods which expose the carbon from PFA such as

carbon burn out. Two methods are discussed below: carbon burn-out and combined process. Consequently, this project used microwave process and air flotation to beneficiate high carbon PFA samples, as discussed in section 3.4.

2.5.3.1 Carbon burn out

Carbon Burn-Out (CBO) process combusts PFA with high carbon, and produces a premium quality PFA that can be readily sold to concrete ‘‘ready-mix’’ facilities. In addition, heat from the process is recovered and returned to the host power plant, making that plant more efficient and resulting in less coal consumption (*i.e.* lower emissions). As a direct result, approximately 400,000 tonnes of PFA is recycled per year from these facilities instead of placed in landfills, and approximately 320,000 tonnes per year saved in CO₂ emissions [Keppeler, 2003]. A CBO plant designed in South Carolina at the Wateree station to process 180,000 tonnes per year, see Figure 2.9 [Fredy *et al.*, 1999].



Figure 2.9: Carbon burn-out unit at Wateree station in South Carolina

[Fredy *et al.*, 1999].

2.5.3.2 Combined processes

Combined beneficiation processes have been employed in stages to produce cenospheres, iron oxide microspheres, carbon component and low carbon PFA.

A flow diagram of the combined processes is shown in Figure 2.10. The gravitational separation process separates cenospheres which are composed of low density hollow spheres. A magnetic separation step then separates iron oxide and iron silicate spheres from the ash. Finally, a froth flotation process is used to recover the unburned carbon. The depleted carbon PFA produced which consists of the silicate sphere component [Hwang *et al.*, 1995a and 1995b].

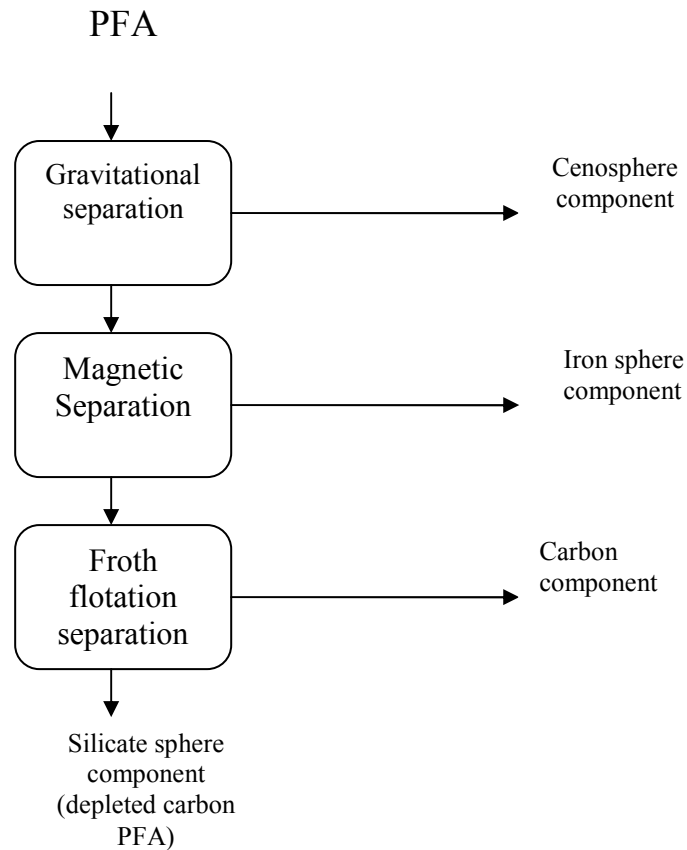


Figure 2.10: Separation schematic for PFA beneficiation process [Hwang *et al.*, 1995a].

It has similar stages to the RockTron process that applied one of the power plants in UK. The RockTron method is used to beneficiate different sources of PFA (dry, stockpile, and lagoons). It produces different quality of PFA such as magnetite PFA (*i.e.* high Fe), delta PFA (*i.e.* coarser particles type-1), and alpha PFA (*i.e.* finer particles type-2). These types of PFAs are classified according to the carbon content, minerals content, and fineness to suit cement constituents [Smalley *et al.*, 2004].

2.6 Carbon activation

Carbon activation is a process conducted to produce carbons with high degree of porosity and produce activated carbons with large surface area. Activated carbons can be derived from different sources including coal, municipal solid waste, oil, biomass etc. The activation processes are carried out either by physical or chemical conditions. The carbon quality depends on the method used, the porosity and the surface area produced. Consequently, the activated carbons are predominantly used as adsorbents according to the porosity texture. The pores in the activated carbon show different dimensions include micropores up to 2 nm, mesopores from 2 to 50 nm, and macropores above 50 nm, and thus it could be accessed by a different range of molecules [Rodriguez-Reinoso, 1997].

During the activation process, the carbon burn-off increases linearly with the activation time. Also, the activation rate (*i.e.* yield) increases when the activation temperature increases. Previous studies show that the activation rate at 900 °C is three times higher than that achieved at 800 °C for palm shell char.

Another study reveals work was conducted on coconut char, which presented similar results (*i.e.* activation rate) in that temperature [Bansal *et al.*, 1988].

Pores are developed during the activation process and their dimensions change significantly according to the activation method used, conditions applied, and carbon types. The carbon activation is depending on many factors including activation method, conditions applied, carbon porosity, carbon reactivity, and inorganic content. Furthermore, the adsorption capacity of the activated carbon depends mostly on the presence of micropores on surface area. It has been reported by Rodringuez-Reinoso [Rodringuez-Reinoso *et al.*, 1992] that the micropore volume increases when the burn-off increases almost linearly and this study conducted on a peach stone. Tomkow (1977) found that this change occurred similarly in brown coal. With regards to the effect of activation, this case is not always followed by the same pattern [Maroto-Valer *et al.*, 2001] as different carbon types were observed differently.

The pore volume reflection is followed similar way as the total surface area for the carbon pores [Zhang *et al.*, 2003]. It has been shown in previous studies that the carbon sources from high carbon PFA samples need one stage activation compared with the carbon source from either coal or biomass fuels [Maroto-Valer *et al.*, 1999a and 2002a]. This is according to the carbon, as it has been devolatilised during the combustion process. It is different from the carbon separated from coal and biomass fuels with no heating which has been conducted. Accordingly, this project uses a physical process to activate the enriched carbon samples. The porosity of these carbons is clearly developed

from microporous into meso-porous where they behaved differently, as discussed in the carbon activation section 3.6.

2.6.1 Carbon activation methods

Physical and chemical activation methods are industrially implemented to produce activate carbon. Physical activation uses steam at temperatures ranging from 800-1000 °C in order to gasify the carbon (*i.e.* char). This char is either separated or obtained by carbonization of the precursor. The purpose of this method is to enlarge the pores (*i.e.* maximum) by gasifying the carbon [VonKienle, 1986 and Baker *et al.*, 1992]. Chemical activation takes place in four stages including dehydrating agents such as ZnCl₂, H₃PO₄, KOH *etc.*, heating the mixture up to 600 °C, impregnating the precursor, and intensive washing to remove the chemical. Further information can be found in section G.2-appendix G.

Carbon precursor can be derived from different sources such as wood (saw dust), lignite, fibre, and cloth [VonKienle, 1986 and Baker *et al.*, 1992]. The disadvantages can be raised from the chemicals (*i.e.* hazardous) used for washing the carbon sample, the chemical waste generates after washing, and the operation is too costly. Therefore, physical activation was a more preferable method compared to the chemical [Jankowska *et al.*, 1991].

The selection of carbon materials for manufacturing activated carbons have subjected to different categories. These include a low content of inorganic matter, affordable and not costly, high yield, the percentage of degradation

which is low upon in storage. Also, the activation process should run easily like wood char but not like calcined coke [Marsh *et al.*, 1989]. There are different carbon precursors used for manufacturing carbon activation with different properties and the expected porosity yield after the activation process [Pastor *et al.*, 1999], as listed in Table 2.8. This table presents biomass fuels with low carbon content compared to coal types. Moreover, the volatile matter higher for biomass than coal and ash content for biomass is lower than coal. The density is generally lower for wood compared to coal types.

However, many countries have preferred to use hard coals as a carbon precursor, because the raw material is not expensive. It is more affordable, low moisture, and high carbon compared to other types of coals [Patrick, 1995]. Moreover, the porosity decreased when the coal rank increased and because more hard and dense compared to other types of coals which are softer, high in moisture and not denser.

It is more interesting that nutshells can produce a large micropore volume compared with other raw materials (Table 2.8). It is more important to know the source of the activated carbon, pore volume or the surface area, and ash content in order to choose the right type to conduct the right process, even more which activation process can be applied to get a good yield of activated carbon from this raw material.

Table 2.8: Raw materials characterisation properties as a precursor for activated carbon [Patrick, 1995].

Raw material	Carbon wt. %	Volatile matter wt. %	Density $\text{cm}^3 \cdot \text{g}^{-1}$	Ash wt. %	Texture of activated carbon
Soft wood	40-50	55-60	0.4-0.5	0.3-1.1	Soft, large pore volume
Hard wood	40-42	55-60	0.55-0.8	0.3-1.2	Soft, large pore volume
Lignin	35-40	58-60	0.3-0.4	-	Soft, Large pore volume
Nutshells	40-45	55-60	1.4	-	Hard, large micropore volume
Lignite	55-70	25-40	1-1.35	5-6	Hard, small pore volume
Soft coal	65-80	20-30	1.25-1.5	2-12	Medium hard, medium pore volume
Pet coke	70-85	15-20	1.35	0.5-0.7	Medium hard, medium pore volume
Semi-hard coal	70-75	10-15	1.45	5-15	Hard, large pore volume
Hard coal	85-95	5-10	1.5-1.8	2-15	Hard, large pore volume

CHAPTER THREE

EXPERIMENTAL PROCEDURES

3.1 Introduction

This chapter presents the experimental procedures followed to develop high value of PFA. The approach taken was to beneficiate high carbon PFA samples to produce two streams: a depleted carbon PFA suitable for cement tests and an enriched carbon PFA for activation. This chapter has four parts: firstly, the characterisation techniques conducted on PFA samples which are presented in Table 3.1, the second part describes the PFA beneficiation processes used, while the third part includes cement tests and mineral analyses for the depleted carbon PFA. The final part explains the carbon activation procedures and adsorption activity tests conducted on the carbon rich samples.

Additionally, the outcomes of the various techniques applied to ascertain the optimum of PFA beneficiation and carbon activation are reported and discussed in the following chapter.

3.2 Samples procurement

Sixteen PFAs were received from different power plants and derived from different fuels (biomass and coals). The PFA samples are presented in Table 3.1. It can be seen that the samples are named with C. It illustrates how these samples are derived from coal. The samples are named with B, resulted from biomass co-firing. It is important to know that B1 sample was derived from sunflower co-firing with Russian coal with ratios 7 wt.% and 93 wt.%, respectively, while B2-B6 samples derived from oat co-firing with Russian coal with ratios 5 wt.% and 95 wt.%, respectively. Moreover, these PFAs were

sampled differently as presented in Table 3.1. It is important to mention that the PFA coal samples were derived from different import coals. PFA co-firing samples and PFA coals were collected from different devices and received from different power plants. These PFAs were sampled in different dates and times.

Table 3.1: PFA samples and characterisation works.

Sample	Sampling point	Fuel type	Characterisation works	Beneficiation	Activation	Cement and adsorption
Power station 1 (P.S.1)						
C1	Electrostatic precipitator	Coal				
C2	Mechanical separator	Coal				
B1	Electrostatic precipitator	Biomass co-firing				
Power station 2 (P.S.2)						
C3	Electrostatic precipitator	Coal				
C4						
C5						
C6						
C7						
C8						
Power station 3 (P.S.3)						
C9	Electrostatic precipitator	Coal				
C10		Coal				
B2		Biomass co-firing				
B3		Biomass co-firing				
B4	Economiser	Biomass co-firing				
B5		Biomass co-firing				
B6	Electrostatic precipitator	Biomass co-firing				

This colour shows ESPs precipitator
 This colour shows mechanical separator

This colour shows economiser
 This colour shows coal source

This colour shows biomass co-firing source
 This colour shows the chosen sample

3.3 Samples characterisation

PFA samples were received from three power stations (P.S.1, P.S.2, and P.S.3). The samples in those power stations collected from different devices and derived from different fuels. They were initially characterised in terms of their carbonaceous content, surface area measurements, ultimate analyses, microscopy studies and particle size distribution.

3.3.1 Thermogravimetric analyses (TGA)

Thermogravimetric analyses were conducted for both LOI and proximate analyses using SDT-TGA 600. These analyses were performed to calculate unburned carbon content (*i.e.* LOI), moisture, volatile matter and ash content. The intention of the first experiment is to identify the LOI value for these samples. The reason for conducting LOI analyses is to find high carbon PFA samples. One has to establish which has higher LOI in order to use these samples in the PFA beneficiation. Moreover, proximate analyses were conducted because of the relevant information collected and therefore could incorporate them in the following analyses. Consequently, thermogravimetric analyses were done in a preliminary stage to obtain mainly the values shown above and translate them for the PFA beneficiation stage. The principles of these analyses are described below.

3.3.1.1 LOI analyses

LOI analyses conducted in duplicate following ASTM C311 in order to calculate the unburned carbon content. Typically around 20 mg of sample was heated from room temperature to 105 °C under air at a flow of 100ml.min⁻¹. It

was then held there for 30 minutes to remove the moisture. The sample was then heated to 805 °C at a heating rate of 50 °C.min⁻¹. The final step was to hold the sample isothermally for 35 minutes at 805 °C. The LOI content was then calculated from the weight loss of the sample Equation 3.1 [ASTM C311, 2006], and the average values are then reported.

$$\text{LOI} = \{(W1-W2)/W1\} * 100 \quad (3.1)$$

W1= Weight of the sample in dry basis (no moisture) (g)

W2= Weight of the sample at the end of the experiment (left) (g)

3.3.1.2 Proximate analyses

The proximate analyses were conducted in duplicate. These analyses measured the moisture content, fixed carbon, volatile matter and ash content. Firstly, around 20 mg of sample was heated up to 105 °C using a flow of nitrogen at 100 ml.min⁻¹ to determine the moisture content. The temperature was then ramped to 805 °C and held isothermally for 45 minutes to determine the volatile matter. The sample was then held isothermally at 805 °C for 85 minutes under a flow of air at 100 ml.min⁻¹. As a result the carbon started to combust, and thus the fixed carbon was measured. Finally, the sample was cooled to 30 °C using a flow of nitrogen at 100 ml.min⁻¹ and the remained weight was reported as the ash content.

3.3.2 Ultimate analyses

The carbon, hydrogen and nitrogen contents of the study samples were measured using a Flash EA 1112 Series- element analyser. The determination

of carbon, hydrogen and nitrogen was made by burning a weight quantity of sample around 2 mg in pure oxygen at ~ 950 °C. A thermal conductivity cell was used for measuring the remaining elemental nitrogen. At the same time as the nitrogen measurement, the carbon and hydrogen infrared cells measured CO_2 and H_2O levels. These analyses were conducted in duplicate runs and the results for each element are calculated in average basis. The results for the three elements are displayed in weight percent. It is important to point out that the sulphur element has not been measured due to very low content in these PFAs, the difficulty to detect any sulphur by this instrument, and most power plants burned lower sulphur coals [Woolley *et al.*, 2000].

3.3.3 Porosity studies

The porous texture of the PFA samples was characterized by conducting N_2 adsorption isotherms at 77K using a Micromeritics ASAP 2000. Around 0.1 g of sample was placed in a tube to degas of approximately 1-2 hours in order to remove moisture completely. This moisture can cause error during the analyses. The sample tube was then transferred from the degas port to the analyses port. For the Brunauer, Emmett and Teller (BET) [Brunauer *et al.*, 1940] surface area ten points were required in the relative pressure P/P_0 ranged from 0.1-0.25 and then it calculated according to the BET equation 3.2 [Patrick, 1995]. For the BJH adsorption-desorption method [Barrett *et al.*, 1951], thirty three points were used in the relative pressure P/P_0 from 0.025-0.8. The purpose of this method was to calculate the mesopore (pores 2-50 nm in width) and micropore (<2 nm in width) volumes. Also, the total volume V_T was measured from the isotherm graph at relative pressure 0.95.

$$S_{\text{BET}} = V_m L \sigma \quad (3.2)$$

Where

S_{BET} = surface area ($\text{m}^2.\text{g}^{-1}$)

V_m = amount of gas required for monolayer coverage of adsorbent (mmol.g^{-1})

L = Avogadro's number ($\text{molecules.mol}^{-1}$)

σ = projected area of adsorbate molecule ($\text{m}^2.\text{molecule}^{-1}$)

3.3.4 Particle size distribution (PSD)

Particle size analyses were conducted using a Malvern Mastersizer S type. Approximately 1 g of sample was placed in a cylindrical tube (stainless steel) filled with liquid to disperse the sample and a small stirrer agitated the particles. It is important to point it out that the liquid should not react with the sample because it can cause error in the particle size measurement. This experiment was carried out with two dispersion liquids (water and isopropanol (IPA)) for all the samples listed in Table 3.1.

A laser beam was applied to sense the particle movement and measure the particle size. This analysis was repeated four times for each sample and the results presented here are the average of the four runs. The purpose of this analysis was to measure the particle size which is required in the beneficiation process (*i.e.* particle size difference) and other analyses (*i.e.* the presence of coarse and fine materials).

3.3.5 Microscopy and X-ray studies

This section describes the different techniques applied for the PFA samples such as scanning electron microscopy (SEM), energy dispersive X-Ray (EDX), and X-ray diffraction (XRD). The aim of these studies is to collect information regarding the particles shape and elements concentration. The procedure of these studies is described below.

3.3.5.1 Scanning electron microscopy (SEM) and Energy dispersive X-Ray (EDX)

Scanning electron microscopy for the PFA samples was conducted using a Quanta 600. The Quanta 600 SEM produces enlarged images of a wide variety of specimens, using magnifications usually from 100x to about 100,000x.

A small amount of PFA around 1 g was fixed onto aluminium pin-type stubs using double sided carbon sticky tabs. This was achieved by sprinkling a spatula end full of sample onto the carbon tab until the tab was just covered. Excess sample was removed from the tab using a gentle jet of air. The prepared samples were stored in desiccators. The samples were then introduced into the chamber of the Quanta 600 SEM. Low vacuum mode was used as the samples were of a non-conducting nature. An accelerating voltage of 25 kV was selected. All imaging was performed using a solid state backscattered electron detector (BSE). EDX studies were conducted simultaneously using same instrument to determine elements concentration. The error is ranged approximately $\pm 5\%$.

3.3.5.2 X-Ray diffraction (XRD)

These analyses were conducted to identify the crystallinity of the minerals contented with the PFAs. XRD studies were carried out on a Hiltonbrooks 3 KW generator model DG3. The conditions applied in the XRD studies were scan speed of 2 degrees 2-theta per minute and a step size of 0.05.

X-ray powder diffraction specimens should be flat, densely packed, very fine-grained powders. This was achieved by pressing the sample powder into a cavity without causing preferential orientation of the crystallites. The amount of the sample used was around 1 g.

The method used included taping a flat piece of clean glass over the upper surface of an aluminium cavity holder, so as to cover the rectangular window. The cavity holder was then inverted and placed so as to overfill the cavity. The powder flat was gently pressed and the excess material from the edges of the window was removed. The chromed 'base piece' was clipped in place, inverted and the taped glass was gently removed. This made a flat densely packed cavity from the sample powder without any cavity. Each cavity mount was numbered and placed in the relevant position inside a 36 position sample holder magazine, ready for XRD analysis.

3.4 PFA beneficiation

The outcomes of the samples characterisation could consequently be used to establish PFA beneficiation. It appeared, there are five samples (B5 and C2-C6) classed for PFA beneficiation. This is because of LOI values of these PFAs showed over the acceptable limit of cement applications as it reported previously. Two methods were selected to beneficiate high carbon PFA

samples; incipient fluidisation and thermal treatment (*i.e.* microwave). Five samples (B5 and C2-C6) were proposed for the incipient method, while two samples (B1 and B3) were used for the microwave method. The concepts of each method are described below.

3.4.1 Microwave treatment (vitrification)

Microwave treatment was selected as a type of thermal treatment to remove unburned carbon from high carbon PFA samples. This is a new technique applied to utilise high carbon PFA that derived from biomass co-firing. This treatment was conducted only on two PFA samples (B1 and B3). This method was applied in order to see how the vitrification process works out on these samples from removing the unburned carbon and the size reduction. The experiment started by placing 90 g of sample in a microwave. The power used was 3 KW for 8 minutes, and the temperature reached 1250°C. High power energy was carried in this treatment which could play a good sign for removing the unburned carbon from PFA.

3.4.2 Incipient fluidisation

The incipient fluidisation process was selected as a physical treatment with no reaction occurred during the carbon removal to beneficiate high carbon PFAs. The error is ranged for LOI measurements approximately $\pm 8\%$. The apparatus of this process is presented in Figure 3.1. This process was carried out on five samples (B5 and C2-C6). As mentioned above, these samples were presented higher LOI values according to the TGA and the particle size different is high, thus they were selected to conduct this process.

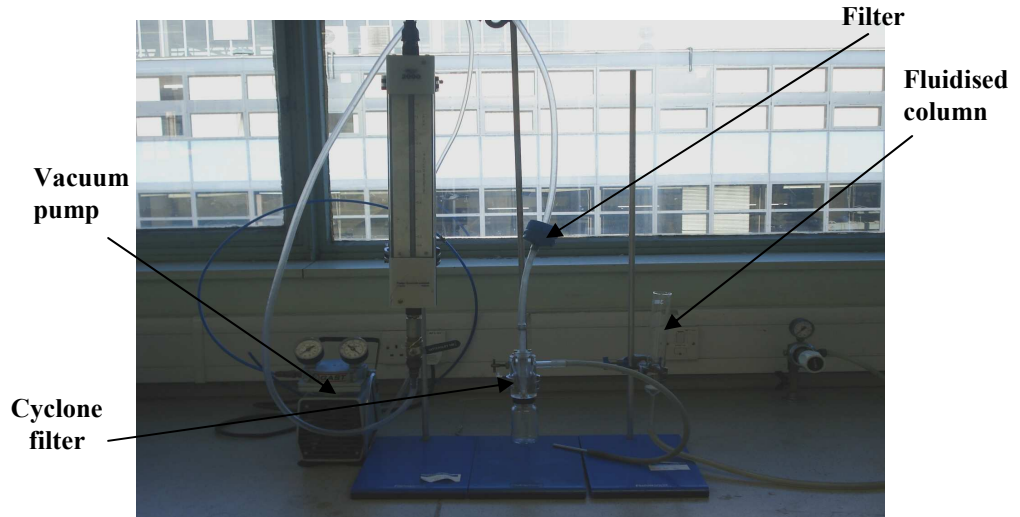


Figure 3.1: Incipient fluidisation apparatus used for PFA beneficiation.

This technique segregates carbon rich particles from mineral-rich particles on the basis of density. The height of the fluidised bed column, shown in Figure 3.1, is 28.5 cm, the inside diameter is 3 cm, and the height of PFA bed ranged from 2-5 cm. A vacuum pump was used to pull the fluidised particles from the fluidised column. These particles were delivered into cyclone filter to collect the coarse ones from the bottom and the fine ones through the top filter, as shown in Figure 3.1.

Basically, 20 g of sample placed inside the fluidised bed column, and then was introduced from the air supply at a flow rate $0.1 \text{ (l.min}^{-1}\text{)}$ fed into the bottom of the bed, as shown in Figure 3.1. The flow rate was kept low in order to generate very smooth particle motion, while avoiding large-scale bed flows that lead to macro-mixing and homogenisation of the sample. Capillary suction employed from a vacuum compressor under pressure applied 430 mmHg and the air flow rate was approximately $10 \text{ (l.min}^{-1}\text{)}$. This capillary suction was

removed the bubbled particles (*i.e.* darkest) and then introduced them into a cyclone filter, where the coarse carbon rich particles dispersed down into a vessel, and the finer particles (*i.e.* white/gray) were removed through the top of the cyclone and collected by a filter, as shown in Figure 3.1.

This process produced two streams depleted carbon PFA and enriched carbon PFA denoted with –d and –e, respectively. This process was repeated four times in every sample for better separation and also followed by dry sieving process under sizes (45 μ -250 μ) for both streams. The purpose of applying dry sieving afterward was helped to remove more carbon (*i.e.* especially fine materials). Previous study had shown the incipient fluidisation presented around 60% of carbon removal by itself [Hurt *et al.*, 1994], and this number might change according the LOI value and the particle size difference. The duration of this process was approximately 30 minutes to beneficiate the placed amount referred above.

The cost of implementation is not high for large scale. Furthermore, the coarse material for each sample can be reverse back to the separator with more added sample to achieve a better separation. However, if the material is coarser (*i.e.* thick), then it may be better keep it separately, which can subject as aggregate material for example. Finally, the waste produced from this method is low, but it will depend on the sample properties.

Other observations took place during the operation like particles size and agglomeration, dust problem, filters blockage and noise problem.

3.5 Cement tests

These tests were conducted on the beneficiated samples (C2d, C4d and B5d) which produced from the incipient fluidisation (*i.e.* depleted carbon stream). The suffix d denotes that this sample was depleted carbon. These samples were mixed with cement into two ratios 5% and 10%. Also, air entrainment agent was added in each mixture in order to examine the concrete blocks strength after carbon removal. The error of these tests is in the range of $\pm 3\%$. Typically, six cubes of 100x100 mm were prepared with 5% and 10% PFA. The mix details of each cube 5% and 10% are shown in Table 3.2.

Table 3.2: Mix details of each cube for 5% and 10% Cement/PFA.

Material	kg-(5%-mixture)	kg-(10%-mixture)
Cement	1.79	1.7
Coarse aggregates	6.86	6.86
Fine aggregates	6.3	6.3
PFA	0.098	0.189
H ₂ O	1 litre	1 litre
AEA	9.5 ml	9.5 ml

The measured amount of each material as specified in Table 3.2 was placed in the mixer and then the water was added last in order to produce homogenous mixture. For C2d and B5d samples were mixed under 10% with cement, while C4d sample was mixed in 5% with cement.

After the mixing, the concrete was placed in cubes size 100 mm x 100 mm. Six cubes were made from each sample for these tests. Afterward, these cubes were

placed in a water bath at temperature $\sim 22^{\circ}\text{C}$. Cement tests were conducted for these cubes after 7 days and 28 days. These tests were took place on concrete test instrument type (GD-10) shown in Figure 3.2. The cube was placed in a square foot controlled by a piston from the top. This cylindrical piston applies weight load on the cube in order to measure the load capacity. Two measure scales are presented in this instrument, top one show the load in N and bottom one in kN.

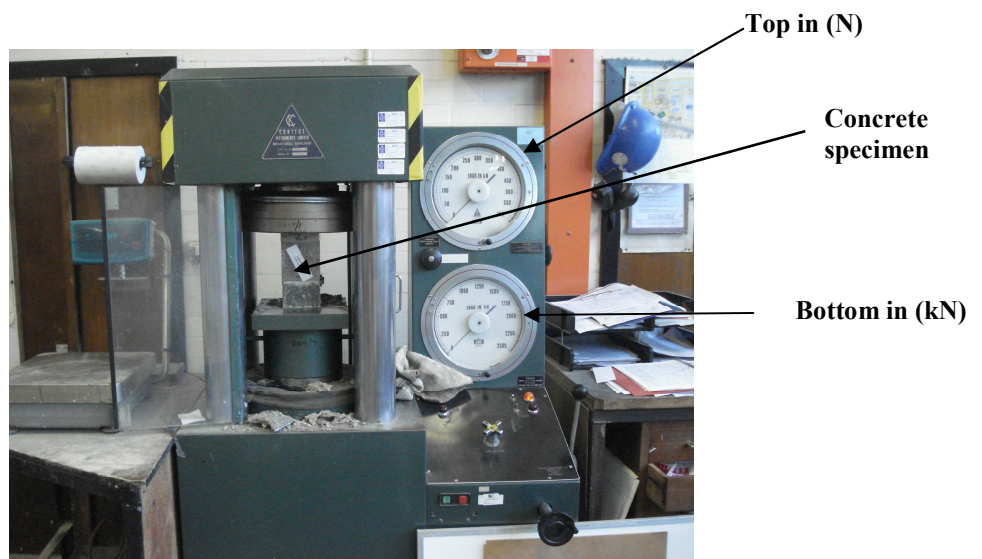


Figure 3.2: GD-10 compression strength tester.

The test illustrates through applying a certain load until the device starts to beep. Then, the final reading is presented to explain the maximum strength resisted by this cube. These readings were recorded for four runs and then presented in average basis for all the samples.

3.6 Carbon activation

The carbon activation experiments were conducted on the enriched carbon streams (C2e, C4e and B5e) produced by incipient fluidisation. The suffix e

denoted that this sample was enriched carbon. The resulted samples after activation were denoted with a. The activation system used for the steam activation is presented in Figure 3.3. Obviously, the purpose of this process is to produce activated carbon which is separated from high carbon PFAs. The furnace length is 670 mm and 85 mm inside diameter. The quartz tube that passed through the furnace is 1000 mm long and 60 mm inside diameter.

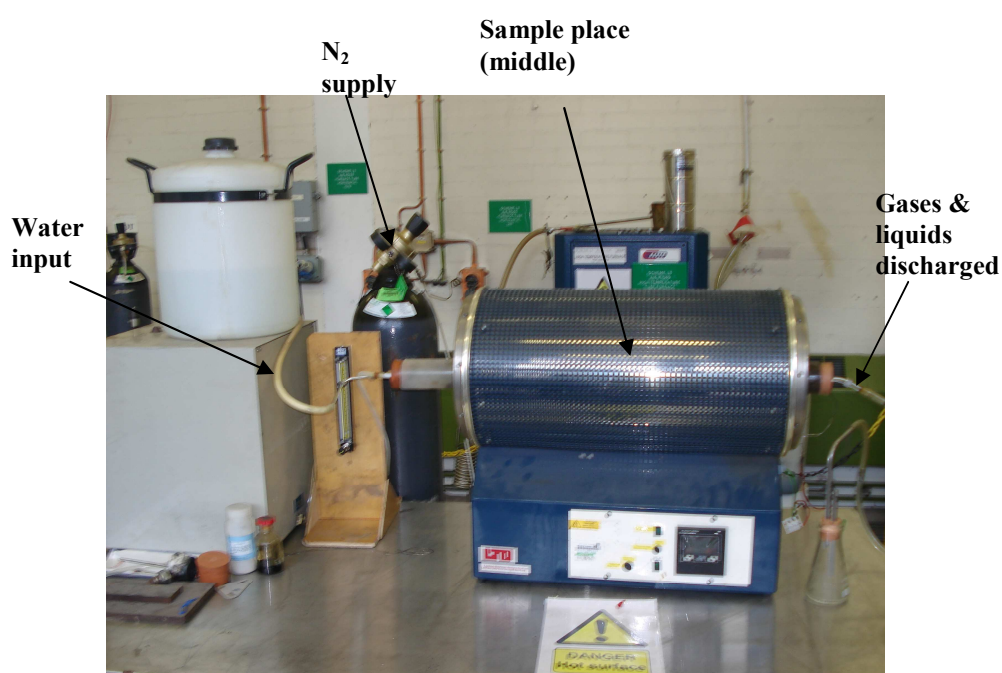


Figure 3.3: Photo of steam activation system.

Typically 2-3 g of sample was placed inside the furnace in a silica boat. The distance from the entry part into the furnace to the silica boat is 450 mm. N₂ gas was firstly passed at 150 ml.min⁻¹ to achieve an inert atmosphere. After 30 minutes, the furnace was heated to the desired activation temperature under a flow of N₂ gas in order to keep an inert atmosphere. A thermocouple was used to monitor the furnace temperature placed underneath the quartz tube.

When the sample reached the desired activation temperature, a flow of deionised water was introduced into the furnace at 8 ml.min^{-1} to generate steam for the activation. The water flow was introduced by gravitational force as the water tank was kept at a higher level than the furnace (Figure 3.3). The steam was swept through the furnace by the flow of N_2 gas. During the activation, liquid and gas products were swept from the pipe outlet into the liquid collector (vessel) as shown in Figure 3.3. After a certain activation period, the feeding water into the furnace was stopped and the heating was shut off. The heating temperature was set at 850°C and activation periods from 60-300 minutes were used.

3.6.1 Calorific value

The calorific value (CV) was measured for enriched carbon streams separated from high carbon PFAs (C2e, C4e and B5e). This experiment was conducted using a calorimeter KA C5001. Around 1.2 g was placed inside a vacuum bomb and the starting fire was ignited by a thread wire. The sample was then ignited using an electric shock supplied with O_2 gas under pressure 30 bars, and thus, the sample started to burn. The software programme in the instrument was calculated to change the temperature of the sample every minute for up to 20 minutes. The calorific value of the sample was reported at the end of the experiment. This calorific value was measured as a received basis (asr). The error was estimated in these values around $\pm 5\%$.

3.6.2 Optical microscopy (Automated analyses)

Optical microscopy studies were conducted for carbon rich samples and the resultant activated samples. The rich samples are (C2e, C4e and B5e) and the activated (C2a, C4a and B5a). The activated samples selected were these produced at 60 minutes and 120 minutes activation. The purpose of these analyses was to understand the possible change in particles morphology due to activation and any variation in carbon types. These analyses report the particles shape and size, wall structure, carbon types, carbon source and minerals type. This experiment consisted of two steps as described below.

A) Blocks preparation:

A set of pans suitable to place the selected samples were prepared. Around 0.2 g from each sample was placed as a first layer, and then second layer of epoxy resin was placed with a weight of around 5 g. This second layer was accomplished with only 25% in volume from the pan. These blocks were placed in a vacuum of 200 mbar for 30 minutes to remove any bubbles that occurred between the layers. A final layer of epoxy resin was placed with a weight around 8 g and occupied the rest volume of the pan (*i.e.* 75%). These blocks were then left to dry for about six hours.

Then, they were polished using grinding paper sizes 600, 1200, and 2400 and water wash was conducted with every grinding. The reason for block polishing was to remove any cracks, to get smoothness and to obtain better images. This step took around one hour and then these blocks were polished again with paper size 4000 and washed with colloidal silica. Afterwards, they were

washed again with water to remove any colloidal silica left which could affect the images taken. The duration was around 20 minutes which meant the blocks were now ready for taking images.

B) Taking images

The step used a coal analyser type KS 400 in order to analyse the blocks. A sample block was placed on stand under the microscope lenses and a drop of immersion oil was put on it before taking any images. The source light was set on 5.2 mps. A calibration should be conducted for the analyser to provide clearer images. The magnification was illustrated on all images at 100 microns. Also, two types of images (full view and particle view) were taken as described in section 4.8.4. Finally, the blocks were cleaned and stored.

3.6.3 Methylene blue studies

Methylene blue measurements were conducted on the activated carbon samples C2a, C4, B5a, and a commercial sample Fisher-DC. These samples were selected due to their high surface areas. The purpose of these analyses is to examine the adsorption capacity. These measurements were designed to provide nominally a 12-points adsorption isotherm plot for each sample tested. A 7.12 g of methylene powder was mixed with 1 litre distilled water. Furthermore, a 0.05 mg of activated carbon for each sample (C2a, C4a, B5a and Fisher DC) was placed in 12 sample bottles (*i.e.* vials), with capacity is 28 ml. Appropriate volumes of distilled water and 20 mmol.litre⁻¹ methylene blue solution were pipette into the vials to give a total volume in each vial of 10 ml solution. These mixtures in each vial are presented in Table 3.3.

Table 3.3: Twelve mixtures of methylene blue & water.

Methylene blue ml	Water ml
0.8	9.2
1.0	9.0
1.3	8.7
1.8	8.2
2.4	7.6
3.2	6.8
4.0	6.0
4.8	5.2
6.0	4.0
7.2	2.8
8.6	1.4
10.0	0.0

The bottles were capped and shaken over a period of 24 hours. Then after seven days, they are carefully filtered with 4 ml of the supernatant solution through a micro-funnel containing a plug of glass wool in the top of the stem, into a 10 mm cuvette. The absorbance of the residual methylene blue in solution was measured at a wavelength of 668 nm using a UV mini-1240 spectrophotometer. Some of the solutions required a greater or lesser degree of dilution in order to accommodate the absorbance within the calibrated range (*i.e.* absorbance should be less than 1 and for better absorbance) of the instrument [Grubbs, 2009]. By determining the initial and final (*i.e.* seven

days) equilibrium concentrations of methylene blue in solution, then it was possible to construct an adsorption isotherm plot for each carbon sample.

In addition, six concentrations with their absorbance (nm) were prepared and presented in Figure 3.4. This figure represents the calibration curve in order to calculate the equilibrium constants. Equation 3.3 observed linear least square. This analysis was applied in different phenomena and implemented for methylene blue measurements to calculate the constants in equation 3.3. This equation was chosen in correspondence with the conditions applied in this analysis [Potgieter, 1991 and Yamin *et al.*, 2007].

$$y = ax^2 + bx + c \text{ -----(3.3)}$$

a= constant 1 is calculated from the calibration curve (Figure 3.4) = -1.2378

b= constant 2 is calculated from the calibration curve (Figure 3.4) = 12.137

c=0

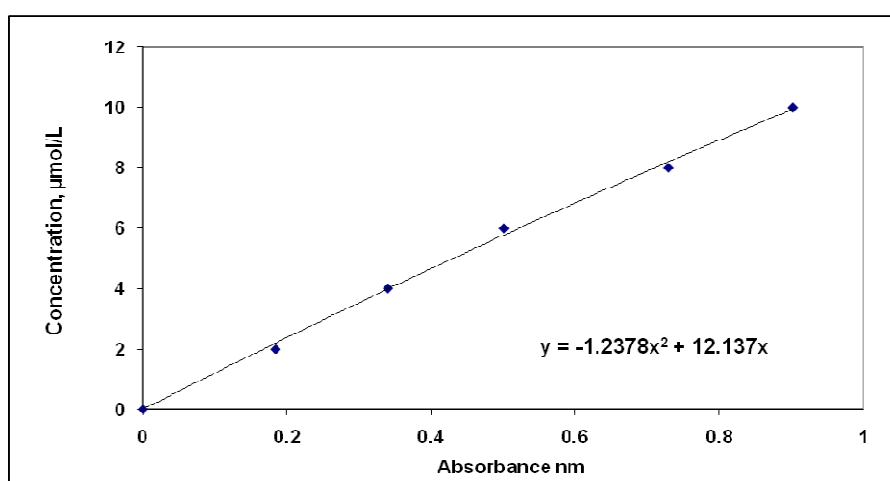


Figure 3.4: Calibration curve to calculate the constants (a & b).

According to equation 3.3, it can be calculated how much has been adsorbed from the dye colour in all samples which is illustrated as follows:

The residual of methylene blue (Ce) (mmol/litre) = $(0.001 * \text{dilution factor}) * (\text{absorbance of diluted solution}^2 * (a)) + (\text{absorbance of diluted solution} * (b))$ ----- (3.4)

Then, it can be calculated dye colour adsorption per gram of carbon according to this equation with substitution of the actual mass of carbon used 0.05 g:

MB uptake mmol/g carbon (qe) = $(\text{Initial MB concentration} - \text{the residual of MB calculated at equation 3.4}) * \text{total volume of (MB+water)} / (1000 * \text{Mass of carbon used})$ ----- (3.5)

3.7 Inductively Coupled Plasma-Atomic Emission Spectrometry (ICP-AES)

This technique was carried out on three PFAs (asr) (C2, C4 and B5), and their beneficiated (C2d, C4d and B5d) and the activated (C2a, C4a and B5a). For the activated samples, these were selected after 120 minutes activation. This experiment was conducted in two parts. Firstly, the samples were digested by microwave to help the carbon separation from PFA. Secondly, the resulting samples were taken into the ICP-AES analyser. ICP-AES analyser can measure the inorganic impurities with a moderate-low detection limit (approximately 0.2-100 ppb). The main minerals (*i.e.* oxides) measured through this analyser were (Si, Al, Fe, Ca, Mg, K, Mn, Na, P, S, and Ti). The error in these analyses was accounted up to $\pm 8\%$. The microwave digestion was divided into three stages:

- 1) **Stage A:** this stage started by weighting around 0.3 g from PFA in a bottle. After this, first acid digestion step was started by adding 10 ml nitric acid HNO_3 per sample, then placed in the tray. This tray can take up to twelve samples. The sample arrangement in each tray was started with a reference sample and in the sixth position was a blank sample. The rest were samples to be analysed. The programme in this stage started heating the samples into 190 °C for 15 minutes at a rate 15 °C.min⁻¹. Next step, the samples were kept isothermally for about 30 minutes, and finally, they were cooled down for about 50 minutes.
- 2) **Stage B:** After cooling, the samples tray was removed from the microwave. Then next acids digestion treatment started first by adding 5 ml of hydrofluoric acid HF and 3 ml of hydrochloric acid HCl into each sample solution. The tray was then placed back in the microwave which commences the second digestion programme. The programme was started by heating the samples to 190 °C for about 20 minutes at a rate 10 °C.min⁻¹. Then the samples were kept isothermally for about 20 minutes. Finally, they were cooled down for about 50 minutes.
- 3) **Stage C:** After cooling, 30 ml of boric acid B(OH)_3 was added into each sample solution and placed again in the microwave tray. The third programme started first by heating the samples to 170 °C for about 20 minutes at a rate 10 °C.min⁻¹, and then the samples were kept isothermally for about 10 minutes. They were then cooled down for about 50 minutes. The resulted samples were placed into

the ICP analyser. The solutions were filtered to prevent a partially or completely clogged nebulizer. This analyser measured the emitted characteristic wavelengths from the electrons in the atom as they specified higher energy levels during their return to the ground state. The intensities of these wavelengths were compared to those generated by known standards [Zhe, 2006], thus, the concentration of the required elements were measured.

Furthermore, the ICP-AES analytical technique can be used to quantitatively determine main and trace elements in PFA samples and is more accurate than EDX analysis especially at lower concentrations of the elements and at very low detection limits, but the sample must be in aqueous solution. The disadvantage is that the instrument cannot handle high concentration of ‘salt, *i.e.* Mg, Na’ without dilution to a level within the range of calibration for that element. Therefore, for coal combustion by-products, the digested sample may require dilution up to 1000 times, thus giving rise to possible uncertainties in transferring and making up volumes for successive dilutions as well as possible misidentification of mass spectra contamination from within the reagent solutions used for dilution.

An alternative analytical procedure involves using high resolution mass spectrometry (MS), which offers a more reliable means of resolving each element over a wide linear range [Lachas *et al.*, 1998]. Also, this technique will help to identify the PFA sample according to these mineral contents and could classify it in terms of the application will integrate into.

CHAPTER FOUR

RESULTS AND DISCUSSION

This chapter presents the results and discussion for the work undertaken to utilise high carbon applications of PFA into value added products. It follows the same parts that were presented in chapter three: samples characterisation, PFA beneficiation, enriched PFA characterisation and carbon activation.

4.1 Thermogravimetric analyses (TGA)

4.1.1 LOI analysis

The determination of the loss-on-ignition (LOI) content was conducted according to the ASTM C311 procedure. These analyses were carried out for PFA samples and LOI values are presented in Table 4.1. These samples were received from three power stations.

Basically, LOI value represents the unburned carbon residue in PFA. It can be seen that the LOI values ranged from 3.6 % for C1 to 35.7 % for C6. The LOI values change between these stations, because of the variations in coal type, particle size, combustion system, boiler operation regime (residence time, temperature, etc.) and type of air pollution control devices used. Furthermore, incomplete combustion in coal-fired power plants may result in LOI values up to 15% [Lesley *et al.*, 1996 and Fan *et al.*, 2001].

Power station 1 (*P.S.1*) has showed different devices were used for collecting the three samples. C1 and B1 samples were collected by ESP (electrostatic precipitator) and their LOI values are 3.6 and 5.7% respectively. C2 sample was collected by a mechanical precipitator and the LOI value is 12.1%. It can

be pointed out that the PFAs collected from ESP present lower LOI, while the PFAs collected mechanically present higher LOI [Couch, 2003]. The LOI value of B1 sample is slightly higher than C1 sample according to biomass co-firing with coal let the LOI value increase approximately 1% [Livingston, 2006].

PFAs at *P.S.2* were sampled from front to back rows of the ESP units, while C7 and C8 samples were collected from the same unit but at different dates. It can be seen that the LOI values increase from front to the back rows of the ESP hoppers for samples C3-C6, as shown in Table 4.1. It can be seen that C7 and C8 samples were collected from same hopper but at different hours. The time difference was two hours, and it had shown the LOI increased due to the changes in combustion conditions, and feedstock.

Moreover, the LOI values of C3-C8 samples are changed significantly across the fields (Table 4.1). Thus, ESP unit at this station presents bigger variation in LOI value for these samples. This is because of flue gas condition and ESP design unit. Consequently, C5 and C6 have shown highest LOI values. This has been previously observed from other power plants [Maroto-Valer *et al.*, 2002b]. Therefore, selected hoppers could be suitable for collection of high carbon ashes as a precursor for carbon materials. ESPs can be classified into two types according to flue gas temperature: cold side ESP operates with flue gas temperatures of <150 °C, whilst hot side ESP operates at higher temperatures up to about 350 °C [Couch, 2003]. Thus, C3 and C4 were collected from the hot side as they presented lower LOI contents, while C5 and

C6 sampled from cold side as they presented higher LOI contents [Maroto-Valer *et al.*, 2002b].

Table 4.1: LOI values for all PFAs received.

Sample	LOI %
<i>P.S.1</i>	
C1	3.6
C2	12.1
B1	5.7
<i>P.S.2</i>	
C3	8.8
C4	15.5
C5	20.4
C6	35.7
C7	8.6
C8	9.5
<i>P.S.3</i>	
C9	8.2
C10	5.0
B2	6.1
B3	5.8
B4	3.9
B5	8.1
B6	5.4

The samples are delivered from P.S.3 either derived from coal only or biomass co-firing with coal. The type of biomass co-fired with coal was oat pellets, and the co-firing ratio between biomass and coal ranged from 1-5%. It can be seen from Table 4.1, that C9 and B5 samples showed higher LOI values (8.2 and 8.1%, respectively). For C9 sample, it could be from the combustion conditions changed in that time and resulted into flue gas stream as it goes into ESP unit. For B5 sample, it could be from the collection point as it was collected from bottom tray of the economiser unit. This point reflects higher unburned carbon

accumulate with PFA compared with top tray accumulate less carbon, as it resulted in sample B4.

Furthermore, the LOI value varies between three stations from lower level 3.6% to higher level 35.7%. ASTM C311 [ASTM C311, 2006] presents acceptable LOI value up to 6 % in order to make this PFA suitable for concrete applications. Thus, samples C2, C4, C5 and C6 observed highest LOI values compared with other samples. It can be considered that these samples are not suitable for cement industry and they are good stock for carbon precursors. Other samples C1, B1, C10, B2, B3, B4 and B6 were appeared with lower LOI from the acceptable value due to the collection device, parent coal, and combustion conditions. These samples are suitable for cement industry. Finally, it can be concluded that the samples collected by ESP show lower LOI value and are suitable as a good admixture for cement. For biomass co-firing samples as the co-firing ratio with coal was 1-5%, there is no significant effect on the LOI value (*i.e.* ~1%) compared to PFA coal samples.

4.1.2 Proximate analyses

The proximate analyses were performed using the same SDT-TGA600 as for LOI analyses, but the procedure applied is different as described in section 3.3.1.2. Proximate analyses conducted on all the PFA samples received from the three power plants. The values in wt.% are presented in Figure 4.1.

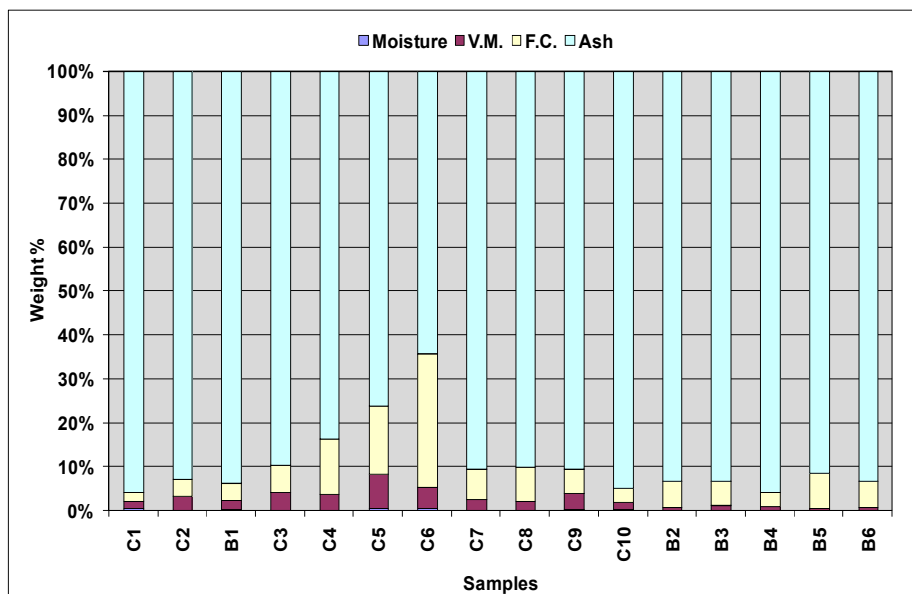


Figure4.1: Proximate analyses for all PFA samples received presented in a column diagram.

Figure 4.1 presents PFAs with low moisture content. Moisture content ranged from 0.1 to 0.5 wt.%, and this is depending on the store room and receiving conditions. Volatile matter (V.M.) values for all PFAs are expected to be low. The reason is because of the original fuels (biomass and coal) had already undergone devolatilization during the combustion process and therefore most PFAs present lower in volatile matter content. Volatile matter values ranged from 0.6-7.9 wt.%, as shown in Figure 4.1. The biomass co-firing samples B1-B6 are presented lower values compared to PFA coal samples. This is reflected from the biomass burned quickly than coal due to high volatile matter of biomass.

Fixed carbon (F.C.) values obtained from the proximate analyses were lower than the LOI values for samples C1-C10 and B1-B6 (Figure 4.1). The sample C2 presents much lower value of fixed carbon. The reason could probably be

the homogeneity of the sample and not been agglomerated like other samples (Figure 4.1).

However, LOI values for all PFA samples were almost equal to the sum of the contents of V.M. and F.C, as shown in Figure 4.2. This figure proves this category in terms of it being not much difference between the LOI results and the total contents of moisture, volatile matter and fixed carbon for all PFA samples. This could be explained by the difference between the analytical methods used to determine LOI and proximate analyses. However, fixed carbon content was calculated by subtracting moisture, V.M. and ash from the total, *i.e.* 100% [ASTM D 5142-90, 1994].

In contrast, some components (*i.e.* volatile matter and inorganic compounds) could decompose at the LOI test temperature (750 ± 50 °C) [Lesley *et al.*, 1996]. However, samples B1-B6 were presented fixed carbon values slightly higher than C1, C2, C9, and C10 samples, with the exception of C3-C8 samples. This is probably due to lower values of volatile matter and ash, as shown in Figure 4.1. PFAs are usually presented as having higher ash content according to inorganic, which are transformed when the parent coals underwent the process inside the boiler [Kenneth, 1987 and Ihsan *et al.*, 2001]. Therefore, these samples are presented over 60 wt.%. Ash content is higher than moisture, volatile matter and fixed carbon contents. It can be pointed out that PFAs with higher LOI value present lower ash content compared to samples which show a lower LOI value, as shown in Table 4.1 and Figure 4.2. This was observed

previously due to work reported by Harold to characterise coal combustion by products [Harold *et al.*, 2001]

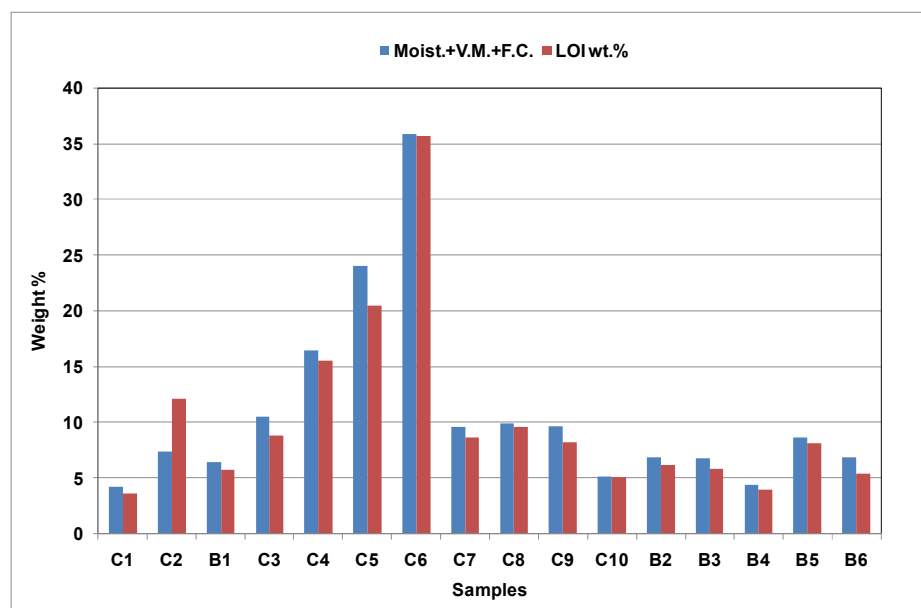


Figure 4.2: LOI results and the total contents of moisture, volatile matter and fixed carbon.

4.2 Ultimate analyses

The ultimate analyses of all the PFAs are presented in Table 4.2. These were conducted in on a received basis. It was approved in previous works that PFAs had contents with elemental carbon, very little hydrogen and nitrogen [Harold *et al.*, 2001]. It can be seen that the hydrogen content were between <0.01 to 0.1%, whereas nitrogen content is lower than <0.01%. This was previously described that these PFAs were derived from fuels devolatilised while in the combustors. Thus, the PFA samples resulted with lower contents of moisture and nitrogen. On the other hand, the sample C9 was received as the ammonia injection was applied during the sample collection. It should content with more nitrogen due to this injection compared to other samples, but it appeared with

low nitrogen. This is probably of a lower amount of ammonia injected into ESP unit.

Table 4.2: LOI values and ultimate analyses for all PFAs received (asr).

Samples	LOI %	C %	H %	N %
C1	3.6	2.9	0.1	<0.01
C2	12.1	9.1	0.04	<0.01
B1	5.7	4.9	0.01	<0.01
C3	8.8	8.0	0.04	<0.01
C4	15.5	15	0.1	<0.01
C5	20.4	17.8	0.1	<0.01
C6	35.7	30.4	0.1	<0.01
C7	8.6	6.8	<0.01	<0.01
C8	9.5	8.4	<0.01	<0.01
C9	8.2	5.1	0.02	<0.01
C10	5.0	3.9	0.04	<0.01
B2	6.1	5.7	0.04	<0.01
B3	5.8	5.7	0.03	<0.01
B4	3.9	4.1	0.02	<0.01
B5	8.1	7.4	0.03	<0.01
B6	5.4	5.8	0.04	<0.01

Moreover the date for conducting the analyses is after receiving the samples. The ammonia in PFA can render the PFA market as it reported by Kulaots [Kulaots *et al.*, 2001]. The elemental carbon follows the same trend with LOI results of all PFA samples (Table 4.2). Carbon content of all PFAs varied from 2.9 to 30.4%. It can be seen that the elemental carbon is higher for samples C2-C6 and C8. This was previously described in section 4.1.1. The biomass samples B1-B6 present higher elemental carbon compared with PFA coal samples which have similar LOI value. This is caused by incomplete combustion of biomass particles due to the particle shape (*i.e.* un-homogenous) compared to coal. Also, the fuel characteristics between biomass and coal are

different as described in section 2.4.1 and illustrated by Baxter and Livingston [Baxter, 2005 and Livingston, 2007].

4.3 Porosity studies

The nitrogen adsorption isotherms at 77K were conducted on all PFAs listed in (Table 4.1) using a Micromeritics ASAP 2000, as described in section 3.5. For the purpose of comparison, isotherms are presented in two Figures 4.3 and 4.4. The adsorption isotherms are Type II according to BDDT [Brunauer *et al.*, 1940] classification and it shows they are typical for nonporous or macroporous adsorbents, where unrestricted monolayer-multilayer adsorption can occur [Harold *et al.*, 2001 and 2003].

Monolayer coverage is succeeded by multilayer adsorption at higher P/P_0 values and this type is not presenting a hysteresis loop. Type II isotherms can also be obtained from carbons with mixed micro- and mesoporosity [Patrick, 1995]. The reasons of not showing any a hysteresis loop by these samples are illustrated of lower of mesoporosity and small surface areas are presented. These isotherms have been previously observed and indicate that the extensive and rapid devolatilization that coal and biomass underwent in the furnace promoted the generation of meso- and macropores.

It can be seen that sample C6 needs a long time to reach the saturation point compared with other PFAs, as shown in Figure 4.3. This indicates that the C6 sample had a higher volume absorbed to approach saturation pressure and this is related to show higher proportion of meso- and macropores.

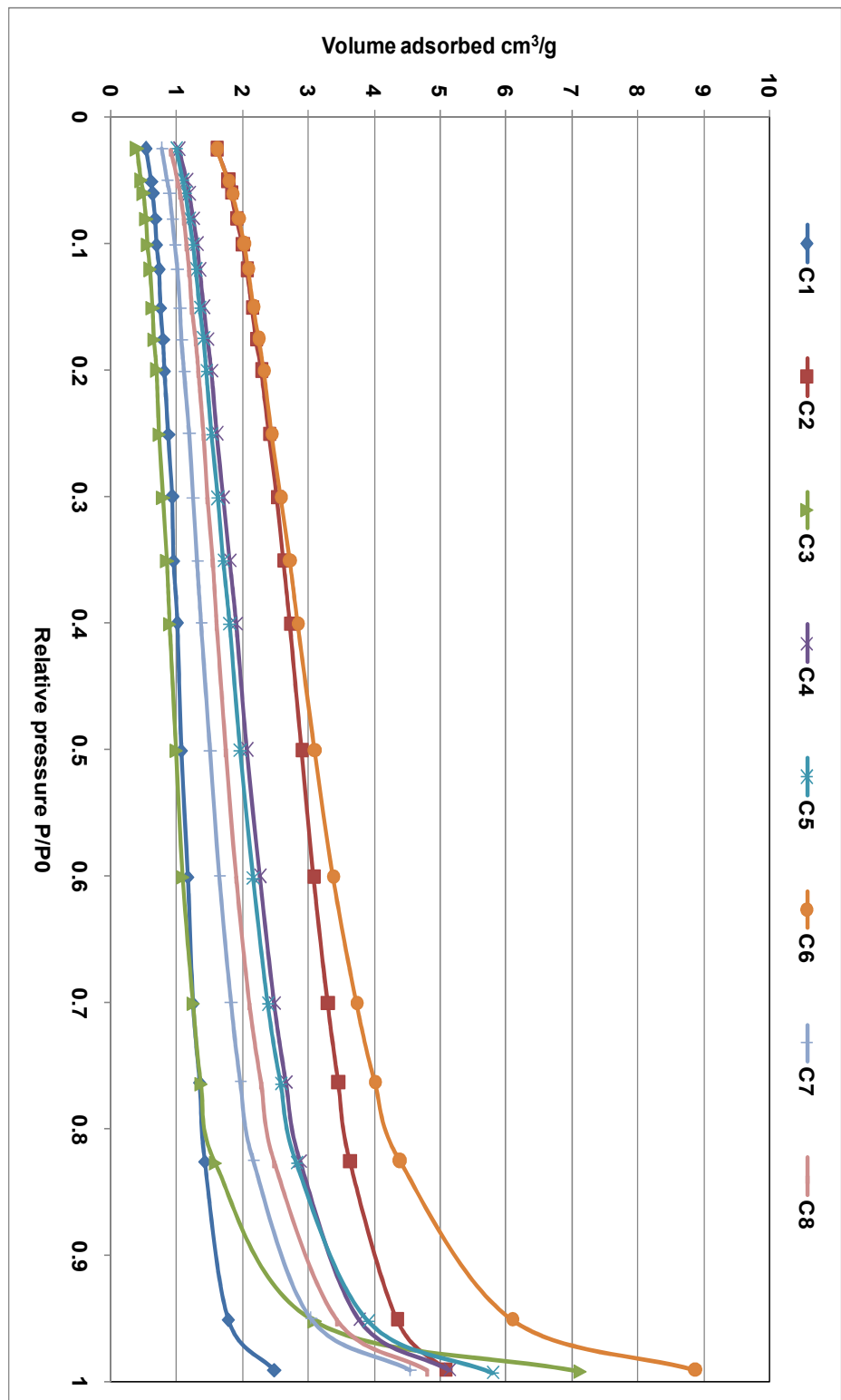


Figure 4.3: Adsorption isotherms.

Samples C1-C5, C7, and C8 presented almost linear isotherms and become convex to the P/P_0 axis. Moreover, samples C1-C5, C7 and C8 presented lower adsorption volumes compared with sample C6, which was observed having a higher proportion of mesoporosity. Samples C9 and B5 presented a tail as saturation pressure was approached, indicating the presence of macropores. In addition, samples C10, B1-B4, and B6 observed similar trends to samples C1-C5, C7 and C8, as shown in Figures 4.3 and 4.4.

The BET surface areas were calculated using the adsorption points at the relative pressures (P/P_0) 0.1-0.25. The surface area and LOI value have been previously reported to be interrelated, where increasing surface area is related to increasing LOI value [Maroto-Valer *et al.*, 2007], as shown in Figure 4.5. All the reported data here for surface area are on a received basis and dry basis for LOI results. The PFAs samples had surface areas in the range of 2.5-17 m^2/g , and it is relatively low. It was clear that this area is generally correlated with LOI value, for example, sample C1 presents LOI value and surface area 3.6% and 2.7 m^2/g , respectively, whereas sample C2 presents LOI value and surface area 12.1% and 5.8 m^2/g , respectively. This relation was observed by the samples received from the three power stations. Moreover, PFAs coal C1-C10 exhibited similar trends between LOI value and surface area to PFAs biomass B1-B6, as shown in Figure 4.5. It can be pointed that PFA biomass samples B1-B6 exhibited higher surface areas than

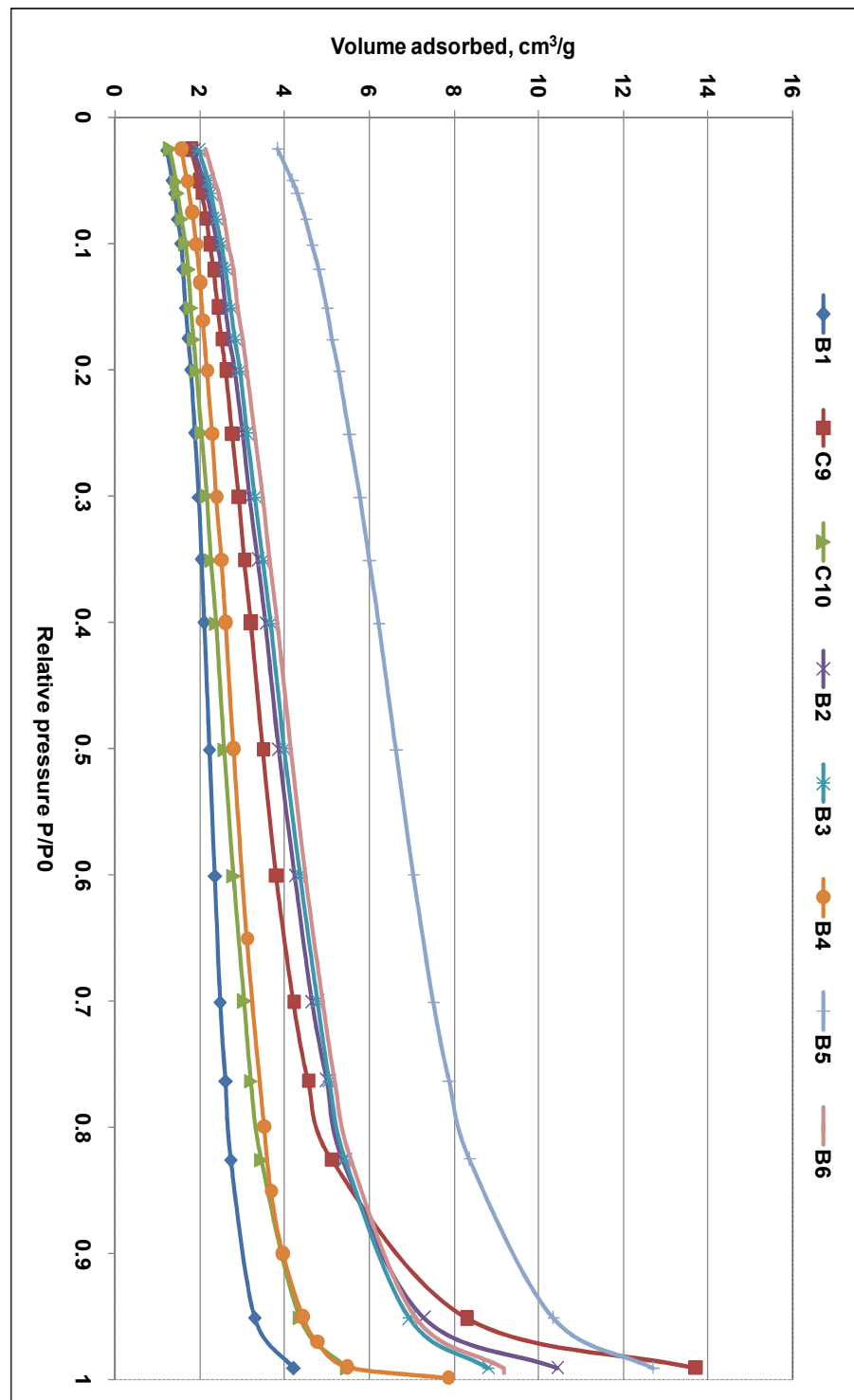


Figure 4.4: cont. adsorption isotherms.

PFA coal samples C1-C10. This is illustrated according to low ash content (*i.e.* inorganic matter) and the porosity generation from the carbon (*i.e.* type) found in biomass samples which is higher than those observed from coal samples. Previous studies generally have used both sources (*i.e.* coal and biomass) to generate high surface areas required for industry reasons [Patrick, 1995 and Harold *et al.*, 2001]. In addition, it was found that the PFAs class F presented surface areas between 30-40 m²/g, whereas class C presented much higher surface areas, with values up to 390 m²/g [Maroto-Valer *et al.*, 2002a].

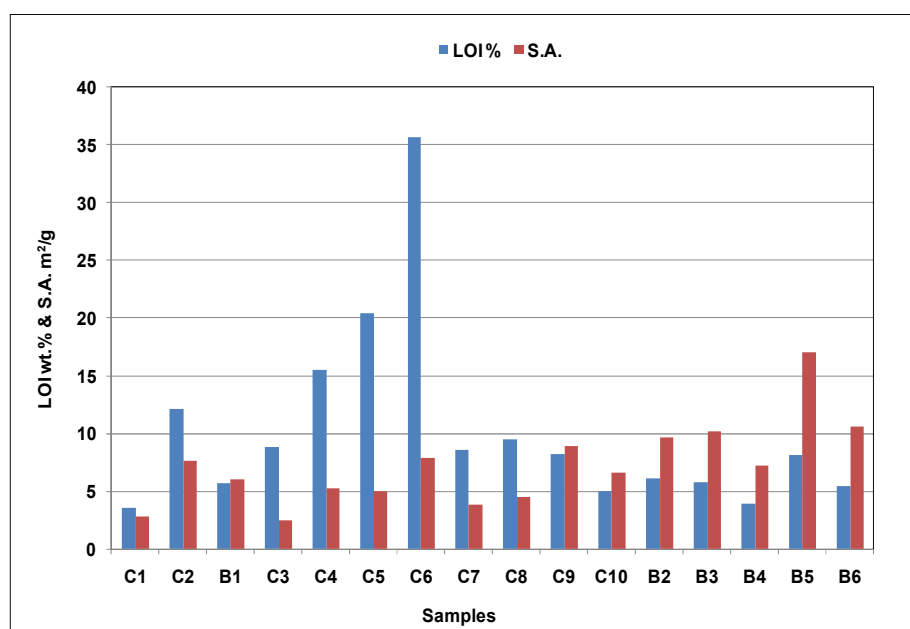


Figure 4.5: The total surface area and LOI % (db) for all PFAs received.

4.4 Particle size distribution

Particle size distribution analyses were conducted on all the samples using a Malvern Mastersizer S-type. These analyses carried out with two dispersant agents (water and iso-propanol-IPA). The reason is because of the difficulty to

disperse fine ash particles below 1μ in water [Rawle, 2008 and Malvern, 2008]. Moreover, PFA is usually a mixture of organic and inorganic, as it was referred in the literature. In contrast, the wetting process by water is more difficult than IPA, but most studies used both agents [William *et al.*, 2002 and Shuanzhen *et al.*, 2008b]. The particle size distribution figures for all the samples are presented in appendix A, but only the representative (*i.e.* high carbon PFA) figures are included here for discussions requirement.

4.4.1 Particle size distribution using water as a dispersant

The particle size distribution of all the samples presented multi peaks in water dispersion. It can be seen that samples C2, C9 and B5 have presented coarser particle size distribution. This was observed from the particle size distribution of these samples after $100\mu\text{m}$ particle size, as shown in Figures 4.6 and 4.7. It seemed to be a large portion of the in-homogeneous particles exhibited by these samples and often the irregular (non-spherical type) introduced the coarsest material. Consequently, the LOI value which was the previously expressed unburned carbon content, presented higher LOI values. Therefore, un-combusted material is accumulated in these samples and usually presents large particle sizes [Ferraris *et al.*, 2004], as illustrated in Figures 4.6 and 4.7.

Moreover, all PFA samples are typically presented bimodal distribution. This was illustrated with small peaks (*i.e.* particle sizes up to $1\mu\text{m}$) and large peaks (*i.e.* over $10\mu\text{m}$, as most of the material concentrates in this area). The bimodal distribution is caused by the presence of fine particles (*i.e.* inorganic) and coarser carbon ones. This was shown in a work study conducted by Power

Technology for the UK Electricity Supply Industries Joint Environmental Programme on opacity measurements [Gibb, 2000].

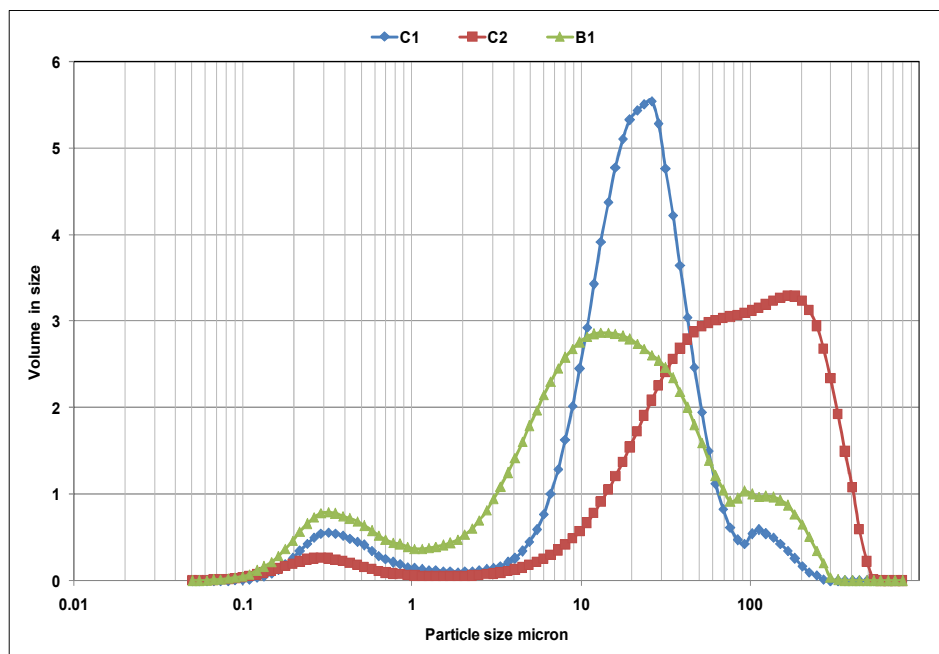


Figure 4.6: Particle size distribution with volume % in size.

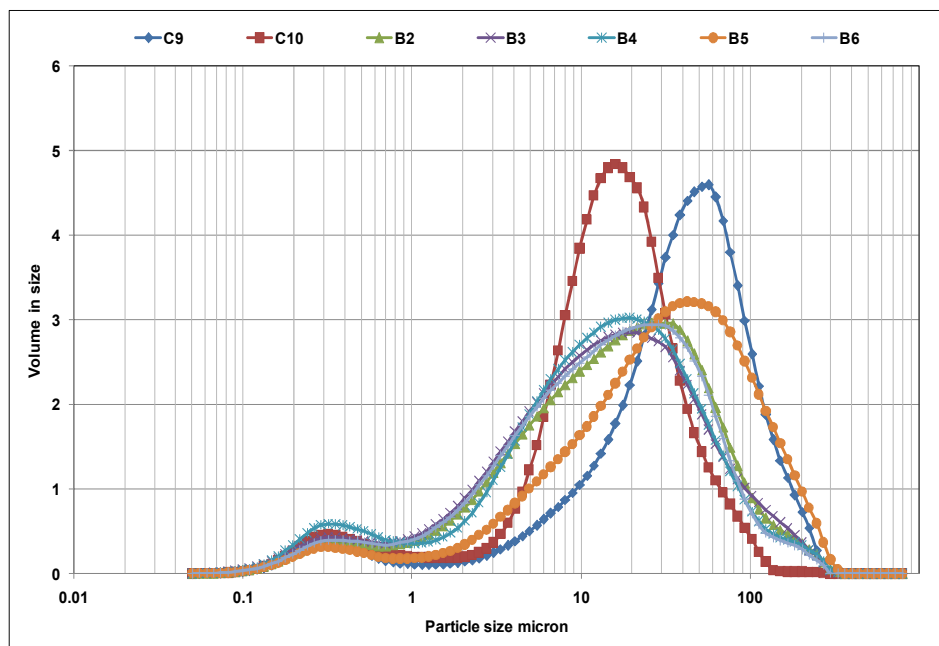


Figure 4.7: cont. particle size distribution with volume % in size.

The PFA biomass samples B1-B6 exhibited a similar distribution trend to PFAs coal C1-C10. One point that can be illustrated is that PFA biomass samples observed wider peaks compared with PFA coal samples which presented narrower and higher peaks.

The d_{50} for all PFA samples were calculated from cumulative graphs. Due to the similarity distribution, two graphs were included in these discussions, but other graphs presented in appendix A. It can be seen that the d_{50} for samples C1 and B1 is 21 μm , 14 μm respectively, while the d_{50} for sample C2 is 80 μm (Figure 4.8). Therefore, the sample C2 trend line observed to the right side due to coarse particles accounted in this sample. Consequently, PFA biomass samples showed similar cumulative graphs to PFA coal samples.

The particle size distribution (*i.e.* fineness) of PFA has a significant effect on the cement admixture, and thus the strength characteristics of the resulting concrete [Wesche, 1991]. Therefore, finer particles in concrete imply greater strength. ASTM C618 and EN-450 specify PFA fineness when mixed with cement up to 70% of 45 μm [McCarthy *et al.*, 1990 and Vom Berg, 1993]. However, samples C1, C10, and B1-B4 are good cement admixtures, due to their fineness which results in high strength concrete (Figures 4.8 and 4.9).

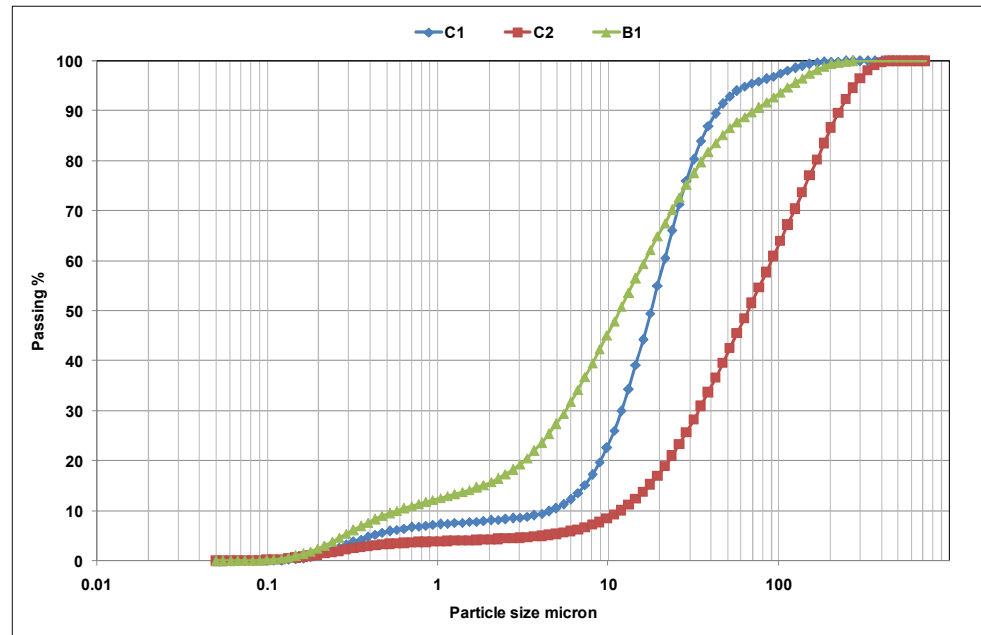


Figure 4.8: Particle size distribution with % passing.

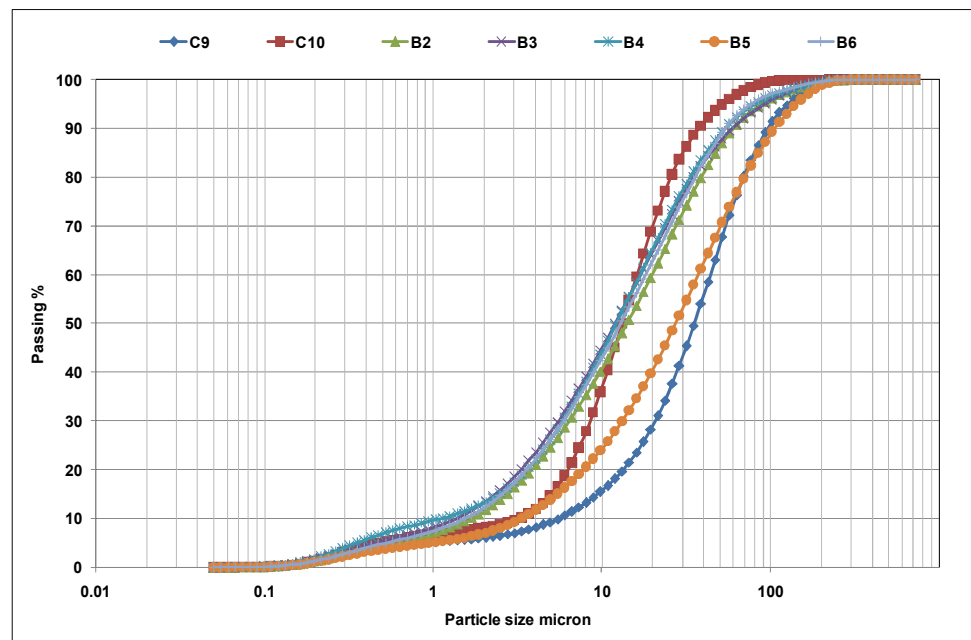


Figure 4.9: cont. particle size distribution with % passing.

4.4.2 Particle size distribution using iso propanol (IPA) as a dispersant

All the samples received from the three power stations were dispersed with IPA. It can be seen that fine particles (*i.e.* sizes up to 1 μm) were wetted through this organic agent, as shown in Figures 4.10, and 4.11. Thus, all samples are presented with a single peak compared with particle size distribution figures which used water as a dispersant agent. Consequently, sample C5 appeared finer (*i.e.* over 50% observed $<10\mu\text{m}$) than the actual graph (*i.e.* over 50% observed $<100\mu\text{m}$) presented with water dispersion, as shown in Figure 4.12. This is illustrated due to less agglomeration for finer particles obtained through this agent, the wetting process achieved all finer particles, and the fragmented particles of carbon which seemed to be finer than coarser.

In addition, the d_{50} in some samples is slightly changed due to the wetting process. This can reduce the agglomeration in order to achieve better distribution to all sizes. IPA is a useful agent to disperse the PFA instead of water and can achieve better particle size distribution [William *et al.*, 2002 and Shuanzhen *et al.*, 2008b]. In contrast, this agent is more expensive to use than water and produces chemical waste not like water.

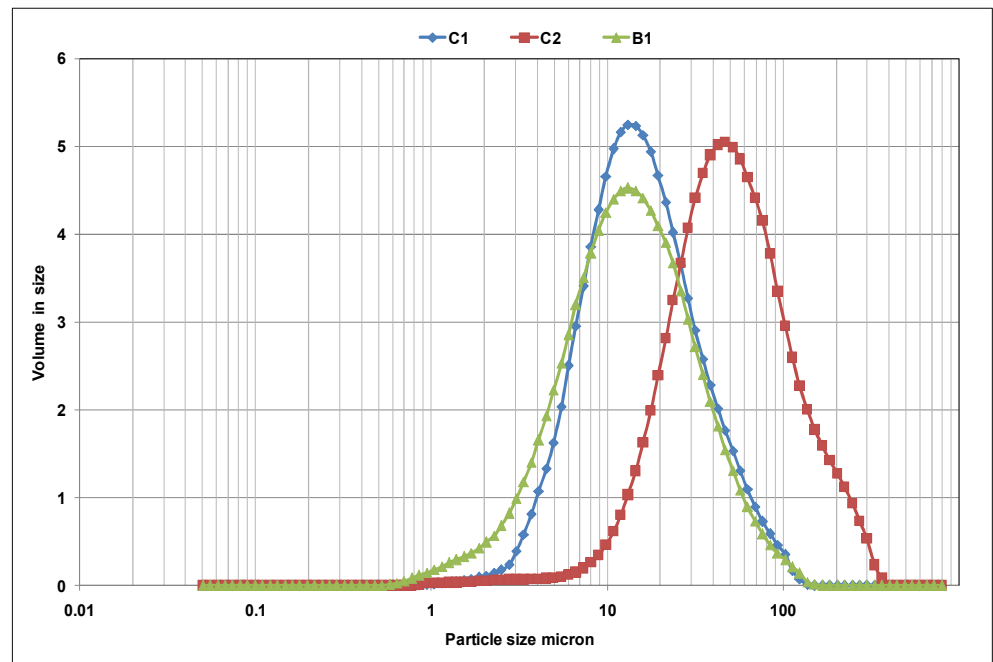


Figure 4.10: Particle size distribution with volume % in size.

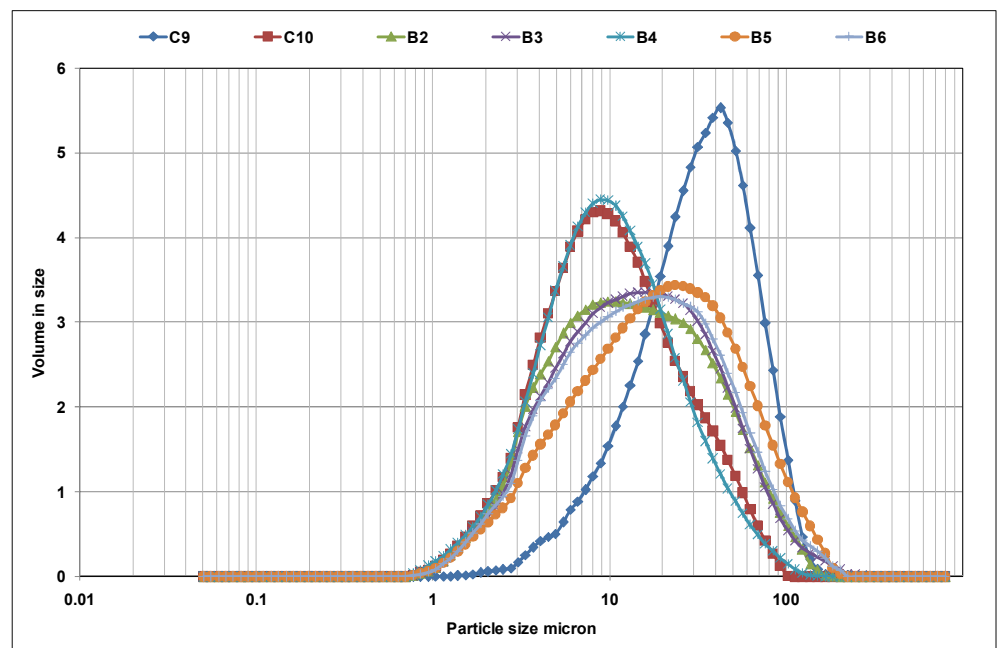
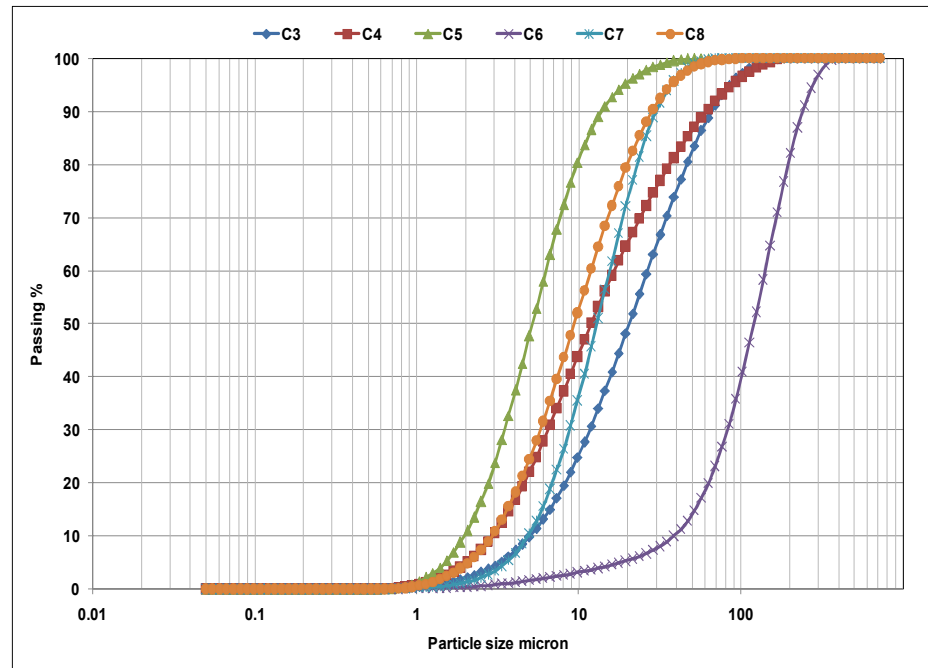


Figure 4.11: cont. particle size distribution with volume % in size.



from these elements can account for 75-85% of the sample weight. Physically, PFA consists principally of glassy spheres together with some crystalline matter and unburned carbon [VomBerg, 2000]. All the figures show mineral particles where some smaller spherical and mineral particles are plastered.

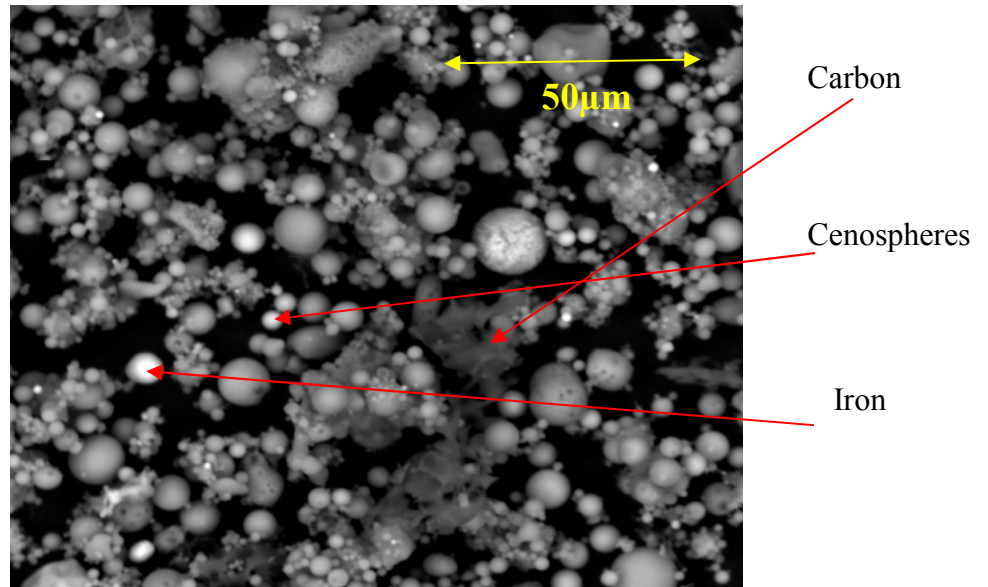


Figure 4.13: SEM image of C1 sample.

It is clearly seen from Figures 4.13-16 that the dark particles are carbon. These particles are porous and present different irregular shapes. Generally, the small spherical particles (ceramic spheres, called cenospheres) range in diameter from 5-75 μm and have many valuable applications due to their insulating properties (Figure 4.13). The mineral particles with white spots have iron, and some of these particles are glassy (*i.e.* silica content) [Barbara *et al.*, 2006 and Shuangzhen *et al.*, 2008b].

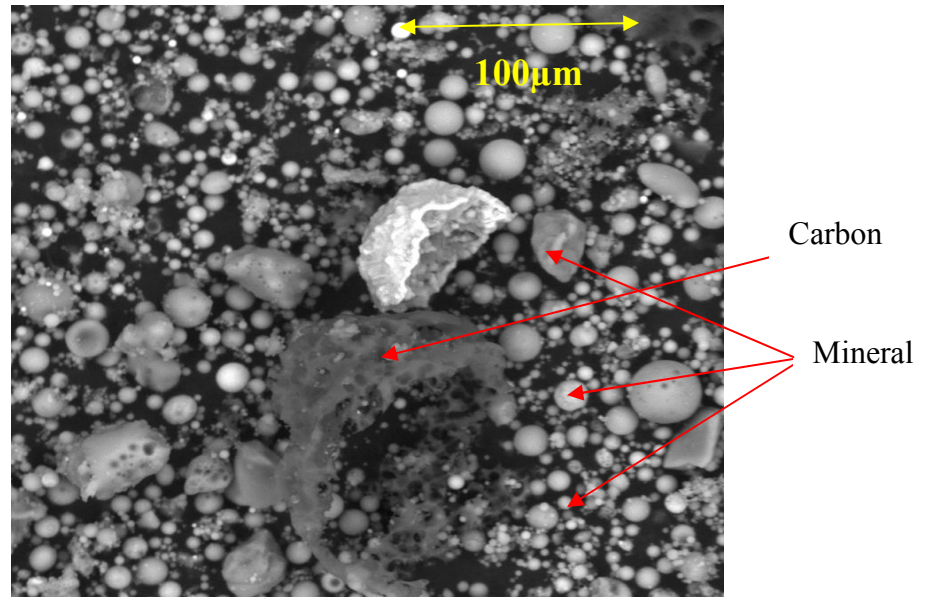


Figure 4.14: SEM image of sample B1.

These particles are formed during different stages as described in the PFA formation section 2.1.2. Rapid cooling in the post-combustion zone results in the formation of spherical and amorphous (non-crystalline) particles. The hollow sphere particles are obtained due to the expansion of trapped volatile matter [Lesley *et al.*, 1996 and Barbara *et al.*, 2006].

Figure 4.14 shows a porous black particle in the middle filled in some parts with ceramic small spheres (*i.e.* minerals). The porosity enlargement in this particle was developed adequately during coal combustion inside the boiler and apparently is different from other particles in this image. This mechanism is often complicated and it is depending on the fuel (coal and biomass), fuel origin, combustion conditions, and boiler design [Barbara *et al.*, 2006 and Zhe, 2006]. It should be pointed out that samples B1 and B5 images are similar (*i.e.* view) to those of samples C1 and C6. Thus, these samples can behave the same

as PFA coals. This was achieved due to low biomass co-firing ratio and has probably contributed more inorganic content from coal rather than biomass [Livingston, 2006 and Shuangzhen *et al.*, 2008].

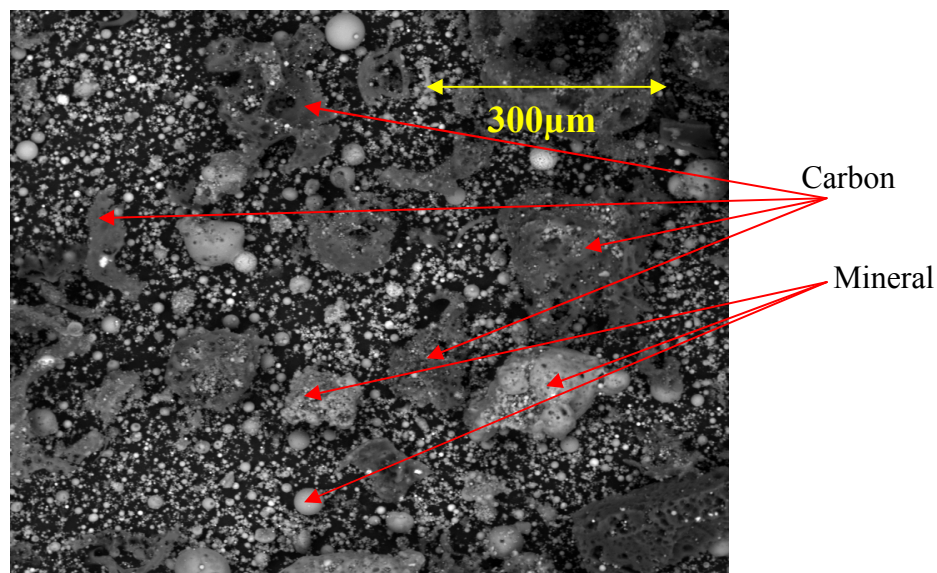


Figure 4.15: SEM image of sample C6.

Samples C6 and B5 presented more unburned carbon particles than samples C1 and B1, as shown in Figures 4.15 and 4.16. This was consistent with LOI and particle size distribution results obtained in sections 4.1.1 and 4.4. However, the dark particles are shaped differently according to the conditions and coal origin. Some particles are more porous than the others and some are fragmented in pieces during the combustion process. Each of these particles was accompanied with small spherical and non spherical particles.

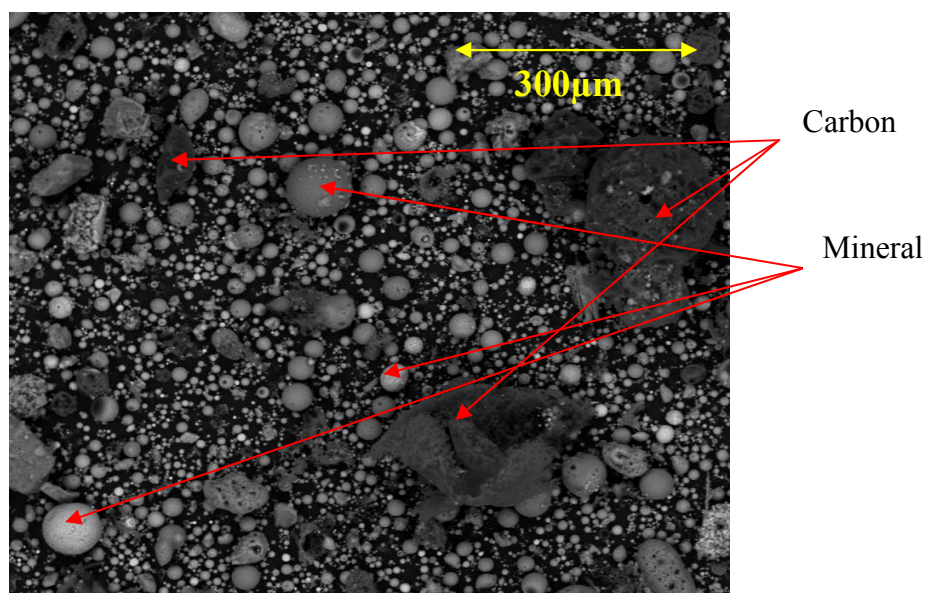


Figure 4.16: SEM image of sample B5.

4.5.2 Energy dispersive X-Ray (EDX)

EDX is the most frequently used technique in a solid state and utilised to study crystal structure. Some figures of the representative (*i.e.* high carbon PFA) samples are illustrated here. Additional figures are placed in appendix C. The elements composition of PFA samples as identified by EDX are included (carbon, oxygen, sodium, magnesium, aluminium, silicon, phosphorous, sulphur, potassium, calcium, titanium, iron and copper), as shown in Figures 4.17-20.

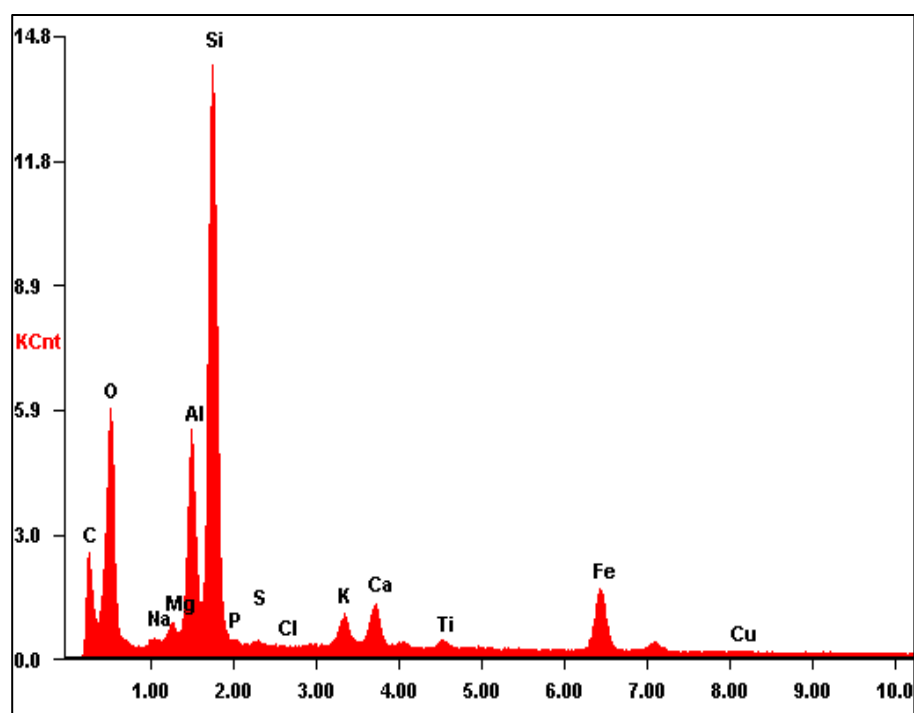


Figure 4.17: EDX graph for C2 sample.

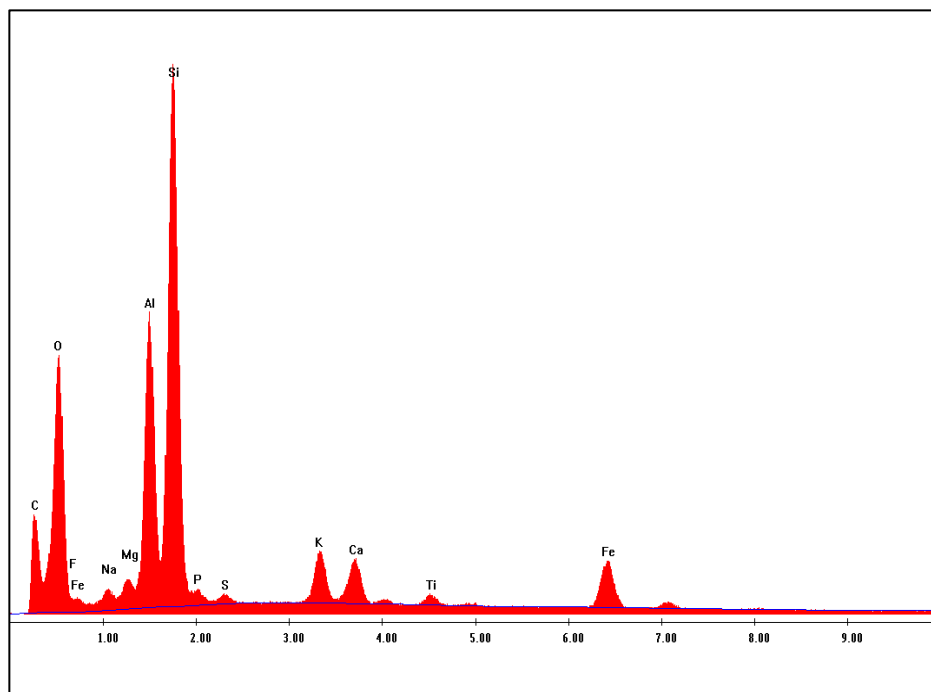


Figure 4.18: EDX graph for B1 sample.

It can be seen that the most needed elements in PFA (*i.e.* cement applications) are silica, aluminium, iron and calcium. Figures 4.17-20 presented these elements and silica element observed the highest peak. These elements (*i.e.* inorganic) transferred during combustion process into PFA are described in section 2.1.2. They are presented as free single particles or associated with carbon particles [Mohamed *et al.*, 2005]. In contrast, these inorganic particles are considerably effective on carbon activity. Previous studies have illustrated the effect of these impurities during carbon activation in terms of catalysing the carbon reactions [Linares-Solano *et al.*, 1979 and Zhe, 2006].

Samples C2 and C5 are attributed with high carbon compositions according to their highest LOI results as discussed in section 4.1.1. This happened due to incomplete combustion inside the boiler unit which resulted in a high carbon composition in these samples. Samples B1 and B5 are observed as having similar elements type as PFA coal samples, as shown in Figures 4.17-20. This happened because of the biomass co-firing ratio to coal (approximately 1-7%). Thus, most of these elements are accounted from coal [Shuangzhen *et al.*, 2008b]. It is clear that sample B5 showed more Cl than B1. The reason could come from the original biomass as it had a lower content.

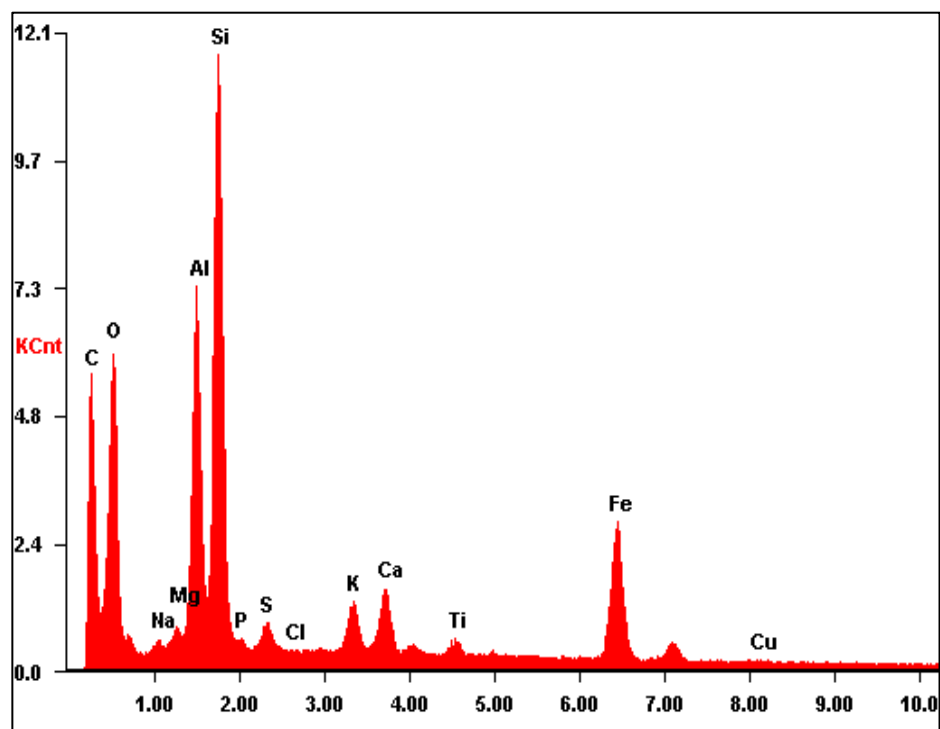


Figure 4.19: EDX graph for C5 sample.

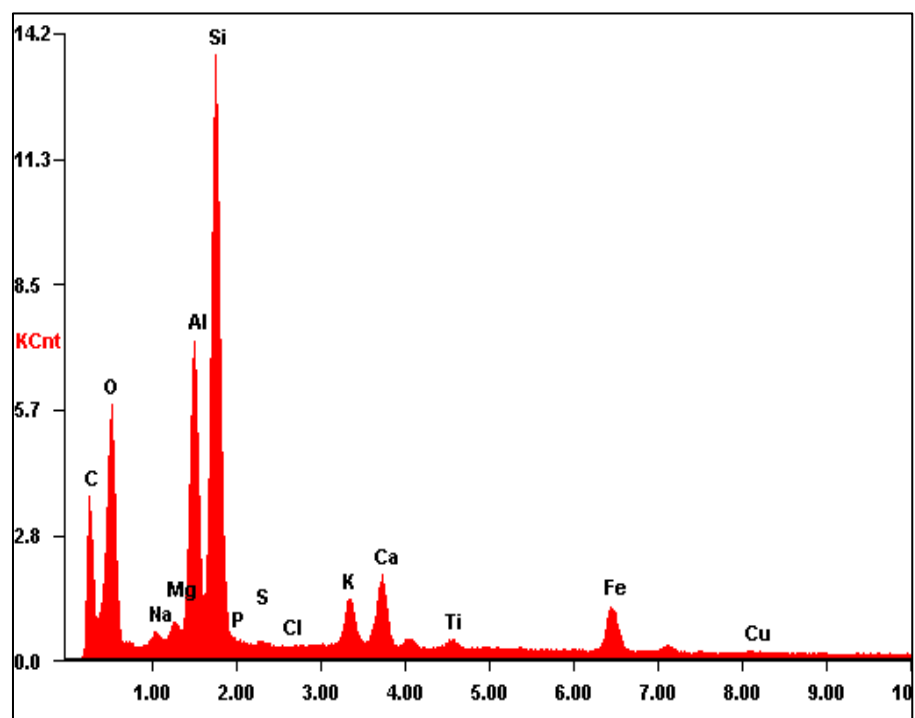
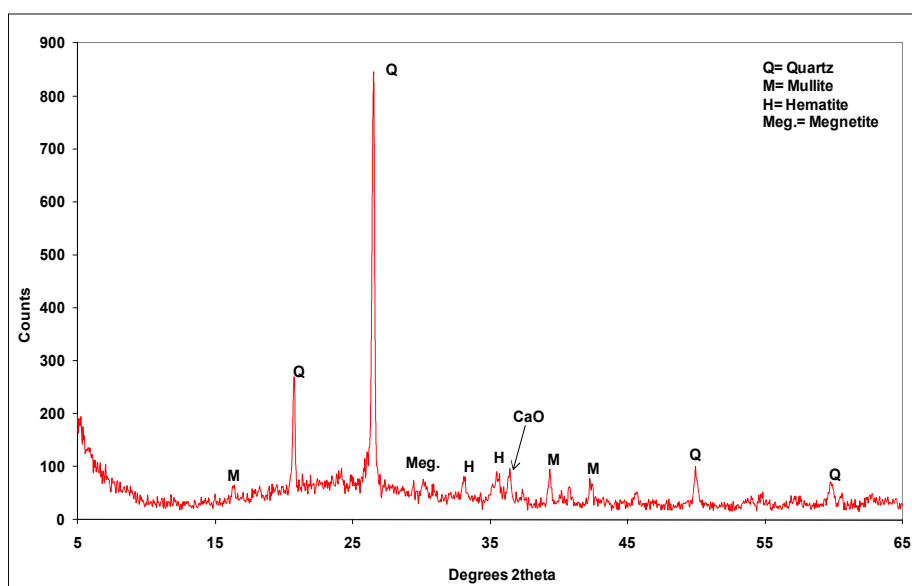


Figure 4.20: EDX graph for B5 sample.

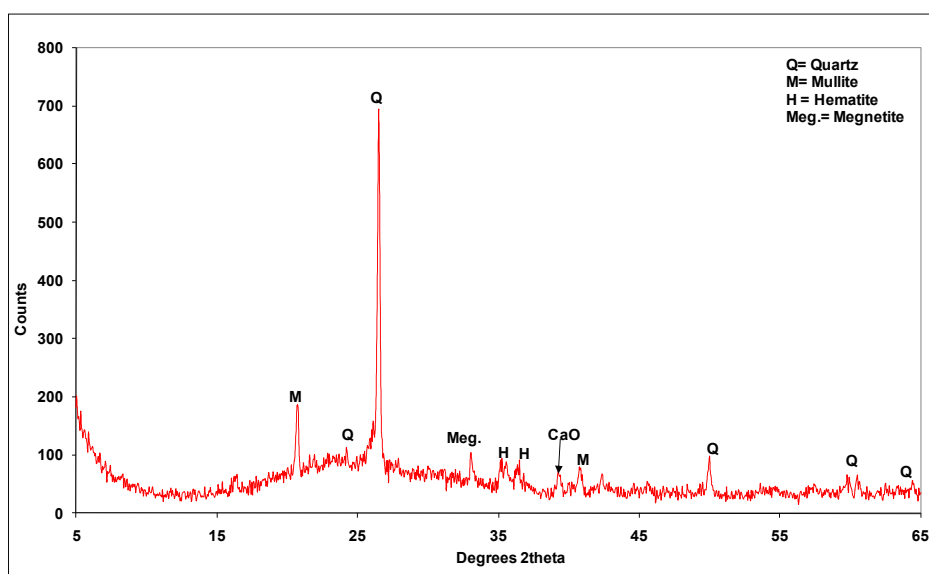
On the other hand, it is important to know the chemical composition of PFA particularly looking into high applications. For instance, work has been conducted by South Africa-Sparton Resources of Toronto on the evaluation of the possibility of extracting uranium and other metals from waste material such as coal ash [Sparton, 2007]. Furthermore, PFA can be presented subjected as a raw material such as fine and coarse ash fractions, magnetic fraction, carbon rich fraction and cenospheres. ICP-AES studies are also conducted for these samples and will be discussed in section 4.10. This is the recommended method for routine multi-element analyses of PFA.

4.5.3 X-Ray diffraction (XRD)

XRD is a more applicable way to identify the crystallinity of the solid structure [Robert *et al.*, 1995]. All figures are illustrated in appendix D and only the representative (*i.e.* high carbon PFA) figures are presented in this section. It can be inferred that these analyses were conducted under normal resolution (*i.e.* 0.05) and scan speed 2 θ as described in section 3.3.5.2. Generally, XRD analyses are used to identify the crystallinity of PFA. They showed the presence of high amounts of quartz, mullite, hematite, magnetite and lime (CaO). The main inorganic phase present is quartz and it varies in these samples. Lime (CaO) and magnetite contents showed very low peaks in all the samples, as shown in Figures 4.21-24. The reason is referred to the parent coal, as it has low content of calcium and iron.

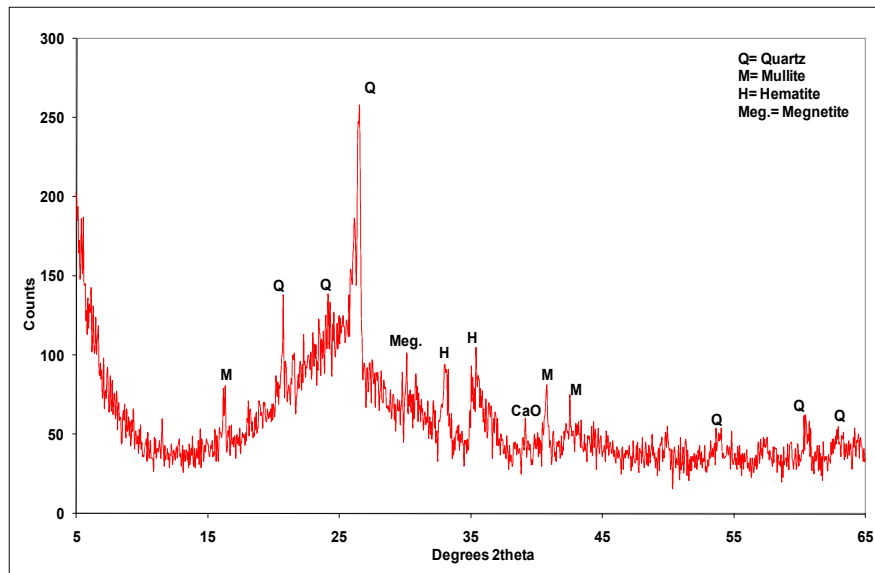


4.21: XRD graph for C2 sample.



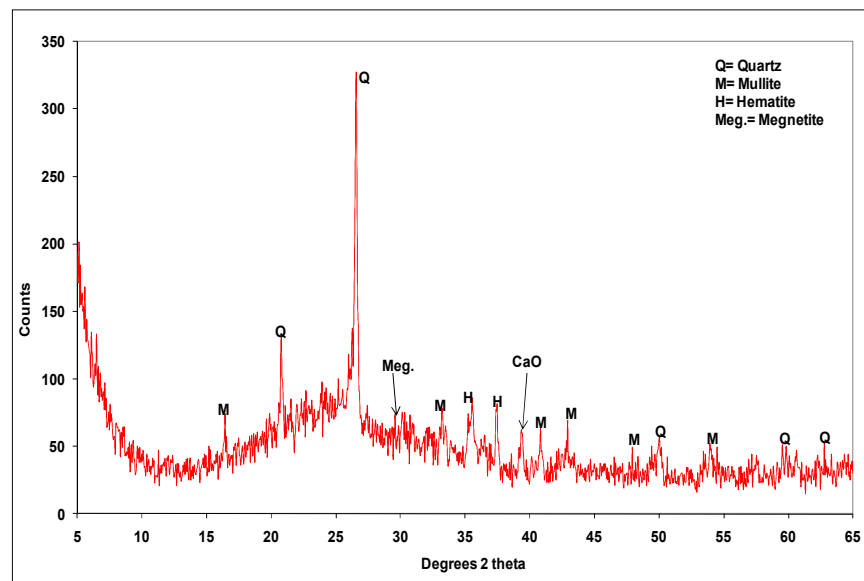
4.22: XRD graph for B1 sample.

It can be seen that sample B1 has lower organic matter and presented only a low noise (*i.e.* narrow peaks). In contrast, C2 sample has higher organic content and reflects similar XRD pattern to B1 sample. This has been obviously observed that the unburned carbon and not amorphous and it might be this sample that reflects higher inorganic contents. This was previously investigated by Manivannan [Manivannan *et al.*, 1997] PFA samples with unburned carbon and how it can effect XRD pattern.



4.23: XRD graph for C6 sample.

Moreover, B1 and B5 samples performed a similar XRD pattern to C2 and C6 samples. This typically showed a higher percentage of inorganic content transferred from coal, rather than biomass in terms of low co-firing ratio (*i.e.* 1-7%). These samples presented slightly higher lime (*i.e.* calcium) counts compared to C2 and C6 samples. This could be exhibited by biomass fuel as it has a higher content than coal.



4.24: XRD graph for B5 sample.

In addition, C6 and B5 samples presented wider broader peaks, compared with samples C2 and B1 samples. These samples have higher LOI value (*i.e.* unburned carbon) and thus broader peaks are caused either by amorphous carbon or amorphous glass. This was achieved by different studies like [Manivannan *et al.*, 1997 and Ward *et al.*, 2005]. Consequently, peak counts are observed differently (*i.e.* not systematic) in these samples. This could relate to different rank coals where the PFA derived.

4.6 High carbon PFA beneficiation

The PFA beneficiation was carried out on high carbon PFA samples, which were identified in the samples characterisation. Two beneficiation methods were used, namely microwave and incipient fluidisation. The objective of the beneficiation was to obtain depleted carbon ash stream for cement tests and concentrated carbon stream for activation studies. The activation studies will

examine the adsorption capacity of the resulted carbons with different activation times. The results for both methods will be discussed below.

4.6.1 Microwave treatment (vitrification)

This method is typically thermal treatment and used the microwave to vitrify PFA by reducing the carbon content under very high electric power in a short period. It removed the unburned carbon by combusting it and produced PFA with low carbon content or neglected.

The objective of this treatment is to vitrify PFA into useful products which can be used as aggregate material (*e.g.* roads surfacing). Microwave vitrification treatment was conducted on two biomass ashes B1 and B3 with LOI values of 5.7% and 5.8%, respectively. These biomass ashes were heated around 1250 °C for a period of 8 minutes. Whole B1 sample vitrified, while the B3 sample was partially vitrified and may need a longer time, see Figures 4.25 and 4.26.

The LOI values for B1 and B3 after vetrification are 5.4% and 2.5%, respectively. Therefore, the efficiency for reducing the carbon content in B3 is higher than in the B1 sample. This might be because carbon particles agglomerated in a larger size compared to the B1 sample and therefore the B3 sample had darker colour to B1. This is coming from the combustion of unburned carbon particles. However, the biomass co-firing ratio observed differently in B1 and B3 samples (*i.e.* 7% sunflower and 5% oat, respectively). Hence, the particles agglomeration resulted in the B1 sample higher to B3. The difference in the behaviour of these two co-firing ashes is probably explained considering that the vitrification method depends on the inorganic content for

both samples. It can be seen from EDX studies, the silicate, alumina and iron contents for B1 sample are 14.56, 7.75 and 3.17 wt.% and for B3 sample are 17.92, 8.73 and 3.63 wt.%.



Figure 4.25: Photo of B1 after vitrification.



Figure 4.26: Photo of B3 after vitrification.

Therefore, the B3 sample presents higher minerals than B1 and made this sample need a longer period to vitrify it completely in a large chunk of particles as shown in B1 sample (Figure 4.25). This was observed by Su-Chen and Robinson to produce light weight aggregates (LWA) from different resources like PFA received from an incinerator and a coal-fired power plant. Both studies aimed for the same thing but the key issue illustrates the inorganic contents in the samples improve the vitrification [Su-Chen *et al.*, 2007 and Robinson *et al.*, 2009].

Consequently, the samples conducted in this process are biomass co-firing and hence the achievement is to produce low carbon PFA. Moreover, the particle size studies showed d_{50} of B1 and B3 samples $<50\mu\text{m}$ and helped to vitrify them in a short period. On the other hand, this method could perform on toxic ashes with higher volumes and produce vitrified ashes with lower volumes suitable as aggregate material [Pierre *et al.*, 2007].

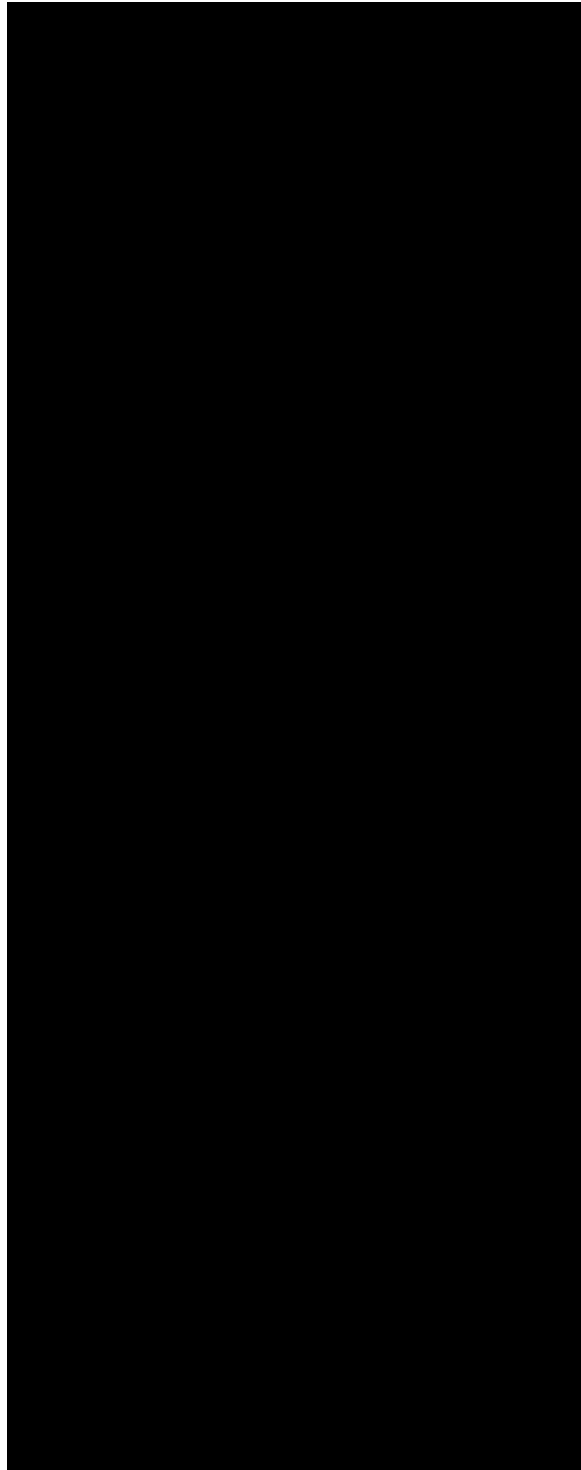
4.6.2 Incipient fluidisation

The incipient fluidisation process was applied on samples with higher LOI values and can be benefited by carbon material resulting from the treatment compared to the vitrification method. This method was carried out on the C2, C4, C5, C6, and B5 samples. Table 4.3 presents the LOI values for each stream (depleted carbon ash and enriched carbon denoted with $-d$ and $-e$, respectively). It can be seen that the LOI value for all the depleted carbon ashes was reduced after the one-stage separation, compared to the original value, particularly for the C2 sample that presented a very good separation with LOI reduction from 12.1% to 1.5%. Conversely, C2e sample presented a very high

LOI value compared to the parent sample (72.2 vs. 12.1%). The LOI values for C4e, C5e and C6e samples were <55%). Hence, C2 sample observed a better unburned carbon separation compared with others. The reason is because of the particle size difference between unburned carbon and minerals which helped the separation. This was described in particle size distribution studies. It can conclude that this method consists on particle size of the beneficiated sample and works with over 75 μm .

For those samples, multi stage separation improved LOI values. For example, the LOI value of B5 sample was reduced from 8.1 to 4% and the efficiency was around 50%, as shown in Table 4.3. Efficiency of separation was lower than that of C2, C4, C5, and C6 samples. Efficiency represents how much carbon has been removed, and this was calculated for the multi stage separation stream. The C2 sample has the highest efficiency (88%) compared with other samples. This was noticed according to LOI values and particle size distribution. It is also interesting that yield percentage was calculated for ash and carbon streams. This yield obtains the average amount retained (*i.e.* separated) to which ash and carbon streams. It depends on the efficiency of separation and it shows again C2 sample presents good yields for both streams. In contrast, B5 sample presents quite close values for efficiency and yield in both. This is because of the particle size difference between unburned carbon and mineral particles which is not significant and the maximum volume of those particles showed <60 μm .

Table 4.3: Incipient data analyses for the PFA samples selected.



This was illustrated in particles size distribution studies and it is an important point which was emphasised by the separation. In addition, this process was achieved of carbon removal and produced samples with LOI acceptable to cement specifications like B5d, C2d and C4d. C5d and C6d samples presented LOI values higher than the acceptable limit (*i.e.* 7%) [Biricik *et al.* 1999 and ASTM C-311, 2006], and therefore need more stages to get lower than 7%. It can be concluded from those samples that the maximum volume (*i.e.* mainly unburned carbon particles) observed $<100\mu\text{m}$. It had been noticed in B5 and C4 samples that a filter blockage occurred frequently. The reasons are probably due to the high amount of fine particles ($<50\mu\text{m}$), irregular particle shape (*i.e.* not spherical) and smaller particle size difference, as described previously in particle size distribution and SEM studies. Finally, C2d, C4d, and B5d samples were chosen for cement tests and C2e, C4e, C5e, C6e, and B5e samples for carbon activation.

4.7 Cement tests

Three samples B5d, C2d and C4d were mixed with cement as well as air entrainment agent AEAs, as described in section 3.5. The air entrainment agent type *AE3 Cormix* was used with these mixes PFA/cement. According to Table 3.2, 50 ml of AEAs was added in each mixture. Table 4.4 presents the results of the 7 days test and Table 4.5 the results of 28 days. It can be seen that the workability (*i.e.* slump) for B5d, C2d and C4d samples were 50 mm, 70 mm and 130 mm, respectively.

Hence, C2d sample showed higher workability compared with others. This was caused by the spherical shape of the mineral particles, as their presences have

more than irregular particles. This was described in SEM studies and also work done by Hobbs and npower [Hobbs, 1989 and RWE International, 2010]. These people were illustrated the water ratio carefully with PFA/cement mixtures. The particle shape can enhance the workability and increase the slump more than the limit (*i.e.* no greater than 70mm) [Hobbs, 1989 and Alhozaimy, 2007].

The workability of B5d sample observed lower than 70 mm, which indicates a high percentage of irregular particles than spherical existed in it, as described by SEM images. Thus, it needs more water during the cement mixing than others. Usually, biomass co-firing PFA particles are irregular in shape, density too low, and higher unburned carbon, which have all been described biomass co-firing characteristics. This is also described by Found and Naik [Foud *et al.*, 1998 and Naik, 2003]. All these aspects can influence on the workability of the cement. Meanwhile, AEAs was added with cement mixture for samples C2d, C4d, and B5d (*i.e.* 5% and 10%). This agent helps to trap carbon particles, increase the workability of the mixture and increase the air voids to prevent thawing and propagation of the concrete during the winter time. It is important to consider water ratio with this agent (*i.e.* liquid phase) in the mixture in order to get good workability.

It can be seen from Tables 4.4 and 4.5 that compressive strength data for all concrete specimens are different. In previous studies found that the compressive strength depends on cement content, type of the cement used, water content, air content, amount of PFA and density of the specimen [Lesley *et al.*, 1996 and Forsroc, 2007]. The compressive strength data present an

increase after 28 days compared to the 7 days tests. This indicates a slower rate of strength development but longer term final strength in all samples. The idea with PFA/cement mixtures which showed the strength developed in a longer period. For example, Europe applies 7 and 28 days strength tests, while USA applies up to 1 year tests. This explains the difference of cement regulations between the countries according to the environmental issues, weather conditions and public awareness [Scotash, 2007 and FLSmidth, 2009]. Consequently, B5d sample approved a good strength after 28 days rather than 7 days. This also applies into C4d sample, while C2d sample gained lower strength. This was influenced by the lower workability obtained in it. In addition, the maximum load was increased after 28 days compared to 7 days tests as it happened with all the samples. This appeared in the same manner with the strength development. Again, B5d sample shows a higher maximum load than the others.

Table 4.4: The test results of concrete mixes after 7 days.

Samples	Max Load (kN)	Compressive strength (N/mm²)	Mass in air (kg)	Mass in water (kg)	Density (kg/m³)	Slump (mm)
C4d (5% admixture)	137	14	2.1	1.1	2128	70
C2d (10% admixture)	93	9.3	2.1	1.1	2060	130
B5d (10% admixture)	156	15.5	2.2	1.2	2180	50

Furthermore, the density results for 7 and 28 days of B5d sample were higher than C2d and C4d samples, as shown in Tables 4.4 and 4.5. This was reflected by the mass (*i.e.* mass in air) and the strength which presented higher than

others. It was observed by Uysal the amount of water contained in concrete mixes effect the density [Uysal *et al.*, 2004]. Meanwhile, C2d sample showed lower density according to the water dispersion between the particles in it. There is no effect occurred from the mass measurements of this sample or even with others. The mass difference in air and water of each sample mixture was 1 kg, so the air voids created after mixing was good. In addition, the colour of C2d and B5d concrete blocks was darker than C4d blocks due to a higher amount of PFA.

Table 4.5: The test results of concrete mixes after 28 days.

Samples	Max Load (kN)	Compressive strength (N/mm²)	Mass in air (kg)	Mass in water (kg)	Density (kg/m³)	Slump (mm)
C4d (5% admixture)	183	18	2.2	1.2	2160	70
C2d (10% admixture)	136	14	2.1	1.1	2080	130
B5d (10 % admixture)	213	21	2.2	1.2	2193	50

4.8 Carbon activation

This section discusses the studies conducted on the samples C2e, C4e, C5e, C6e and B5e. They were activated at a temperature of 850°C and different times 60-300 minutes. These samples characterised through calorific value, BET surface area measurements, optical microscopy and methylene blue measurements. In addition, the resulted samples were also characterised in the above techniques.

4.8.1 Calorific value

The calorific value was measured for C2e, C4e, C5e, C6e and B5e samples. The calorific values (CV) recorded in as received basis are presented in Table 4.6.

Table 4.6: Calorific values for the carbon rich streams (asr).

Sample	Calorific value J/g
C2e	29487
C4e	27929
C5e	21947
C6e	26094
B5e	30498

Basically, the calorific values presented in Table 4.6 with the exception of C5e sample, are within the range expected for UK bituminous coals (24000-35000 J/g) [Krevelen *et al.*, 1993 and Mott MacDonald, 2004]. The reason is because of the mineral content is higher than the carbon residual (*i.e.* unburned carbon) and lower in volatile matter as described at proximate analyses. It can be seen that the CVs of samples C2e, C4e, C6e, and B5e are within the range above. So, these samples could be considered as a supplemental fuel, as it is been tried at Harbor power station in USA [Bittner *et al.*, 2001].

Moreover, B5e sample presents highest CV (*i.e.* fuel value). This is a good sign as it showed carbon rich material. This separated from high carbon PFA subtitle high fuel value which would benefit for the utility industry.

4.8.2 Adsorption-desorption isotherms

Adsorption isotherms were conducted for samples C2e, C4e, C5e, C6e and B5e before and after activation. The activation conditions applied for these samples were 850 °C and activation times of 60, 90, 120 and 180 minutes. All the

isotherms are presented in appendix E and the representative (*i.e.* high carbon PFA) figures are included in this section. The adsorption isotherm of all samples are Type II according to the BDDT (Brunauer, Deming, and Teller) [Brunauer *et al.*, 1940] classification which was previously described in section 4.3.

It can be seen that B5e sample presents an isotherm with a long tail compared with others (Figure 4.27). This indicates that this sample adsorbs higher volumes at saturation pressure and this is related to a larger proportion of meso- and macropores. C2e, C4e, C5e and C6e samples adsorb lower volume (*i.e.* maximum 20cm³/g) and follow the same trend. This shows that these carbons have a lower surface area and don't show hysteresis loop. Consequently, isotherms line of C2e and C6e samples cross with each other, similar to C4e and C5e samples. This resulted because of the lower porosity and similar adsorbed volumes, as shown in Figure 4.27.

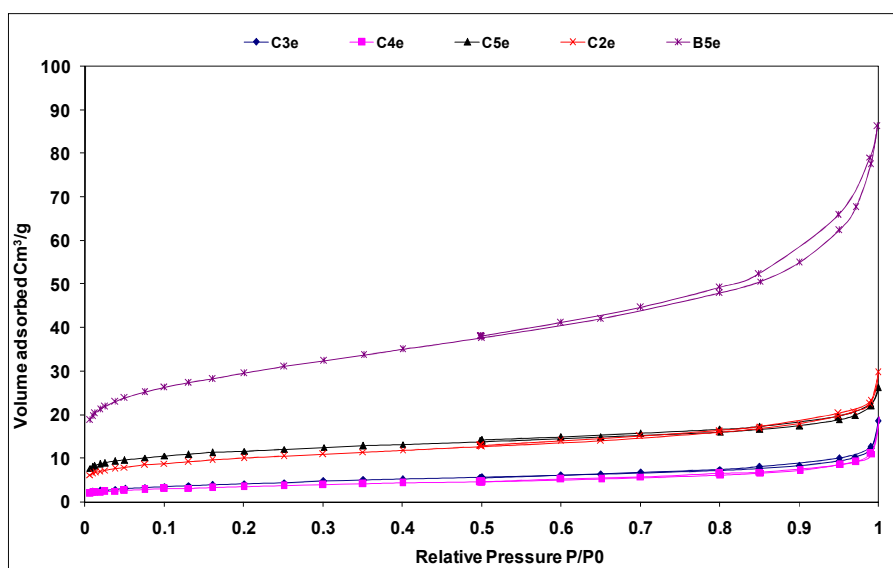


Figure 4.27: Isotherms of carbon rich samples prior activation.

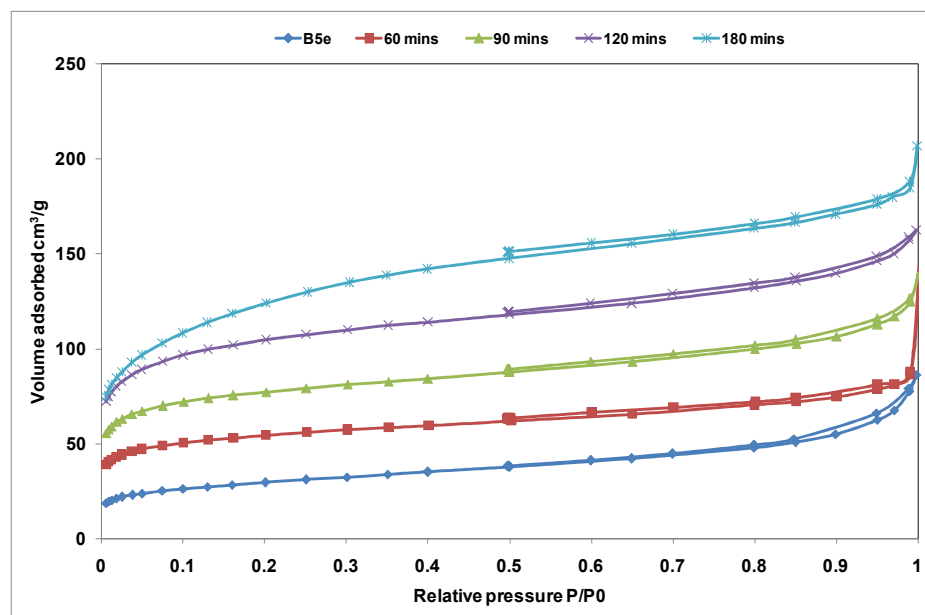


Figure 4.28: Isotherms of B5e sample before and after activation.

Figure 4.28 shows the isotherms of sample B5e with different activation times. With increasing activation time, the adsorbed volume is higher than that the parent sample. The isotherms are followed by the same type (*i.e.* Type II) as a parent sample. It appeared with a concave shape when the activation time increased. Moreover, sample C2e isotherms change significantly between 60-120 minutes activation, as shown in Figure 4.29. This is because of the porosity in B5e and C2e samples which reacted differently.

Therefore the development with activation times resulted in different findings. This was described by Bansal discussing how the porosity in different precursors may differ during the activation process because the mineral matter in some of them will catalyze the activation process. Hence, this will cause changes in the porosity as compared with parent sample [Bansal *et al.*, 1988]. This is consistent with the variations observed in surface areas and carbon burn-out that will be discussed in the carbon burn-out section 4.8.3.

Furthermore, it can be observed that the adsorption isotherms change from Type II to Type IV for sample C2e with different activation times compared to B5e sample. The reason has resulted from the adsorbed volume which increases rapidly at low relative pressure, while at higher pressures, the adsorbed volume increases very slowly. This appears that most of the pores are in the micropore range. It was observed by Maroto-Valer from carbon separated from PFA and steam activated that the isotherms type change with activation time [Maroto-Valer *et al.*, 2002a]. This also depends on the precursor type and mineral matter existed with pores [Bansal *et al.*, 1988].

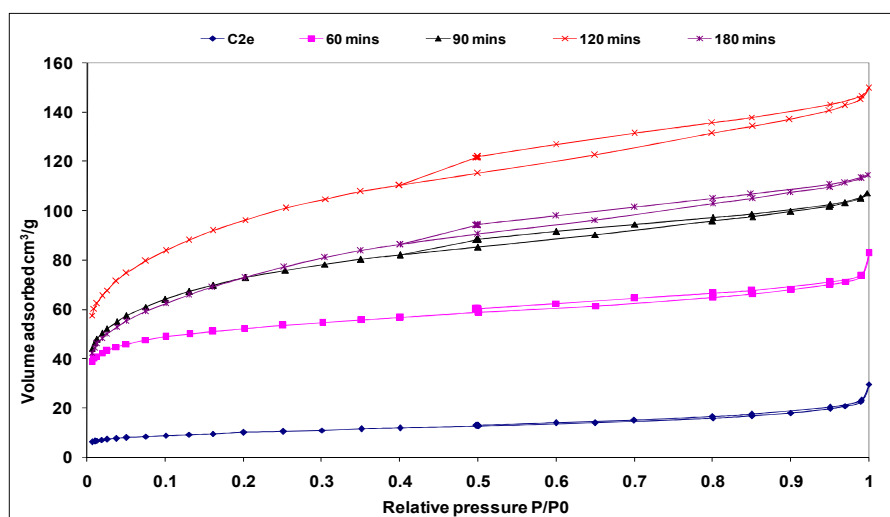


Figure 4.29: Isotherms of C2e sample before and after activation.

Figure 4.30 compares the adsorption isotherms of all the activated samples using steam at 850°C and for 120 minutes. It can be seen that the B5e and C2e samples present an isotherm with higher volumes adsorbed (≈ 165 and $150 \text{ cm}^3 \cdot \text{g}^{-1}$, respectively) to reach saturation pressure. This is consistent with those two samples presenting higher surface areas compared with the other enriched

carbons (section 4.8.3). Therefore, those two samples could be a good source of activated carbon within the samples studied here.

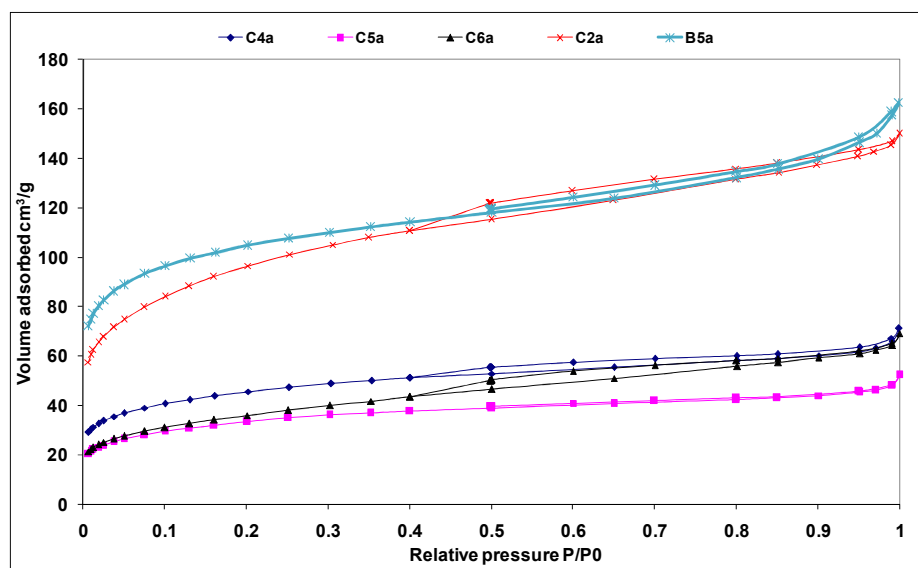


Figure 4.30: Isotherms of activated carbons after 120 minutes activation.

It is speculated that the difference in adsorption volumes of the samples studied is probably due to the different combustion temperature and heating rate that their parent-coals underwent while in the boilers.

It should also be noted that the B5e sample is derived from biomass (5% oat) and Russian coal (95%), and C2e sample is derived from a Colombian coal, while the other samples are derived from a US Pittsburgh coal. Hence, this obtained different behaviour with the same experimental conditions for all the resultant carbons. For example, B5e and C2e samples showed a concave region at a low relative pressure.

In addition, they exhibit higher adsorption isotherms at lower and higher relative pressures compared to C4e, C5e and C6e samples. This was indicated by the pore development and surface areas of them which were lower, as

shown in Figure 4.30. It can be seen that the pore development and the increase in surface areas were achieved after longer periods of activation. The reason is the wall structure of the unburned carbon in these samples observed thicker walls compared with others and need longer time of activation to get break up in order to achieve high value of pore development. Thus, the surface area depends on the heat treatment temperature [Marsh *et al.*, 1964].

On the other hand, B5e, C2e and C6e samples are mostly mesoporous, as shown in Figure 4.31. Samples C4e and C5e samples did not show any micropore volumes compared with others. This was indicated by the isotherm shape (Figure 4.30) and lower surface areas resulted by them. It can be added that the pores in these samples were mainly represented mesopores rather micropores. However, the steam activation process increases the pore volume of the samples, and enhances the development of micropores more than the mesopores volume (Figure 4.32).

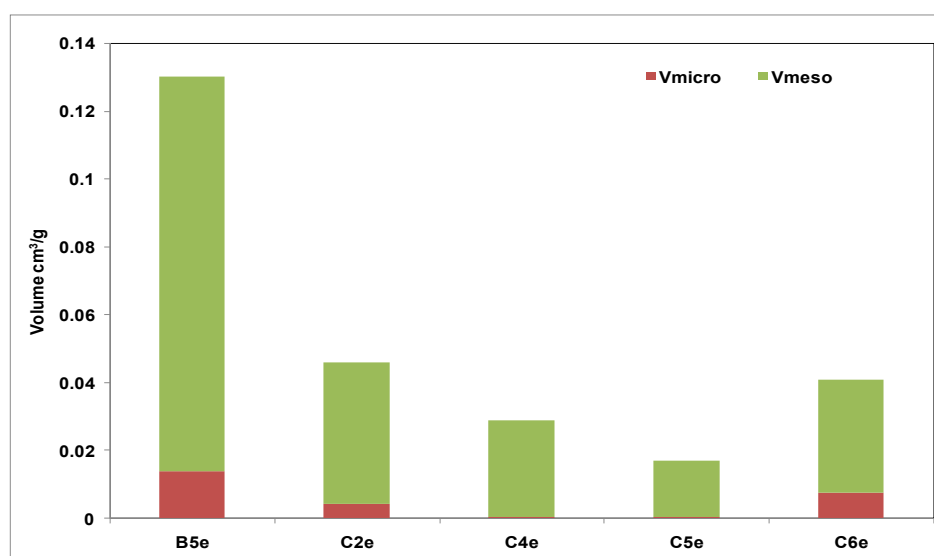


Figure 4.31: Micropore and mesopore volumes of enriched carbons before activation.

Samples B5a and C2a illustrate a good level of micropore volume perhaps more than others. This is because of the wall structure of the carbon particles which accept the conditions mentioned above in terms of the development of micropores. Previous studies conducted by Harold describe the activated samples with high surface areas and narrow microporosity, which are more suitable for commercial adsorbent materials [Harold *et al.*, 2001]. There are more information in regards the classification of the isotherms in section G.4- appendix G.

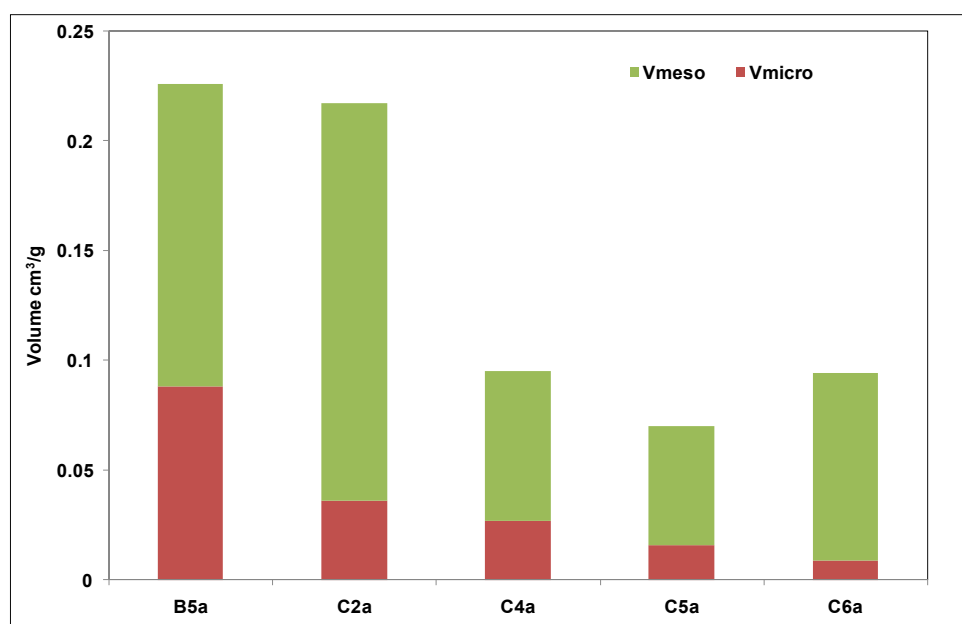


Figure 4.32: Micropore and mesopore volumes of activated carbons after 120 minutes activation.

4.8.3 Carbon burn-out, porosity development and solid yield

This section discusses the relationships between carbon burn-out, porosity development and solid yield for the activated samples. Figure 4.33 presents the variation of surface areas (carbon basis) with carbon conversion for the

enriched carbon samples B5e, C2e, C4e, C5e and C6e, and the resultant samples after activation. It is important to point out that the surface areas and carbon burn-out for all the samples are based on carbon. The carbon burn-out was calculated by subtracting the weights before and after the activation process and then divided by original carbon. The error of the surface areas is in the range of $\pm 6\%$, including the error from the activation process by running duplicates and surface area studies by measuring duplicates using BET method.

It is well known that the porous properties of the activated carbons, such as surface area, depend on the carbon burn-out [Lizzio *et al.*, 1990]. It can be seen that the surface areas of the activated counterparts develop gradually with increasing carbon burn-out. This development reaches a maximum value and then decreases as the burn-out level increases (Figure 4.33). This behaviour was also reported for the activation carbon separated from PFA [Koba, 1980 and Harold *et al.*, 2003]. Those studies illustrated this behaviour after 120 minutes activation while in this project only C4 followed it and other samples achieved it after 180 minutes, as shown in Figure 4.34.

Moreover, the behaviour of burn-out level takes place differently between these precursors. This is because of the raw materials, conditions applied and the compositions of inorganic in every precursor. B5 and C2 samples present higher surface areas with lower burn-out level. It can be considered that this reflection focused to preserve the destruction of porosity. Because of a longer period applied of activation, this will reduce the pore development and the surface area.

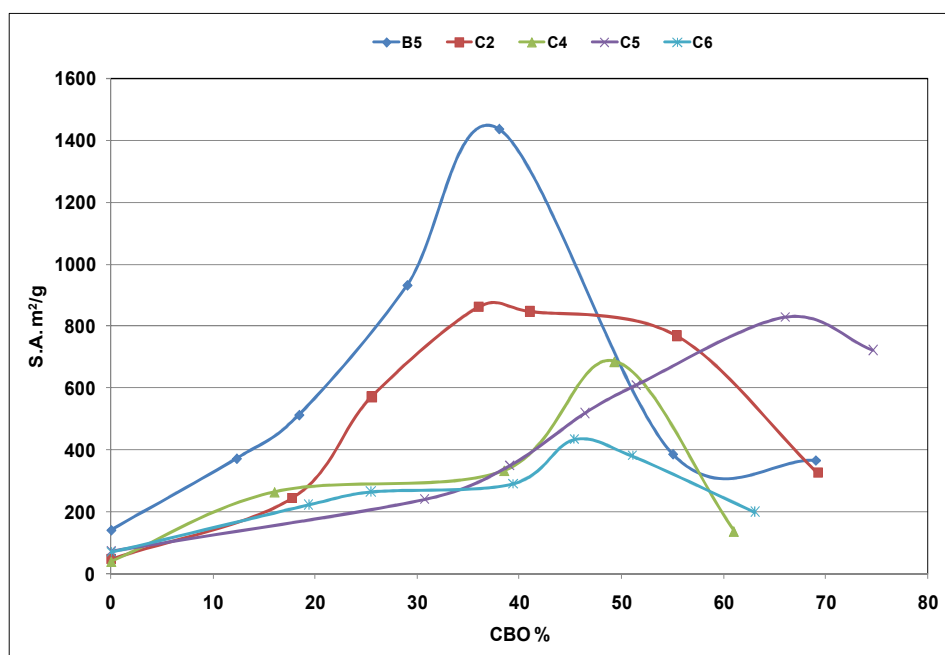


Figure 4.33: Variation of surface area (carbon basis) with carbon burn-out (carbon basis) for unburned carbons with steam activation at 850°C.

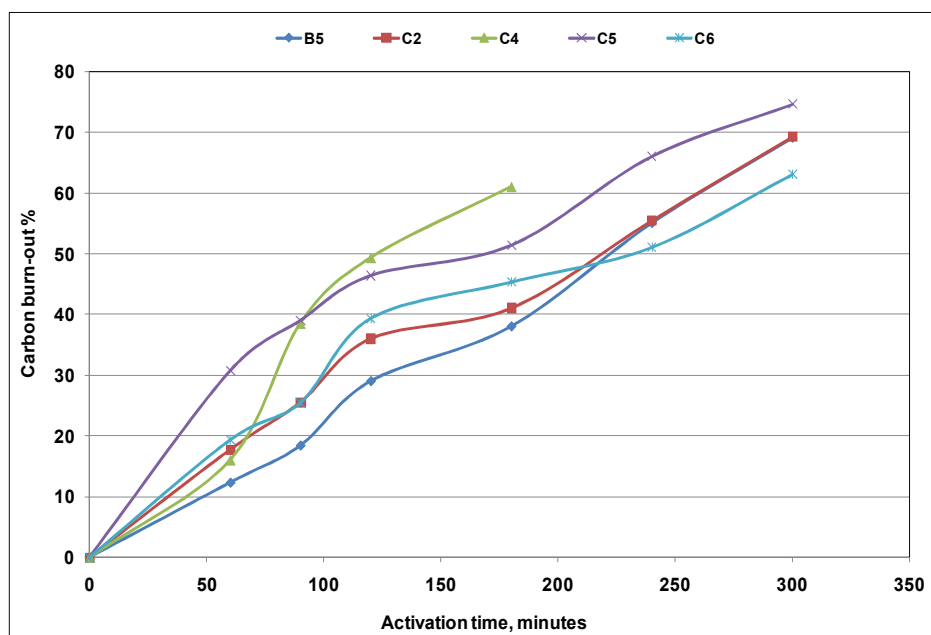


Figure 4.34: Carbon burn-out levels with activation time for the activated carbons selected.

The burn-out level at a maximum surface area presents differently in these samples, for example, B5 and C2 samples present 38% and 35%, respectively, while C4, C5 and C6 samples present higher burn-out 50%, 65% and 45%, respectively. The lower burn-out for the B5 and C2 samples could be possibly due to its low reactivity, as previously described in the TGA studies. In addition, the inorganic content reduces the reactivity and burn-out level, which was observed by them, as described in EDX and XRD studies.

Previous work has reported on high carbon concentrates in PFAs and activated chemically [Harold *et al.*, 2003]. The chemical process was chosen as it can produce activated carbon with a surface area up to 1075 m²/g. Compared to the work reported here, it should be noted that the carbon concentrates separated by incipient fluidisation and activated using steam at 850 °C present LOI values up to 70-80%. Furthermore, the highest surface obtained is up to 862 m²/g. Although the chemical method is more effective than steam activation in terms of producing samples with highest surface areas, this method present some disadvantages. This includes the used of costly and toxic chemicals, and generated chemical waste. Finally, it should be noted that the different samples which were used in both studies presented and showed different surface areas according to the conditions applied and the removal of inorganic content.

Figure 4.35 presents the change of surface area with activation times of unburned carbon samples during steam activation. It can be seen that the variation in surface area with activation times showed differently by these

samples. B5 and C2 samples present higher surface areas after 180 minutes while C4 sample after 120 minutes.

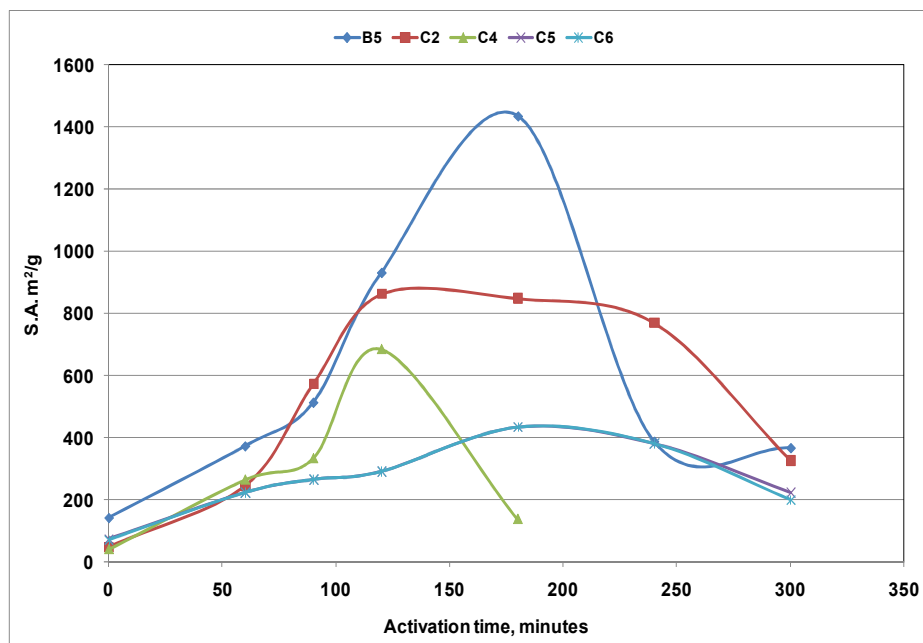


Figure 4.35: The surface area plotted with the activation times.

The reasons are accordingly to inorganic content and the wall structure of unburned carbon. These samples illustrate the surface area, which increases after 180 minutes except C4 sample. In contrast, a previous work illustrates the maximum surface area achieved within 120 minutes and decreases after this time [Maroto-Valer *et al.*, 1999a]. Consequently, it may keep increasing during the activation due to pore enlargement and pore coalescence. This was observed by Maroto-Valer and Sun as they presumed this increase took place smoothly after two hours and tried different carbon resources (*i.e.* coals and PFA) [Sun *et al.*, 1997 and Maroto-Valer *et al.*, 1999a].

The increasing in surface area with carbon burn-out level at the early stage of activation indicates the development of porosity by burning out of active carbon structure and opening of blocked pores [Maroto-Valer *et al.*, 1999a and

Harold *et al.*, 2003]. The subsequent decrease of the surface area is caused by extensive gasification. This is presumably due to the pore widening and the destruction and merging of the pore walls between the micropores after a certain carbon burn-out level, which varies from different raw materials (parent coal), combustion conditions, and boiler type [Bansal *et al.*, 1988 and Chi *et al.*, 1989].

Table 4.7 presents the solid yield and surface area for the resulted samples after activation in duration 60 and 120 minutes. It can be seen that the solid yield is decreasing when the activation time is increasing for the five enriched carbons, while the surface area is increasing until reaching the maximum and then it drops back.

Table 4.7: The solid yield and surface area for all the samples at 60 and 120 minutes activation.

Sample	Time (minutes)	Solid Yield (%)	S.A. m ² /g
B5	60	91	372
	120	80	930.6
C2	60	87	243.3
	120	74	862
C4	60	94	264
	120	82	685
C5	60	88	239
	120	81	517
C6	60	89	222
	120	78	290

The reduction in solid yield had been noticed after 120 minutes in terms of the duration of carbon gasification and occurred differently in these samples. The solid yield depends on the carbon-out level. For example, if it decreases, then the carbon burn-out increases. The solid yield is always decreased due to the

gasification process. B5, C2, C4 and C5 samples present a significant increase in the surface area going from 60-120 minutes activation 372 vs. 930, 243.3 vs. 862, 264 vs. 685, and 239 vs. 517 m²g⁻¹, respectively while C6 presents a little increase in the surface area 222 vs. 290 m²g⁻¹. This change in the surface area is related to the open pores inside the carbon particles and controlled by the wall thickness and inorganic content, as described previously.

As mentioned above, the char gasification starts with the elimination of disorganised carbon, and this occurs at a relatively high rate. The result is the opening of blocked pores of the char. Subsequent gasification affects the skeleton of the carbon structure, thus resulting in the widening and deepening of the pores. Consequently, increasing burn-off produces an increase in pore volume and surface area of the activated carbon [Maroto-Valer *et al.*, 2001 and Harold *et al.*, 2003]. This is the general behaviour found for most activated carbons prepared by steam activation from different precursors. It is observed that there is an initial increase in micropore volume up, mainly produced by the opening of partially blocked pores in the char. Thereafter, the increase in pore volume is smaller, and generally after 40-50% burn-off the micropore volume continually decreases [Zhang *et al.*, 2003].

Finally, this work has showed that the surface area reaches a maximum value from 1-2 hours activation only for C4 samples. In contrast, B5, C2, C5 and C6 samples observed increase in the surface area after three hours activation. This indicates when the surface area reaches the maximum value, the higher carbon burn-off level resulted (*i.e.* very low solid yields). This followed to the char wall structure, active sites in every carbon particle, minerals content and the

carbon porosity. Therefore, B5, C2 and C4 samples could be considered as good precursors for activation, due to high surface areas, while the solid yields were still high (>50%).

4.8.4 Optical microscopy (Automated analyses)

Optical microscopy studies were conducted on B5e, C2e, and C4e and their activated counterpart at 850 °C and activation times 60 and 120 minutes. This study presented two types of images such as full view and particle view. Full view considered whole parts (*i.e.* particles group) which focused on different particles shapes, while particle view covered only 1-3 particles. The full view images were discussed as it explained the general view (*i.e.* morphology) of the sample, whereas particle view is related to random particles in terms of particles identification. All images presented in appendix F. The representative (*i.e.* high carbon PFA) images were included in this section. It is more important that all these images were compared with the atlas in order to identify the char types and minerals [Hower, 2001].

However, the ash contents for C2e, C4e and B5e samples are 20%, 60% 40%, respectively. The mineral particles were devolatilised during coal combustion and shaped differently, as previously described in section 2.1.2 and SEM studies. Some of these particles are also diffused during the activation according to their structure properties and heat rate.

The unburned carbon present in PFA is composed of three petrographically distinct carbon types, namely inertinite, isotropic coke, and anisotropic coke [Maroto-Valer *et al.*, 1998 and 1999b]. Both coke forms are most likely derived from vitrinite macerals and are artifacts of incomplete combustion. Porous carbons are a non-graphitic form of carbon and they characterised by

internal surface areas (*i.e.* micropore areas) [Patrick, 1995]. Isotropic coke comprises non-graphitizable carbon particles, while anisotropic coke consists of more highly aligned carbon particles, and they can be differentiated by the optical activity of the latter ones [Zhang *et al.*, 2003].

It can be seen that the walls of unburned carbon particles are often incomplete, either as a result of porosity or wall breakage during coal combustion and carbon activation (Figures 4.36-38). B5e sample showed that the isotropic coke particles are more abundant than the anisotropic coke as showed one in the centre-top (Figure 4.36-a and b). It can also be observed that the char walls are thinner for the biomass sample compared to the samples derived from coals (C2e). Moreover, the C2e sample shows that there are more isotropic coke type particles than anisotropic (Figure 4.36-c and d). There are few white solid unfused particles that are identified as inertinite.

Figure 4.37 presents optical microscopy images of the activated samples after 60 minutes activation. There is an (a) letter added with each sample to specify that this sample has been activated. The wall thickness of the carbon particles has become thinner during activation, due to the carbon gasification and it is expected that this may result in an increase in the surface area and reduce the wall thickness. The B5a shows isotropic cokes, anisotropic cokes and inertinite particles. It can be seen that more particles have more walls breakage compared with C2a images (Figure 4.37-a-d). The images of the C2a sample after 60 minutes activation show isotropic cokes, anisotropic cokes, inertinite and glass particles.

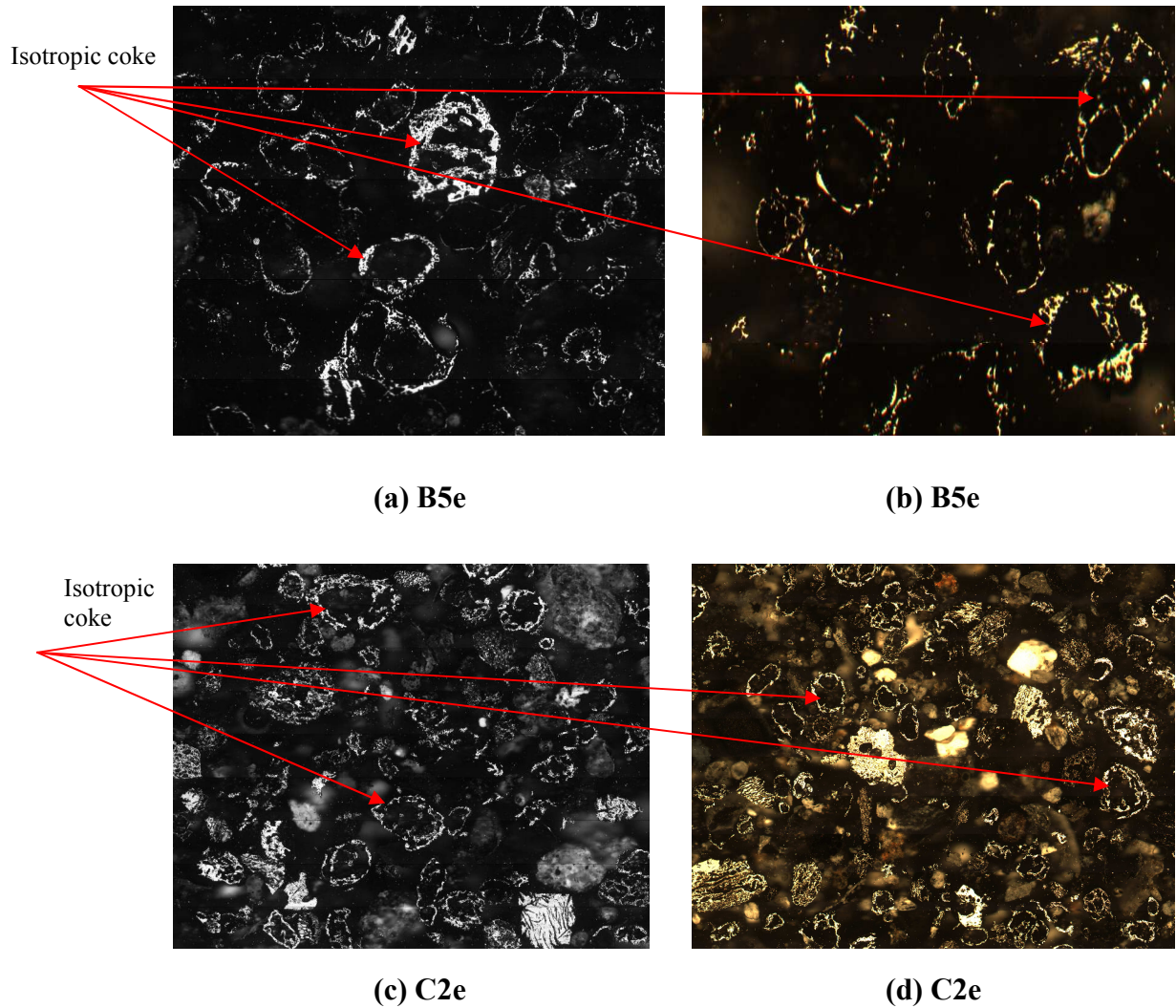


Figure 4.36: Optical microscopy images of carbon rich samples

Furthermore, inertinite and anisotropic coke presented in this sample, as shown in Figure 4.37-d (top left). It can be seen that the char walls of C2a have become thinner or have been fused, due to the carbon gasification process during activation.

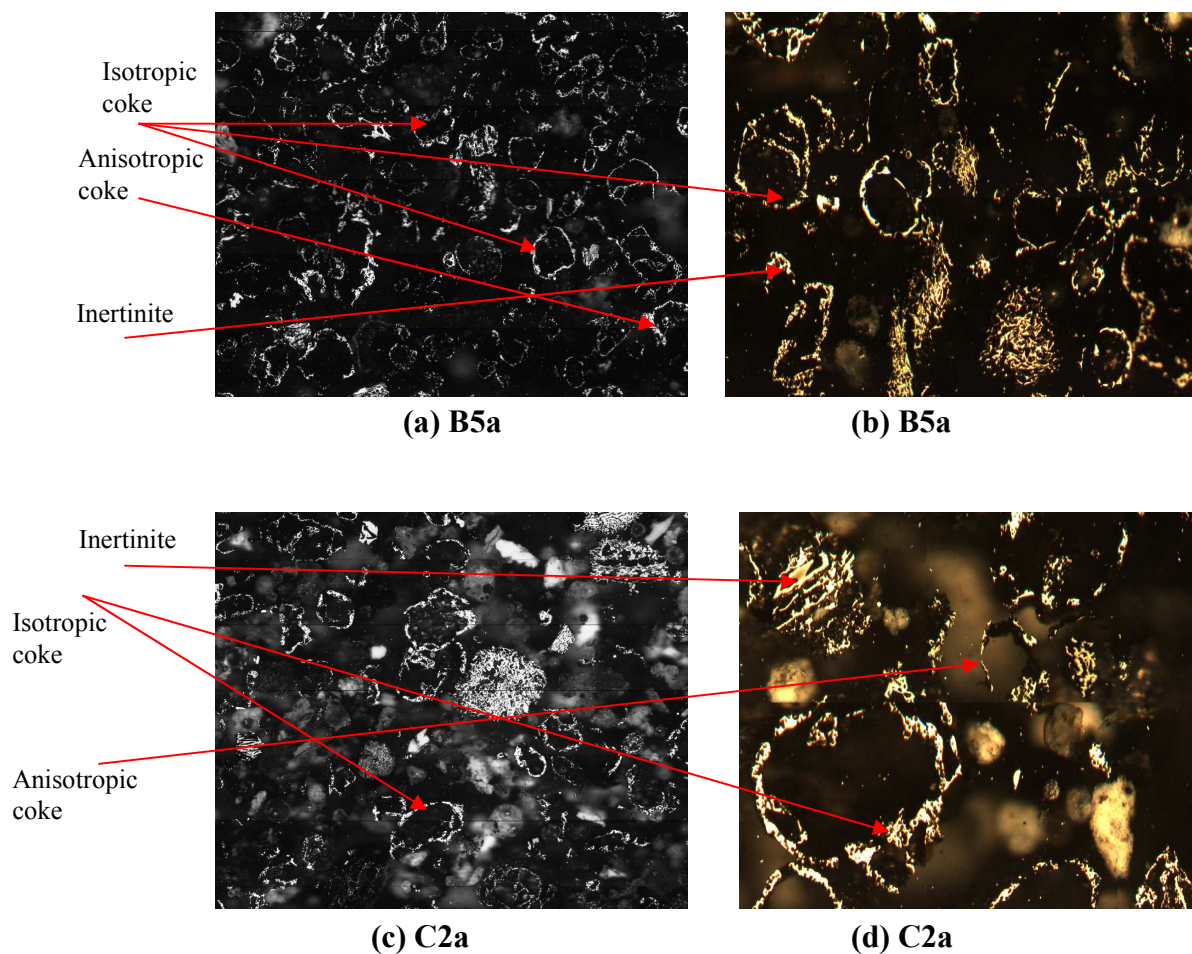


Figure 4.37: Optical microscopy images of activated carbons after 60 minutes.

Figure 4.38 presents the images of activated carbons B5a and C2a after 120 minutes activation. As described previously, the char wall thickness became thinner but some particles are appeared with thicker walls. This is because of the breakage in the char walls which occurred during the activation and some other walls joined with each other to make thicker wall. This is complicated mechanism consisted of many factors such as wall thickness, char reactivity and type, heat rate and mineral content. In contrast, the carbon particles present

more fragmented walls compared to the samples after 60 minutes activation, as shown in Figures 4.37 and 4.38.

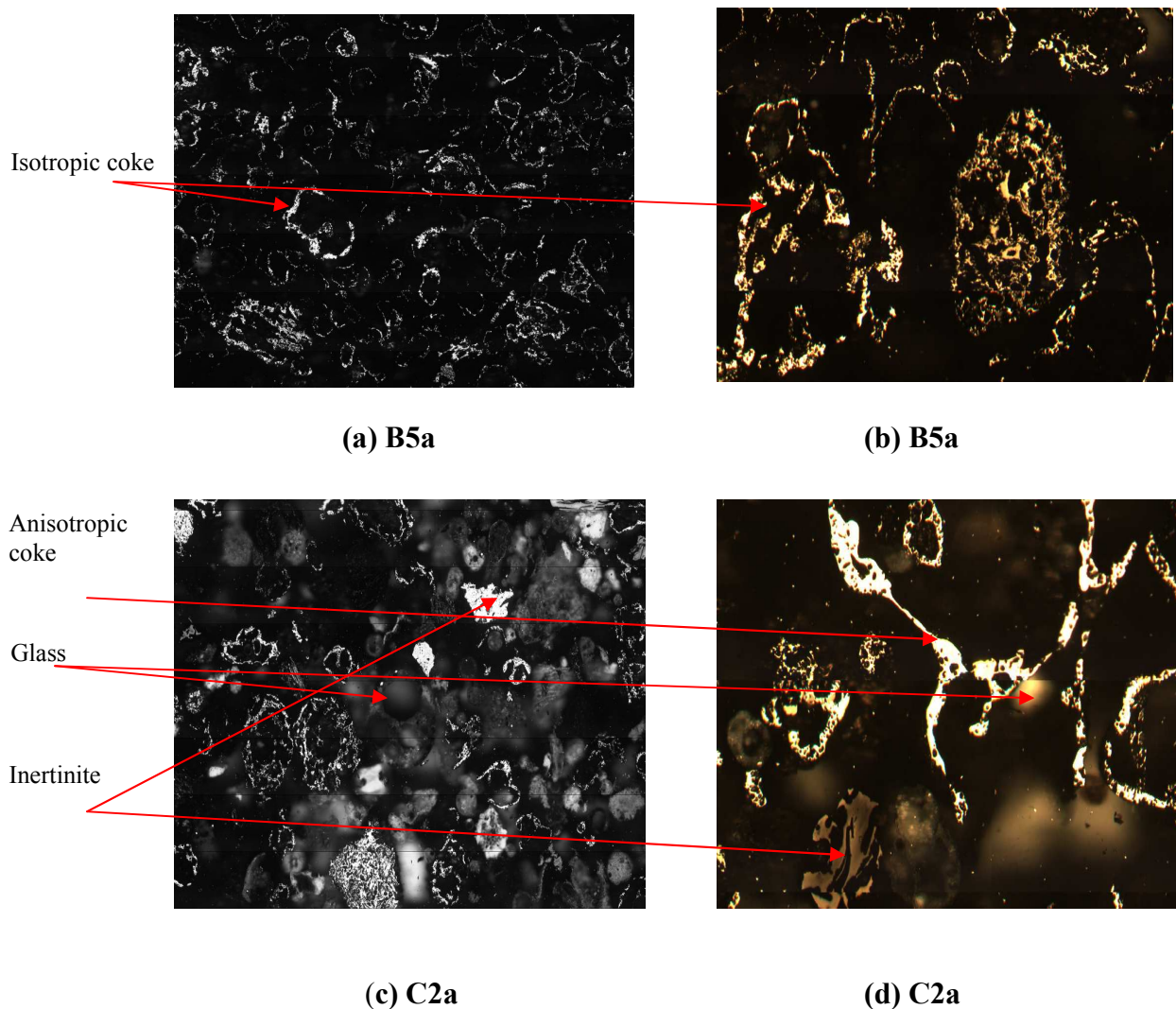


Figure 4.38: Optical microscopy images of activated carbons after 120 minutes.

Moreover, inertinite and glass spherical particles type quartz are shown in Figure 4.38 (c and d). It can be seen that the fragmented char particles joined together and made larger particles. Consequently, the majority type is isotropic cokes presented in all the samples compared with few anisotropic cokes. These

carbon types may change during the activation and varies into their parent coal. It is also the carbon reactivity changed to a low reactivity. This was observed by Zhang on unburned carbon in PFA [Zhang *et al.*, 2003].

There are few iron oxide particles and several showing mixed iron oxide/glass particles (Figures 4.36-38). This is also observed by Hower which conducted petrology studies on class F PFA sample. These studies showed a variety of iron oxide phases [Hower *et al.*, 1999]. Nevertheless, the surface area of char particles increases during the activation, as shown in Figures 4.37 and 4.38. This was discussed previously as char walls breakage are trapped with each other to make a larger particle. It can be noticed from the solid yield that some particles presented a large surface area before the activation and then confer a low surface area with expense of the solid yield (Table 4.7). The solid yield is gradually reduced according to carbon gasification, but on the other hand, the surface area increases due to pore enlargement.

4.8.5 Optical microscopy comparison of the biomass co-firing char and coal char samples.

This section summarizes the main findings reported from the optical microscopy studies for the purpose of comparison the char derived from biomass co-firing and coal only before and after the activation process. It should be pointed out that the biomass was co-fired in a lower ratio compared to coal (5%) and biomass particles are expected with high volatile matter than coal particles, as described in the literature review section 2.4. Hence, the resulted particles in the biomass co-firing sample B5 may come predominantly

from coal, rather than from the biomass due to the burning period very short compared to coal.

When comparing the chars from the biomass and coal derived samples prior to activation, it can be seen that the char particles present in the B5e sample have a more open structure (*i.e.* char walls) compared to the char particles derived only from coal C2e (Figures 4.36-4.38). The wall thickness of the char particles of the B5e sample was thinner than that of the char particles of the coal sample C2e. It can also be seen that the B5e sample has more round char particles compared to the coal sample C2e which observed irregular particles.

Consequently, the images in Figure 4.37 presented the particles with open end (*i.e.* char walls) and some particles decrease in size compare to the samples prior to activation. The C2a sample present high inertinite unfused and some semifusinite, whereas B5e sample showed thinner walls, open in some ends and broken walls.

The B5a images in Figure 4.38 illustrated to be darker than C2a images. This is probably due to the glass content resulting in low light reflection between the particles. C2a sample presented fragmented char walls and open walls. This sample also showed particles with thicker edges. The particle size changed depending on the wall thickness and the surface area. The particles in B5a sample developed open walls, and some particles appear in a bigger shape due to have joined with others.

Moreover, the sample B5a presented more fragmented walls, and open end particles. Isotropic coke type seems to appear more frequently in biomass co-

firing chars, compared with coal chars that are presented with more anisotropic coke type.

Finally, C2a images presented minerals trapped inside the char particles, while B5a images showed particles with thin walls, low in inertinite bright particles (*i.e.* it might be the coal itself had lower inertinite content), and few cenospheres. This is also described in the SEM images for these samples.

4.9 Methylene blue studies

The methylene blue provides an indication of the adsorption capacity of an activated carbon for molecules having similar dimensions to it in order to get adsorption. It can assess the adsorptive behaviour of activated carbon in terms of its propensity to adsorb higher molecular mass in aqueous solutions. Furthermore, it can compare its effectiveness as an adsorbent to that of a commercial equivalent. This test was conducted on three activated carbons B5a, C2a and C4a and one commercial sample Fisher-DC. The surface area of all these samples is listed in Table 4.8. The surface areas were taken after 120 minutes activation for all the samples except Fisher-DC provided by the manufacturer.

Table 4.8: The surface areas for the selected samples.

Sample	Surface area (m ² /g)
B5a	931
C2a	862
C4a	685
Fisher-DC	974

Fisher-DC sample presents surface area higher than other samples, as shown in Table 4.8. It can be seen previously that B5a, C2a and C4a samples were separated from high carbon PFAs, as they already devolatilised in the combustor

and then activated afterwards. Hence, the inorganic content for Fisher-DC is much lower (less than 10%) compared with the activated samples (around 60%).

Tables 4.9 and 4.10 present the methylene blue adsorption test for the activated carbons and commercial sample after seven days. These tests took place after this period in order to provide adequate adsorption. The calculations of the concentrations were carried out according to the equations presented in section 3.6.3. Twelve points were selected to conduct the methylene blue solution with water as presented in Tables 4.9 and 4.10. Both tables have four sections: (1) dilution factor applied when it is piped from the stock and then made up to 100 ml, (2) absorbance measured according to maximum wavelength of 665 nm, (3) residual concentration of methylene blue in each sample (C_e) (*i.e.* calculated from equation 3.4), and (4) methylene blue absorbed per gram of carbon (q_e) as calculated using equation 3.5.

It can be seen that the sample needed less water in dilution process showed high absorption of methylene blue. Thus, Fisher-DC and C4a samples (400 ml) present a lower amount of dilution factor compared to C2a and B5a samples (540) when all the samples were only diluted with 10 ml of methylene blue and no water. For a lower volume of methylene blue used (0.8 ml), Fisher-DC and B5a observe lower dilution factors (10 and 14.3 ml, respectively), while C2a and C4a show higher dilution factors (50 and 100 ml, respectively). This depends on the amount of methylene blue added in each solution.

Table 4.9 Methylene blue measurements after seven days for samples C2a and C4a.

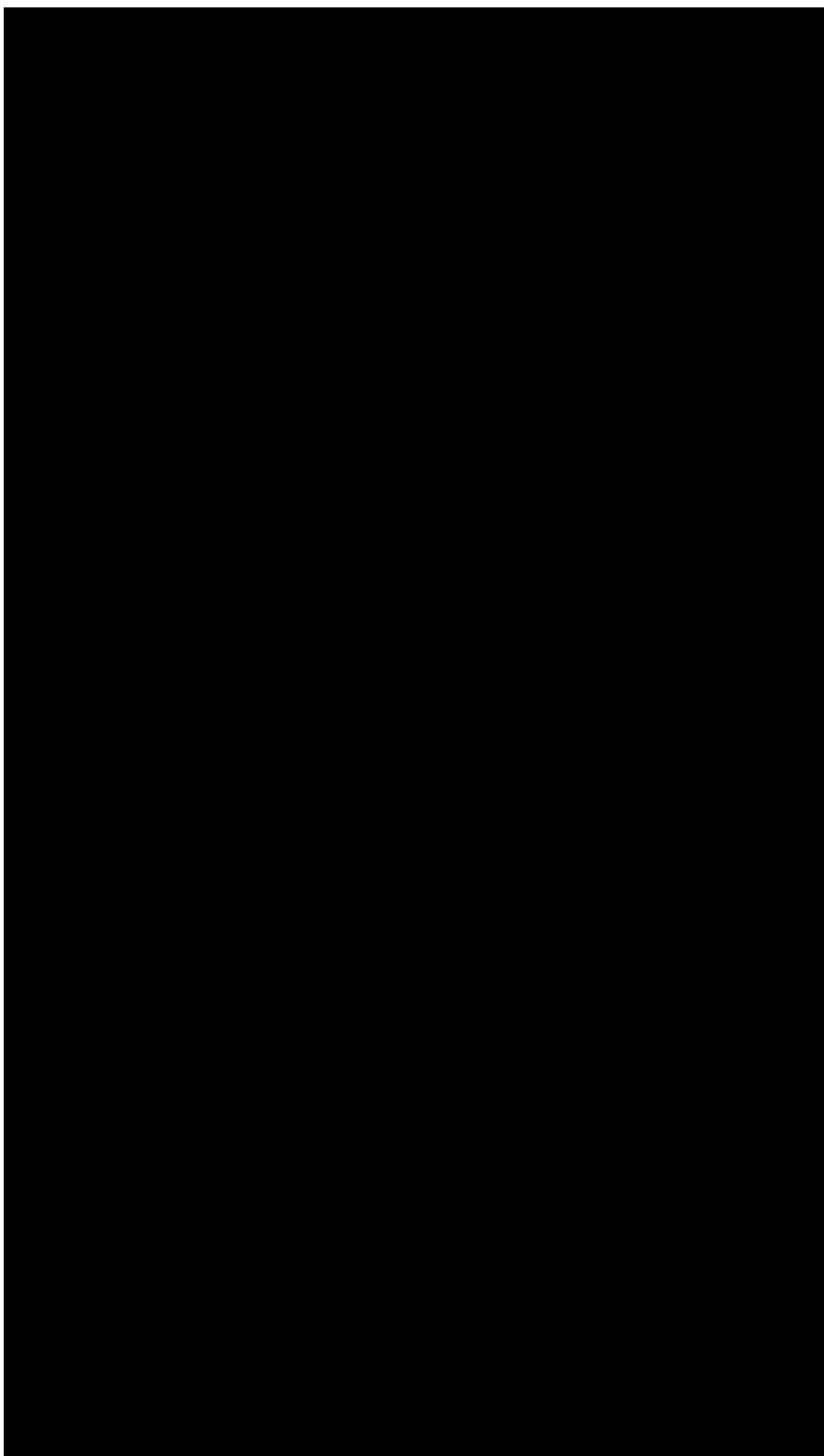
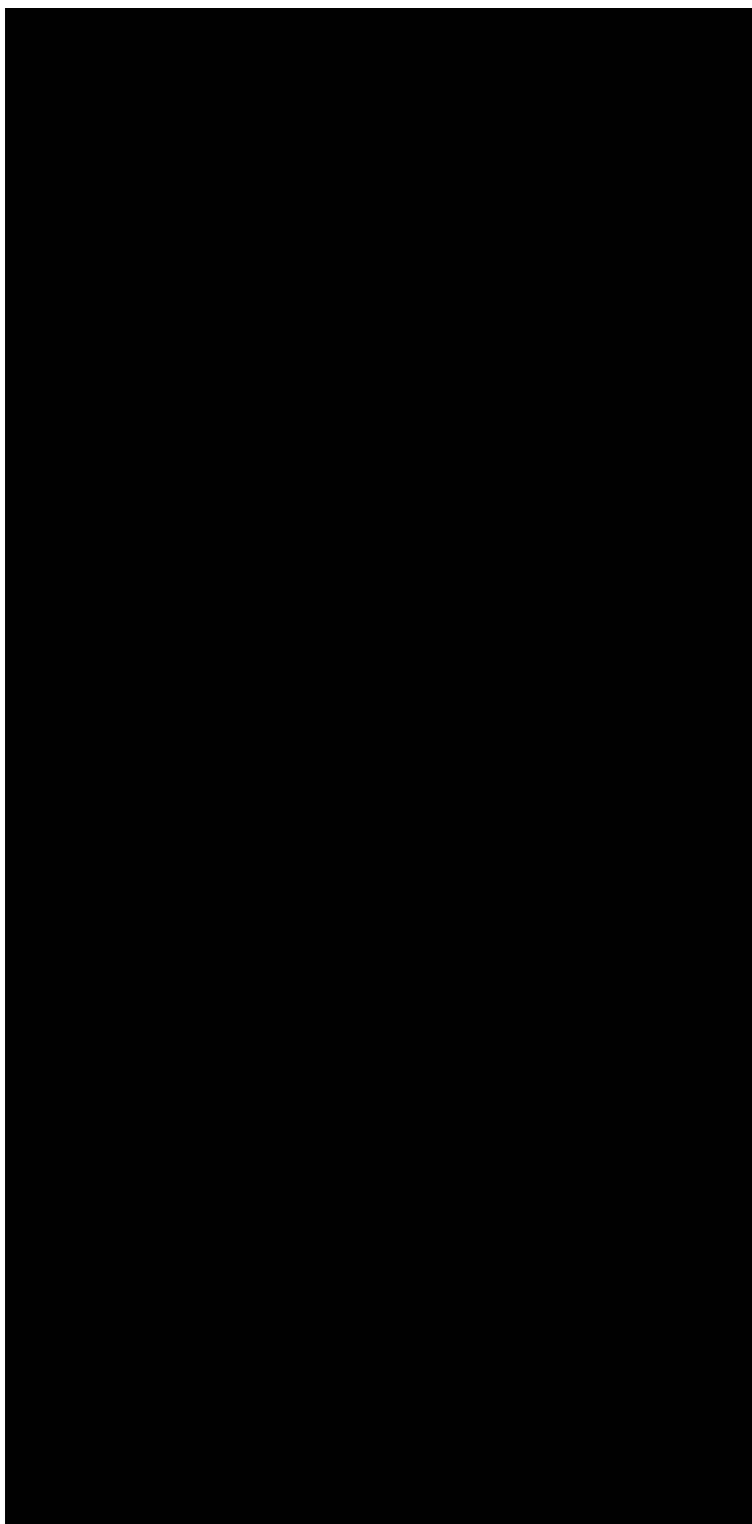


Table 4.10: cont. methylene blue measurements after seven days for samples B5a and Fisher-DC.



It was reported previously that the solution should present absorbance lower than 1nm in order to give better absorbance (*i.e.* calibration curve) [Yamin *et al.*, 2007]. The error was accounted up to $\pm 5\%$ for the dilution factor.

It can be seen that the absorbance of diluted solution increases with the methylene blue volume. The reason is because the blue colour was darker at higher dosage of methylene blue and lighter at a lower dosage. After seven days, the residual concentration of dye blue colour (C_e) was calculated through equation 3.4. It can be seen that C4a and Fisher-DC samples (higher methylene blue volume 10 ml) presented less methylene blue dye residual concentrations (3.95 and 4.26 mmol/litre, respectively) than C2a and B5a samples (5.79 and 5.73 mmol/litre, respectively). This was probably due to the mesoporosity generated, as discussed previously for these samples. This removal gradually decreased when the methylene dosage is decreased, as shown in Tables 4.9 and 4.10.

It is important to mention that C4a sample should present higher residual methylene blue concentration compared to others. This is because of the lower porosity and surface area exhibited by this sample and thus should adsorb lower concentration of methylene blue. Moreover, C4a sample presents higher methylene blue residual (0.8 ml methylene blue volume) compared with other samples. This could be an error resulted from the dilution and also the porosity of this sample was unable to adsorb at a lower concentration of methylene blue. Consequently, C4a and Fisher-DC samples (10 ml methylene blue volume) present higher methylene blue uptake (q_e) (3.21 and 3.15 mmol/g carbon, respectively) than C2a and B5a samples (2.84 and 2.85 mmol/g carbon,

respectively). This reflected by (C_e) as it was lower for samples C4a and Fisher-DC and then (q_e) calculated by equation 3.5 which resulted higher value, as described in section 3.6.3. Also, sample C4a should not observe high uptake of methylene blue as it already explained above.

It is also relevant to point out that the samples C2a and B5a showed quite similar methylene blue uptake concentrations (2.84 and 2.85 mmol/g carbon, respectively). This is because of the high mesoporosity which took place and the ability to adsorb high numbers of methylene blue molecules, as shown in Figure 4.39. This figure is to compare the overlaid adsorption isotherms. B5a and C2a samples presented straight lines compared to C4a and Fisher-DC samples. The reason is because the error occurred during the dilution factor measurements. Hence, the methylene blue removal from the solution is higher for C2a and B5a samples same as Fisher-DC sample. This is observed that the adsorption capacity for the resulted samples higher as the commercial sample.

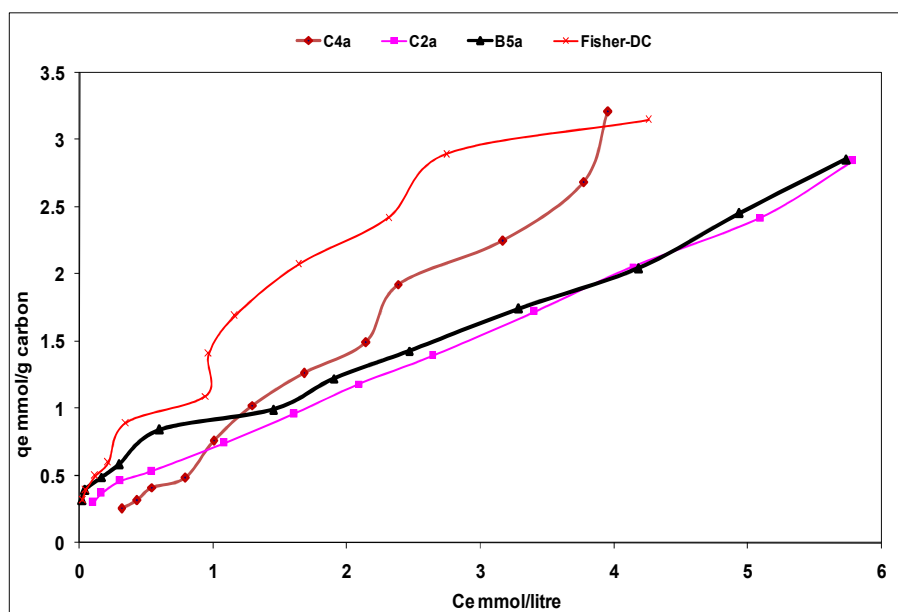


Figure 4.39: Adsorption isotherms for all the activated carbons.

4.10 Inductively Coupled Plasma-Atomic Emission Spectrometry (ICP-AES)

The determination of major elements on the initial PFA feedstock samples B5, C2, and C4 and their derivatives after beneficiation was carried out using inductively Coupled Plasma Atomic Emission Spectrometry (ICP-AES) following a three stage microwave digestion procedure. The analysed samples comprised of PFA (asr), the streams produced after PFA beneficiation for the selected samples (*i.e.* depleted carbon ash and enriched carbon), and activated carbon for these samples (conditions 850 °C and 120 minutes), as listed in Table 4.11. The major elements measured were Si, Al, Fe, Ca, Mg, Na, K, Mn, P, S, and Ti. These elements were presented in the same range of values as previous works [Maoming *et al.*, 2005 and Shuangzhen *et al.*, 2008a].

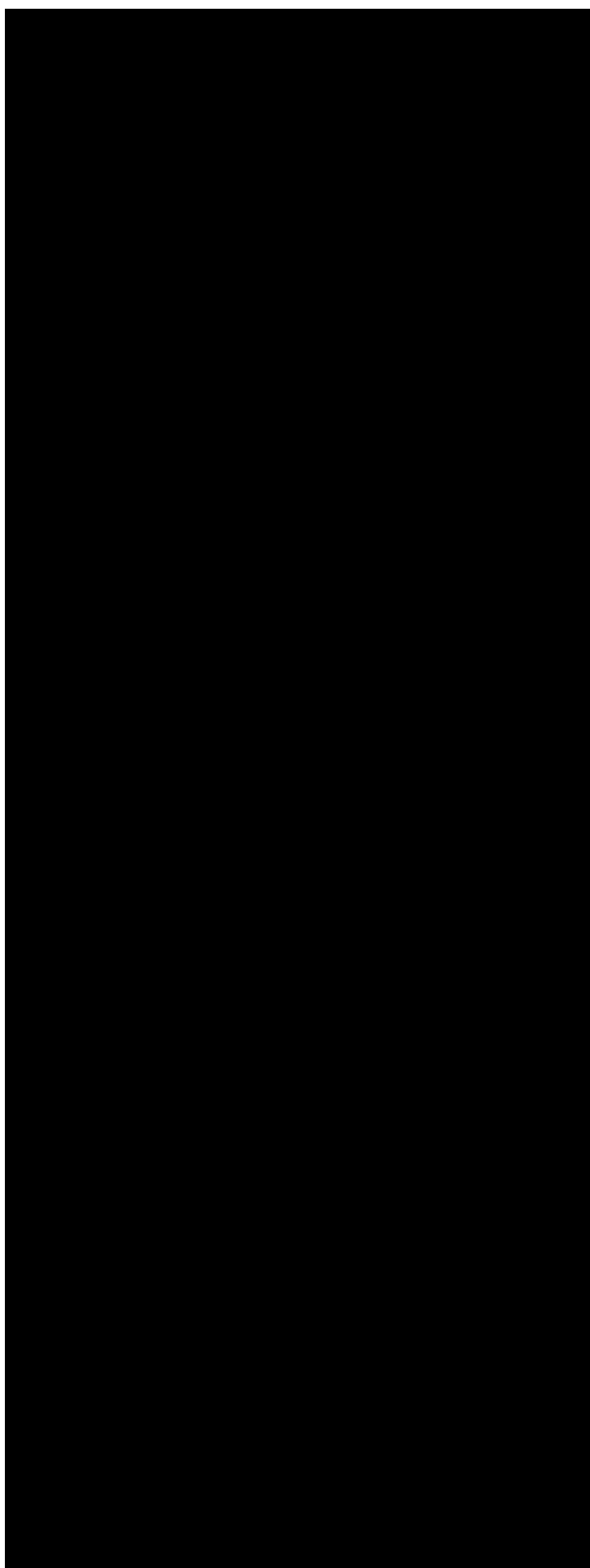
It can be seen that for all these samples, the main components were Si, Al and Fe, and presented altogether in total over 70 wt.% (Table 4.11) typical of Class F [ASTM C-311, 2006]. However, B5d, C2d and C4d were improved after the incipient fluidisation process (*i.e.* less carbon content) compared with untreated samples B5, C2 and C4 (asr). For the enriched and activated carbons, C2 showed lower minerals, less than 20%, while B5 and C4 showed over 50%. This probably is due to particle size difference between carbon and minerals higher than others, as described in particle size distribution studies.

These analyses measured the inorganic content in the activated carbons and indicated the purity of the precursor. For example, C2e presents less mineral compositions than others. In contrast, B5 sample showed more calcium content

compared to the C2 and C4 samples, as this sample was co-fired with biomass (oat) and the latter samples were derived only coal. The calcium content in the ash is important because in conjunction with others (Si, Al, and Fe), which contributes to the strength of concrete [Shuangzhen *et al.*, 2008b]. The magnesium content is fairly similar for depleted carbon stream ranging from (1.5-2.3%) and for the enriched carbon stream ranging from (0.4-1.0%), see Table 4.11.

Furthermore, B5 sample presents higher alkali contents (Na and K) than the C2 and C4 samples. Typically, B5 sample has greater alkalis than C2 and C4 samples and should be lower amount in order to be used with cement [Shuangzhen *et al.*, 2008a]. Consequently, the remaining elements (Mn, Ti and P) appeared with lower values in all the samples B5, C2 and C4, included the resulted samples. This is resulted from the original fuel content as accounted lower contents. Finally, these analyses were approved why some samples activated better than others. This is because of the mineral contents found by these analyses and the efficiency of PFA beneficiation in order to get enriched carbon with less ash. This technique also added another benefit in terms of the mineral content in the depleted ash samples and the alkalis for the co-firing samples when they will be used in the cement industry.

Table 4.11: ICP-AES data for the PFA (asr) and resulted streams.



CHAPTER FIVE

CONCLUSIONS AND FUTURE WORK

5.1 Overview

The aim of this project was to provide an insight into the utilisation of high carbon pulverised fuel ash derived from biomass co-firing and imported coals into a value added product. The approach chosen to achieve this entailed:

1. Utilisation high carbon PFAs derived from biomass co-firing and imported coals.
2. Production depleted carbon PFA and enriched carbon from PFA beneficiation using incipient fluidisation.
3. Assessment of the depleted carbon PFA by the cement application in order to produce high quality concrete from alternative fuels.
4. Assessment of the enriched carbon to regenerate pure carbon substrates in:
 - a. Sorbent material
 - b. Fuel Supplement

5.2 The resulting impacts from using alternative fuels.

Biomass has been exhibited more variation in both composition and amount of inorganic material compared to coal PFA. The main minerals in biomass ash such as Si, Al, and Fe were accounted in lower ratios. These minerals either fused within char particles or found as a free single particles. In addition, incomplete combustion in coal-fired power plants may result in LOI values up

to 15%. Biomass co-firing has been increased the amount of carbon content in PFA subjected to co-firing ratio.

The results indicated that the biomass co-firing samples still dominate a portion of coal. This was illustrated in the microscopy studies obtained no much difference between biomass co-firing PFA and PFA coal in mineral types and shapes. It has been shown that the compressive strength, slumps, durability all followed cement specifications. Also, concrete specimen with higher amount of PFA showed higher compressive strength compared to lower PFA/cement mixture. Air entrainment agent has been developed the workability and the strength of the concrete blocks. Cement tests had shown that the PFA/cement compressive strength developed after 28 days and could achieve higher levels in 56 days and 1 year. This strength consists on the amount of PFA and the cement specifications.

The resulted impacts of biomass co-firing were illustrated in the unburned carbon presented with PFA from un-combusted particles (*i.e.* particles not pulverised), un homogeneity of biomass PFA, and high alkali matter (Na and K). Moreover, biomass ash/cement has been shown lower workability which improves that these mixes need more water, whereas PFAs coals/cement required less water.

5.3 The main factors are affecting the surface area of the activated carbon produced from PFA beneficiation.

High carbon PFAs including biomass co-firing were beneficiated using incipient fluidisation process to produce PFA with low carbon. It was found that there was a significant difference in surface areas of activated carbons produced from different sources at similar carbon burn-out levels. Furthermore, the surface area was increased gradually with carbon burn-out and reached maximum level. This increase was approved after three hours and four hours compared with other studies.

The results indicated that the surface area depends on the porosity of the activated carbon, moisture content, and inorganic impurities accounted in the pores which have been identified by ICP-AES. Moreover, the factors that could influence the activation behaviour of unburned carbon are active sites (*i.e.* amount of oxygen uptake), wall thickness, carbon source, and carbon type. It was observed that biomass co-firing samples has higher surface area compared with PFA coal under same LOI value.

Steam activation was used in this investigation to activate the carbon as it conducted with moderate conditions in terms of destruction of pore walls. The unburned carbons were mainly mesoporous and up to 45% of their pore volume due to the contribution of mesopores. It is important to point out that the rapid devolatilization of the fuels underwent inside the combustor, promoted the generation of mesoporosity. In addition, the porosity developed

during steam activation, thus, the pores enlarge and shift from mesoporosity to microporosity.

5.4 PFA applications developed from alternative fuels.

LOI values were different between PFAs due to different collection devices applied into different power plants. Moreover, the fuel type was shown to effect the LOI value. It was found that there is a great level of carbon in the PFAs collected through the ESP hoppers (front to back), economiser (side B), and the mechanical separator.

Microwave treatment was efficiently reduced the carbon content in the PFAs. The method has also been adapted to reduce the size of PFA and developed to aggregate material. Consequently, incipient fluidisation did not expose the carbon particles or alter the properties and reactivity. The efficiency of separation was consisted on the materials density and differences between the unburned carbons and mineral particles.

Morphology studies have been investigated the carbon type before and after activations. Char walls fragmented during the activation process and the carbon type changes from isotropic to anisotropic, but this is depending on the wall thickness, active site and inorganic content. However, biomass char appeared with more isotropic coke compared with char PFA coals. The char walls observed thinner shape compared to chars derived from PFA coals. Consequently, biomass char observed lower inertinite particles, whereas chars from PFA coals observed more inertinite and minerals such as spinal and glass.

Methylene blue was used to measure the adsorption capacity for the activated carbons. The samples with higher surface area adsorbed more methylene blue which appeared with biomass co-firing and PFA coals.

5.5 Final conclusion

High carbon PFA applications were utilised into value added products. The utilisation conducted through using secondary raw materials for power generation (*i.e.* alternative fuels) and applied PFA beneficiation to remove the residual carbon. This is going to be either fuel to reduce the consumption of coal or carbon precursor. Depleted carbon PFA can be used in the replacement of Portland cement in concrete applications. However, this could help the power industry and make a good return either in energy saving or reducing the waste disposal. However, this study proved no significant impact from using biomass co-firing or PFA derived from imported coals with cement application. Nevertheless, microwave treatment was applied to transform the shape of PFA into aggregate admixture and reduce the size of the by-products.

Moreover, the carbon rich fractions were activated to produce activated carbons to carry out methylene blue measurements. The carbon sourced from biomass co-firing observed higher uptake of methylene molecules due to higher surface area. Morphology studies showed the carbon type could change according to activation process and the conditions applied.

5.6 Future work

There are several areas that are worthy of additional research in the field of high carbon PFA utilisation that have been investigated in this project. However, the future work should cover PFA applications derived from more types of biomass co-firing (high ratio biomass to the coal) and other alternative fuel such as pet coke. This will help to understand the marketability of new PFA generation.

PFA beneficiation process could be considered for these applications using wet process and microwave treatment in order to get more details. Further work will include morphological studies to identify the carbon types for different sources. This step will consist of automated analyses for the carbon rich material and the activated carbon. High surface area of the activated carbon should be achieved to obtain better adsorption. In addition, the activated carbon will be tested to establish the adsorption performance through different areas such as CO₂ and mercury. Finally, the inorganic material could play a significant factor in the adsorption capacity needed to look at.

References

Adriano, D. C., and Weber, J. T. (2001). Influence of PFA on soil physical properties and turfgrass establishment. *Journal of Environmental Quality*. Mar-April 2001, 30(2), p. 596.

Alhozaimy, A.M. (2007). Effect of retempering on the compressive strength of ready-mixed concrete in hot-dry environments. *Cement and Concrete composites*, 29, p. 124-127.

Amanda, M. (2003). Phyto-remediation of PFA from coal-fired power plants, <http://rydberg.biology.colostate.edu/Phytoremediation/2003/Mikel/phytoflyash.html>, [Accessed 10th July 2006].

ASTM C-311, (2006). Test methods for sampling and testing PFA or natural pozzolans for use as a mineral admixture in Portland cement Concrete. www.rediff.com, [Accessed 6th December 2006].

ASTM D5142-09, (1994). Standard Test methods for Proximate Analysis of the Analysis Sample of Coal and Coak by Instrumental Procedure.

Babcock, Renfrew, Scotland. Presented at IEA Exco Workshop on Biomass Co-firing, Copenhagen.

Backman, R., Skrifvars, B.J. and Yrjas, P. (2005). The influence of aerosol particles on the melting behaviour of ash deposits in biomass-fired boilers. *Aerosols in Biomass Combustion*, Graz, March.

Baker, F.S., Miller, C.E., Repik, A.J., and Tolles, E.D. (1992). *Kirk-Othmer Encyclopaedia of Chemical Technology*, 4th Ed. John Wiley, New York, 2, p. 1015-1037.

Bansal, R., Donnet, J.B., and Stoeckli, F. (1988). *Active Carbon*, Marcel Dekker, New York, p. 481.

Barbara, G.K. and Ann, G.K. (2006). Fly ash characterisation by SEM-EDS. *Fuel*, 85, p. 2537-2544.

Barns, D.I. and Lindon, K.A.S. (2004). Ash utilisation from coal-based power plants. United Kingdom Quality Ash Association, Regent House, Bath Avenue, Wolverhampton, West Midlands, WV1 4EG, UK. www.ukqaa.com, [Accessed 10th April 2007].

Barrett, P. H., Joyner, L. G. and Halenda, P. H. (1951). *Amer. Chem. Soc.*, 73, p 373-380

Baxter, L. (2005). Biomass-coal co-combustion: opportunity for affordable renewable energy, *Fuel*, 84, 10, p. 340-349.

REFERENCES

Biedermann, F. and Obernberger, I. (2005). Ash-related problems during biomass combustion and possibilities for sustainable ash utilisation. Austrian Bioenergy Centre GmbH.

Biricik, H. and Akoz, F. (1999). Study of pozzolanic properties of wheat straw ash, Cement and Concrete Research, p. 637-643.

Birkeland, P.W. (1999). Soils and geomorphology, 3rd Edition. New York:

Bittner, J.D. and Stephen, A. G. (2001). STI's commercial beneficiation of high LOI PFA. Separation Technologies Inc. USA.

Bourrat, X., Oberlin, A., and Escalier, J.C. (1986). Fuel, 66, p. 1490.

Brunauer, S., Deming, L.S., Deming, W. S., & Teller, E. J. (1940). Amer. Chem. Soc., 62, p. 1723.

Bryers, R. (1996). Fireside slagging, fouling and high temperature corrosion of heat transfer surfaces due to impurities in steam raising fuels. Programme Energy Combustion Science.

BS 3892: Part 1, (1982). Pulverised fuel ash for use as a cementitious component in structural concrete, BSI.

BS 3892: Part 2, (1996). Specification for pulverised fuel ash for use as a Type I addition, London, BSI, ISBN 0 580 26444 0.

BS EN 450, (1995). Fly ash for concrete-Definitions, requirements and quality control, BSI, ISBN 0 580 24612 4.

BS EN 450, (2008). Sustainable solutions for construction specialists. Scotash, www.scotash.com, [Accessed 30th June 2010].

Byrne, J.F. and Marsh, H. (1995). Introductory overview. In Porosity in Carbon, Patrick, J. W. (Eds). Halsted Press. An Imprint of John Wiley & Sons, Inc., New York, Toronto, p. 2-24.

Castle Cement Ltd (2006). www.castlecement.co.uk, [Accessed 10th October 2006].

Cecil, C.B., Stanton, R.W., and Dulong, F.T. (1981). Geological survey open file report 81-953-A, p.92.

Cen, European Committee for Standardisation, (2005). Fly ash for concrete (EN 450-1), Part 1. www.cen.eu, [Accessed 18th June 2010].

Chi, W.K., and Perlmutter, D.D. (1989). The effect of pore structure on the char-steam reaction. *AIChE Journal*, 35, 11, p. 1791-802.

Clarke, L.B. (1993b). The behaviour of trace elements during coal combustion and gasification: an overview. In: *Managing Hazardous air Pollutants: State of the Art*, Boca Raton, USA, Lewis Publishers, p. 358-370.

REFERENCES

Couch, G. (2003). Opportunities for coal preparation to lower emissions, IEA CCC/30, March, Coal research.

Demirbas, A. (2004). Combustion characteristics of different biomass fuels. Progress Energy Combustion Science, 30, p. 219-30.

Derbyshire, F., Jagtoyen, M., Patric, J.W., and Thwaites, M. (1995). In: Porosity in Carbons. Edward Arnold, London.

DTI (Department of Trade and Industry), (2005). Best Practice Brochure: Co-firing of Biomass (Main Report). Report No. Coal R287 DTI/Pub URN 05/1160. <http://www.dti.gov.uk/publications/index.html>, [Accessed 8th March 2008].

ECOBA (European coal combustion products association), (2004). www.ecoba.com, [Accessed 20th May 2007].

EPRI (Electric Power research Institute), (2009). Is coal ash toxic, CP-INFO Database, August 5th.

ERTD (Environmentally Related Taxes Database), (2007). [www.oecd.org/document/29/0.2340.en_2649_34295_1894685_1_1_1_1.0.html](http://www.oecd.org/document/29/0,2340,en_2649_34295_1894685_1_1_1_1.0.html), [Accessed 20th May 2007].

REFERENCES

Fan, M. and Brown, R. (2001). Comparison of the Loss-on-Ignition and Thermogravimetric analysis techniques in measuring unburned carbon in coal fly ash. *Energy and Fuels*, 15, p. 1414-1417.

Fernando, R. (2005). Fuels for biomass cofiring. IEA Clean Coal Centre, PF 05-09, November.

Ferraris, C.F., Vincent, H. and Ana, I.A. (2004). Measurement of particle size distribution in Portland cement powder: analysis of ASTM round Robin studies. *Cement, Concrete and aggregates*, 26, 2.

FLSmidth, (2009). World Coal Ash Conference Exhibitor, Kentucky USA. www.flsmidth.com, [Accessed 10th June 2009].

Forsroc ltd. (2007). High performance medium weight concrete reinstatement mortar. CI/SfB: February.

Fouad, F.H., and Copham, C.A. (1998). Evaluation of Concrete Containing Fly Ash with High Carbon Content and/or Small Amounts of Wood, Department of Civil Engineering, The University of Alabama at Birmingham.

Fredy, W.T. T., Keppeler, G.J., and Jimmy, C. K. (1999). South Carolina Electric & Gas successful application of carbon burn out at the Wateree Station. International Ash Utilisation Symposium.

Freeman, E., Gao, Y.M., Hurt, R.H., and Suuberg, E.M. (1997). Fuel, 8, p.761.

Georgakopoulos, A., Filippidis, A., and Kassoli-Fournaraki, A. (1994). Morphology and trace element contents of the PFA from main and northern lignite fields, Ptolemais, Greece. Fuel, 73 (11), p. 1802-1804.

Gibb W.H. (2000). An investigation into the suitability of opacity-based measurements for the monitoring of fine dust emissions, November, Power Technology report PT/00/BE1235/R.

Giulio, B. and Prompilio, C. (2000). Production of high value coal PFA. ENEL Production Research-Italy.

Graham, J. (1992). Chapter 1, Fuel and oil, In a modern power station practice. Chemistry and Metallurgy, 3rd edition, Volume E, Pergamon Press.

Grubbs, (2009). Adsorption isotherms: methylene blue on activated carbon. www.stetson.edu, [Accessed 16th July 2009].

Guo, Y.M., Shim, H.S., Hurt, R.H., Suuberg, E.M., and Yang, N.Y.C. (1997). Effect of carbon on air entrainment in PFA concrete: The Role of Soot and carbon black. Energy & Fuels, 11, p. 757.

Hall, P. (2005). Environmental process engineering report. School of Chemical, Environmental and Mining Engineering. University of Nottingham report.

Hamley, P., Lester, E., Thompson, A., Cloke, M., and Poliakoff, M. (2001). The removal of carbon from fly ash using supercritical water oxidation. International Ash Utilisation Symposium, Centre for Applied Energy Research, University of Kentucky.

Harold, H.S., Maroto-Valer, M.M. and Zhe, L. (2001). Development of activated carbons from coal combustion by-products. Annual Technical Progress Report. The Energy Institute, The Pennsylvania State University.

Harold, H.S., Maroto-Valer, M.M. and Zhe, L. (2003). Development of activated carbons from coal combustion by-products. Annual Technical Progress Report. The Energy Institute, The Pennsylvania State University.

Harvey, R.D. and Ruch, R.R. (1986). Mineral matter in Illinois and other US coals. Mineral Matter and Ash in Coal, American Chemical Society ACS, Series 301, p. 10-40.

Heinzel, T., Siegle, V., Spliethoff, H., and Hein, K.R.G. (1998). Investigation of slagging in pulverised fuel co-combustion of biomass and coal at a pilot-scale test facility. Institute for Process Engineering and Power Plant

REFERENCES

Technology (IVD), University of Stuttgart, Stuttgart, Germany, Fuel Processing Technology, 54, p. 109-125.

Hill, R.L., Sarkar, S.L., Rathbone, R.F., and Hower, J.C. (1997). Cement and Concrete Research, 27, p. 193.

Hobbs, D.W. (1989). Portland pulverised fuel ash concretes: water demand, 28 day strength, mix design and strength development. Process Institution Civil Engineers, part 2, 87, March, p. 147-153.

Hoinkis, E. and Robens, E. (1989). Carbon, 27, p. 157.

Hower, J.C. (2001). Petrographic atlas of fly ash. Centre for applied Energy Research, University of Kentucky, Lexington.

Hower, J.C., Robert, F.R., David, J.R., Gilman, P. and Alan, S.T. (1999). Petrology, mineralogy, and chemistry of magnetically-separated sized fly ash. Fuel, 78, p. 197-203.

Huffman, G.P. and Huggins, F.E. (1978). Fuel, 57, p. 592-604.

Hurt, R.H. and Gibbins, J.R. (1994). Residual carbon from pulverised coal fired boiler: size distribution and combustion reactivity.

Hwang, J.Y., Huang, X., Tieder, R., and Hein, A. (1995b). Refractory Material Produced From Beneficiated PFA. In: 11th International Symposium on Use and Management of Coal Combustion by-Products, Orlando, FL, USA, 15-19, Palo Alto, CA, USA, American Coal Ash Association/Electric Power Research Institute, January 1995b, TR-104657-V1, p. 1-32.

Hwang, J.Y., Liu, X., Zimmer, F.V., Thiruvengadam, T.R., and Patzias T. (1995a). Beneficiation Process for PFA and the Utilisation of Cleaned PFA for Concrete Applications. In: 11th International Symposium on Use and Management of Coal Combustion by-Products, Orlando, FL, USA, 15-19, Palo Alto, CA, USA, American Coal Ash Association/Electric Power Research Institute, January 1995a, TR-104657-V1, p. 1-16.

IEA, (2000). Addressing the constraints for successful replication of demonstration technologies for co-combustion of biomass/waste, booklet DIS 1743/98-NL. 1st World Conference and Exhibition on Biomass for Energy and Industry, June 6th.

Ihsan, A.K. and Gayer, A.R. (2001). Characterisation of fly ash from the Kangal power plant, Eastern Turkey. International Ash Utilisation Symposium, Centre for Applied Energy Research, University of Kentucky.

James, D.B. and Stephen, A. G. (2000). Triboelectrostatic PFA beneficiation. An update on separation technologies, International Operations.

Jan, R.P., Danielle, S.D., and Jacob, H.A.K. (2005). Utilisation of ashes from biomass combustion and gasification. 14th European Biomass Conference and Exhibition, Paris, France, October 17-21.

Jankowska, H., Swiatkowski, A., and Choma, J. (1991). Active Carbon, Warsaw, Poland, p. 280.

Jensen, P.A., Sander, B., and Dam-Johansen, K. (2001). Pre-treatment of straw for power production by pyrolysis and char wash. Biomass and Bioenergy, 20, p. 431-446.

John, M.S. and Tian, X.L. (1999). Technology Development for Carbon-Ash Beneficiation by Pneumatic Transport, Tribo-electric Processing. International Ash Utilisation Symposium.

Joshi, R.C. and Lotia, R.P. (1995). PFA Classification System Based on Loss on Ignition (LOI). In: 11th International Symposium on Use and Management of Coal Combustion By-Products, Orlando, FL, USA, Palo Alto, CA, America Coal Ash Association/Electric Power Research Institute, January 1995, TR-104657-V2, p. 1-61.

Joshi, R.C. and Achari, G. (1992). PFA Research and Utilisation in Canada. In: Energy and environment: transitions in eastern Europe, Prague, Czechoslovakia, Grand Forks, ND, USA, North Dakota University, p. 419-431.

Karayigit, A.I. and Gayer, R.A. (2001). Characterisation of fly ash from the Kangal power plant, Eastern Turkey, International Ash Utilisation Symposium, Centre for Applied Energy Research, University of Kentucky.

Karner, F.R., Zygarlicke, C.J., and Brekke, D.W. (1994). New analysis techniques help control boiler fouling. Power Engineering, March 1994, 98, 3, p. 35-38.

Kawahata, M. and Walker, P.L. (1963). In Proceedings of the 5th Carbon Conference. New York: Pergamon Press, 2, p. 251.

Kenneth, W.R. and Baker, A.J. (1987). Mineral matter in coal and wood-replications for solid fuelled gas turbines. The Combustion Institute, May 11-12, Argonne IL.

Keppeler, J.G. (2001). Carbon burn-out an update on commercial applications. International Ash Utilisation Symposium, University of Kentucky Centre for Applied Research.

Keppeler, J.K. (2003). Electric Fuels Corporation, Coal combustion products partnership.

Khan, A.A., de Jong, W., Jansens, P.J., and Spliethoff, H. (2009). Biomass combustion in fluidised bed boilers: Potential problems and remedies. Fuel Process Technology, 90, p. 21-50.

Kiel, J. (2005). Co-utilisation of coal, biomass and other fuels, Presented at JRC-Integration and Enlargement Workshop on the Perspectives for Cleaner Fossil Fuel Energy Conversion Technologies in an Enlarging EU, ECN, Petten, the Netherlands, November 10-11.

Koba, K. and Ida, S. (1980). Fuel, 59, p. 59-63.

Krevelen, D.W., and van, D. W. (1993). Coal: Typology, Physics, Chemistry, Constitution.

Kulaots, I., Gao, Y.M., Hurt, R.H., and Suuberg, E.M. (1998). The role of polar surface area and mesoporosity in adsorption of organics by PFA Carbon. ACS Div. Fuel Chemistry, 43, p. 980.

Kulaots, I., Yu-Ming, G., Hurt, R.H., and Suuberg, E.M. (2001). Adsorption of ammonia on coal fly ash. International Ash Utilisation Symposium, Centre for Applied Energy Research, University of Kentucky.

Lachas, H., Richard, R., Jarvis, K.E., Herod, A.A., Dugwell, D.R., and Kandiyoti, R. (1998). Determination of 17 trace elements in coal and ash reference materials by ICP-MS applied to milligram sample sizes. Department of Chemical Engineering and Chemical technology, Imperial College, University of London.

Lesley, L.S., Irene, M.S., and Deborah, M.B.A. (1996). Pulverised coal ash requirements for utilisation. June, IEA CR/88.

Li, T.X., Jiang, K., Neathery, J.K., and Stencel, J.M. (1999). Triboelectrostatic process of combustion fly ash after carbon burn out. International Ash Symposium, University of Kentucky Centre for Applied Research.

Linares-Solano, A., Mahajan, O.P. and Walker, P.L.J. (1979). Reactivity of heat-treated coals in steam. Fuel, 58, May, p. 327-332.

Lindon, K.A.S., Andrew, J.W., and Andrew, D. (2000). The environmental impacts of using PFA-the UK producers perspective.

Linsay, J., and John, P. (1997). What price coal quality in electric power generation. The Australian Coal review.

Livingston, W.R. (2005). A review of the recent experience in Britain with the co-firing of biomass with coal in large pulverised coal-fired boilers. Mitsui Babcock, Renfrew, Scotland. Presented at IEA Exco Workshop on Biomass Co-firing, Copenhagen.

Livingston, W.R. (2006). Ash related issues in biomass combustion. ThermalNet workshop, Glasgow, Scotland.

Livingston, W.R. (2007). Biomass ash characteristics and behaviour in combustion, gasification and pyrolysis systems. Doosan Babcock Energy, Technology and Engineering report, report no. 34/07/005.

Lizzio, A.A., Jiang, H. and Radovic, L.R. (1990). On the kinetics of carbon (char) gasification: reconciling models with experiments. Carbon, 28, 1, p. 7-19.

Lowenthal, G., Wanzl, W., and Van Heek, K.H. (1986). Fuel, 65, p.346.

Malvern (2008). Wet method development for laser diffraction measurements. Application note by Malvern Instrument, www.malvern.co.uk, [Accessed 24th April 2008].

Manivannan, A. and Seehra, M.S. (1997). X-ray diffraction analysis of the particulate matter in residual oil fly ash. Physics department, West Virginia University.

Maoming, F., Qingru, C., Yuemin, Z., Daniel, T., Zhenfu, L., Xiuxiang, T., Yufen, Y., Xingkai, J., and Jinbo, Z. (2005). Coal ash beneficiation and utilisation in coal separation process. Department of Mining Engineering, University of Kentucky.

Maroto-Valer, M.M., Taulbee, D.N., and Hower, J.C. (1998). American Chemical Society, Fuel Chemical, 43, 4, p. 1014-1018.

Maroto-Valer, M.M., Darrell, N.T., Harold, H.S., James, C.H., and Andrésen, J.M. (1999a). Use of Unburned Carbon in PFA as Precursor for Development of Activated Carbons. International Ash Utilisation Symposium, Centre for Applied Energy Research, University of Kentucky, Paper 19.

Maroto-Valer, M.M., Darrell, T., James, H., and Harold, S. (1999b). Characterization of the carbon types present in PFA separated by density gradient centrifugation. The energy institute, the Pennsylvania State University.

Maroto-Valer, M.M., Taulbee, D.N., and Hower, J.C. (2001). Characterization of differing forms of unburned carbon present in PFA. Fuel, 80, p. 795-800.

Maroto-Valer, M.M., Zhang, Y., Lu, Z., Andrésen, J.M., and Harold, H.S. (2002a). Chapter 30: Development of value-products from PFA carbons, Book: Environmental challenges and greenhouse gas control for fossil fuel utilisation in the 21st century, Kluwer Academic/Plenum Publishers, New York, p. 431-444.

Maroto-Valer, M.M., Andresen, J.M. and Zhang, Y. (2002b). Toward a green chemistry and engineering solution for the US energy industry: reducing emissions and converting waste streams into value-added products. *In: Advancing sustainability through green chemistry and engineering.* 823. Washington, D.C.: American Chemical Society, p. 225-241.

Maroto-Valer, M.M. and Mahmud M. (2007). Applications for high carbon pulverised fuel ash, Technical Progress Report, E-ON UK, 4, May.

Marsh, H. and Wynne-Jones, W.F.K. (1964). Carbon, 1, p. 269-279.

Marsh, H., and Menedez, R. (1989). Introduction to Carbon Science, Butterworths and Co. Ltd., London, p. 37-73.

McCarthy, G.J., Solem, J.K., Manz, O., and Hassett, D.J. (1990). Use of Database of Chemical, Mineralogical and Physical Properties of North American PFA to Study the Nature of PFA and its Utilisation as a Mineral Admixture in Concrete. Materials Research Society Symposium Proceedings, 178, p. 3-31.

McMahan, L.G., Kenneth, J.C., Yee, S., Richard, P.K., Maroto-Valer, M.M., Andrésen, J.M., Michael, V.C., and Paul, H.Z. (2002). Physical cleaning of high carbon PFA. Fuel Processing Technology, 76, p. 11-21.

Miles, T.R., Baxter, L.L., Bryers, R.W., Jenkins, B.M. and Oden L.L. (1995). Alkali deposits found in biomass power plant: a preliminary study of their extent and nature. National Renewable Energy Laboratory, Golden, Co. USA.

Mindness, S. and Young, J.F. (2002). Concrete, Pearson Education, Inc.

- Mohamed, R.M., Aly, H.M., El-Shahat, M.F. and Ibrahim, I.A. (2005).** Effects of the silica sources on the crystallinity of nanosized ZSM-5 zeolite. *Microporous and Mesoporous Materials*, 79, (1-3), p. 7-12.
- Mott MacDonald, (2004).** UK Coal Production Outlook: 2004-16. March, final report. Department of Trade and Industry.
- Muhlen, H.J. and Sulimma, A. (1986).** Thermochemical Activation, 103, p. 163.
- Naik, T.R. and Kraus, R.N. (2003).** A new source of pozzolanic material. *Concrete Int.*, 25, 12, p. 55-62.
- NREL (National Renewable Energy Laboratory), 1998.** Fireside Issues Associated with Coal-Biomass Co-firing. NREL/TP-570-25767. <http://www.p2pays.org/ref/19/18953.pdf>, [Accessed 8th March 2008].
- Ollila, H.J. (2004).** A SEM-EDS and XRD study of the factors affecting the melting behaviour of biomass ash. 6th Science in Thermal and Chemical Biomass conversion. Victoria, BC, Canada, CPL Press.
- Palmer, C.A. and Fliby, R.H. (1984).** Distribution of trace elements in coal from the powhatan no. 6 mine, Ohio. *Fuel*, 63, p. 318-328.
- Pastor, A. C., Rodriguez-Reinoso, F., Marsh, H., and Martinez, M. A. (1999).** *Carbon*, 37, p. 1275-1283.

Patrick, J.W. (1995). Porosity in Carbons: Characterization and applications. Halsted Press.

Pflughoeft-Hassett, D. and Hassett, D. (2001). Developing Beneficial Use Rules for Coal Combustion by-Products. In Proceedings of University of Kentucky Centre for Applied Energy Research, International Ash Utilisation Symposium.

Philadelphia, (1993). American Society for Testing and Materials. ASTM Standards in Building Codes, 2, p. 1449-1451.

Pierre, C. and Jean-Rene, G. (2007). Plasma gasification and vitrification of ash-conversion of ash into glass-like products and syngas. World of Coal Ash, May 7-10.

Pierre, C. and Jean-Rene', G. (2007). Plasma gasification and vitrification of ash-conversion of ash into glass-like products and syngas. World of Coal Ash (WOCA), Covington, Kentucky, May 7-10.

Pietersen, H.S. (1993). Reactivity of fly ash and slag in cement. Geochemistry. Delft, Delft University of Technology.

Pimenow, A.V., Lieberman, A.I., and Cheh, H.Y. (1995). Separation Science Technology, 30, p. 3183-3194.

Potgieter, H.J. (1991). Journal of Chemical Education, 68, p. 349.

Rawle, A. (2008). Basic principles of particle size analysis. Malvern Instruments Limited. www.malvern.co.uk, [Accessed 24th April 2008].

Remero, J.M. and Maranon, T. (1996). Allocation of biomass and mineral elements in *Melilotus segetalis* (annual sweetclover): effects of NaCl salinity and plant age. New phytologist, 132(4), p. 565-573.

Robert, H.H., Kevin, A.D., Nancy, Y.C.Y., Thomas, J.H., and Gareth, D.M. (1995). Residual carbon from pulverised coal fired boilers. Fuel, 74, 9, p. 1297-1306.

Robinson, A.L., Baxter, L.L., Dayton, D., Freeman, M., and Goldberg, P. (1997). Biomass-coal co-firing experience among three laboratories. NYSEG review meeting, Geneva, New York, October 15-16.

Robinson, A.L., Baxter, L.L., Freeman, M., James, R. and Dayton, D. (1998). Issues associated with coal-biomass co-firing. Bioenergy 98, Madison, WI.

Robinson, J.P., Perry, R.A., Grenfell, J.R.A., and Ghazireh, N. (2009). Microwave vitrification for lightweight aggregate manufacture. ICE, p. 167-174.

Rock Talk, (2005). Coal mining glossary. 8 (2).

Rodri'guez-Reinoso, F. (1991). Controlled gasification of carbon and pore structure development, Fundamental Issues in Control of Carbon Gasification Reactivity, Edt. Lahaye, J. and Ehrburger, P., Kluwer Academic Publishers, p. 553.

Rodrigues-Reinoso, F. (1997). Introduction to Carbon Technologies, Publications Universidad de Alicante, Alicante, Spain, p. 35-101.

Rodrigues-Reinoso, F. and Sabio, M.M. (1992). Carbon, 30, p. 1111-1118.

Rouquerol, F., Rouquerol, J., and Sing, K.W. (1999). Adsorption by Powders and Porous Solids-Principles, Methodology and Applications. Academic Press, San Diego, London, Boston, New York, Sydney, Tokyo, Toronto.

Rustu, S.K. (2001). Coal Combustion Products, www.pubs.usgs.gov, [Accessed 14th July 2006].

Rustu, S.K. and Donald, W. O. (2006). Coal combustion products. US Geological survey. www.pubs.usgs.gov, [Accessed 5th October 2006].

RWE Power International, (2010). Generation aggregates. www.generationaggregates.com, [Accessed 28th September 2010].

ScotAsh Power Technology, (2006). www.scotash.com, [Accessed 21st December 2006].

Shuangzhen, W. and Baxter, L. (2007). Comprehensive study of biomass fly ash in concrete: Strength, microscopy, kinetics and durability. *Fuel Processing Technology*, 88, p. 1165-1170.

Shuangzhen, W., Emilio, L., Baxter, L., and Fernando, F. (2008a). Durability of biomass fly ash concrete: Freezing and thawing and rapid chloride permeability tests. *Fuel*, 87, p. 359-364.

Shuangzhen, W., Amber, M., Emilio, L., Fernando, F., and Baxter, L. (2008b). Biomass Fly Ash in Concrete: Mixture Proportioning and Mechanical Properties. *Fuel*, 87, p. 365-371.

Sing, K.S.W., Everett, D.H., Haul, R.A.W. Mocou, L., Pierotti, R.A., Rouquerol, J. and Siemieniowska, T. (1985). *Pure and Applied Chemistry*, 57, p. 603.

Smalley, N., Philip, M., and John, H.W. (2004). Implementation of a RockTron PFA beneficiation process plant. RockTron Ltd., UK. www.rocktronplc.com, [Accessed 20th June 2006].

Soud, H.N. (1991). Emission standards handbook: air pollutant standards for coal-fired plants. IEACR/43, London, UK, IEA, Coal Research, December, p.448.

Sparton (2007). Sparton produces first yellowcake from Chinese coal ash. World Nuclear News (Wnn), 16th October.

Straszheim, W.E., Yousling, J.C., and Markuszewski, R. (1986). Analysis of ash forming mineral matter in raw and supercleaned coals by automated image analysis-scanning electron microscopy. American Chemical Society series 301, p. 449-461.

Strehlow, R.A., Harris, L.A., and Yust, C.S. (1979). Fuel, 57, p. 185-186.

Su-Chen, H., Fang-Chih, C., Shang-Lien, L., Ming-Yu, I., Chu-Fang, W., and JyH-Dong, L. (2007). Production of lightweight aggregates from mining residues, heavy metal sludge, and incinerator fly ash. Journal of Hazardous Materials, 144, p. 52-58.

Sun, J., Hippo, E.J., Marsh, H., O'Brien, W.S., and Crelling, J.C. (1997). Activated carbon produced from an Illinois basin coal. Carbon, 35, 3, p. 341-52.

Swamy, R.N. (1994). Alkali-Aggregate Reaction, The Bogeyman of Concrete, ACI SP-114.

Tazaki, K., Fyfe, S., Sahu, K.C., and Powell, M. (1989). Observations on the nature of fly ash particles. *Fuel*, June, 68, p. 727-734.

Thy, P. (2006). High temperature elemental losses and mineralogical changes in common biomass ashes. *Fuel*, 85, p. 783-795.

Tomkow, T., Siemienińska, T., Czechowski, F. and Jankowska, A. (1977). *Fuel*, 56, p.121.

Turn, S.Q. (2003). Fuel characteristics of processed, high-fiber sugarcane. *Fuel Process Technology*, 81, p. 35-55.

UKQAA (United Kingdom Quality Ash Association), (2007). www.ukqaa.co.uk, [Accessed at 15th January 2007].

Unsworth, J.F., Barratt, D.J., and Roberts, P.T. (1991). Coal quality and combustion performance- an International prospective. *Coal Science and Technology*, Elsevier, 19.

Uysal, H., ramazan, D., Remzi, S., and Rustem, G. (2004). The effects of different cement dosages, slumps, and pumice aggregate ratios on the thermal conductivity and density of concrete. *Cement and Concrete Research*, 34, p. 845-848.

Veijonen, K., Vainika, P., Jarvinen, T., and Alakangas, E. (2003). Biomass co-firing-an efficient way to reduce greenhouse gas emissions. European Bioenergy Networks.

Villar-Cocina, E., and Valencia-Morales, (2002). Kinetics of pozzolanic reaction between lime and sugar cane straw ash by electrical conductivity measurement: a kinetic-diffusive model, Cement and Concrete Research, 33, p. 517-524.

Vom-Berg, W. (1993). New European Standards Concerning the Use of PFA in Concrete. In: Proceedings of the 10th International Ash Use Symposium. Washington, DC, USA, American Coal Ash Association, January, 3, p. 1-93.

Vom-Berg, W. (2000). CCP Utilisation in Europe-Outstanding Option and Continuous Challenge. ECOBA 10th Anniversary Conference CCP-Utilisation in Europe, Essen Germany.

Von Kienle, H. (1986). Ullmann's Encyclopaedia of Industrial Chemistry, A5, p. 124-140.

Vooy, D.E.F. (1983). Activated Carbon-A Fascinating Material. Norit, Amsterdam, 2nd Ed., Chapter 1.

Ward, C.R. and David, F. (2005). Relation between coal and fly ash mineralogy, based on quantitative X-ray diffraction methods. Co-operative

REFERENCES

Research Centre for Coal in Sustainable Development: School of Biological, Earth and Environmental Sciences, University of New South Wales, Sydney, Australia.

WCI (World Coal Institute), (2010). www.worldcoal.org, [Accessed 6th January 2010].

Wert, C.A. and Hzieh, K.C. (1981). Proceedings International Conference on Coal Science, Dusseldorf, September 7-9, p. 780-785.

Wesche, K. (1991). Fly ash in concrete-properties and performance. RILEM report 7.

Wicke, E. and Hedden, K. (1953). Zeitschrift fur Elektrochemie, 57, p. 636.

William, P.L., Andrew, M., Wayne, S.S., Jost, O.L.W., Tadashi, I., Yoshihiko, E. and Shigehiro, M. (2002). On trimodal particle size distributions in fly ash from pulverised coal combustion. Proceedings of the Combustion Institute, 29, p. 441-447.

Woolley, G.R., Simpson, D.T., Quick, W., and Graham, J. (2000). Ashes to assets. Studies of the usefulness and environmental management of ash from coal fired power stations. Powergen UK plc.

Yamin, Y., Mohd, Z.H., and Faujan, H.A. (2007). Adsorption of methylene blue onto treated activated carbon. The Malaysian Journal of analytical Sciences, 11, 11, p. 400-406.

Yangkyu, A., Dae-Sup, K., Jung, H.Y., and Hun, S.C. (1998). Characteristics of unburned carbon particles recovered from fly ash.

Zhang, Y., Maroto-Valer, M.M., Lu, Z., Andrésen, J.M., and Schobert, H.H. (2003). Comparison of high unburned carbon containing PFAs from different combustor types and their steam activated products in Energy and Fuels, 17, p. 369.

Zhe, L. (2006). Factors affecting the behaviour of unburned carbon upon steam activation. Department of Energy and Geo-Environmental engineering, The Pennsylvania State University.

Zuwala, J. and Sciazko, M. (2005). Co-firing based energy systems-modelling and case studies. Paper presented at the 14th European Biomass Conference and Exhibition Biomass for Energy, Industry and Climate Protection, Paris, October 17-21.

Appendix A

Figures of particle size distribution used water as a dispersant

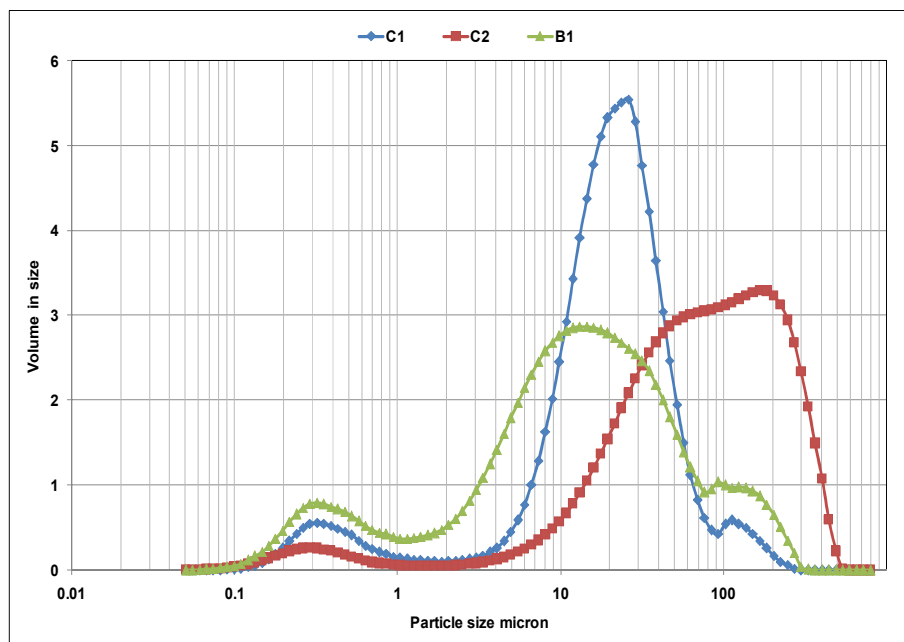


Figure A.1: Particle size distribution with volume % in size for P.S.1.

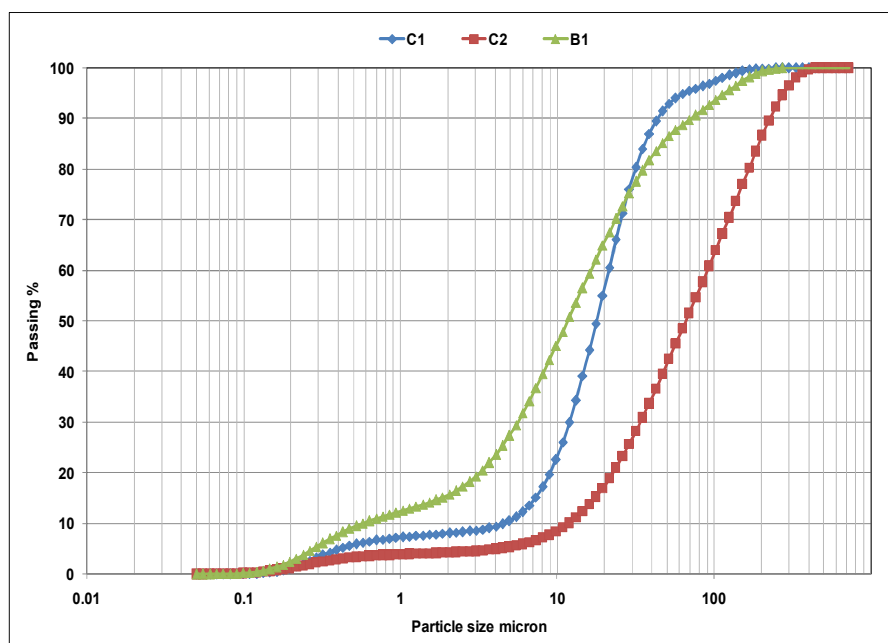


Figure A.2: Particle size distribution with % passing for P.S.1.

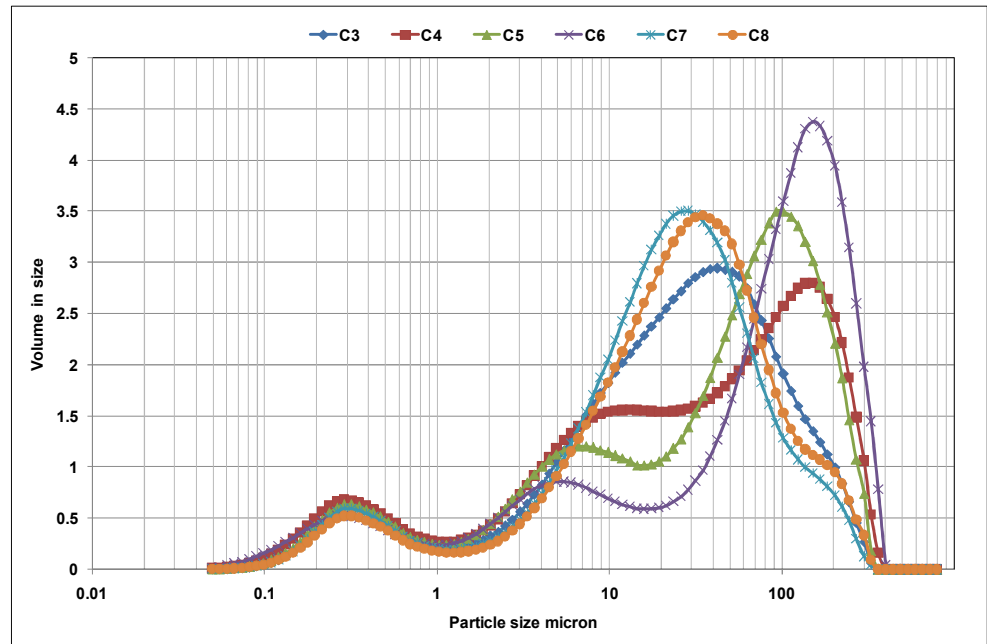


Figure A.3: Particle size distribution with volume % in size for P.S.2.

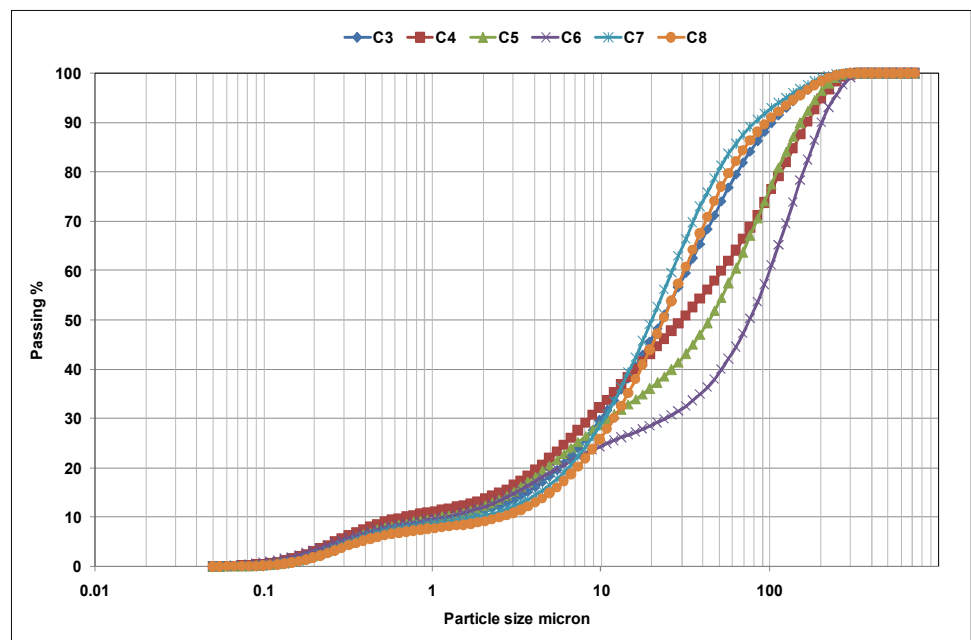


Figure A.4: Particle size distribution with % passing for P.S.2.

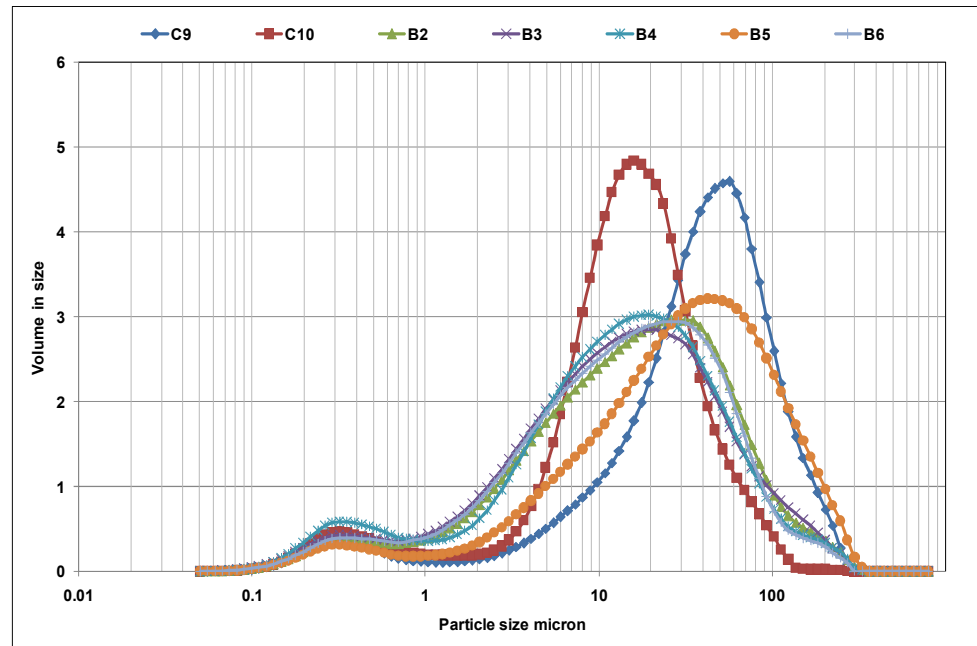


Figure A.5: Particle size distribution with volume % in size for P.S.3.

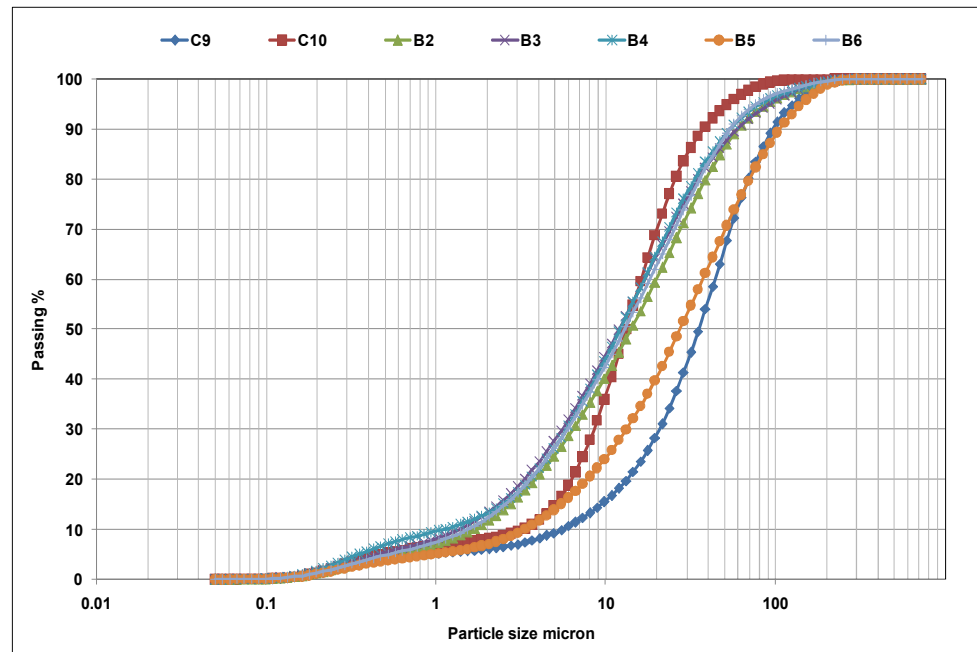


Figure A.6: Particle size distribution with % passing for P.S.3.

Figures of particle size distribution used IPA as a dispersant

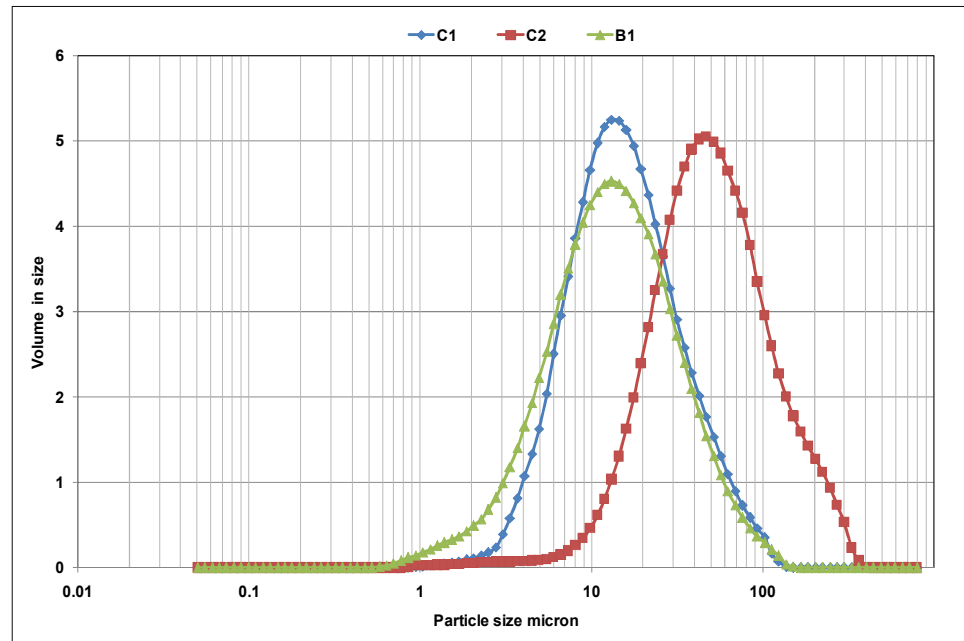


Figure A.7: Particle size distribution with volume % in size for P.S.1.

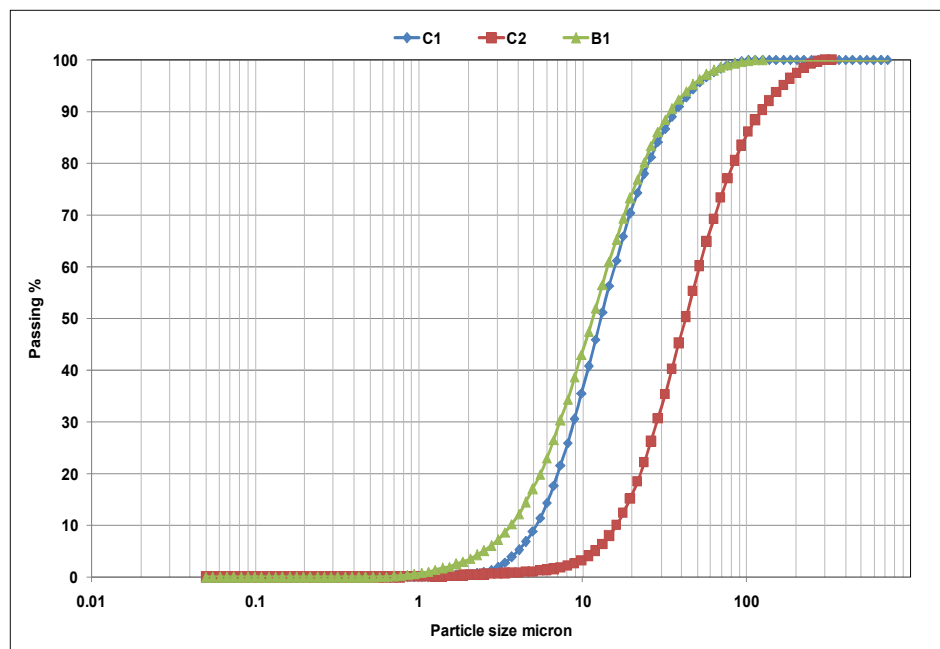


Figure A.8: Particle size distribution with % passing for P.S.1.

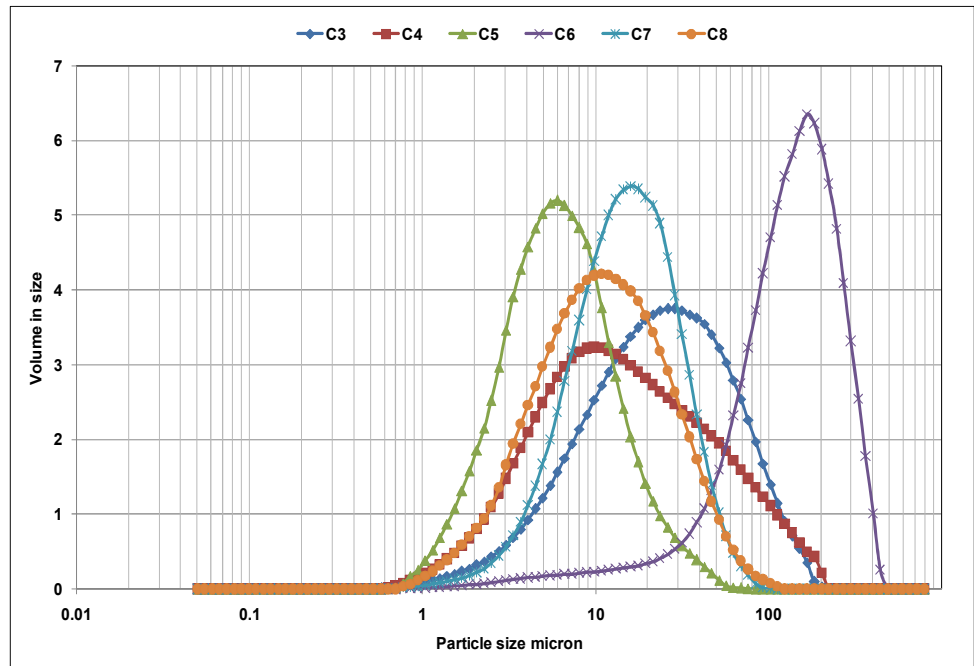


Figure A.9: Particle size distribution with volume % in size for P.S.2.

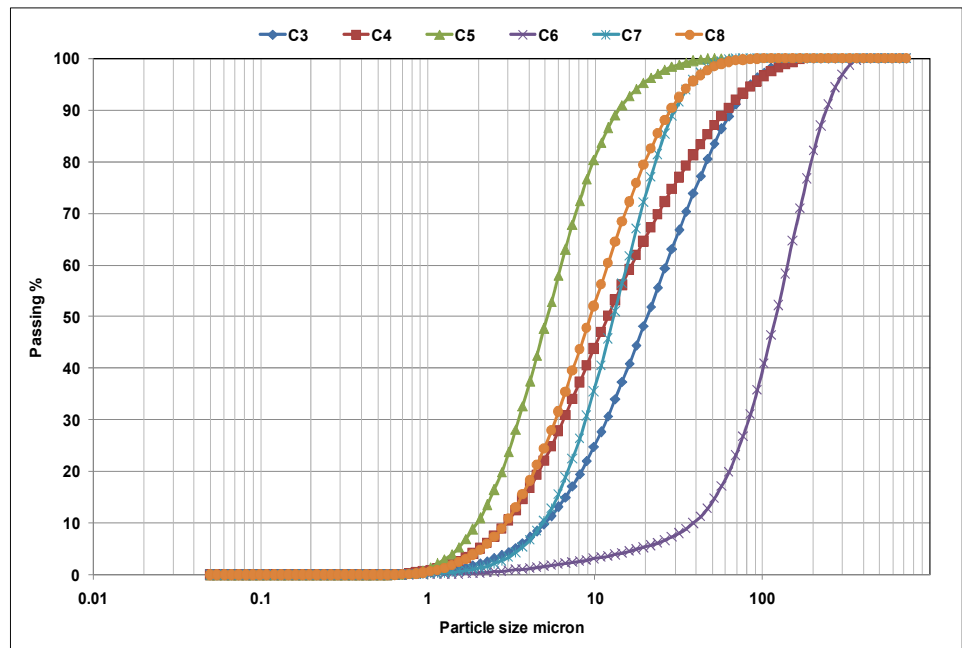


Figure A.10: Particle size distribution with % passing for P.S.2.

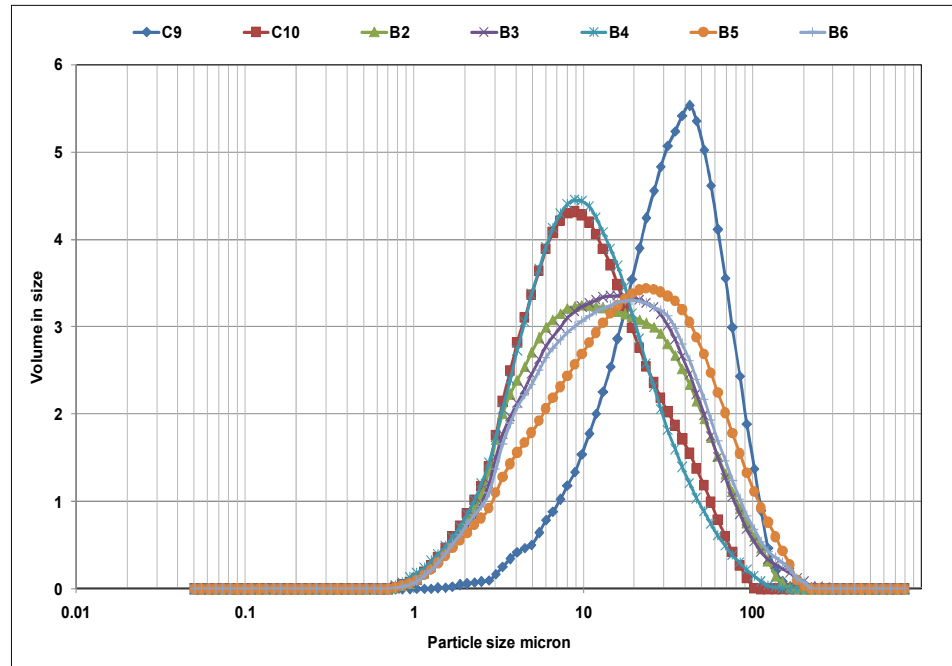


Figure A.11: Particle size distribution with volume % in size for P.S.3.

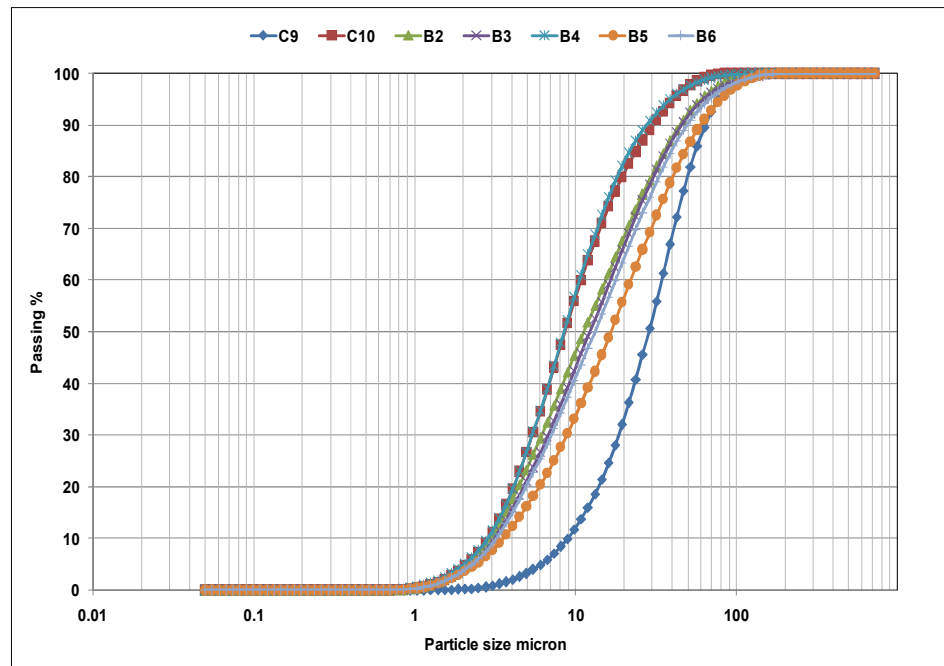


Figure A.12: Particle size distribution with % passing for P.S.3.

Appendix B

SEM images for all the samples

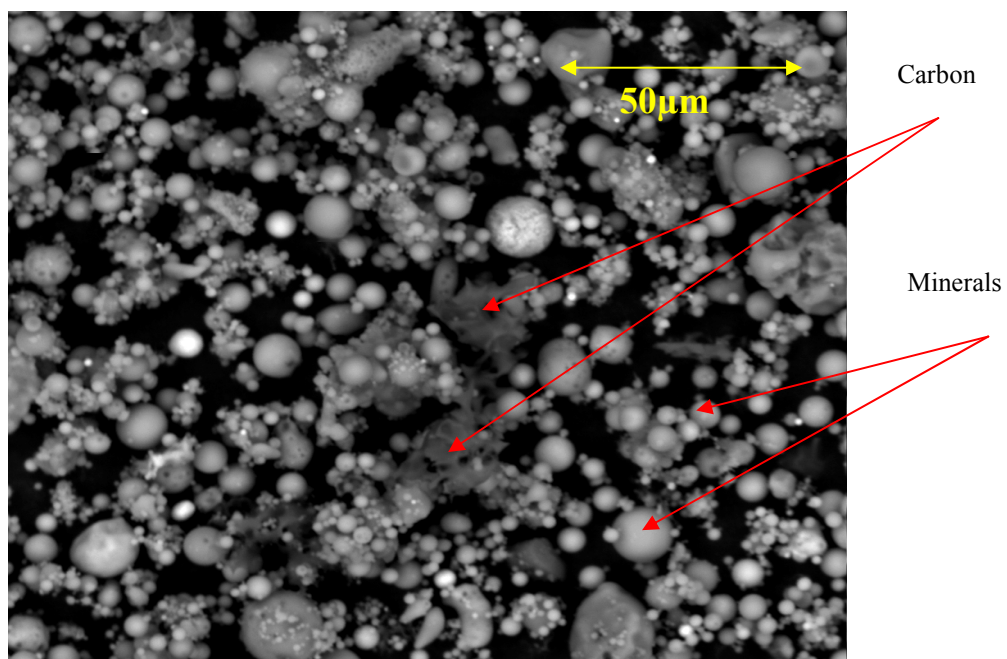


Figure B.1: SEM image of C1 sample.

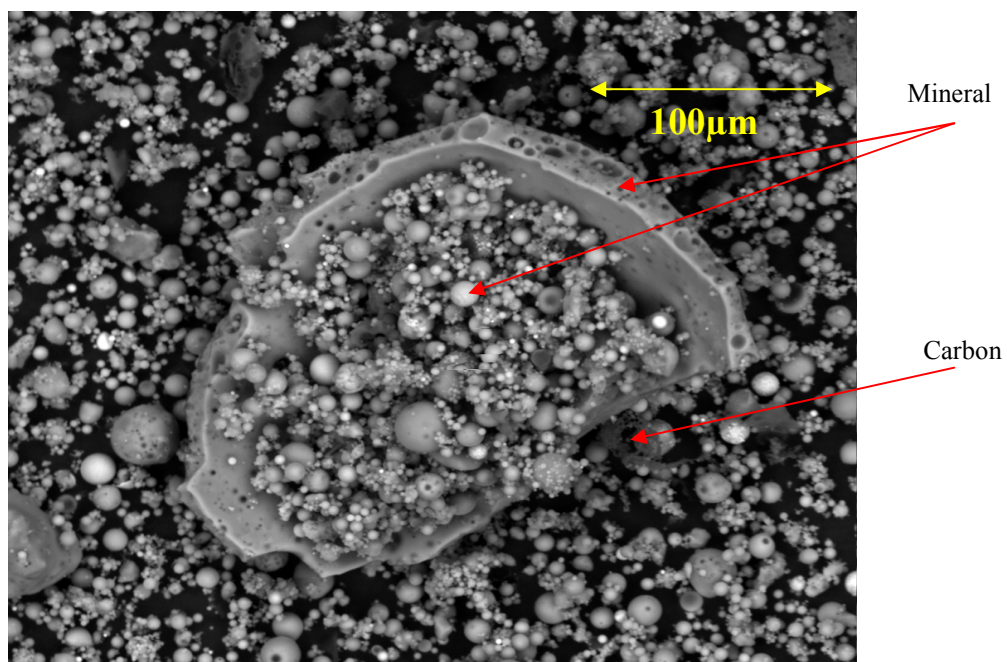


Figure B.2: SEM image of C1 sample.

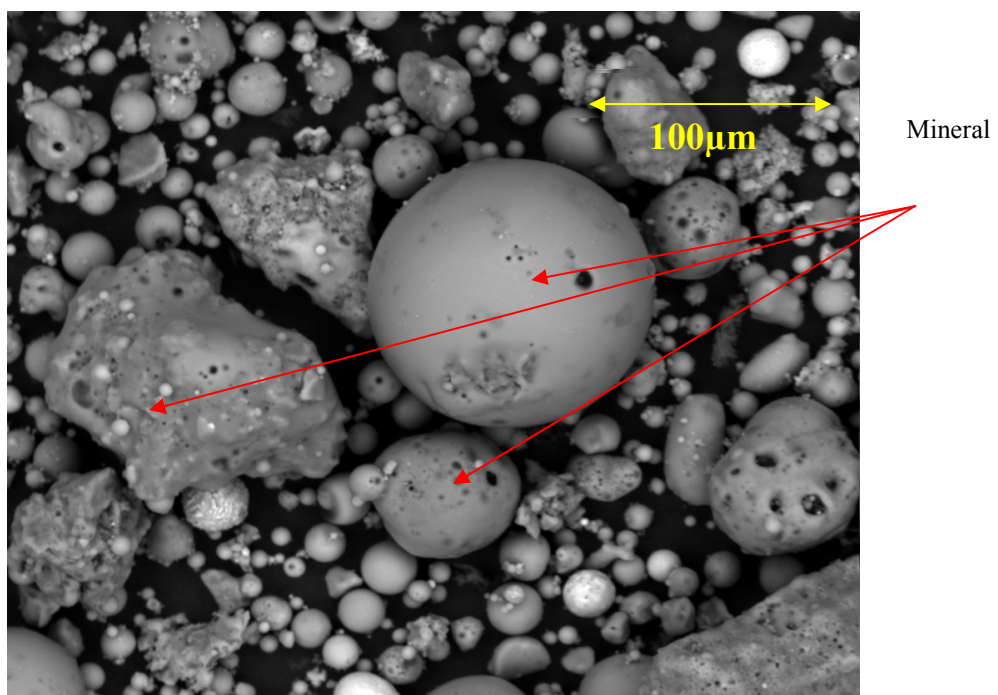


Figure B.3: SEM image of C2 sample.

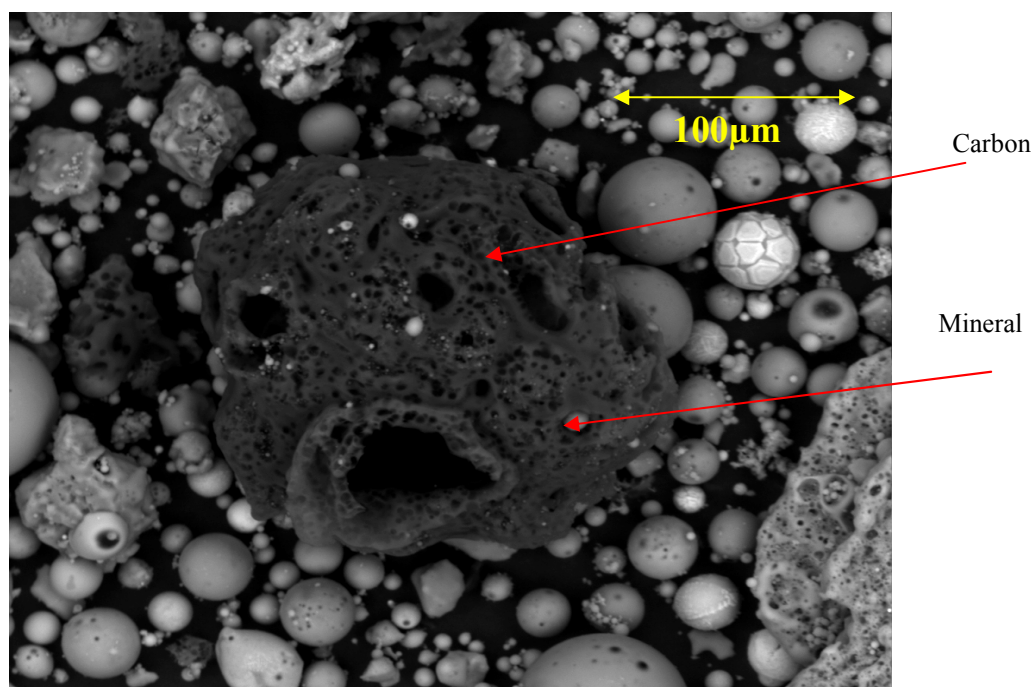


Figure B.4: SEM image of C2 sample.

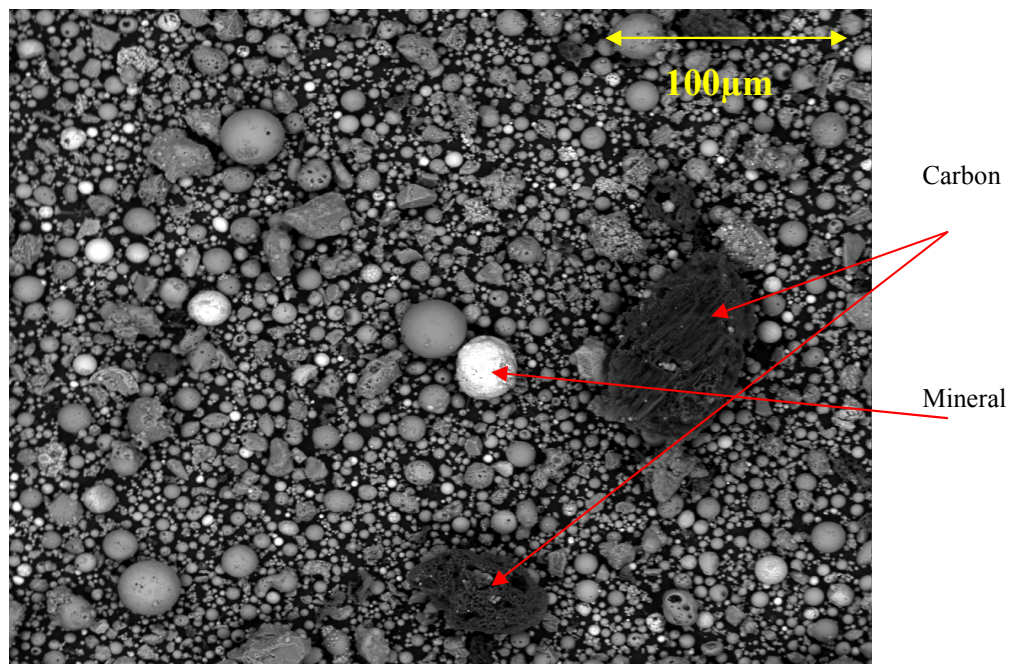


Figure B.5: SEM image of C2 sample.

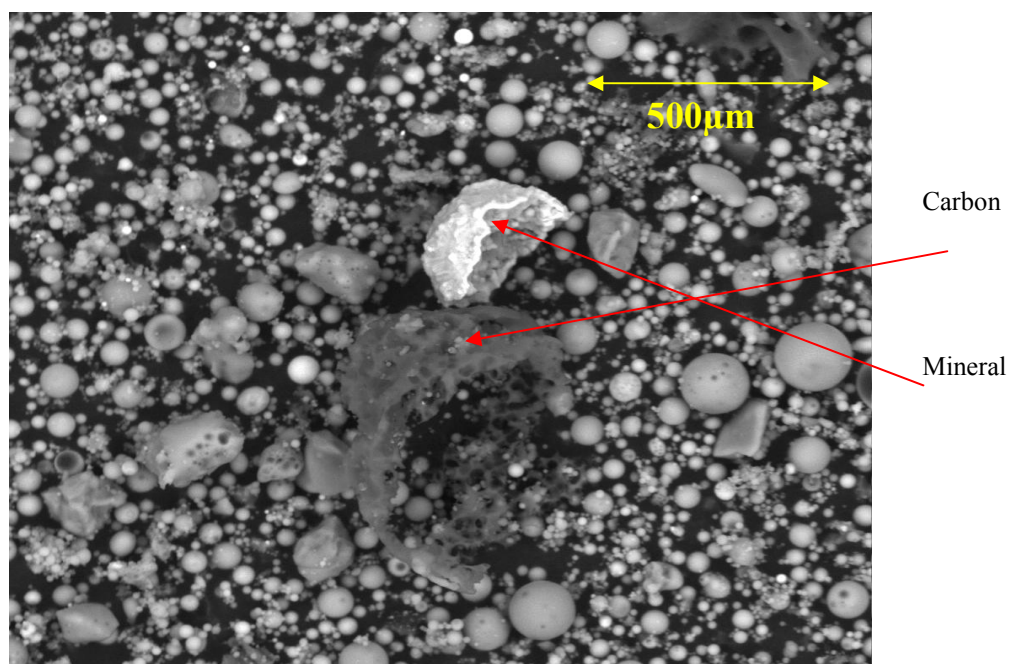


Figure B.6: SEM image of B1 sample.

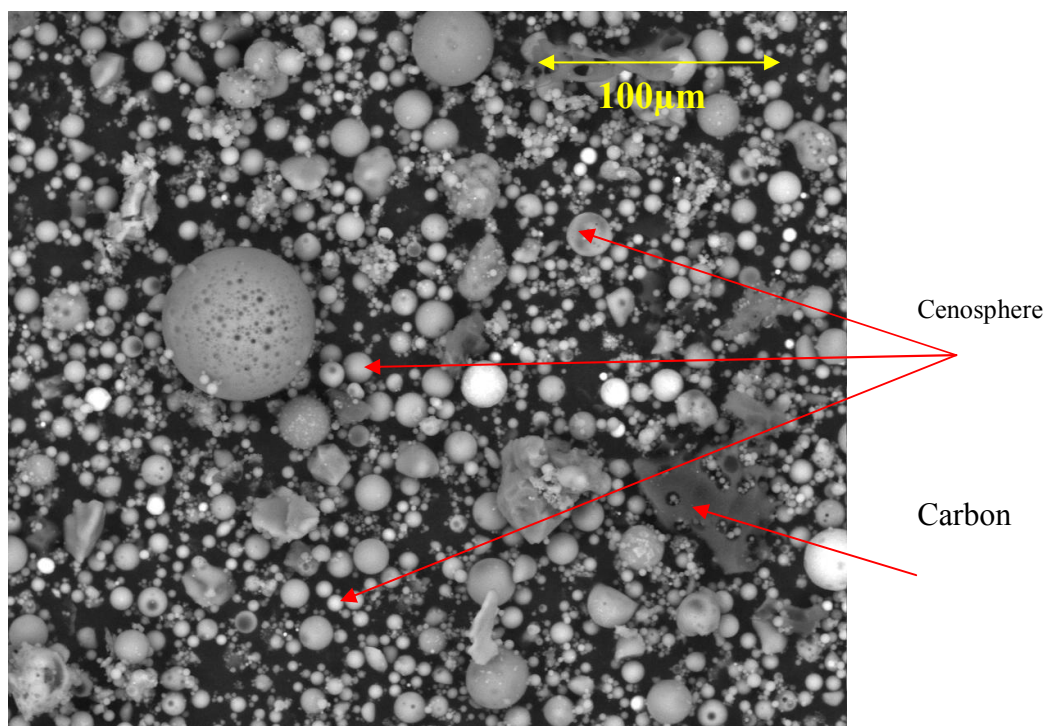


Figure B.7: SEM image of B1 sample.

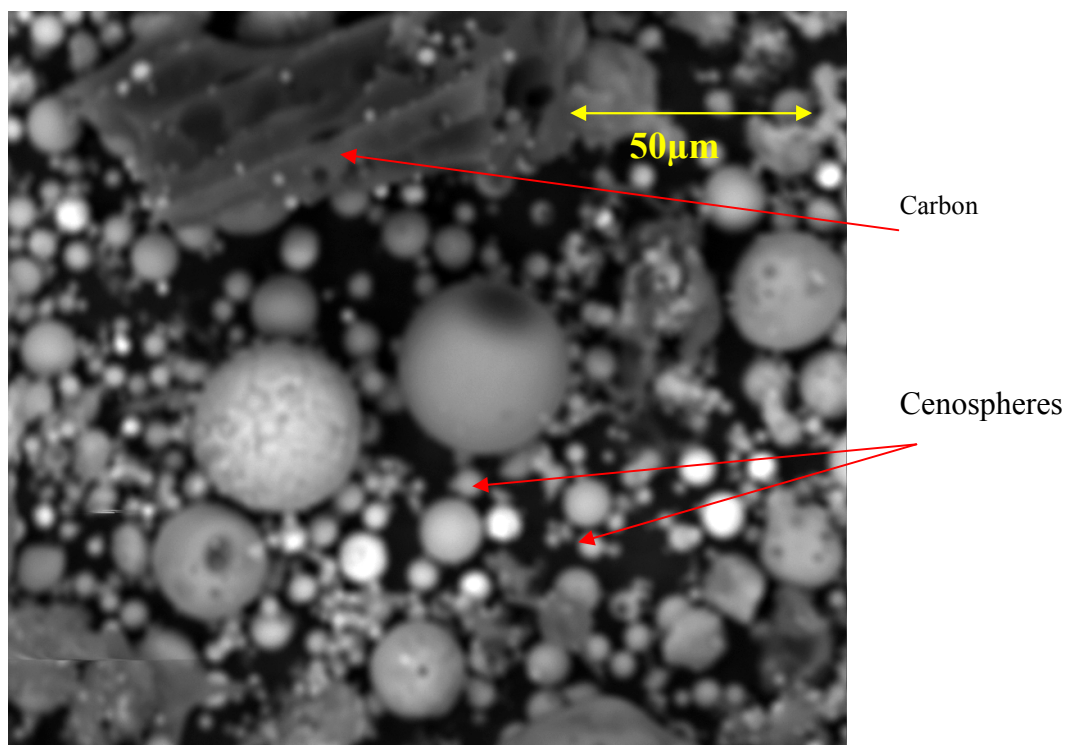


Figure B.8: SEM image of C3 sample.

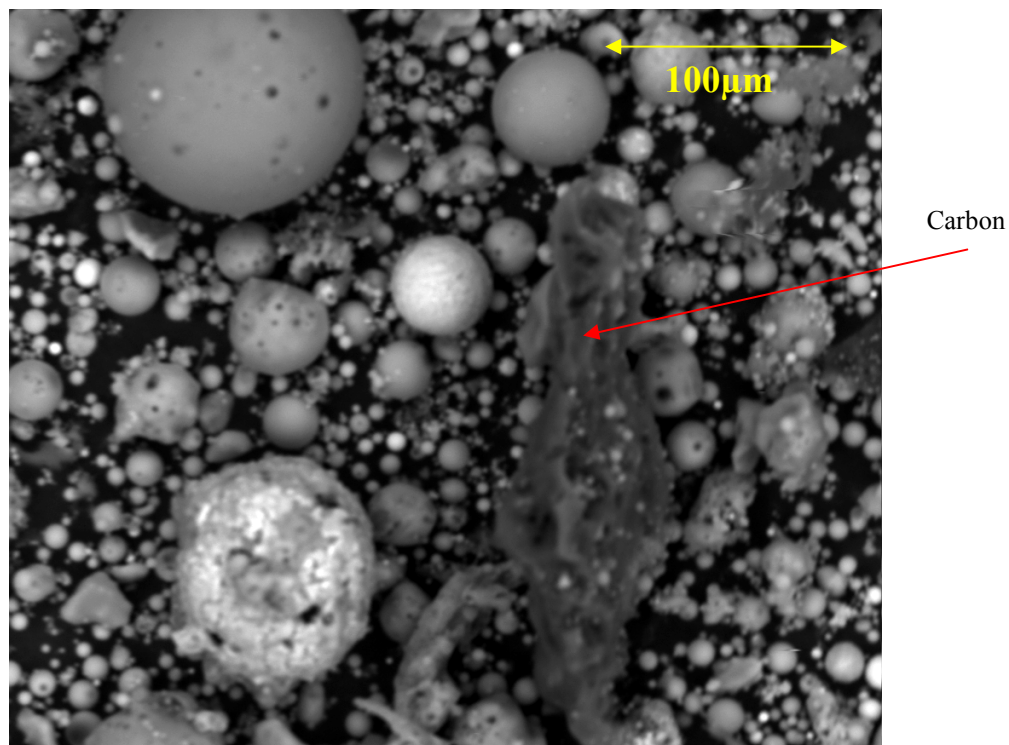


Figure B.9: SEM image of C3 sample.

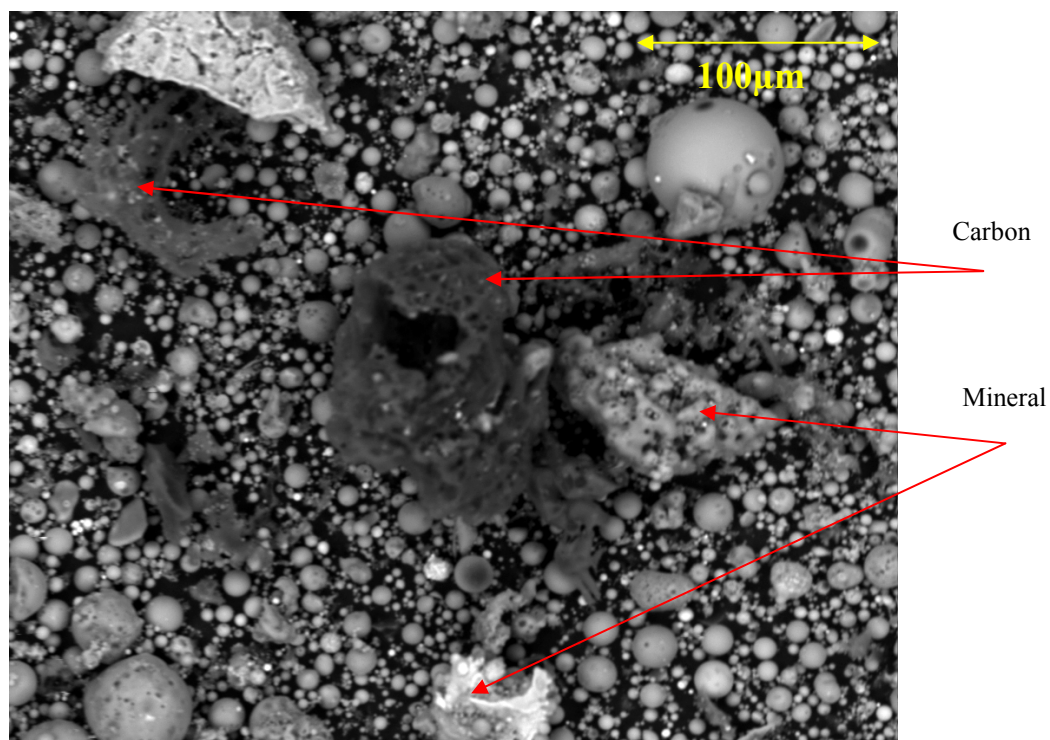


Figure B.10: SEM image of C3 sample.

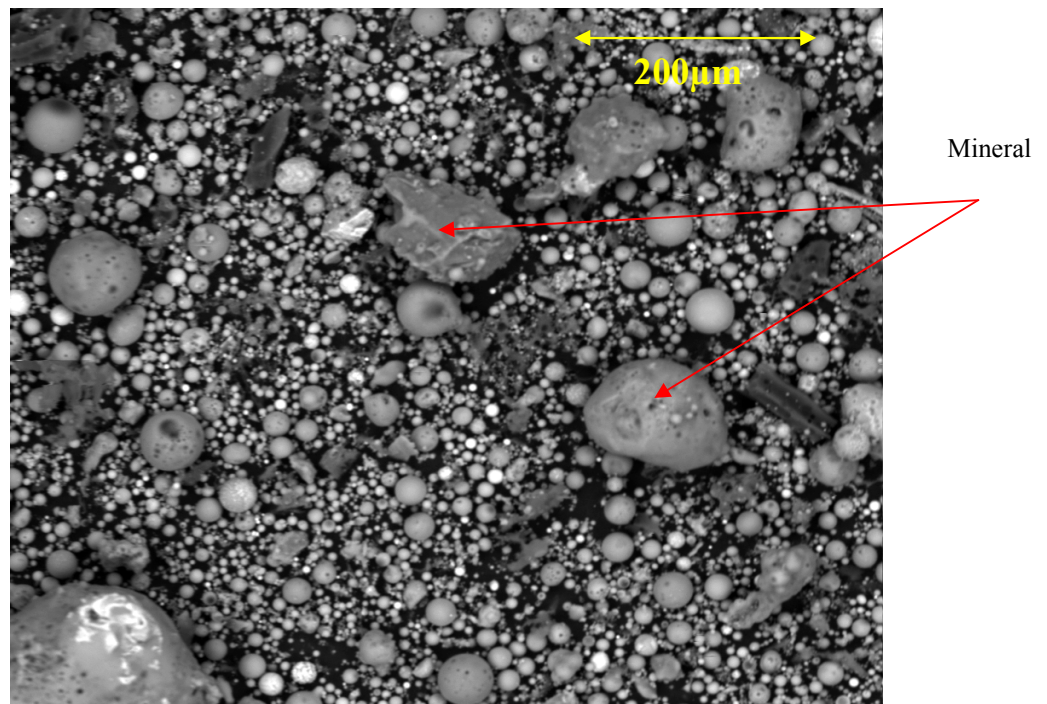


Figure B.11: SEM image of C3 sample.

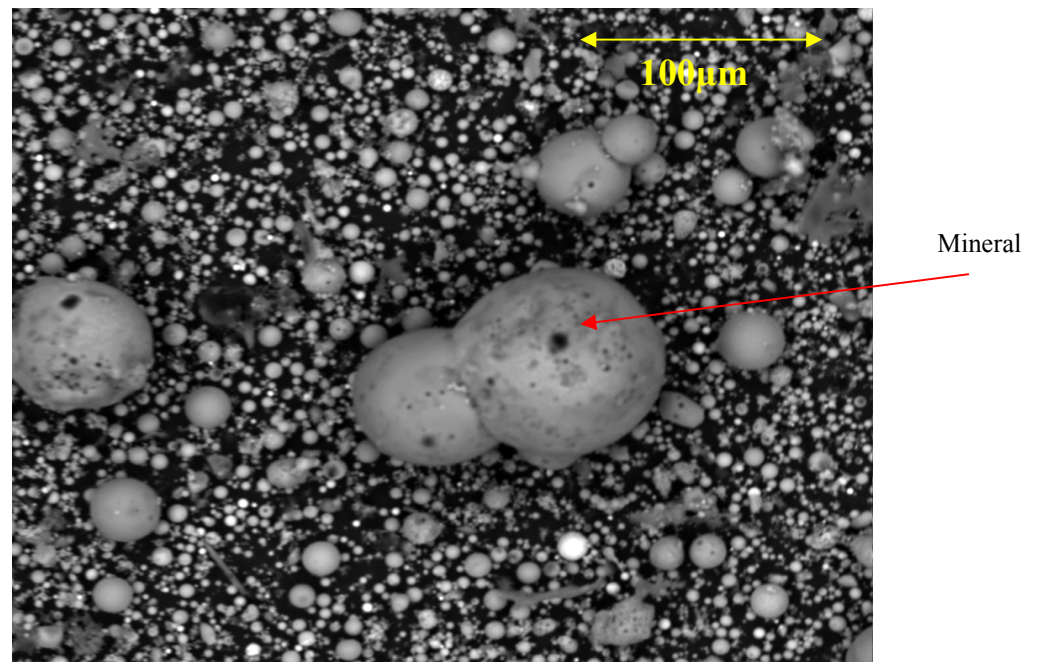


Figure B.12: SEM image of C4 sample.

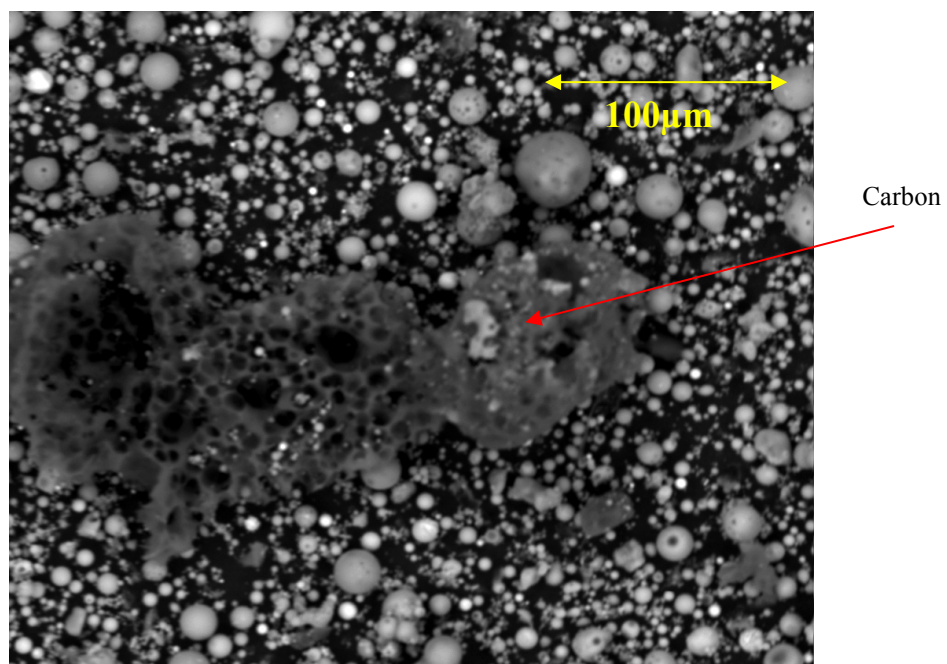


Figure B.13: SEM image of C4 sample.

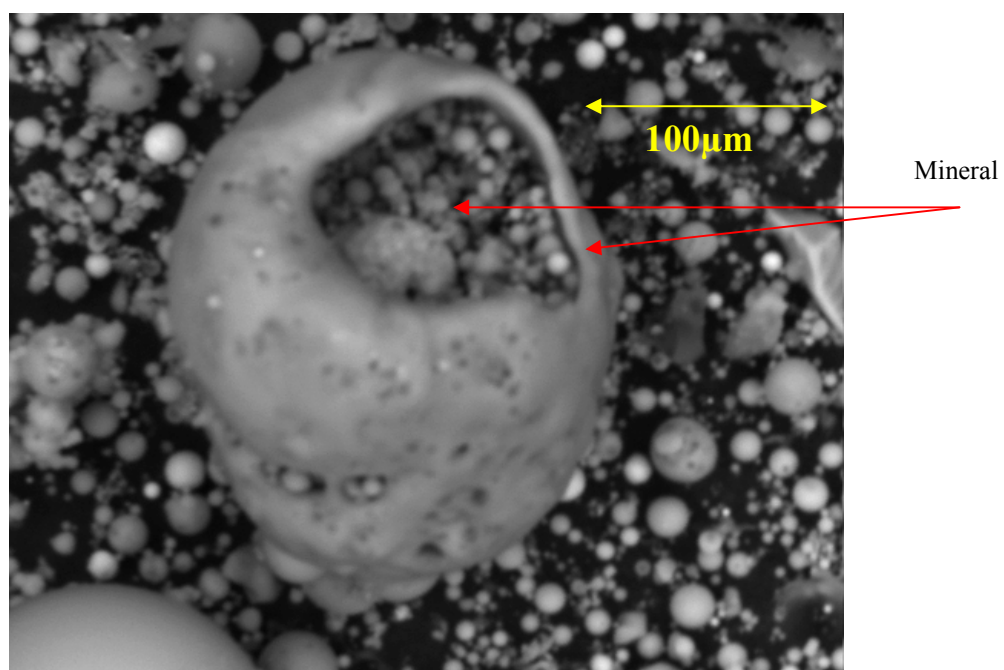


Figure B.14: SEM image of C4 sample.

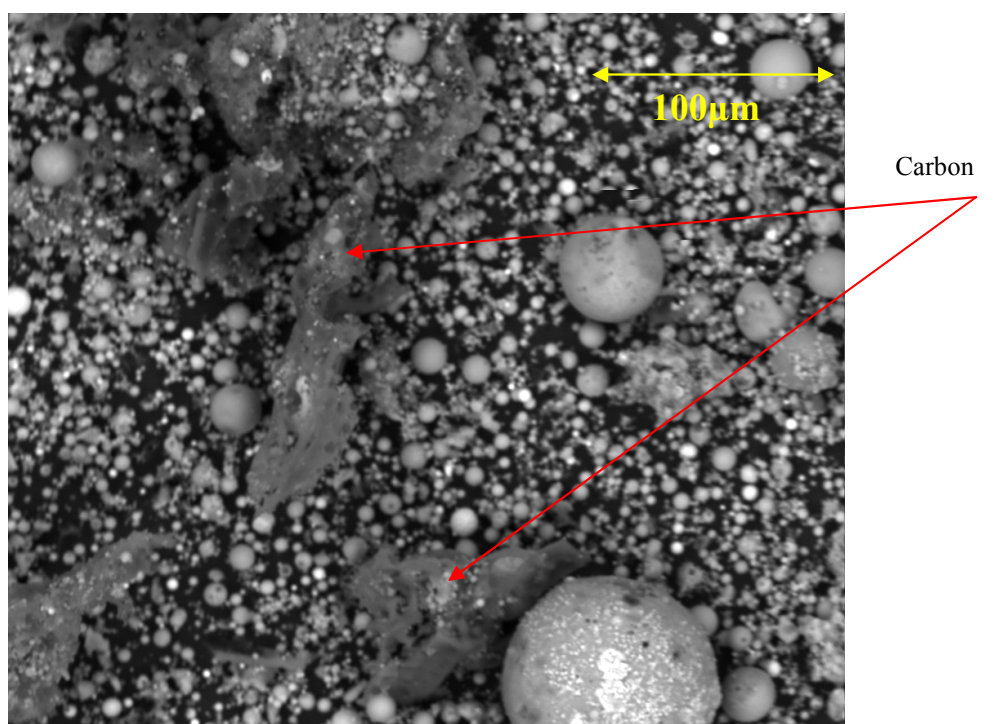


Figure B.15: SEM image of C5 sample.

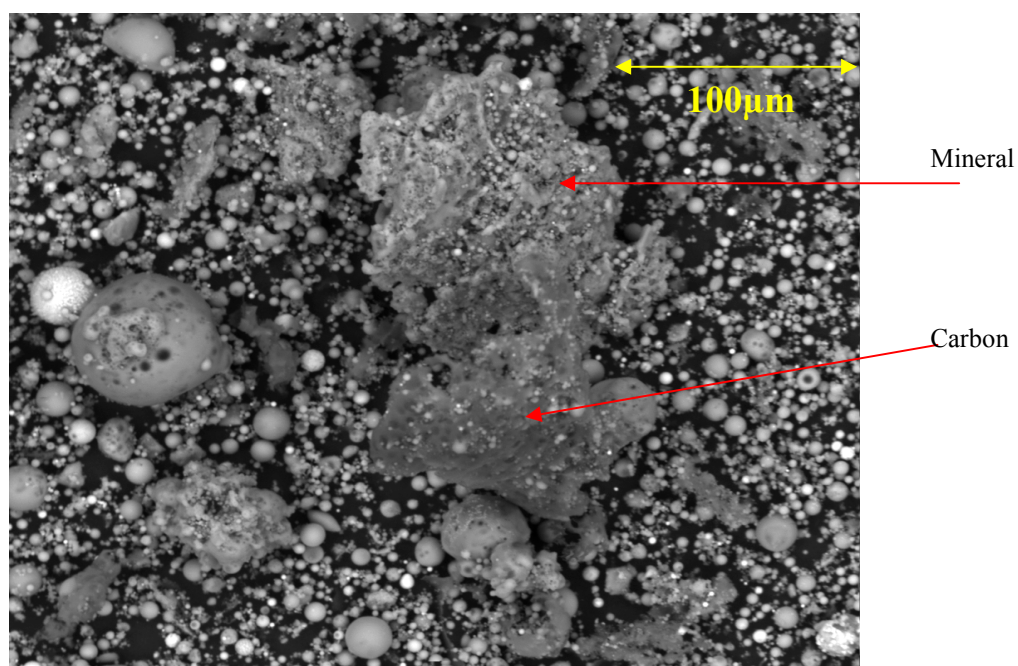


Figure B.16: SEM image of C5 sample.

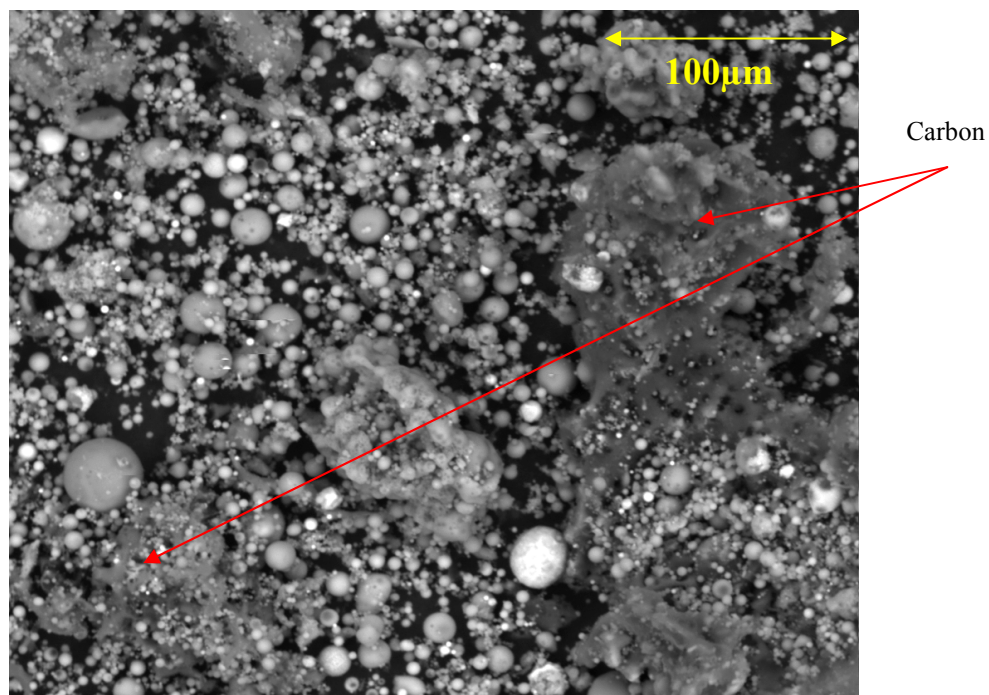


Figure B.17: SEM image of C5 sample.

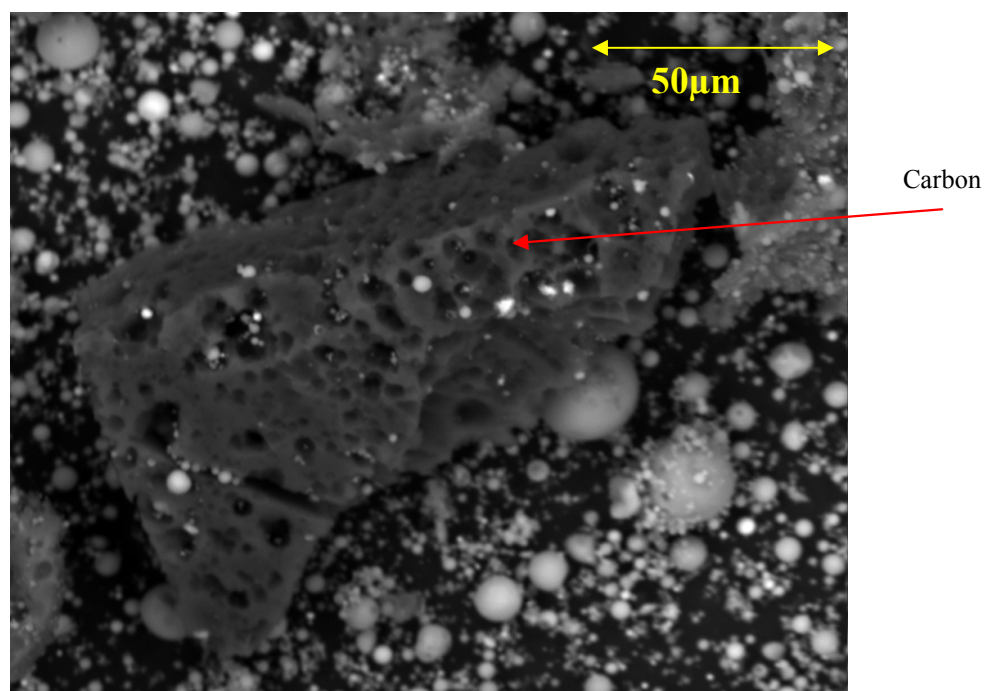


Figure B.18: SEM image of C6 sample.

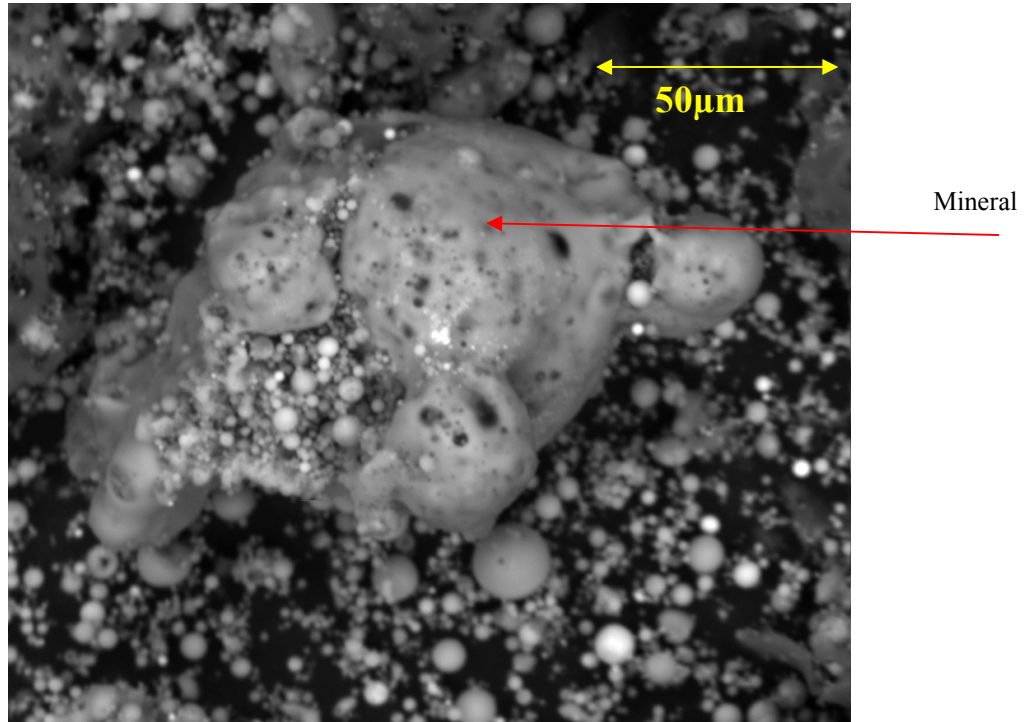


Figure B.19: SEM image of C6 sample.

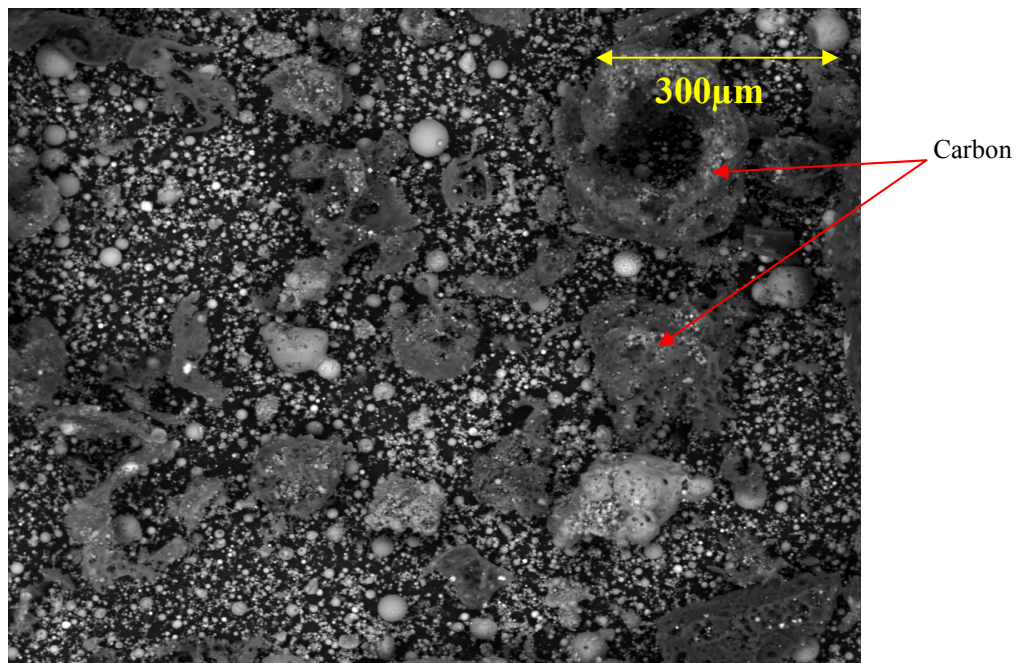


Figure B20: SEM image of C6 sample.

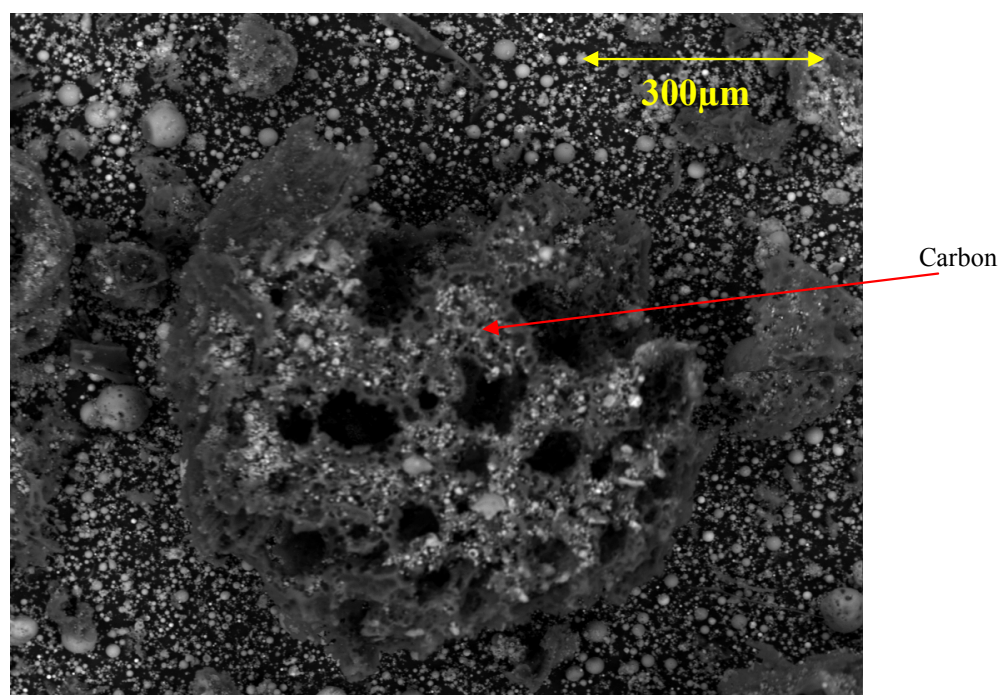


Figure B.21: SEM image of C6 sample.

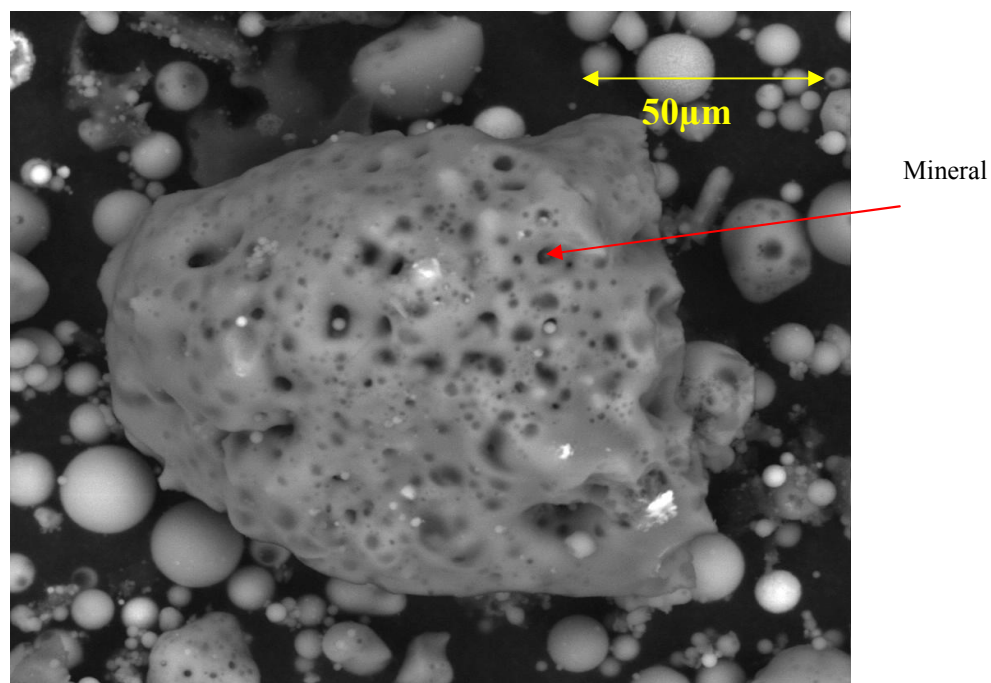


Figure B.22: SEM image of C7 sample.

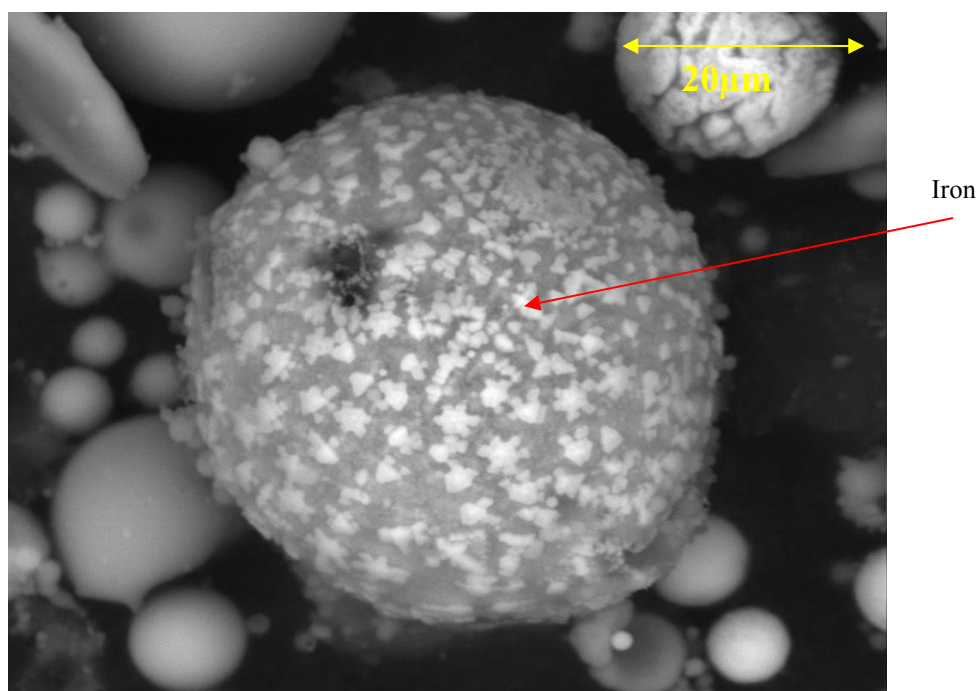


Figure B.23: SEM image of C7 sample.

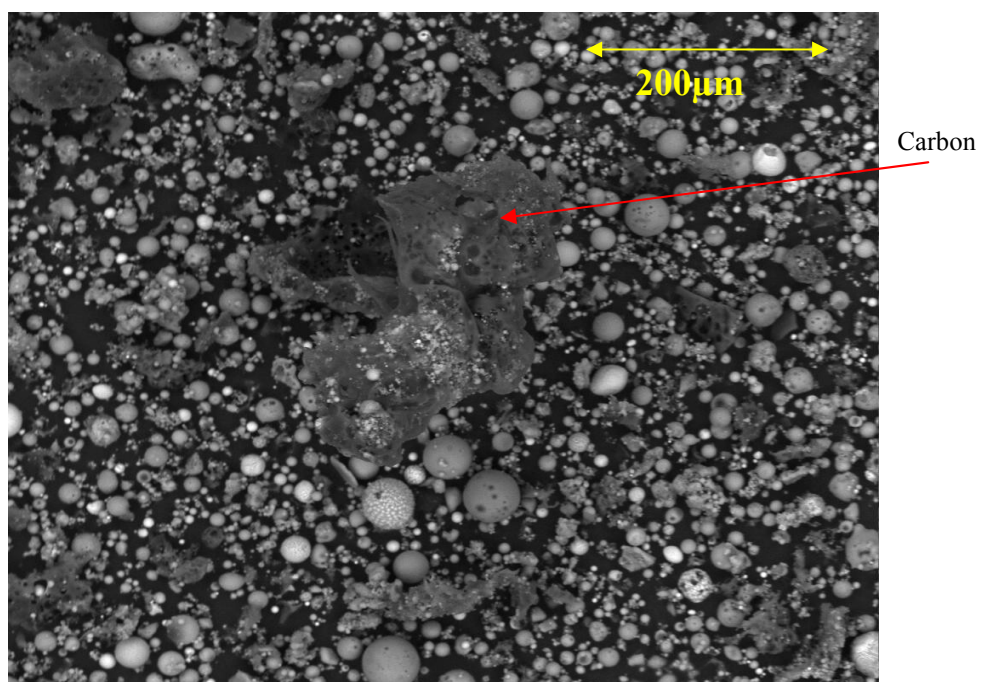


Figure B.24: SEM image of C7 sample.

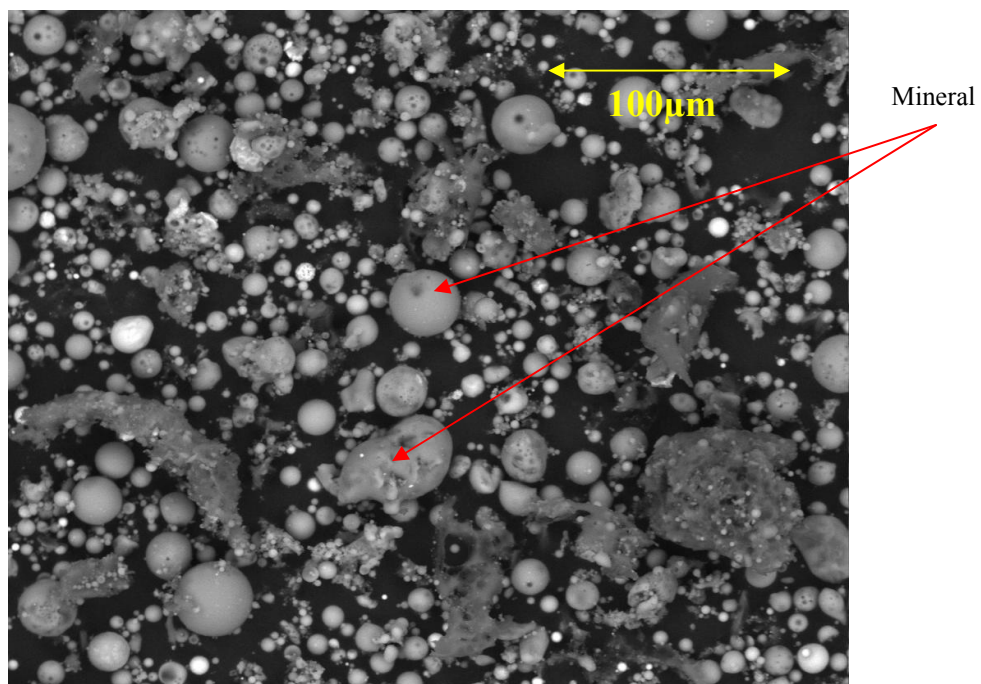


Figure B.25: SEM image of C8 sample.

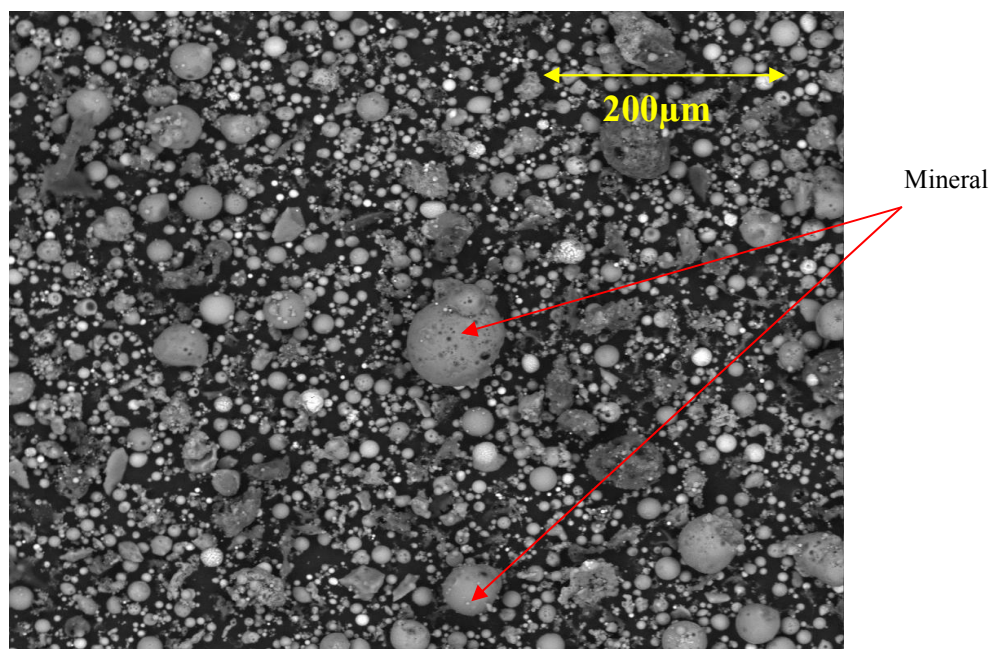


Figure B.26: SEM image of C8 sample.

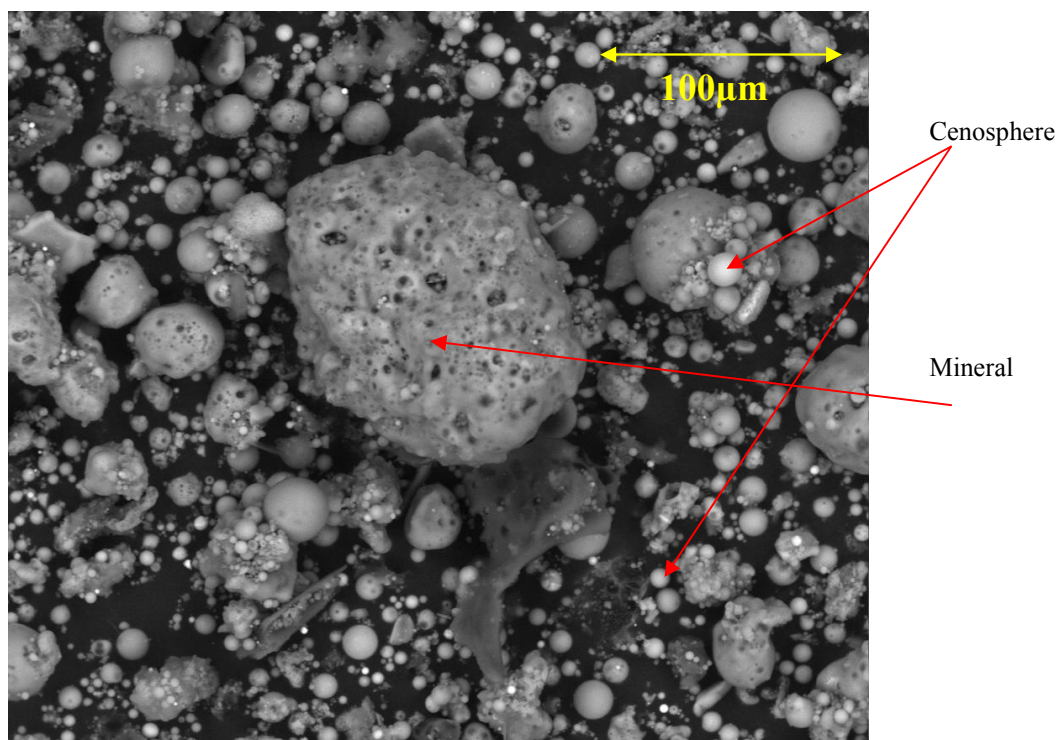


Figure B.27: SEM image of C9 sample.

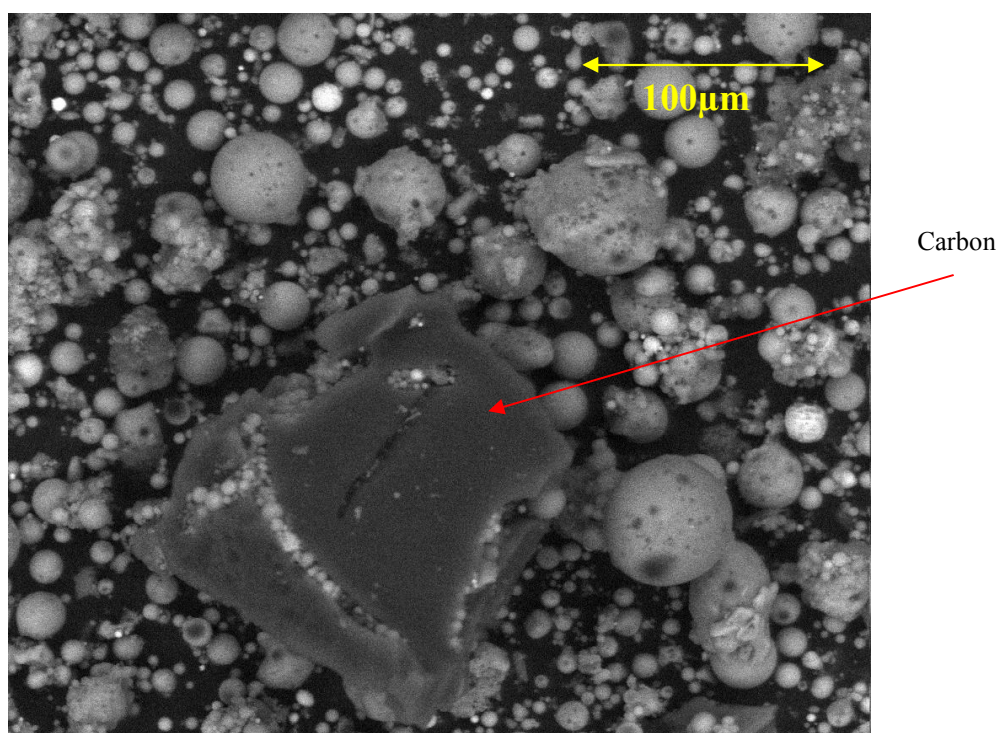


Figure B.28: SEM image of C9 sample.

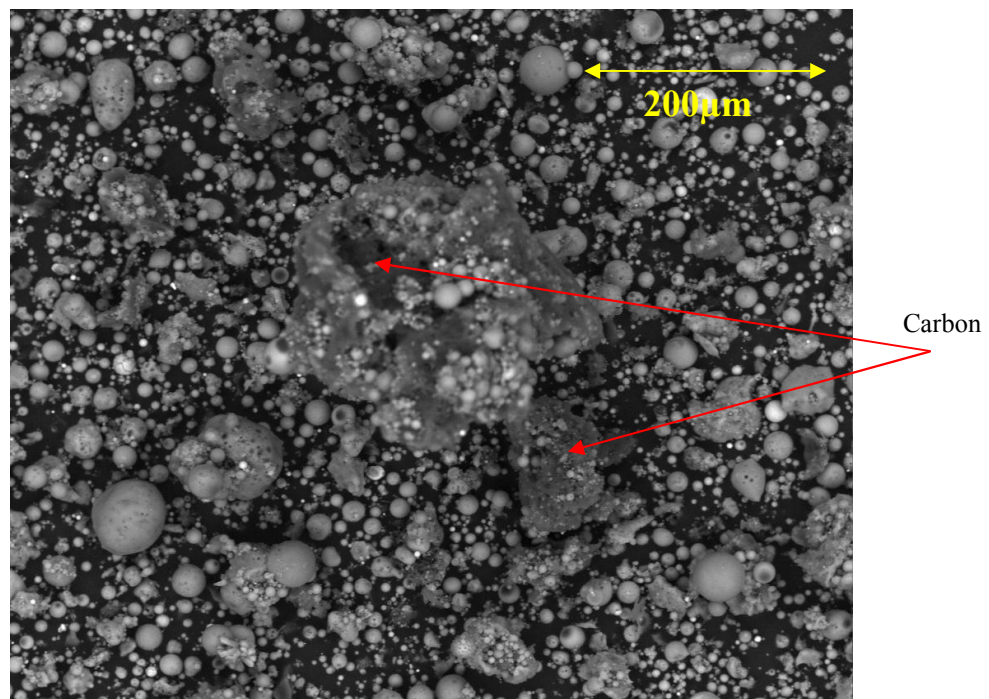


Figure B.29: SEM image of C9 sample.

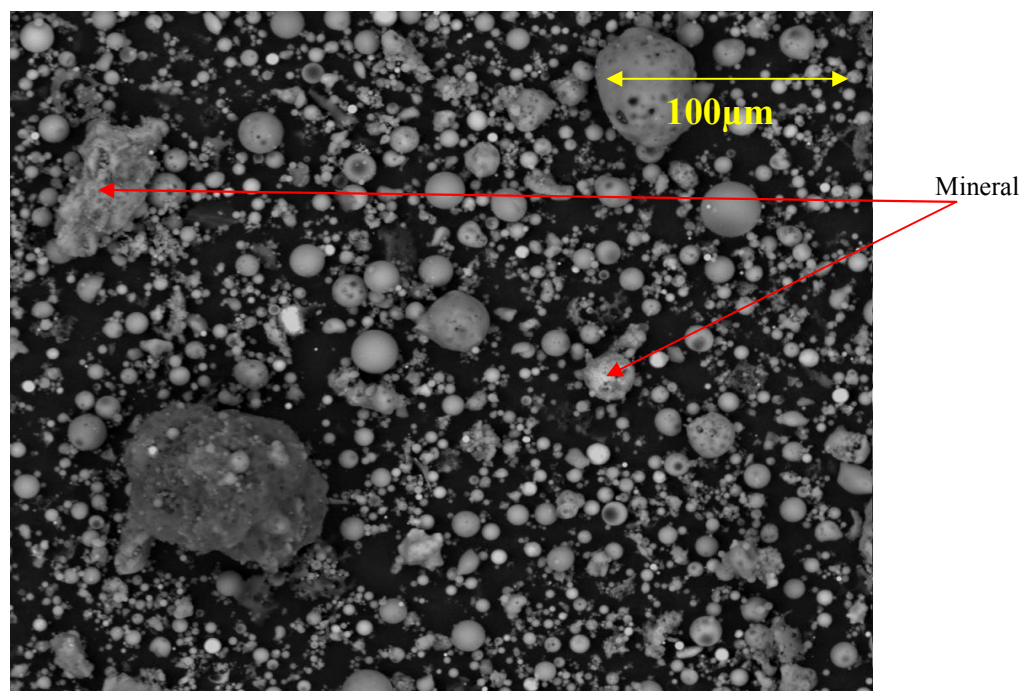


Figure B.30: SEM image of C10 sample.

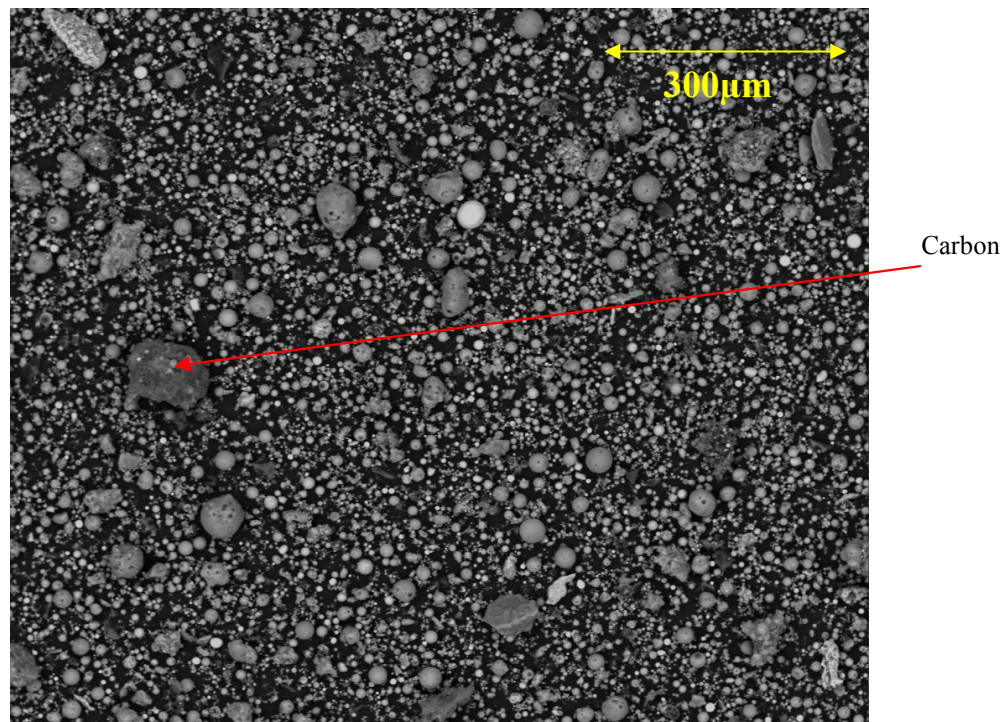


Figure B.31: SEM image of C10 sample.

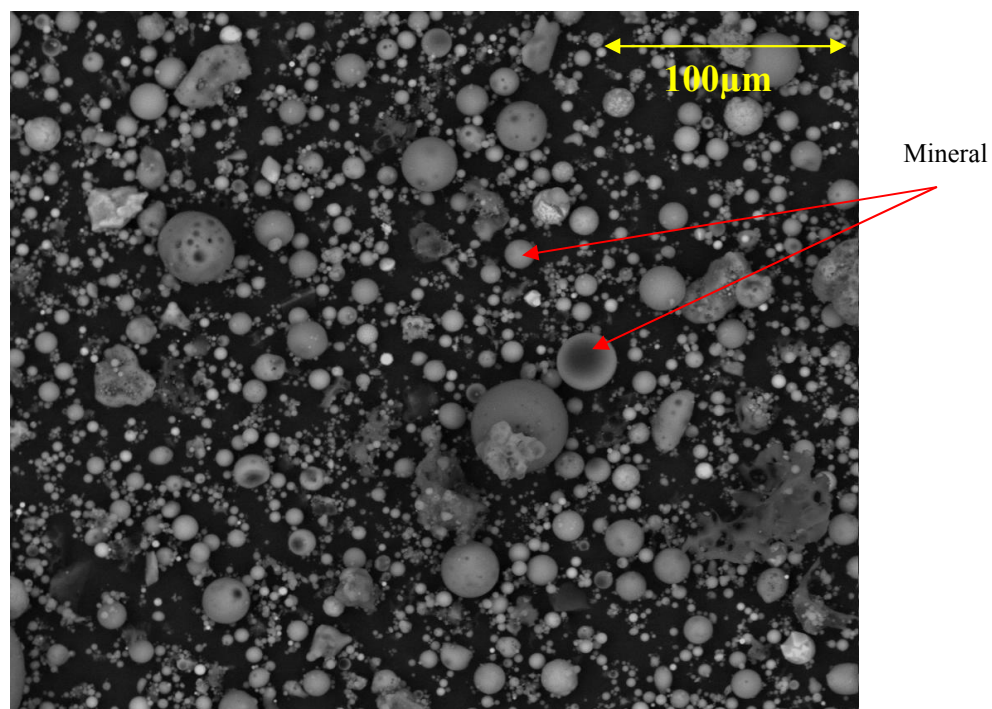


Figure B.32: SEM image of B2 sample.

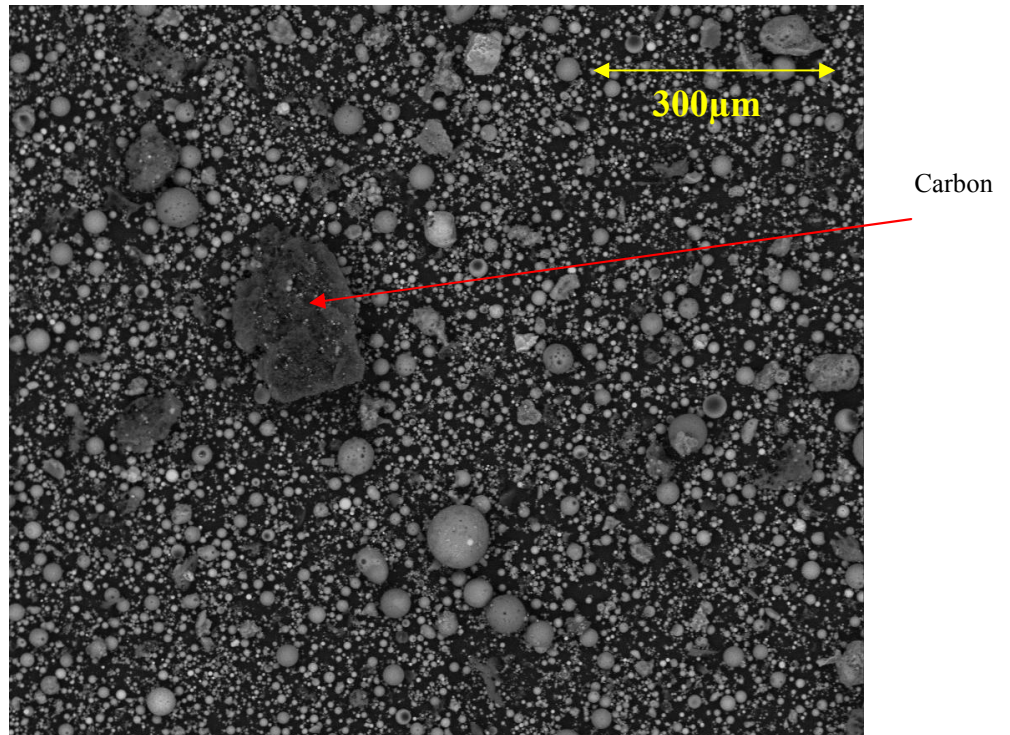


Figure B.33: SEM image of B2 sample.

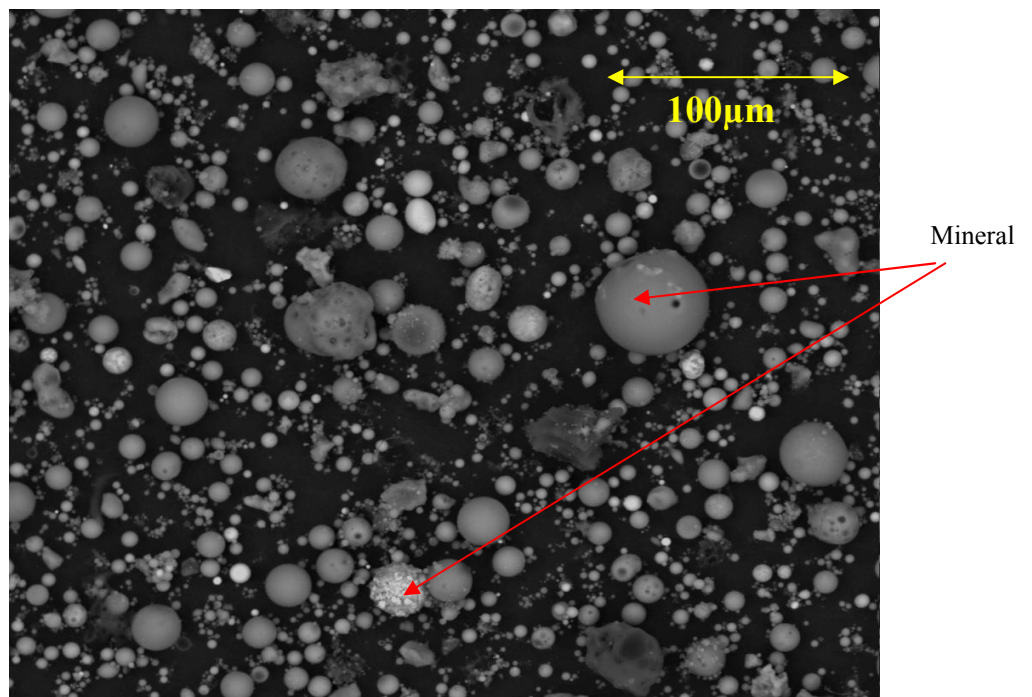


Figure B.34: SEM image of B3 sample.

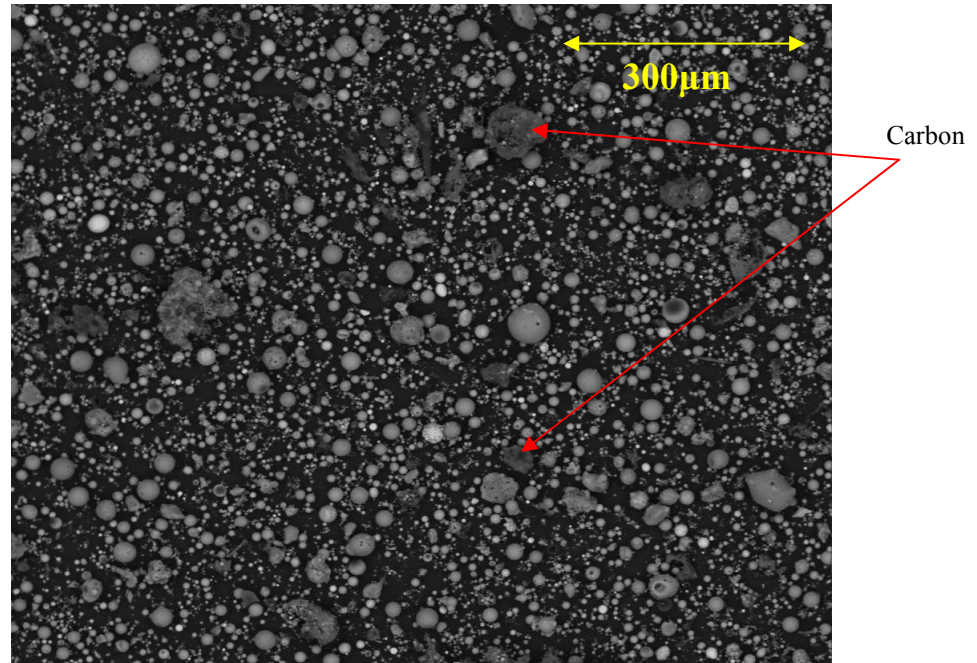


Figure B.35: SEM image of B3 sample.

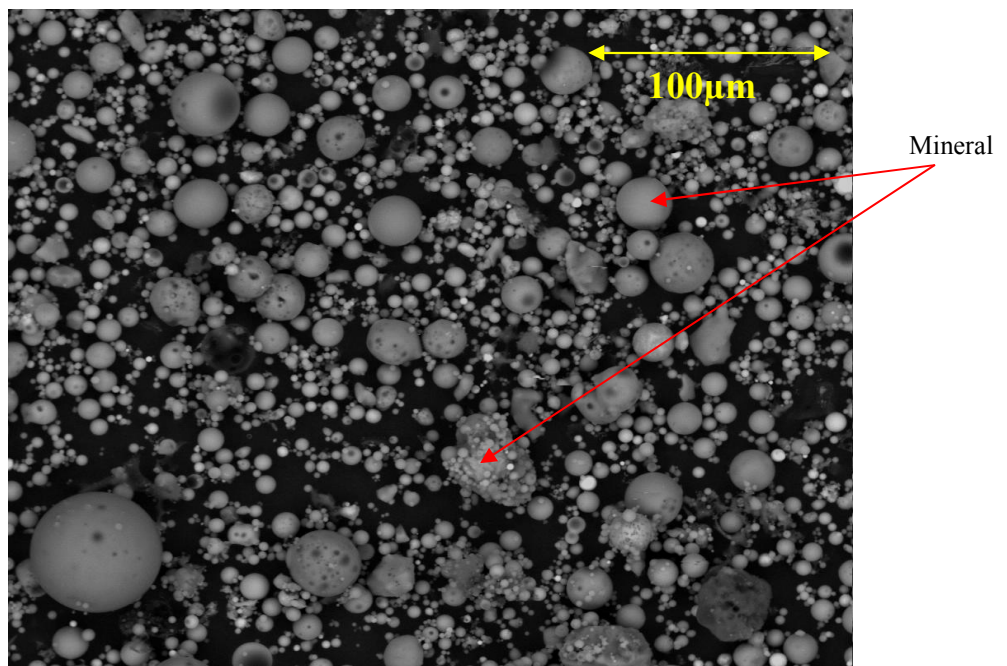


Figure B.36: SEM image of B4 sample.

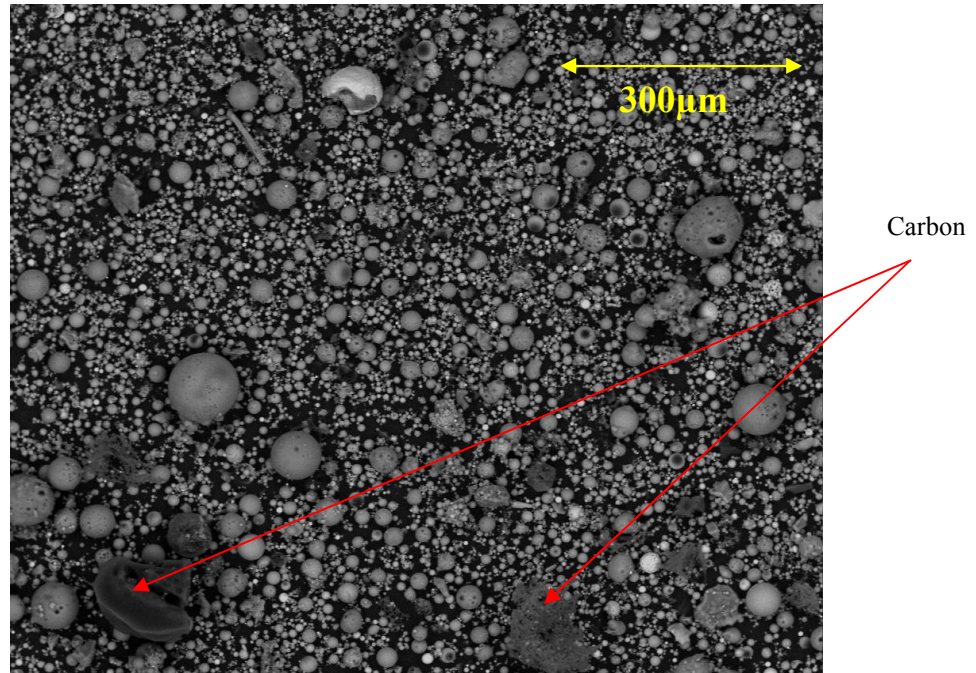


Figure B.37: SEM image of B4 sample.

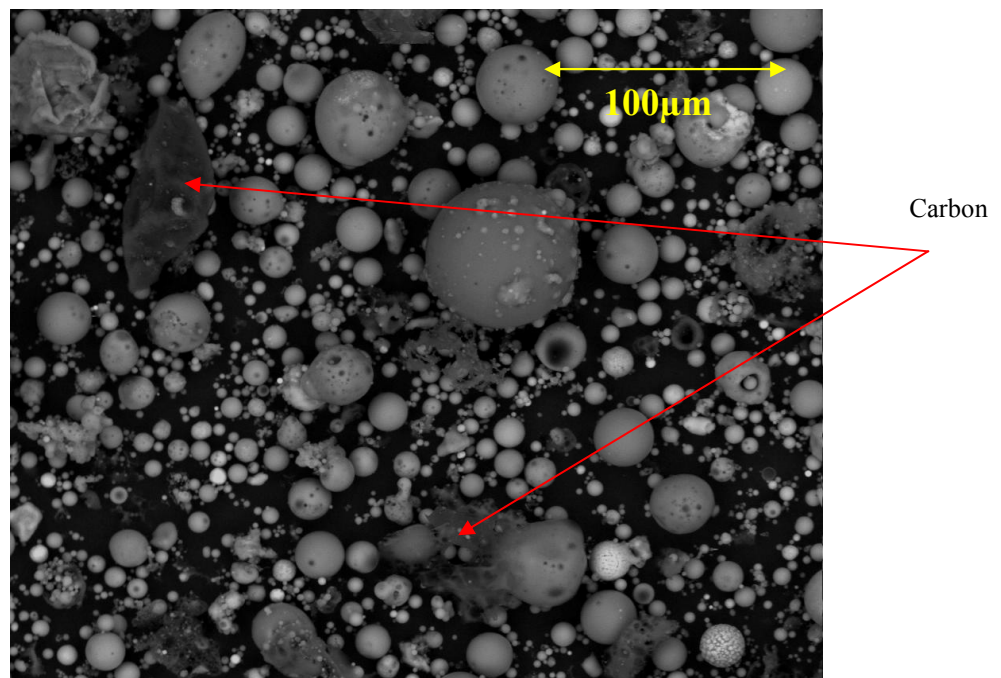


Figure B.38: SEM image of B5 sample.

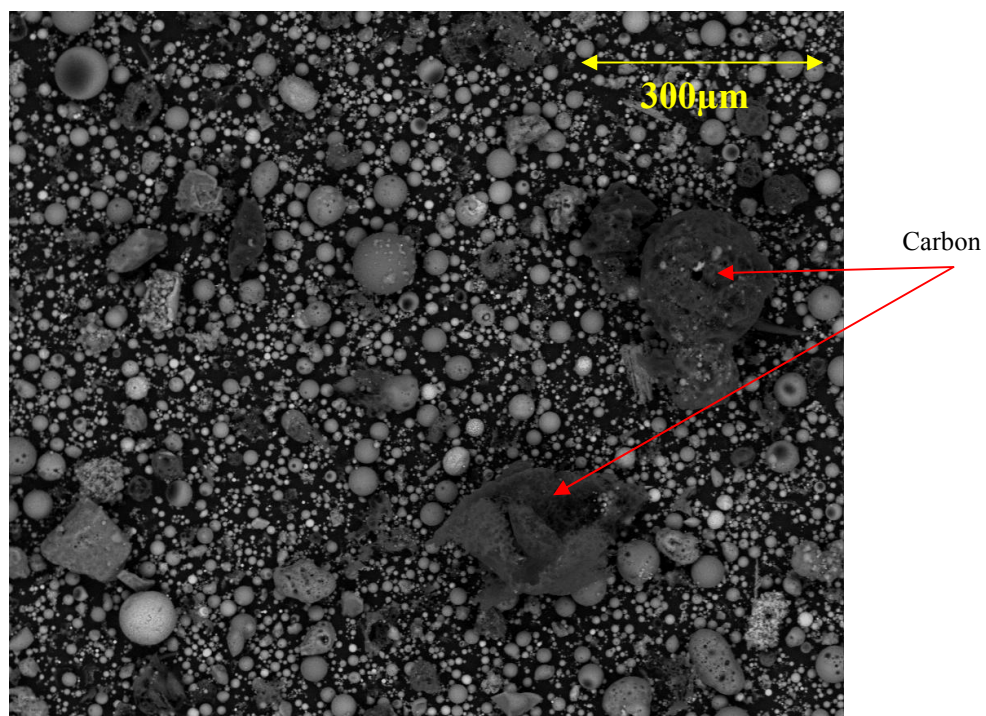


Figure B.39: SEM image of B5 sample.

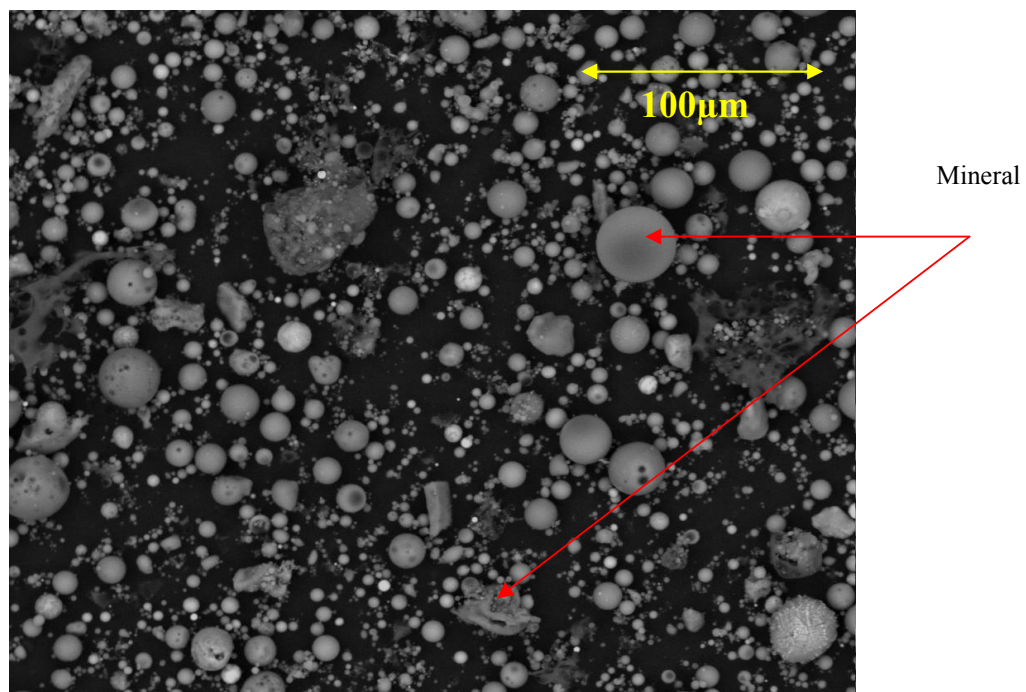


Figure B.40: SEM image of B6 sample.

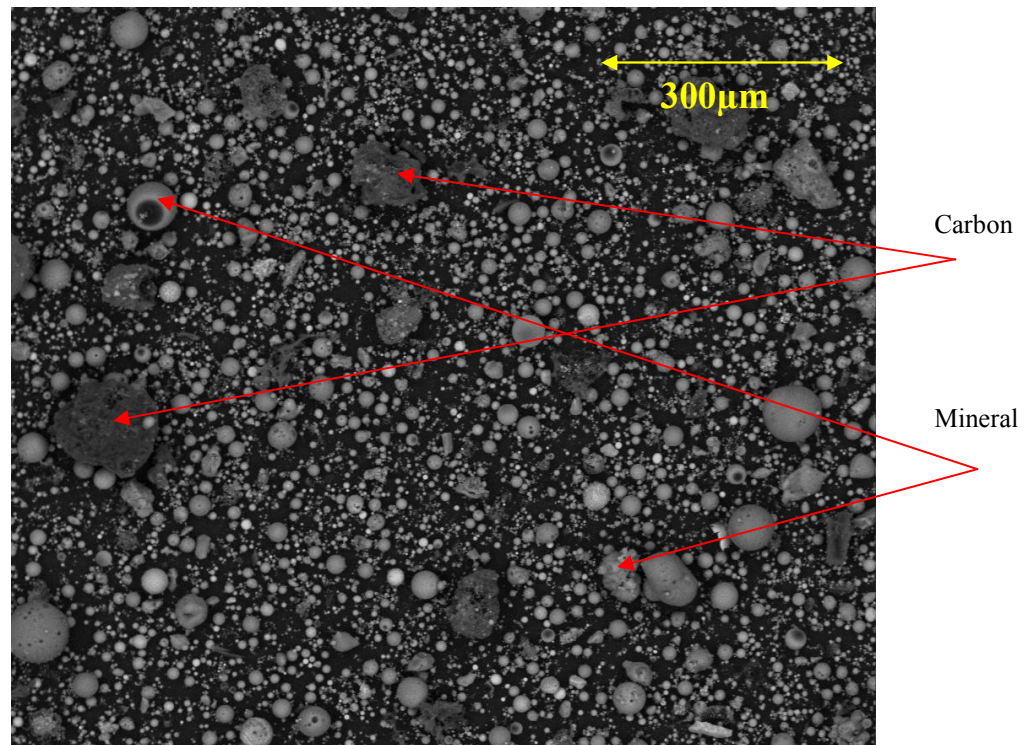


Figure B.41: SEM image of B6 sample.

Appendix C

Figures of EDX-graph for all the samples

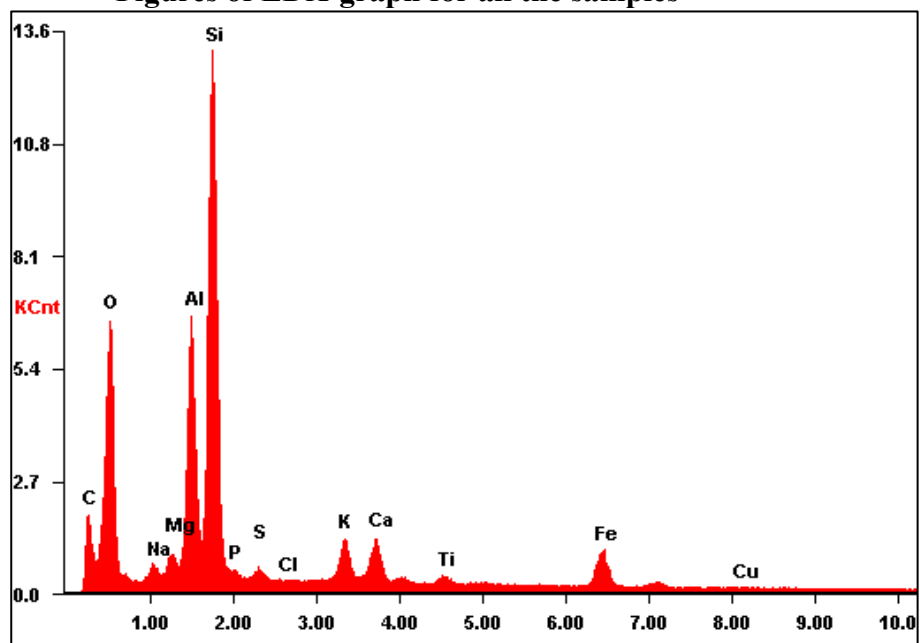


Figure C.1: EDX-graph for C1 sample.

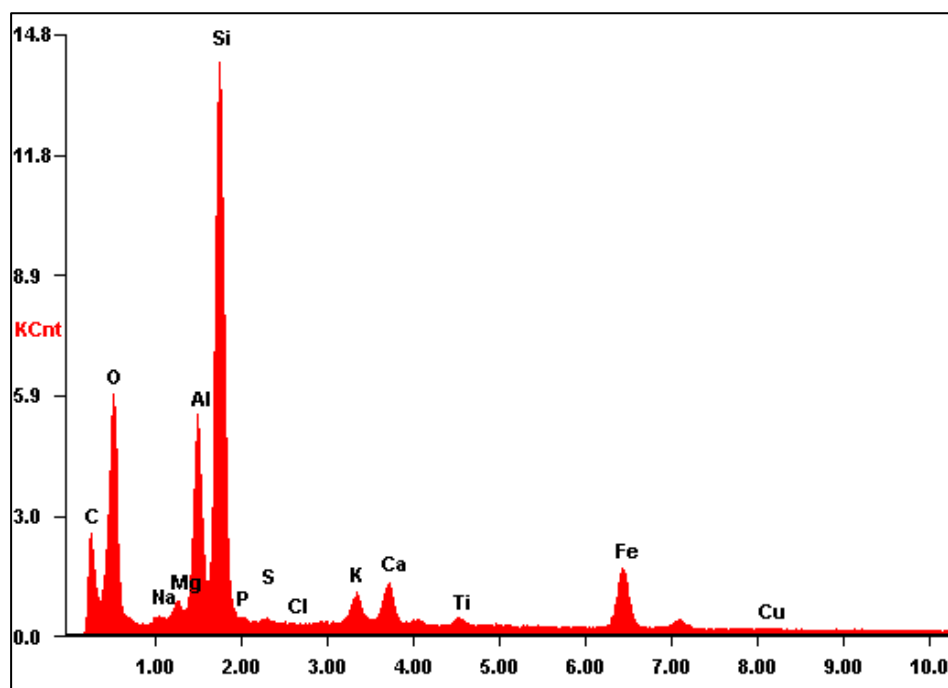


Figure C.2: EDX-graph for C2 sample.

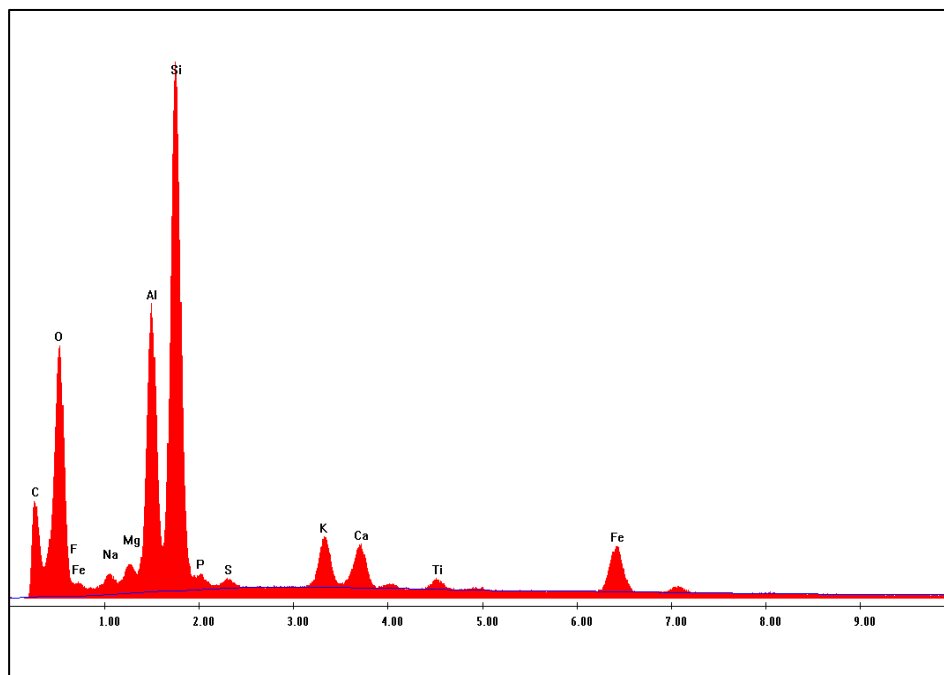


Figure C.3: EDX-graph for B1 sample.

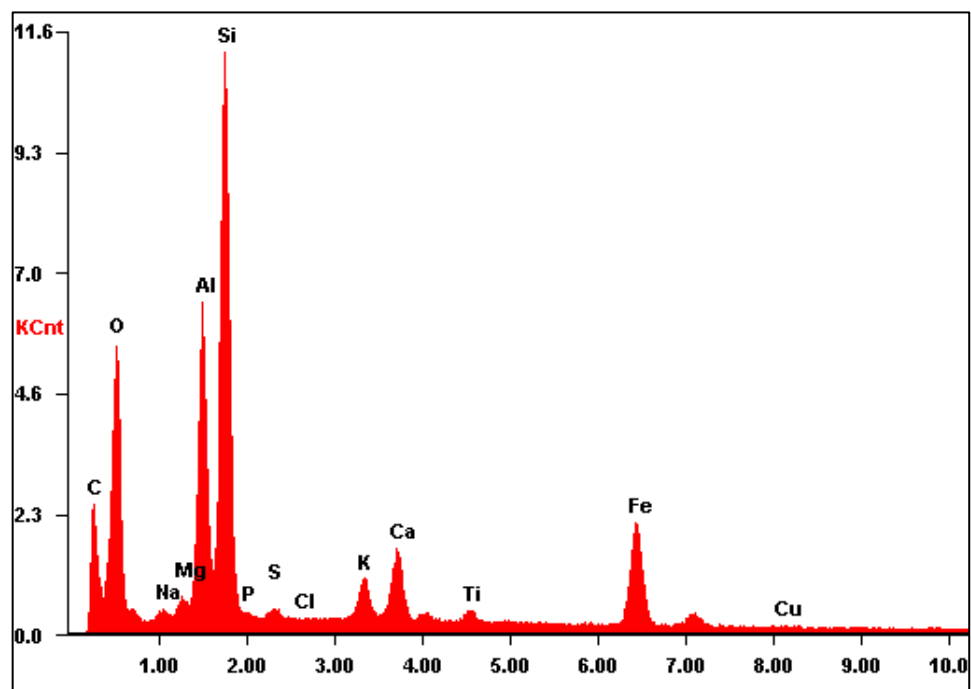


Figure C.4: EDX-graph for C3 sample.

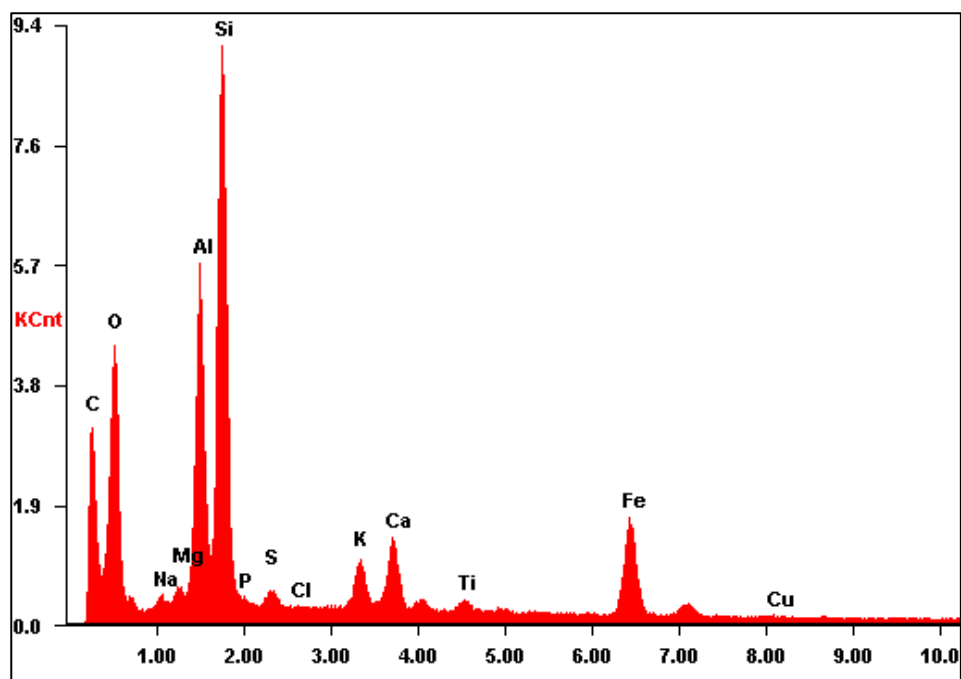


Figure C.5: EDX-graph for C4 sample.

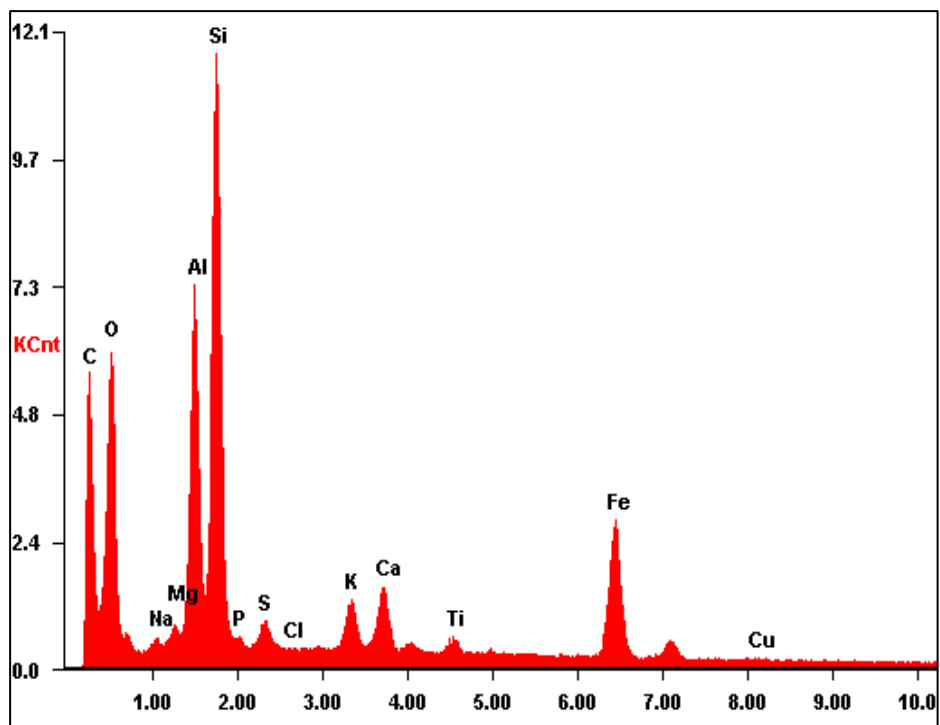


Figure C.6: EDX- graph for C5 sample.

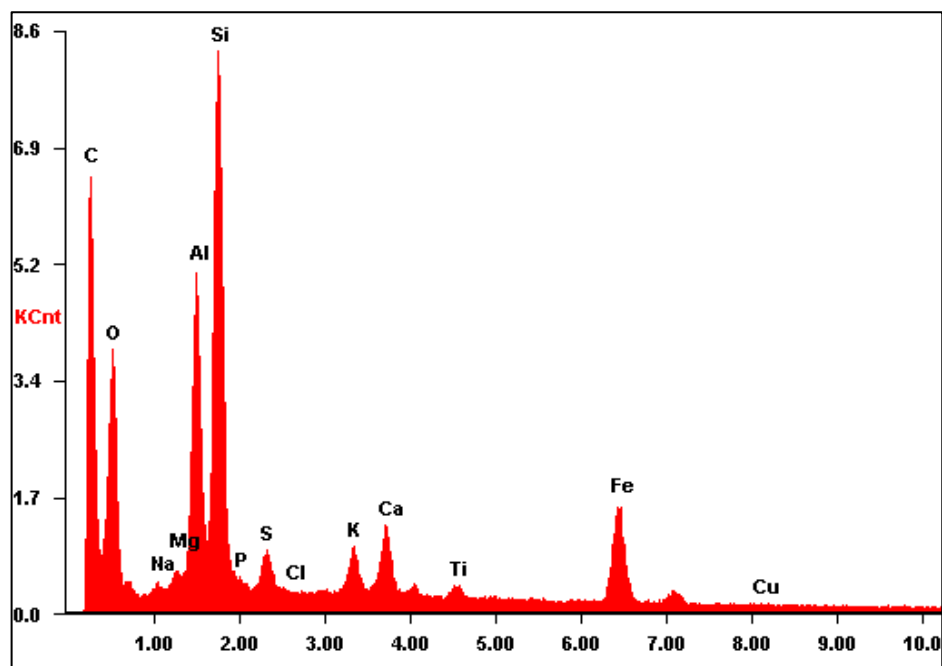


Figure C.7: EDX- graph for C6 sample.

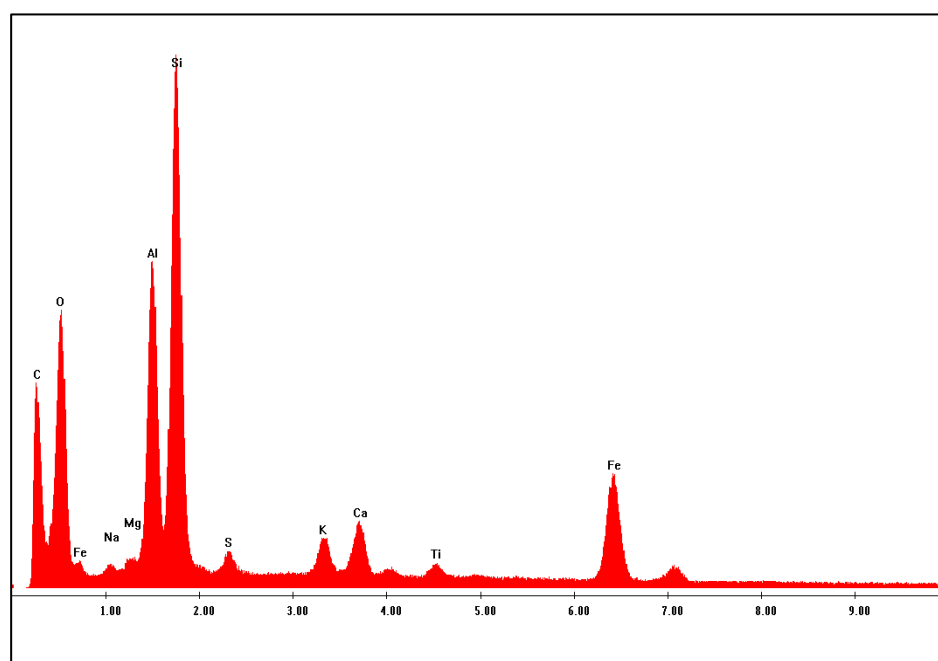


Figure C.8: EDX-graph for C7 sample.

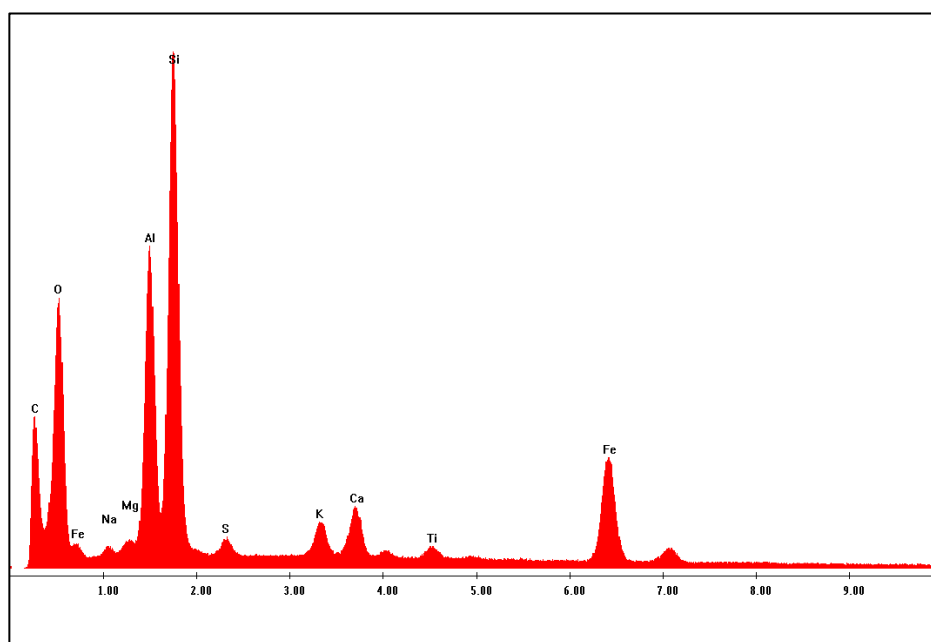


Figure C.9: EDX-graph for C8 sample.

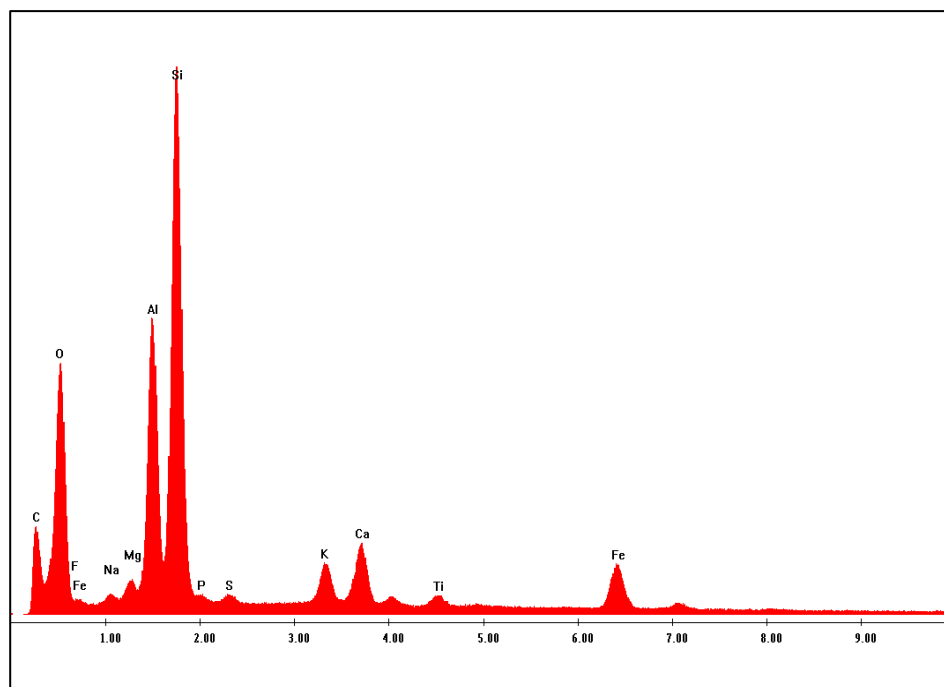


Figure C.10: EDX- graph for C9 sample.

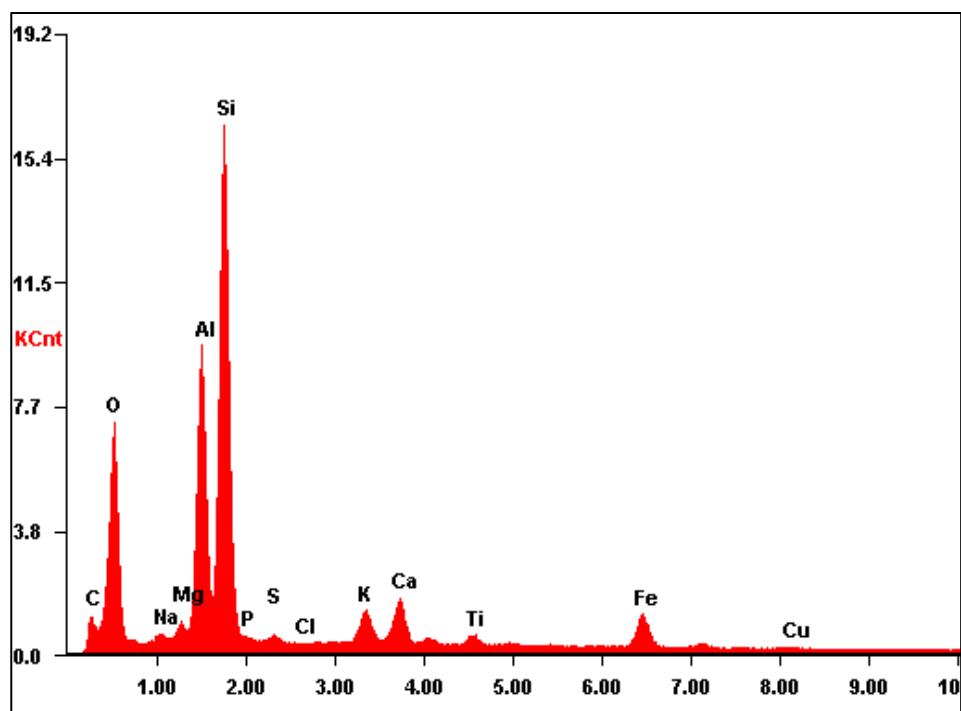


Figure C.11: EDX- graph for C10 sample.

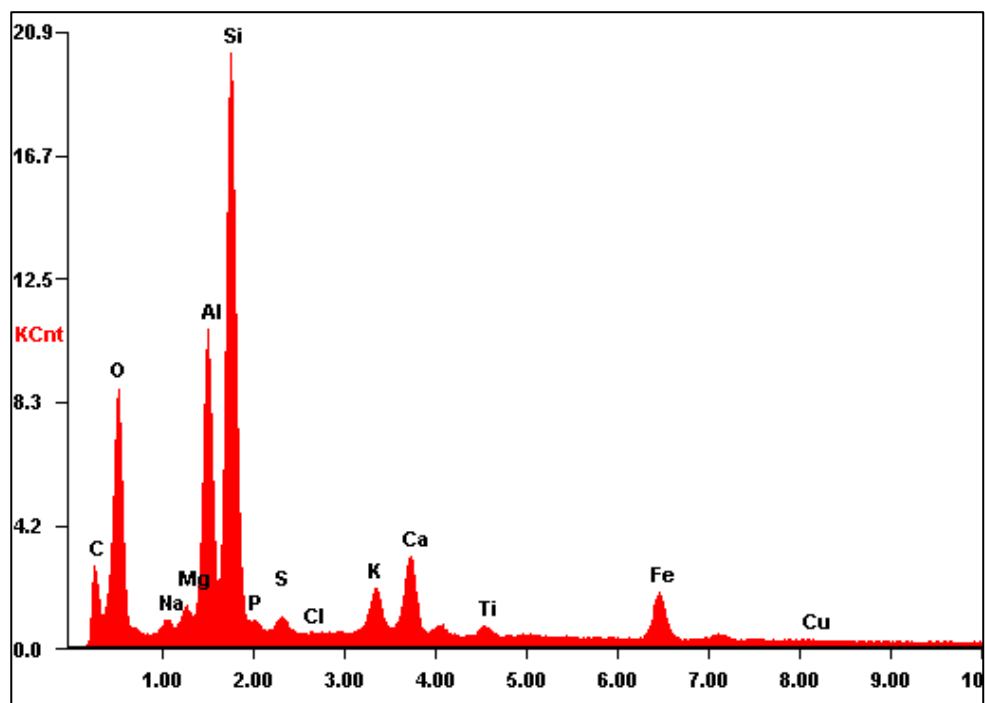


Figure C.12: EDX- graph for B2 sample.

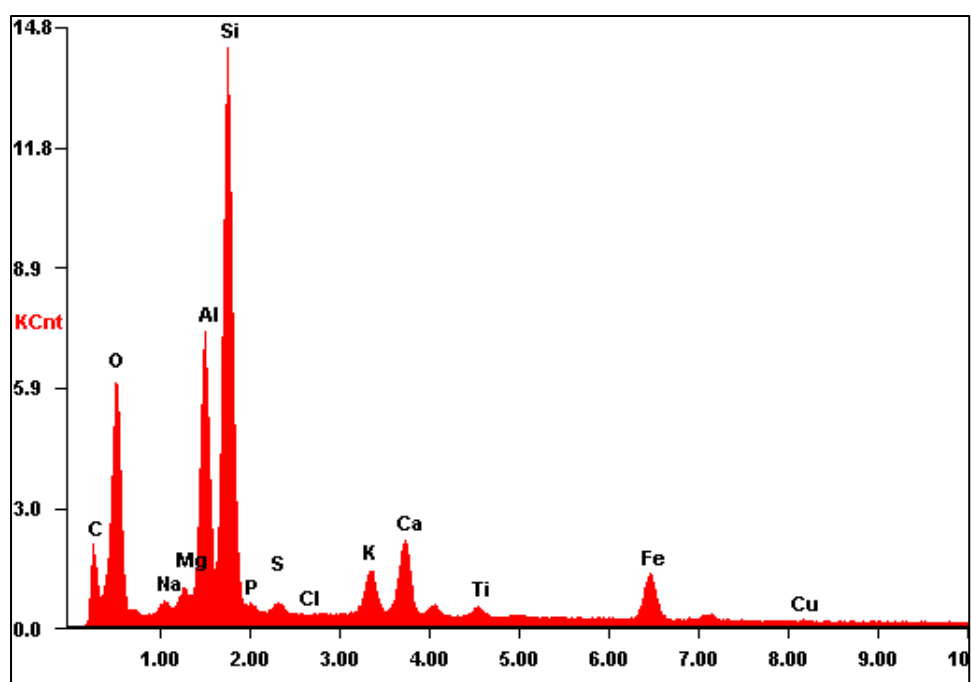


Figure C.13: EDX- graph for B3 sample.

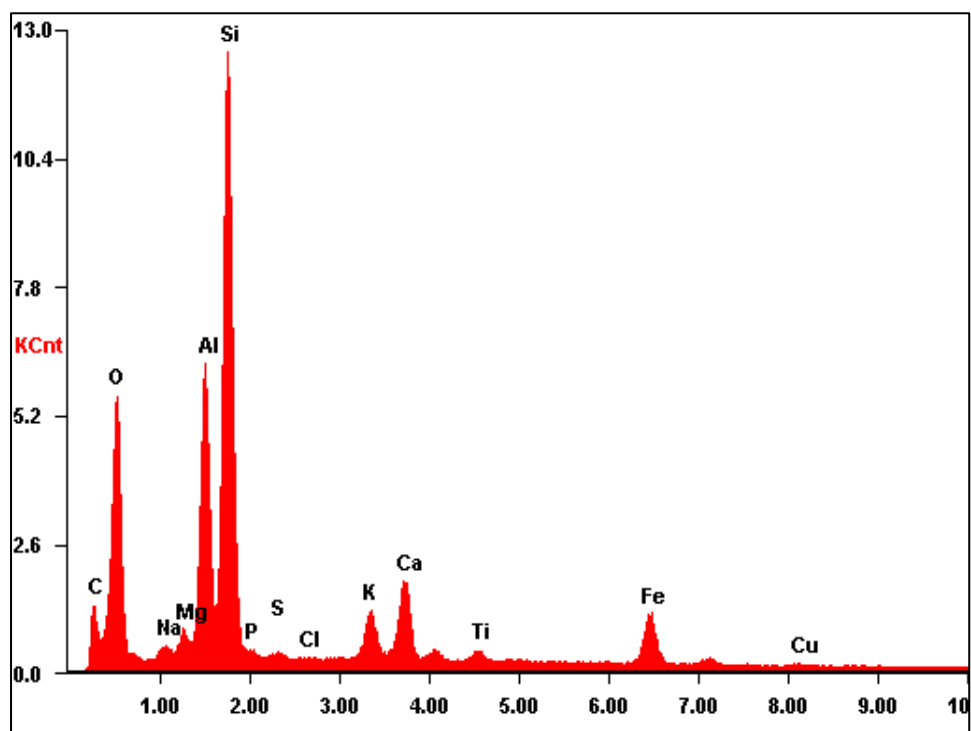


Figure C.14: EDX- graph for B4 sample.

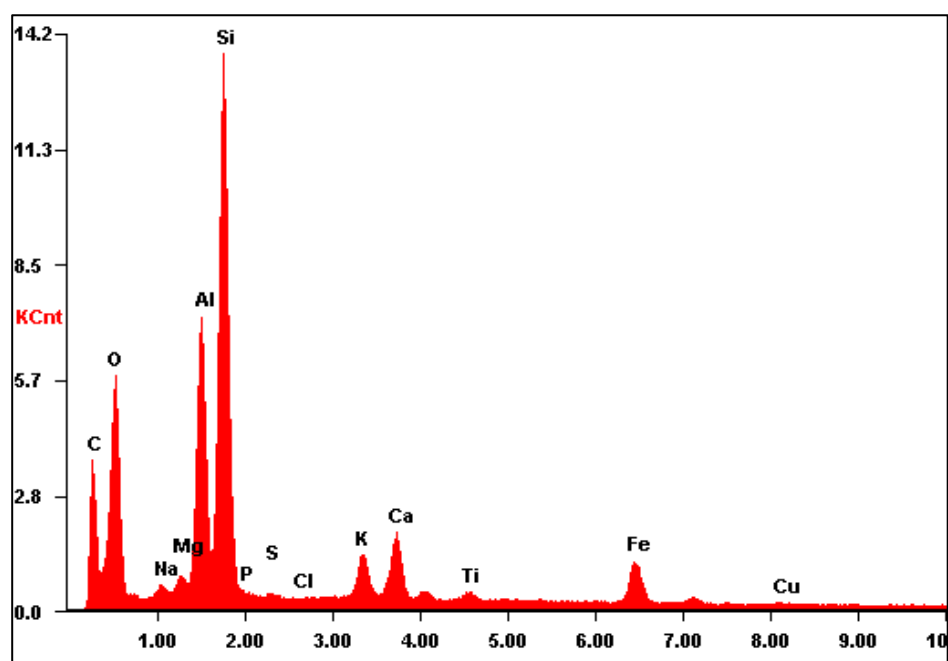


Figure C.15: EDX- graph for B5 sample.

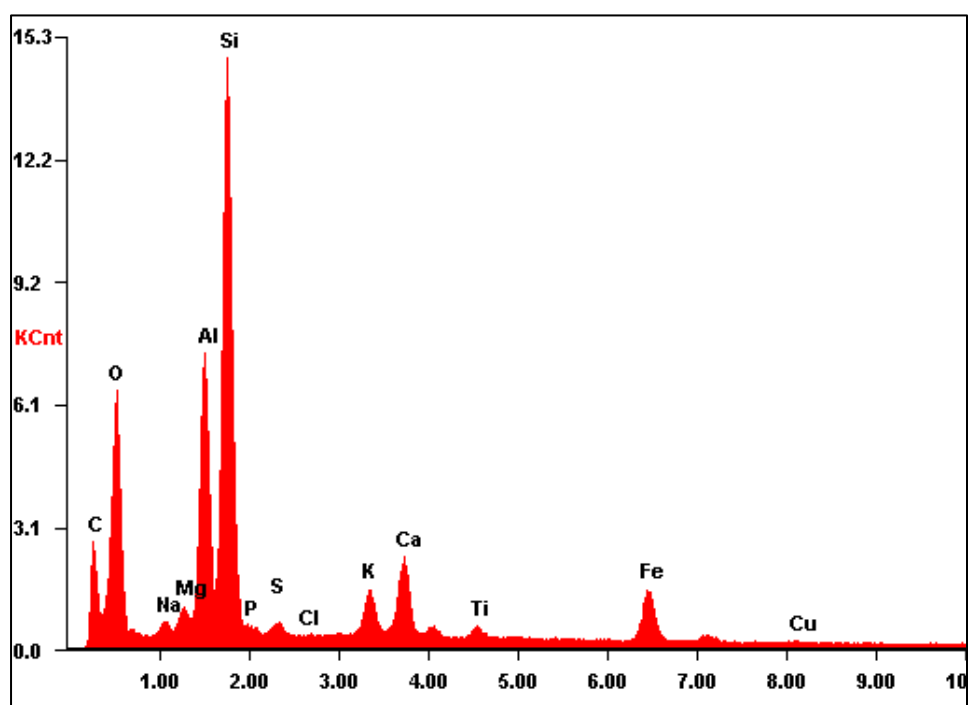


Figure C.16: EDX- graph for B6 sample.

Appendix D

Figures of XRD-graph for all the samples

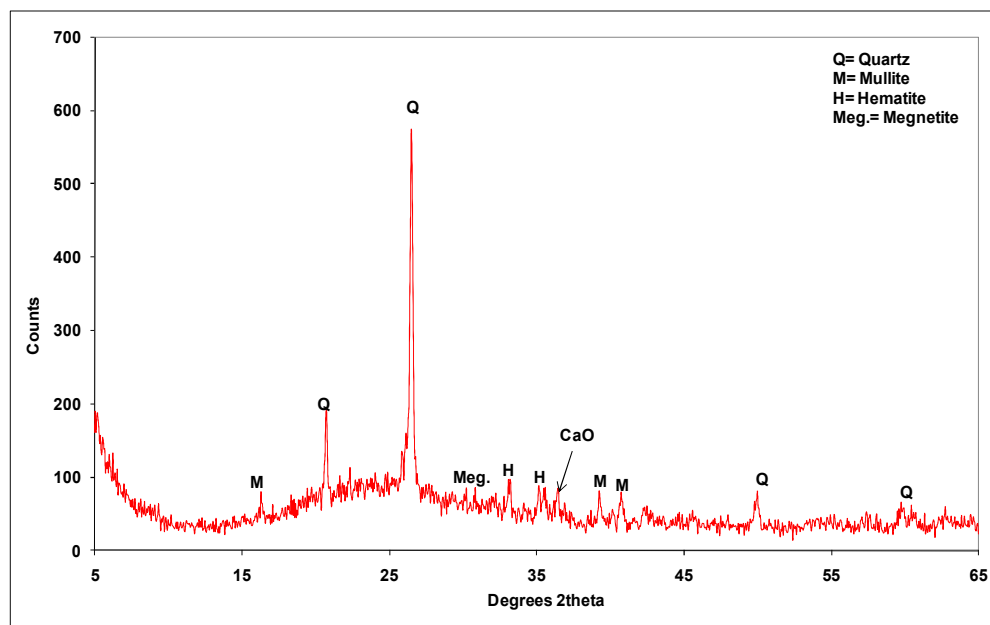


Figure D.1: XRD graph for C1 sample.

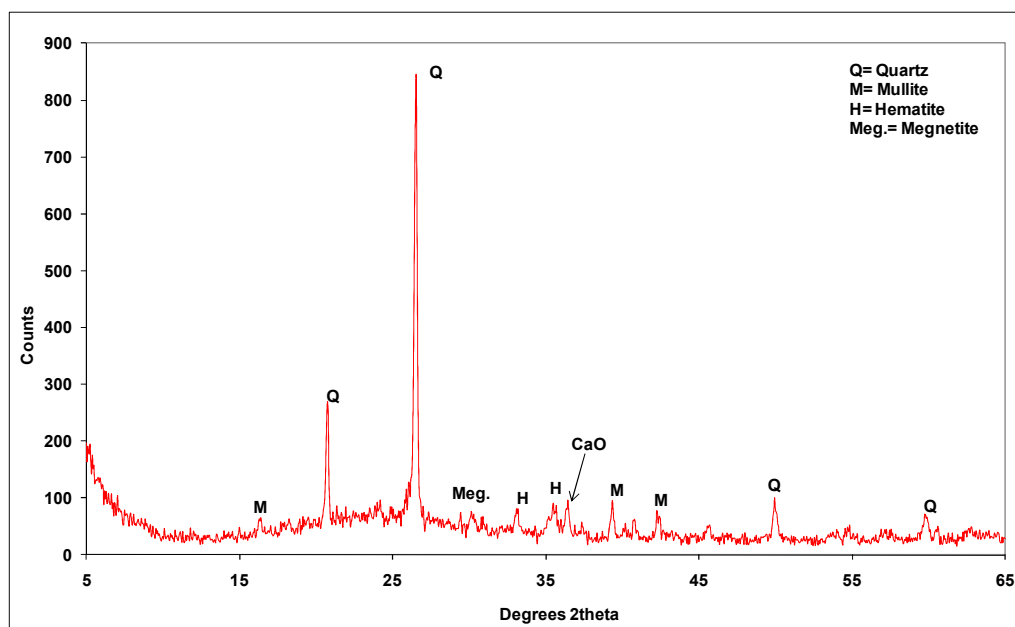


Figure D.2: XRD graph for C2 sample.

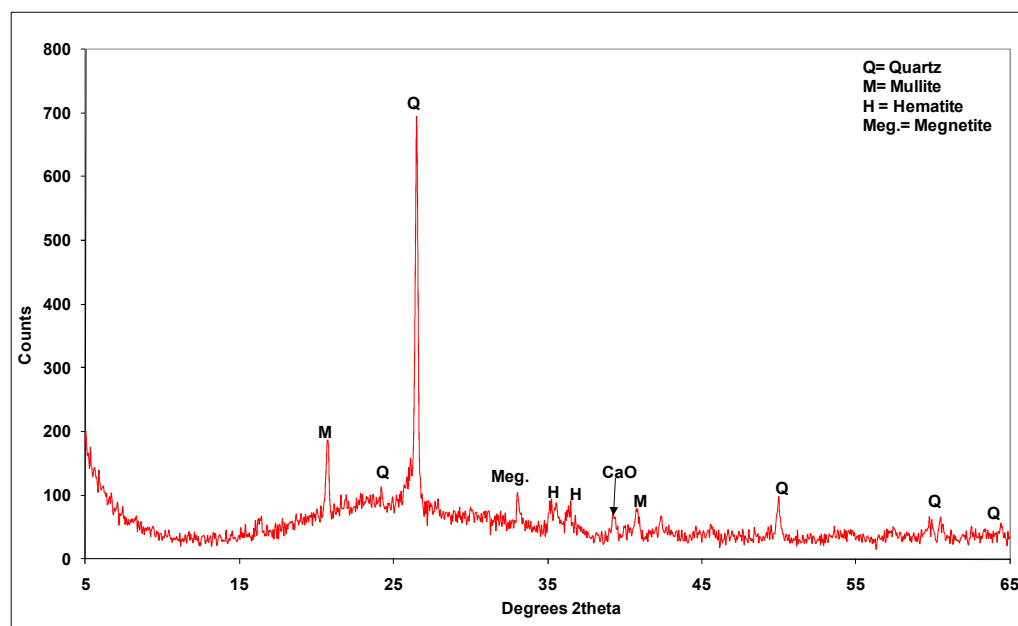


Figure D.3: XRD graph for B1 sample.

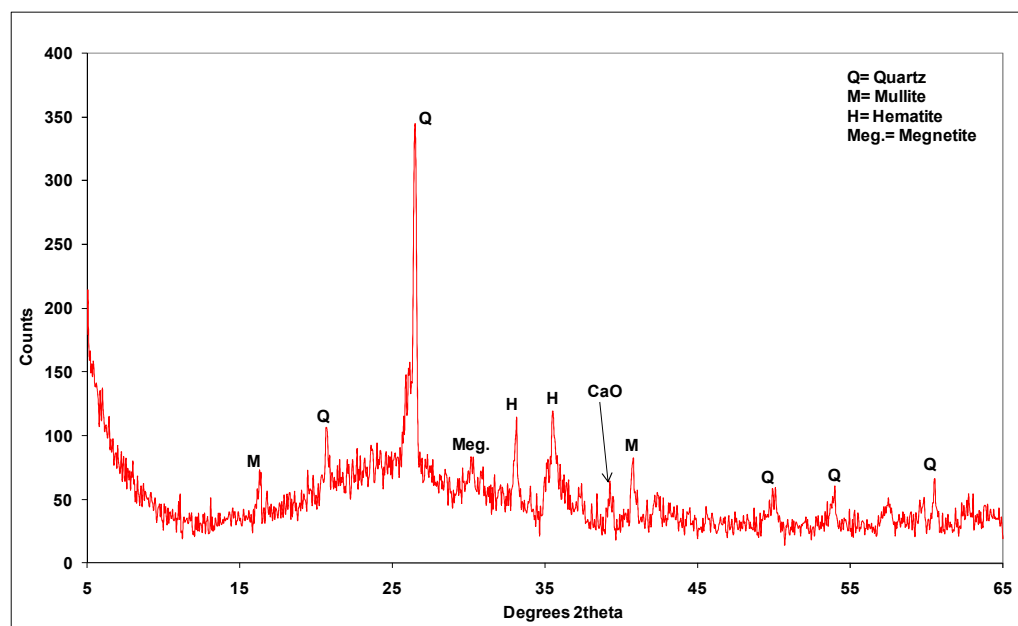


Figure D.4: XRD graph for C3 sample.

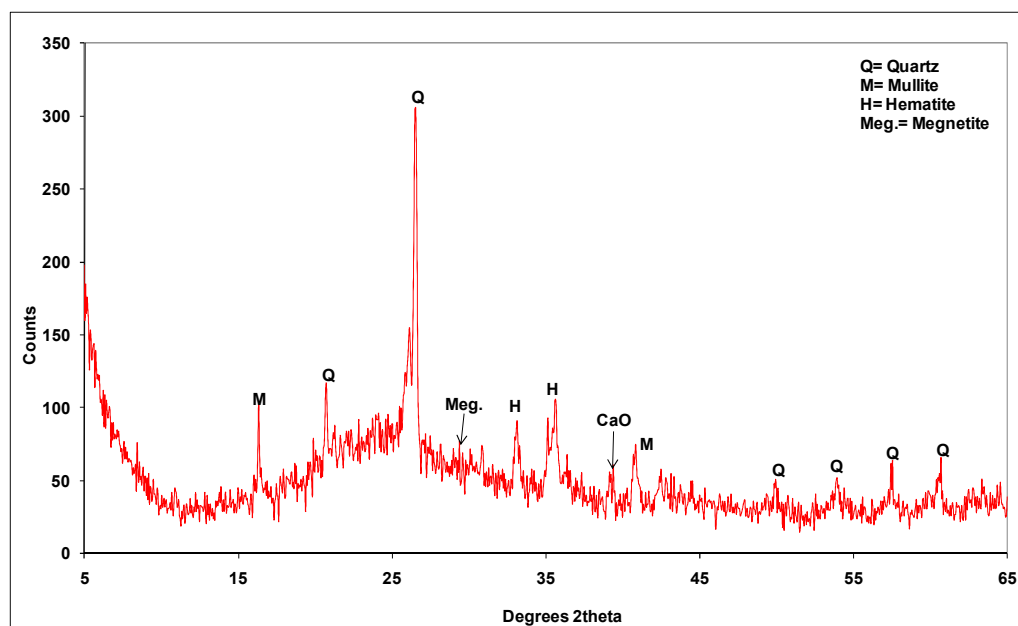


Figure D.5: XRD graph for C4 sample.

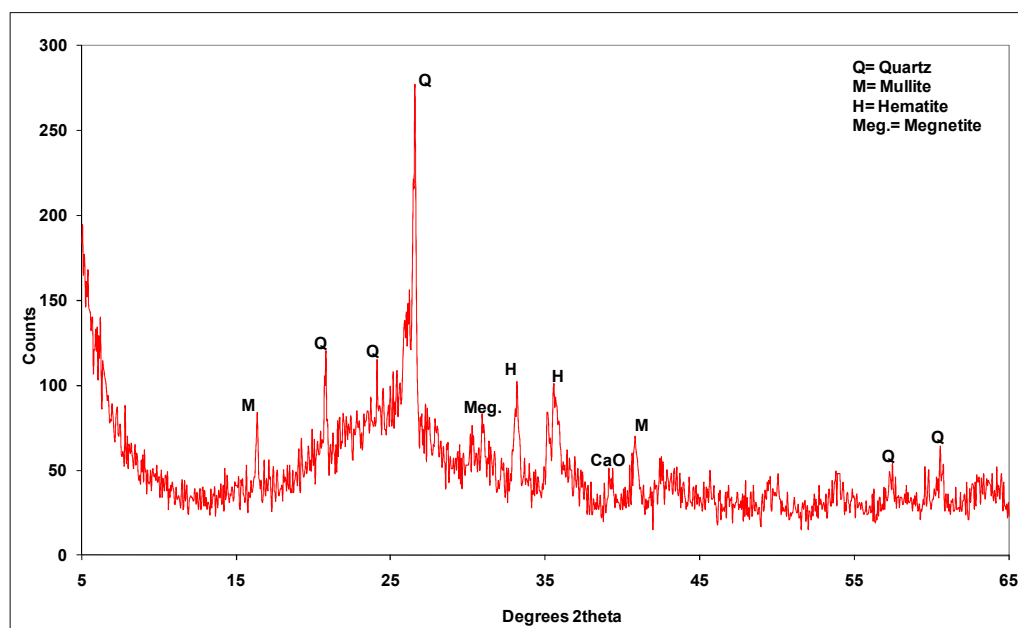


Figure D.6: XRD graph for C5 sample.

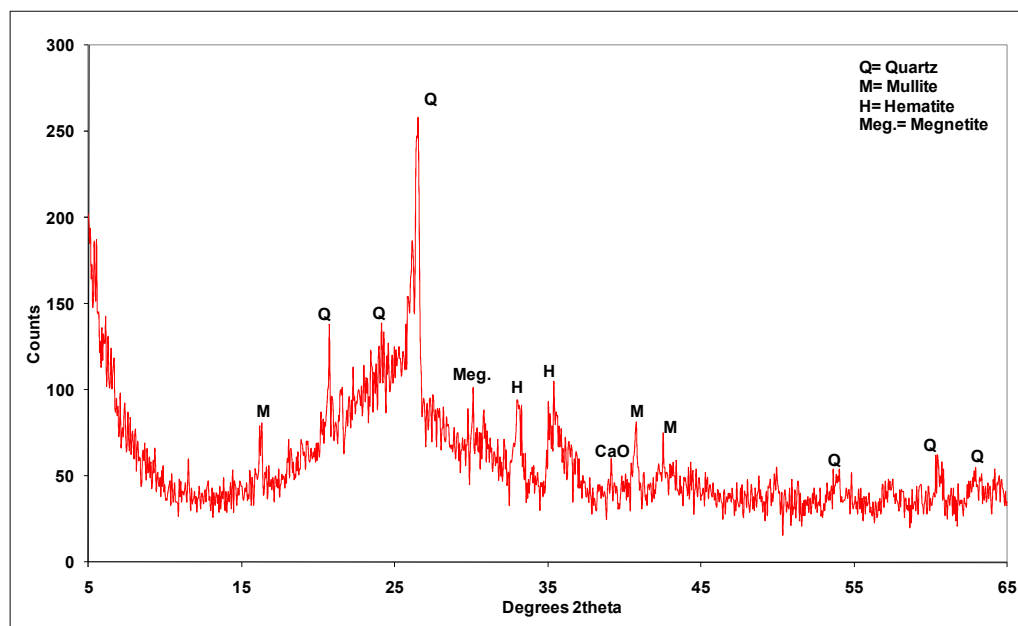


Figure D.7: XRD graph for C6 sample.

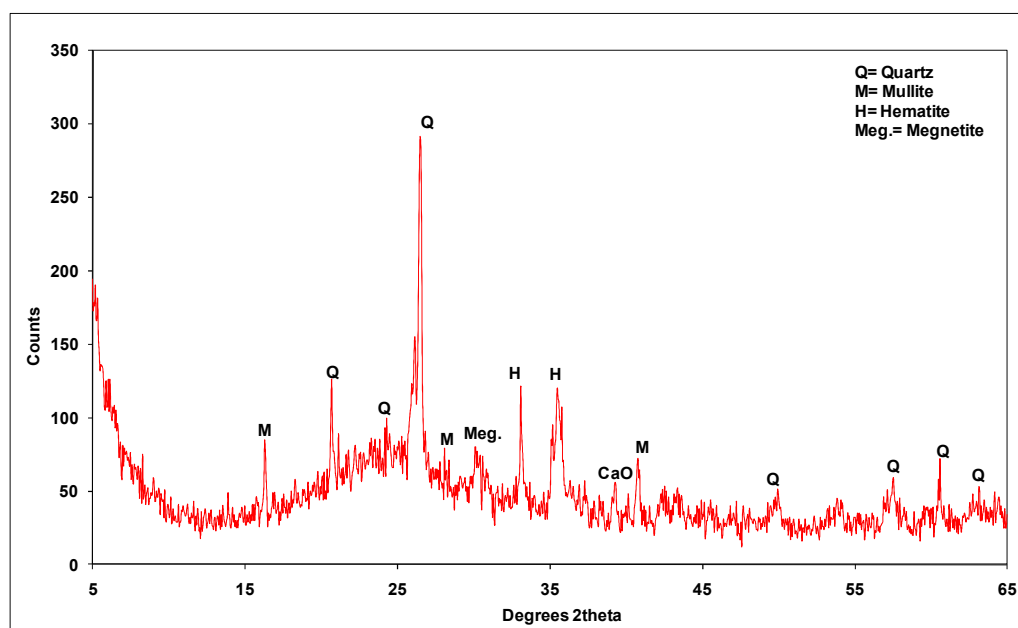


Figure D.8: XRD graph for C7 sample.

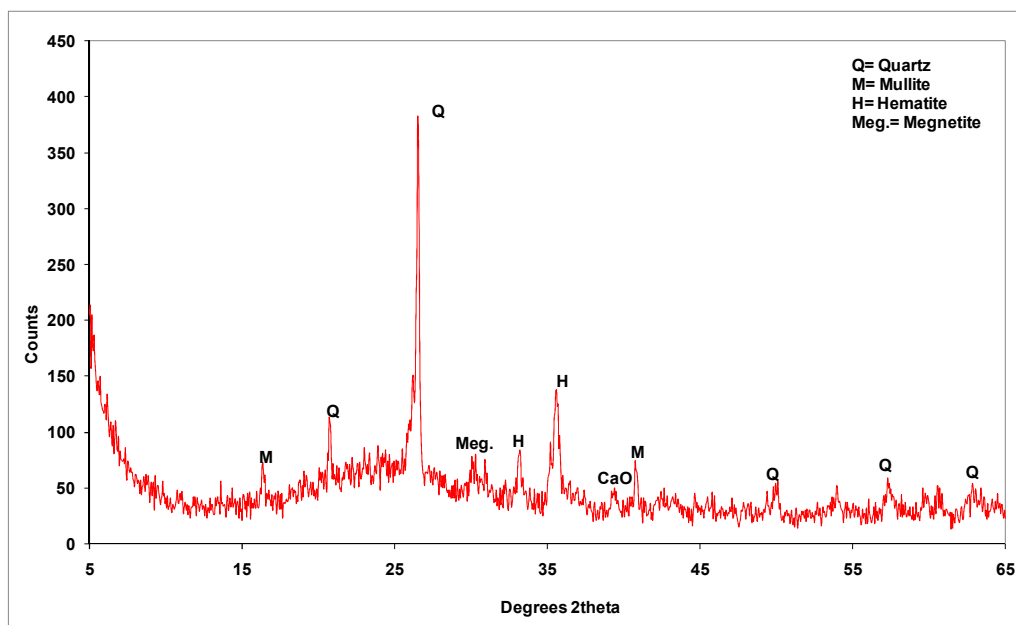


Figure D.9: XRD graph for C8 sample.

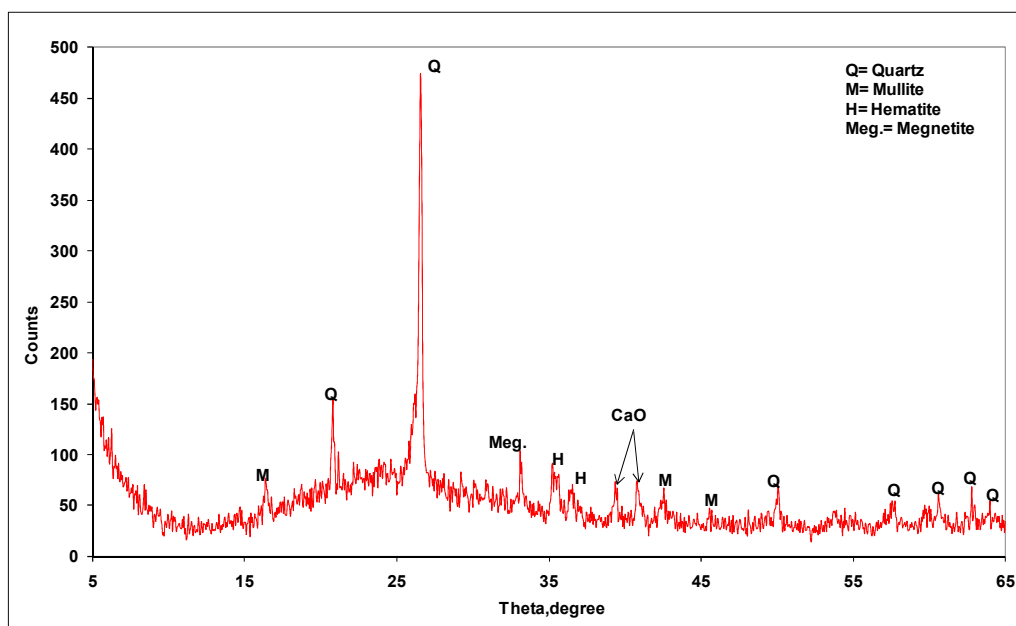


Figure D.10: XRD graph for C9 sample.

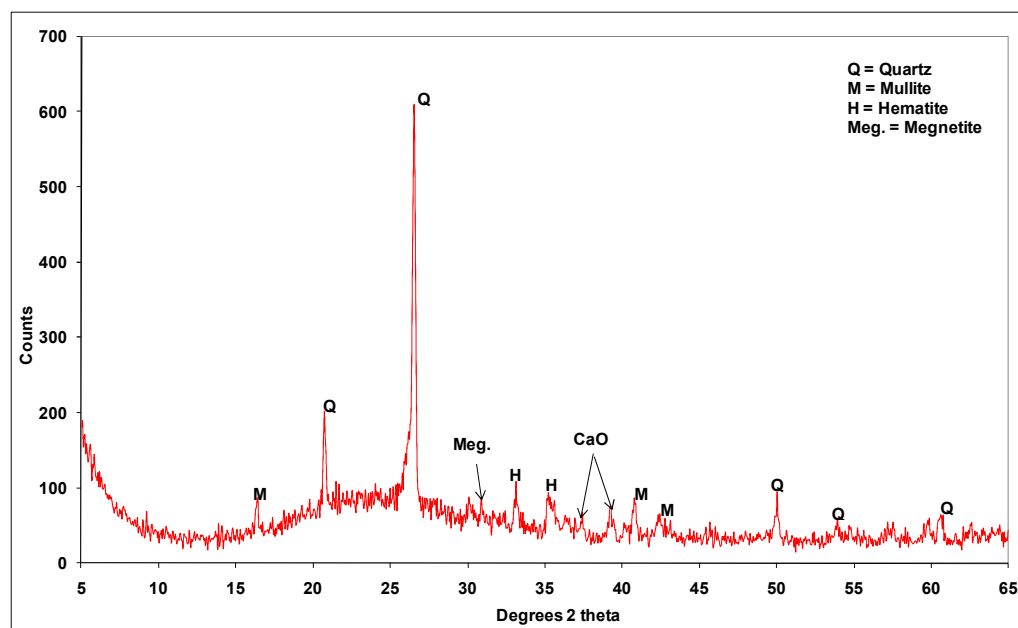


Figure D.11: XRD graph for C10 sample.

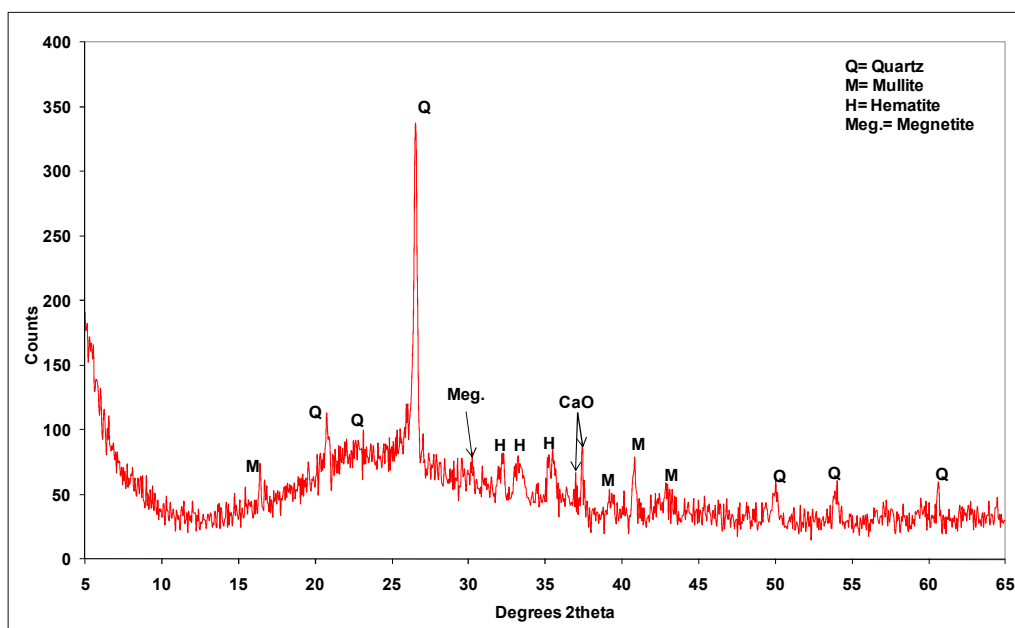


Figure D.12: XRD graph for B2 sample.

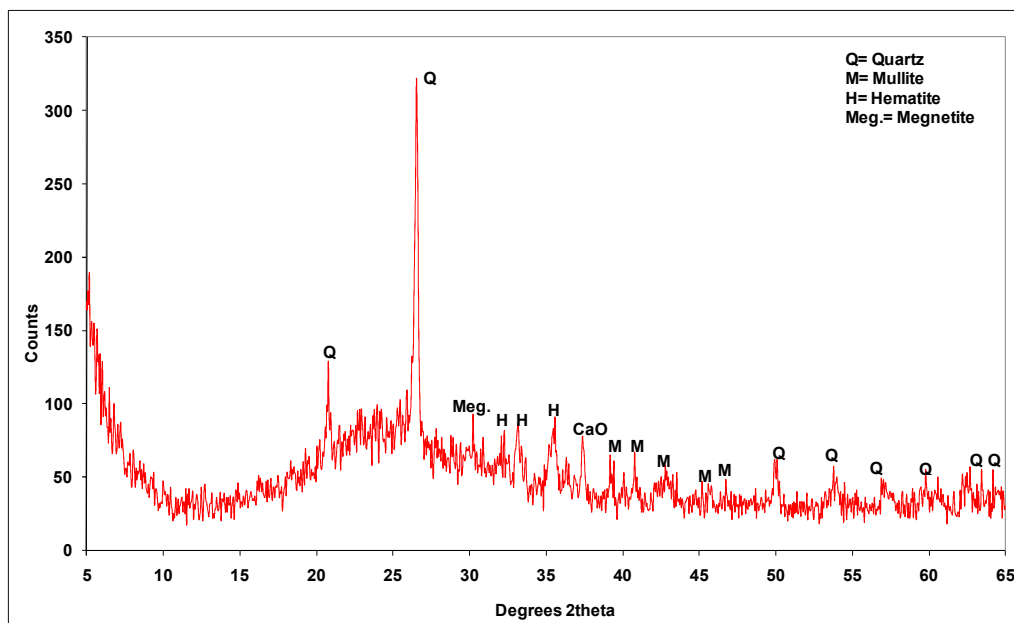


Figure D.13: XRD graph for B3 sample.

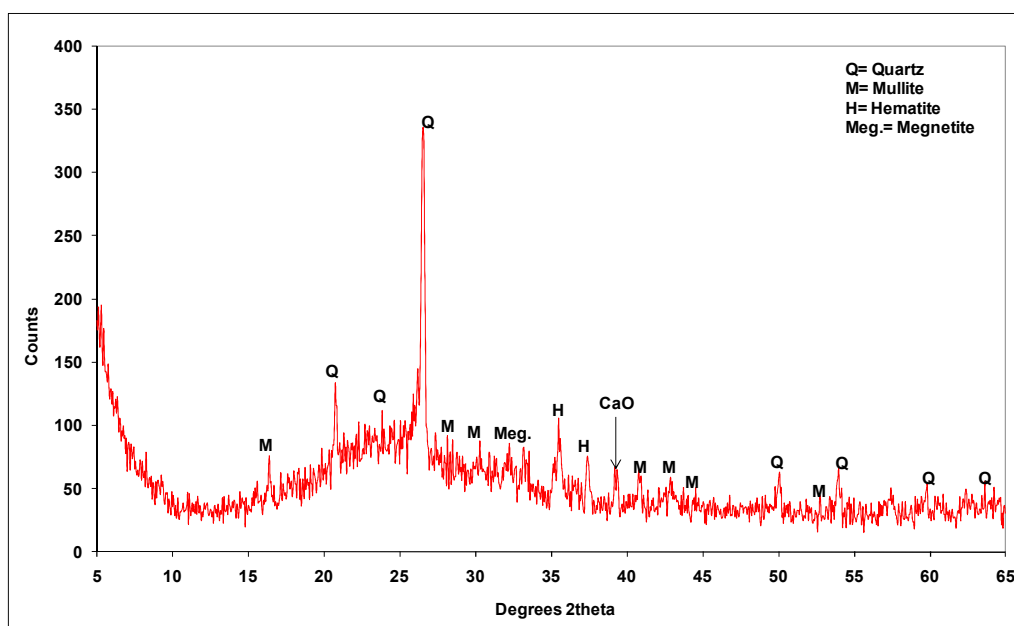


Figure D.14: XRD graph for B4 sample.

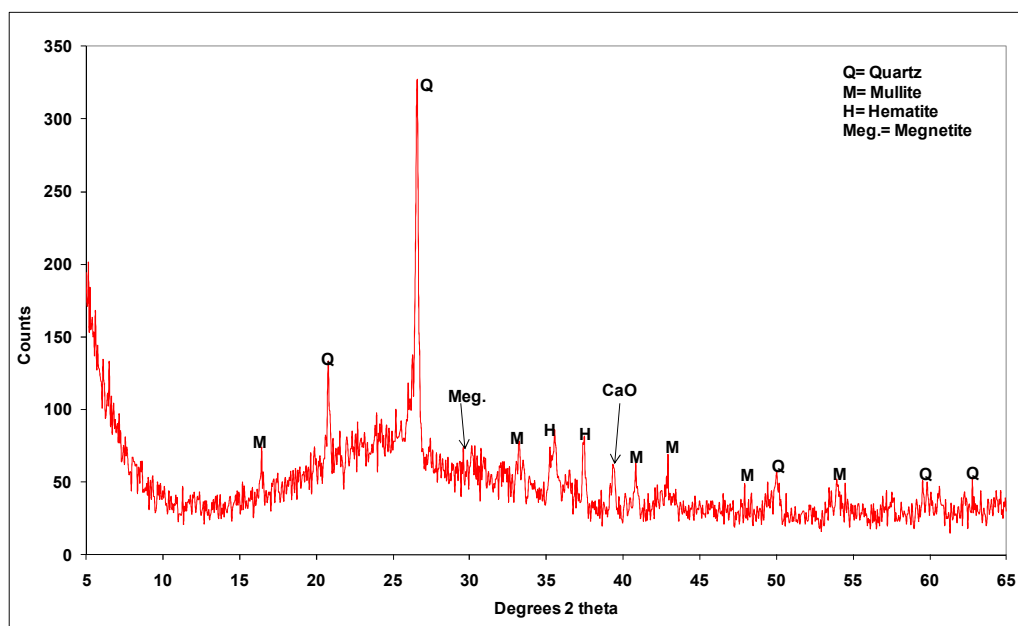


Figure D.15: XRD graph for B5 sample.

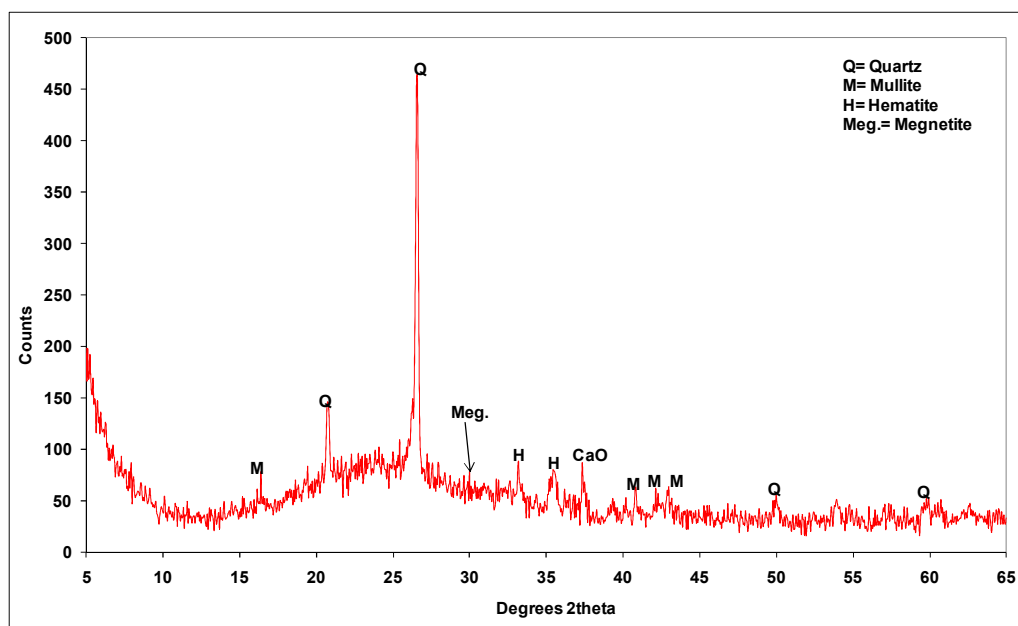


Figure D.16: XRD graph for B6 sample.

Appendix E

Adsorption isotherms for the enriched and activated carbons

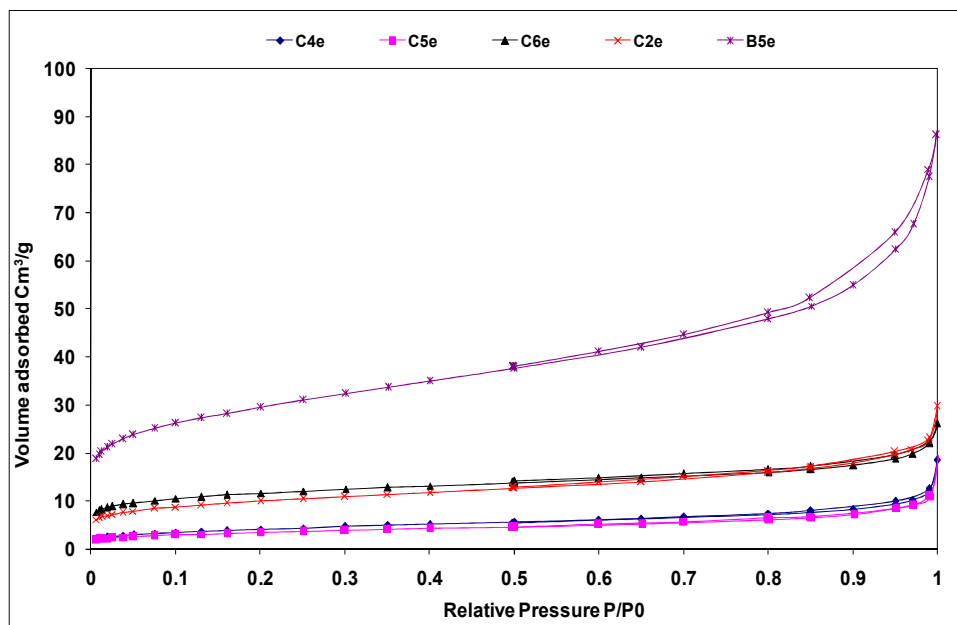


Figure E.1: Isotherms of the carbon rich samples prior activation.

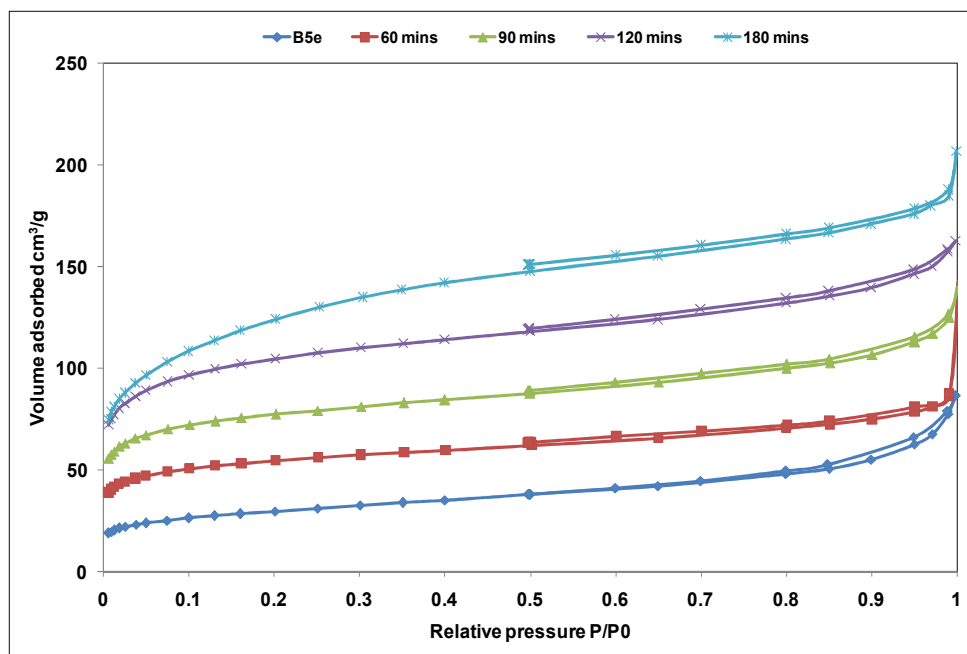


Figure E.2: Adsorption isotherms for B5e before and after activation.

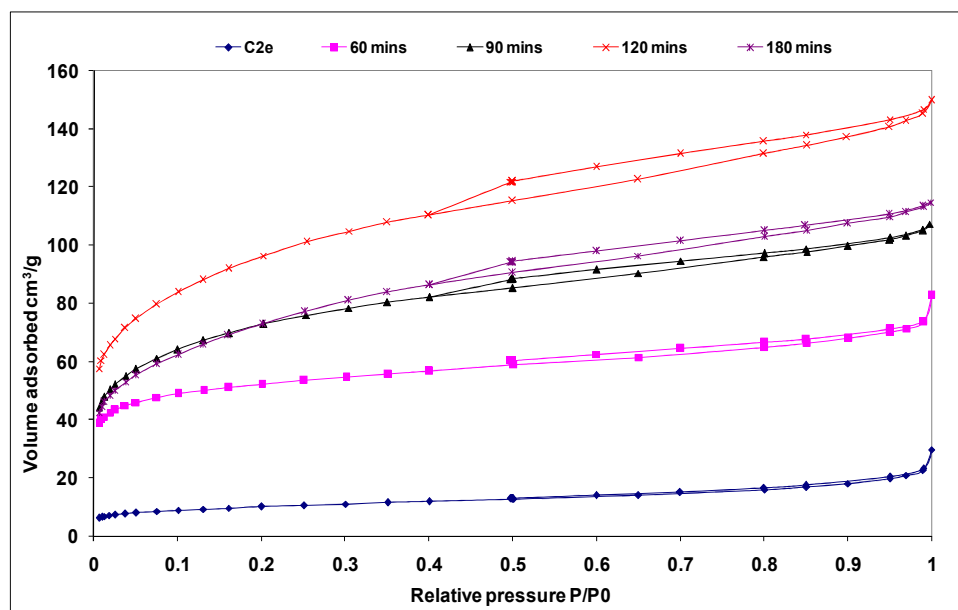


Figure E.3: Adsorption isotherms for C2e before and after activation.

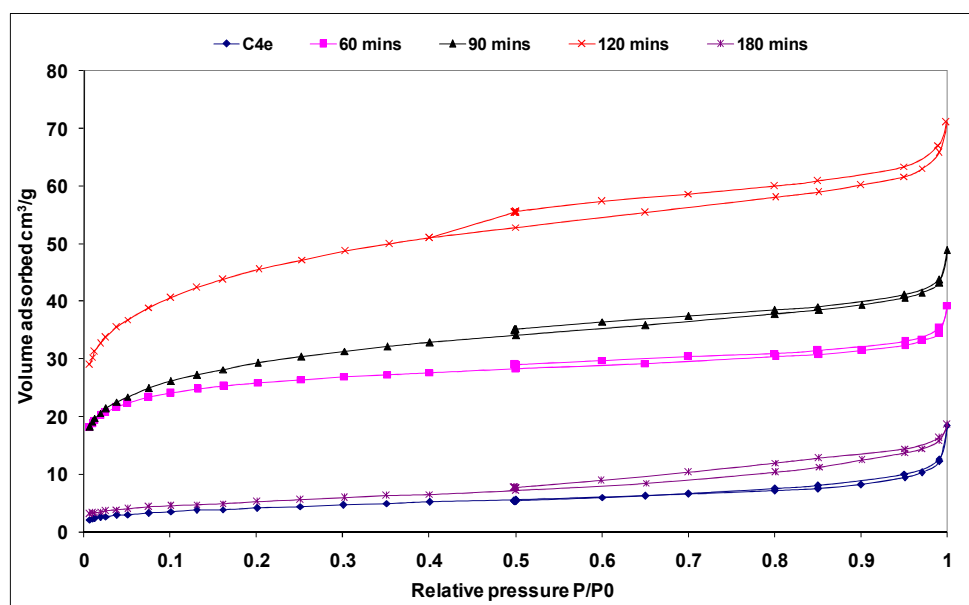


Figure E.4: Adsorption isotherms for C4e before and after activation.

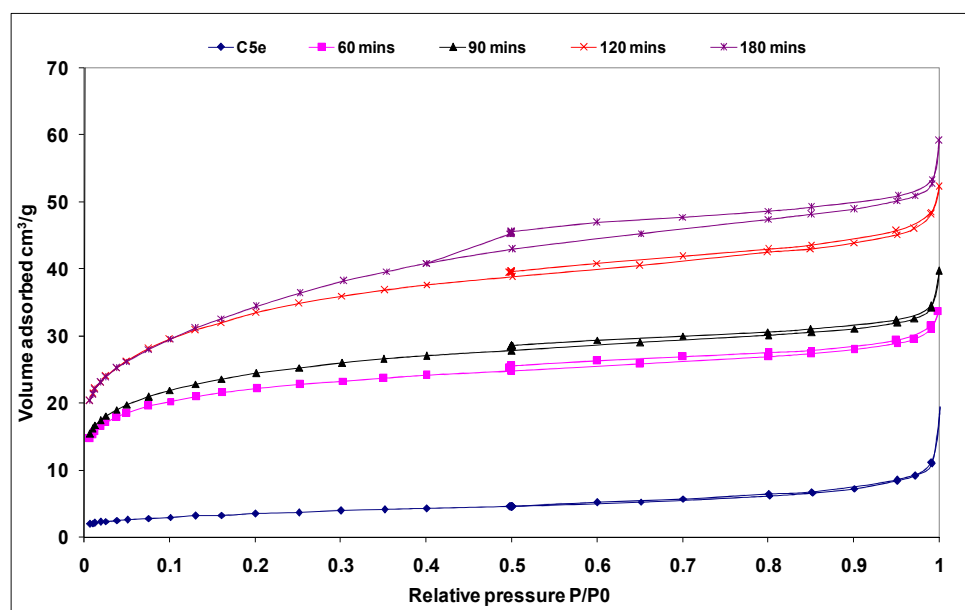


Figure E.5: Adsorption isotherms for C5e before and after activation.

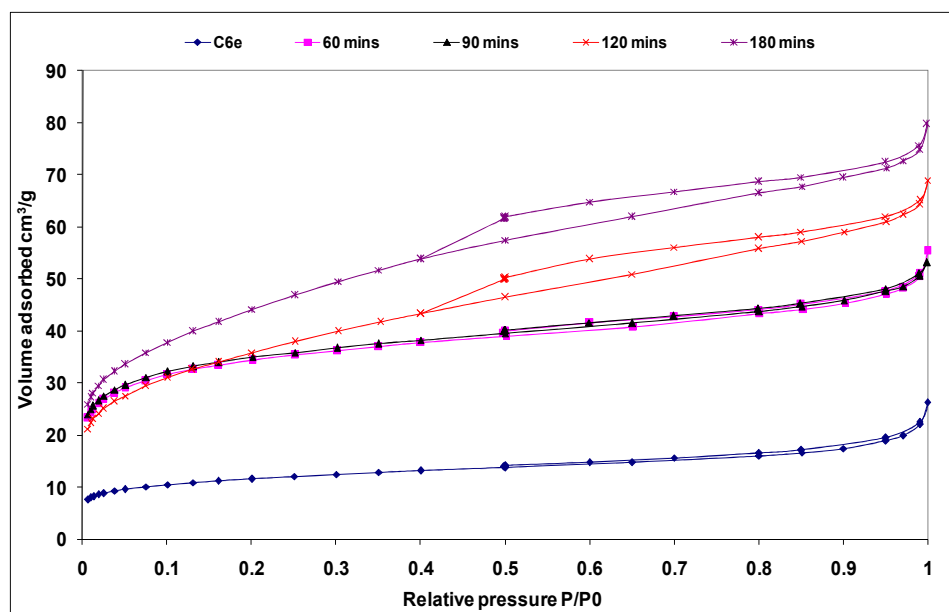


Figure E.6: Adsorption isotherms for C6e before and after activation.

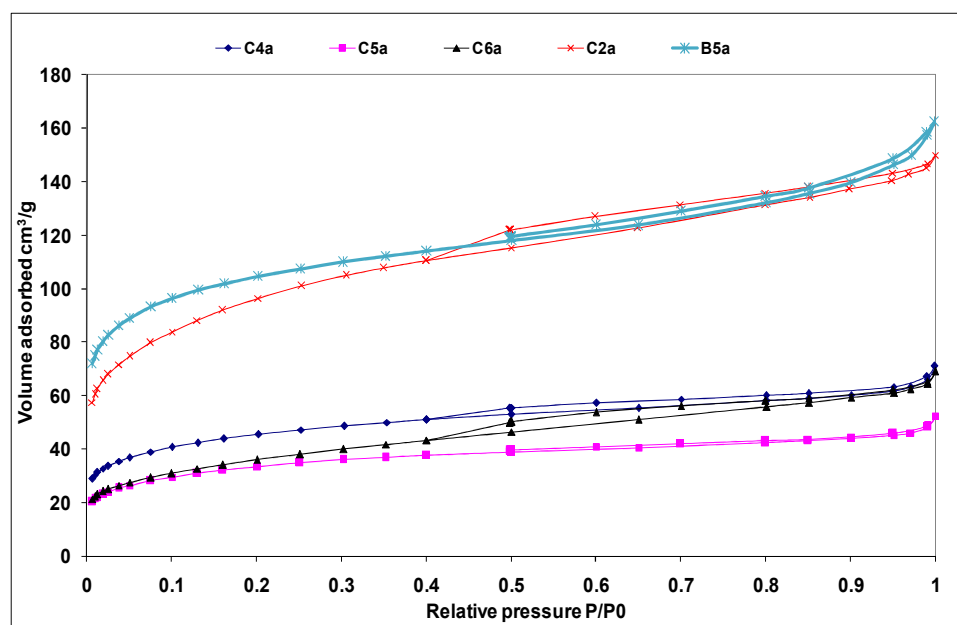


Figure E.7: Adsorption Isotherms for all the samples activated at 850 °C and 120 minutes.

Appendix F
Optical microscopy images for the enriched and activated carbons

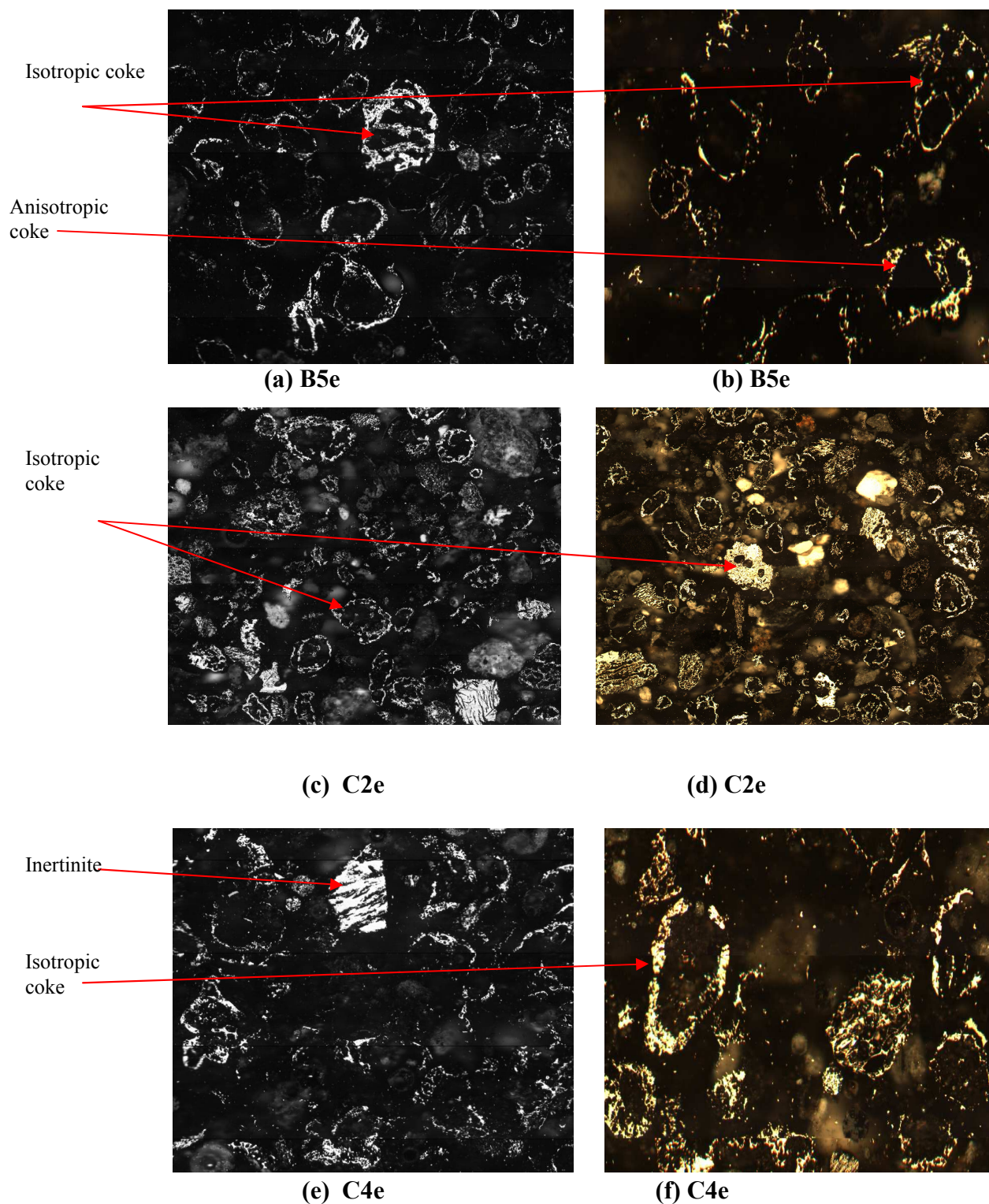


Figure F.1: Optical microscopy images of carbon rich samples.

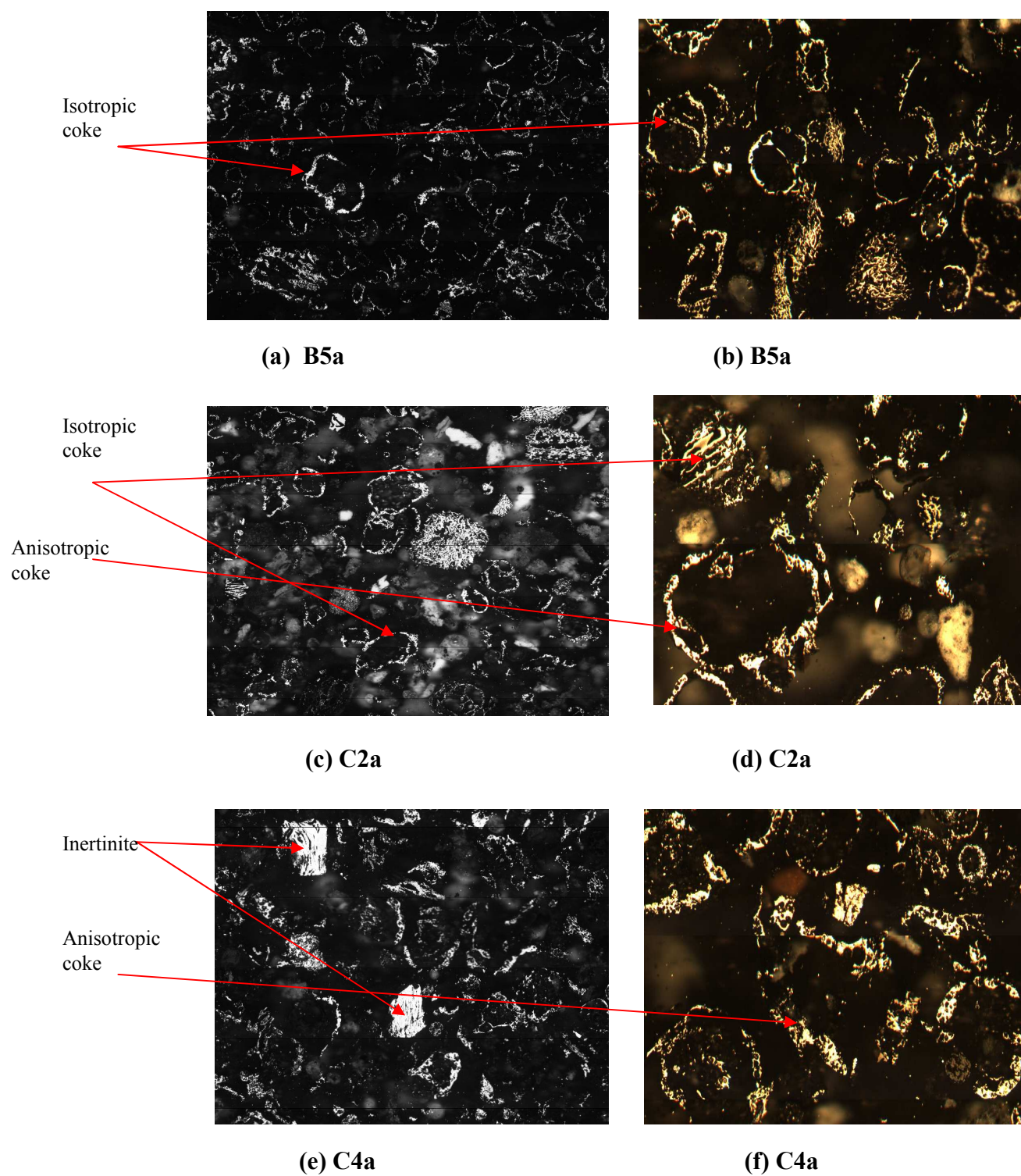


Figure F.2: Optical microscopy images of activated carbons after 60 minutes.

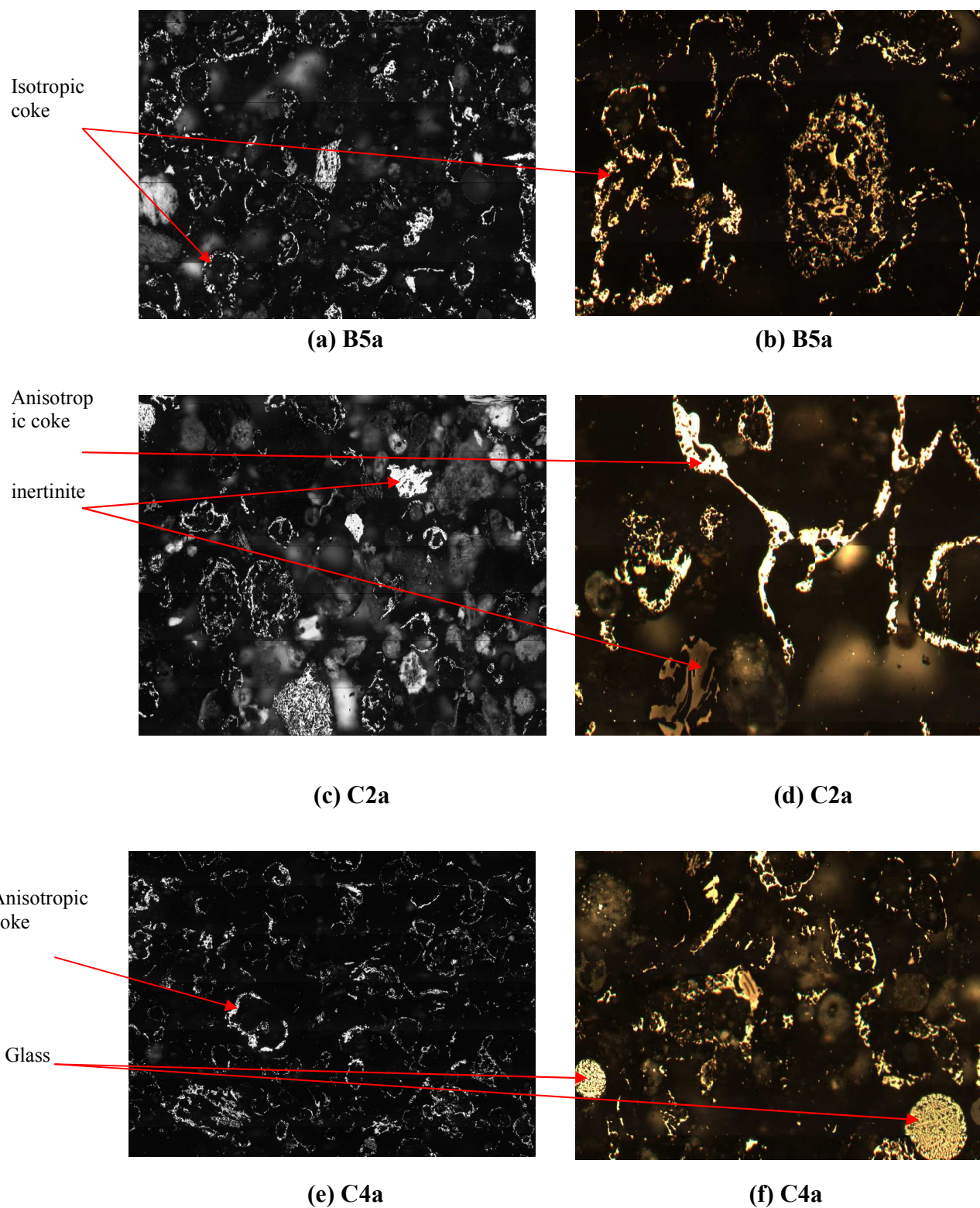


Figure F.3: Optical microscopy images of activated carbons after 120 minutes.

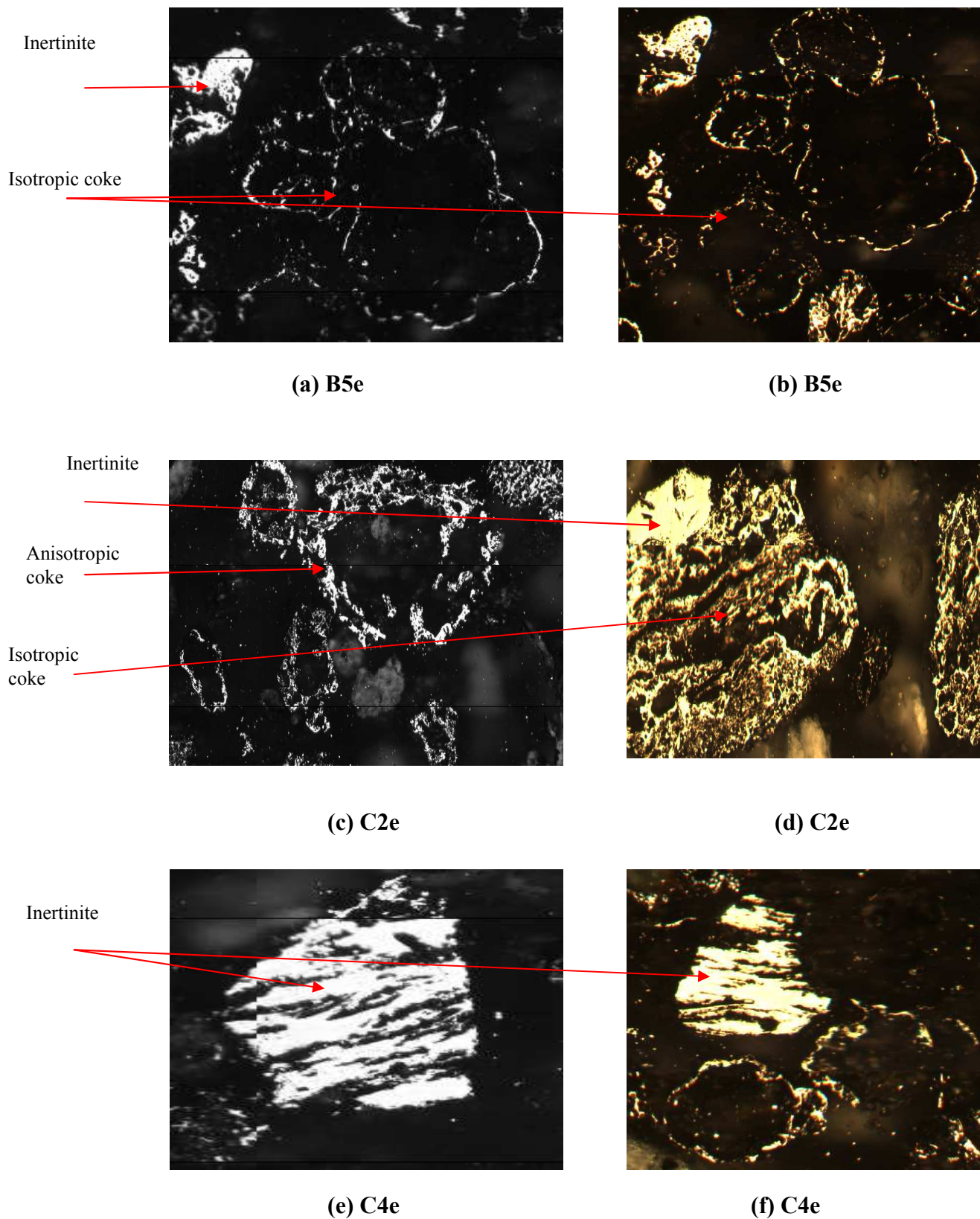


Figure F.4: Optical microscopy images of carbon rich samples with particle view.

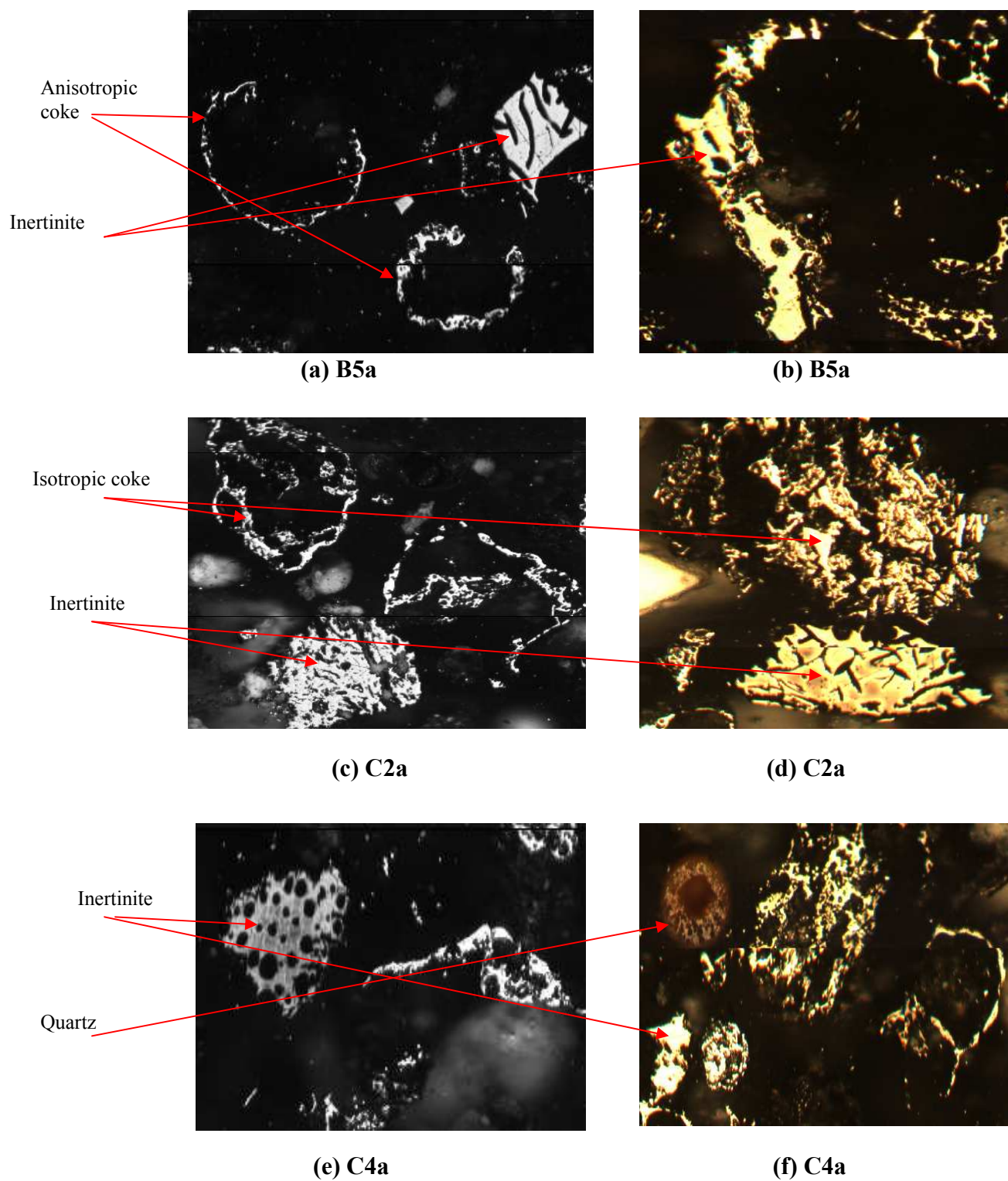


Figure F.5: Optical microscopy images of activated carbons after 60 minutes.

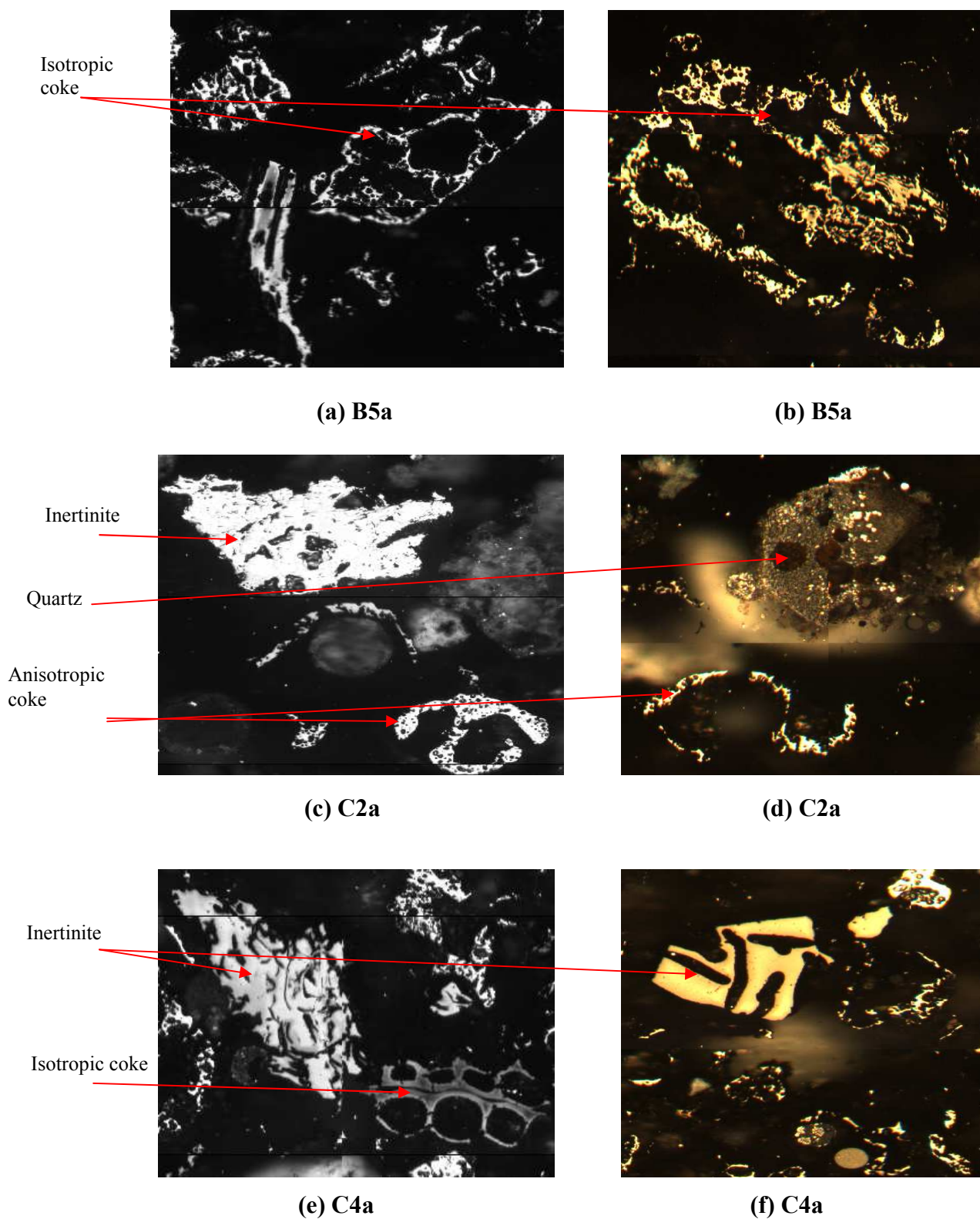


Figure F.6: Optical microscopy images of activated carbons after 120 minutes.

Appendix G
Porosity development and isotherm types

G.1 Porosity

A porosity is a form that is inhabited by the carbon structure. This is an important phase for the carbon as activated carbons are useful in a wide range of applications. According to the IUPAC classification (International Union of Pure and Applied chemistry) [Bourrat *et al.*, 1986], porosity can be divided into three groups as follows:

- 1) Micropores: width less than 2nm;
- 2) Mesopores: width between 2 and 50 nm;
- 3) Macropores: width greater than 50 nm.

Moreover, it is useful to classify micropores further into ultra (<0.5 nm width) and super (1.0-2.0 nm) micropores. These classifications are considering adsorption behaviour, as shown in (Figure G.1) [Sing *et al.*, 1985 and Patrick, 1995].

Micropores are considered as being relatively the size of adsorbate molecules and accommodate one, two or perhaps three molecules. Mesoporosity is wider and is characterised by hysteresis loops during adsorption and desorption at high relative pressures of adsorption. Macroporosity has little interest for the surface chemist, as they are transport pores to the interior of particles and are considered as external surface [Vooys, 1983].

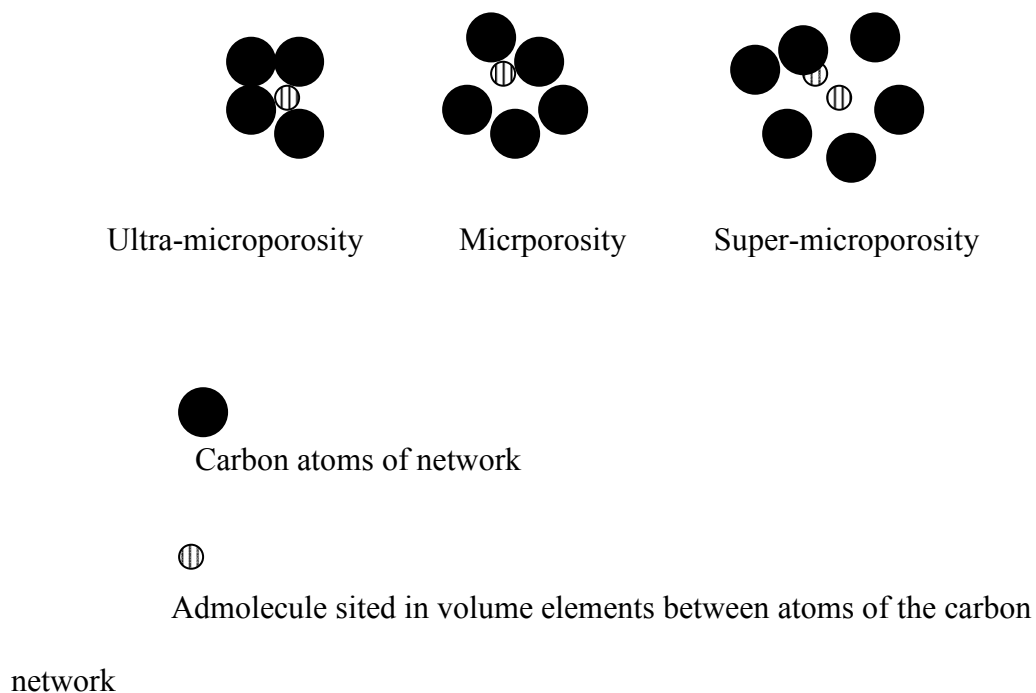


Figure G.1: Models of sizes of microporosity showing an admolecule of constant size in porosities (volume elements) of increasing size [Patrick, 1995].

Some activated carbons contain all of these sizes of porosity associated with botanical composition of the material, as shown in (Figure G.2). Porosity in carbons has disadvantages and advantages. In nuclear graphites, for example, porosity is undesirable as it allows for gasification within the carbon structure, which results in corrosion and loss of mechanical strength, while on the other hand, its presence in activated carbons is highly desirable.

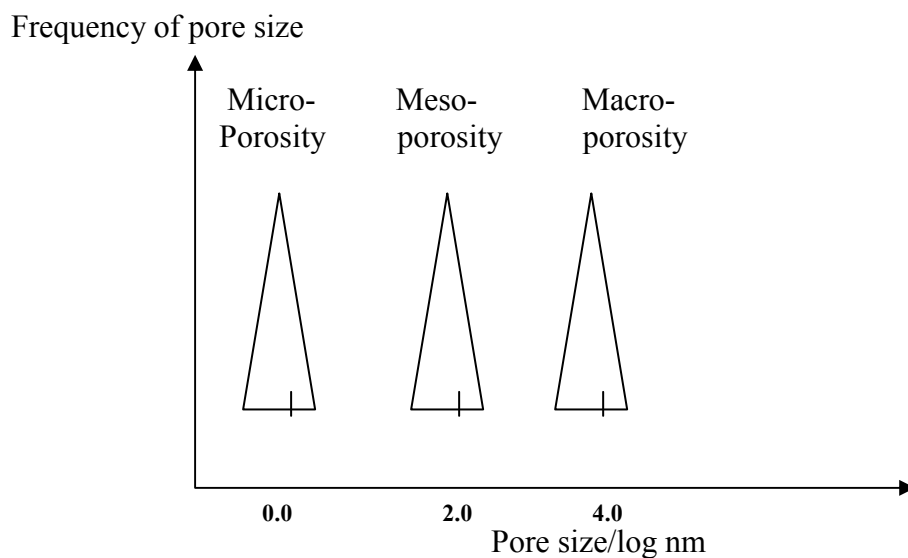


Figure G.2: The trimodal distribution of porosity found in carbons from natural precursors [Patrick, 1995].

Furthermore, porosity structure can be characterised through physical adsorption and the following properties can be determined:

- Pore size distribution, or potential energy distribution;
- Average pore size;
- The shapes of the pores;
- The relative positions of porosities of different sizes (*i.e.* wall thickness);
- The surface chemistry of the pore;
- Diffusion paths controlling rates of adsorption.

G.2 The activation process

Carbons can be derived from parent materials such as wood, nut shells and coal. Carbons may be activated chemically or physically (steam and CO₂) and their microporosity will then be enhanced considerably.

G.2.1 Chemical activation

This process usually applied to woody precursors which involve carbonizing the parent material after impregnation with e.g. phosphoric acid, zinc chloride, sulphuric acid, potassium sulphide, carbonates of alkali metals and metal chloride [Lowenthal *et al.*, 1986 and Muhlen *et al.*, 1986]. The purpose of these acids is to act as dehydrating agents, which affect the pyrolytic decomposition and enhance tar formation. The temperature condition applied from 400-800 °C. The impacts can be detected like lack of adequate control over porosity development, and the hazardous of chemical agents used in this process.

G.2.2 Physical activation

This process gasifies the carbon using gas (steam or CO₂) at 700-1100 °C. Several types of ovens are used commercially to activate the carbon like rotary kilns, multiple hearth furnaces and fluidised beds.

The porosity development is a function of the temperature, flow rate, pressure, and the gas used. Porosity in some types of char can reach a maximum within two hours of activation and then after three hours, the porosity development will decrease until reaching the minimum with no effect if the activation time increases or any of the above conditions change. However, this process varies depending on the sample. Thus, the porosity development depends on [Wicke *et al.*, 1953]:

- The structure of the initial carbon;

- The pressure of catalytic inorganic impurities in the carbon;
- The oxidising gas;
- Temperature of gasification;
- Pressure of the gas;
- Activation time;
- Carbon particle size.

Usually, the gasification conducted in a slower way would achieve the development of porosity within the particle. For example, CO₂ gas molecule must penetrate into the interior of the particle to remove a carbon atom from that position. Therefore, many carbon atoms within porous carbon can be passed during penetration without gasification occurring for these atoms [Wicke *et al.*, 1953 and Patrick, 1995]. During the gasification process, an oxygen atom has to be transferred and bonded to the carbon atom of the network, and the resultant carbon monoxide has subsequently to be ‘desorbed’ from the network, see Figure G.3.

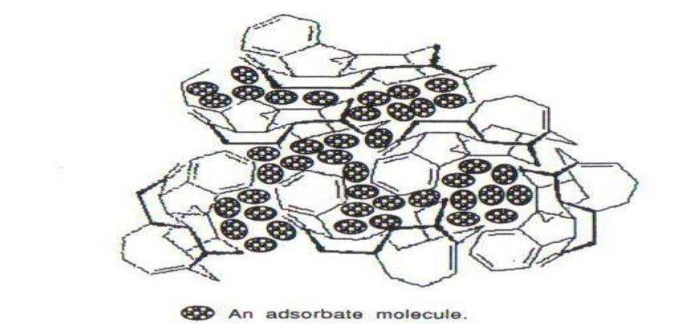
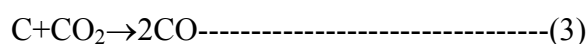
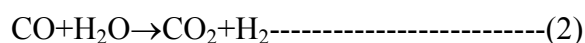
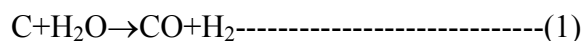


Figure G.3: Model illustrates in carbon network the physical activation process by removal carbon atoms to enhance adsorption capacity [Patrick, 1995].

These reactions are complicated during the process and may never be understood other than in general terms as described below for both oxidising gases (H₂O and CO₂):



Activation by steam is preferred over CO₂ because the water molecule has smaller dimensions than the carbon dioxide molecule. It also has faster diffusion into porous network, easier access into the micropores, faster reaction rate (approximately three times faster than carbon dioxide at temperature 800°C and a pressure of 10 kPa), and higher porosity than CO₂ as the temperature condition (800°C is lower than CO₂ over 1000°C) [Kawahata *et al.*, 1963].

G.3 Porosity development with burn-out

In a previous work by Hoinkis [Hoinkis *et al.*, 1989], it was reported concerning the porosity development for different levels of burn-off for carbon graphite type. This study has shown in the early stages, a considerable amount of either micro- or mesopores at small degree of gasification 3.4 wt.% (Figure G.4). It can be seen that the slope of the isotherms in the range up to $P/P_0 = 0.4$, as measured by N₂ at 77K, increases steadily, indicating the enlargement of microporosity. Moreover, the hysteresis indicating the mesoporosity of the

sample becomes increasingly pronounced with burn-off, as shown in Figure G.4.

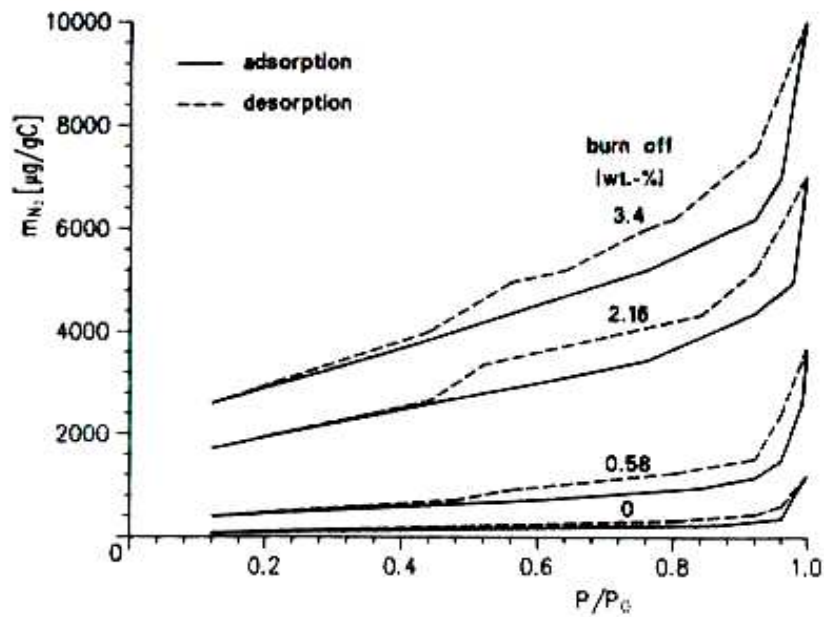


Figure G.4: Nitrogen adsorption and desorption isotherms at 77K before and after gasification for graphite [Hoinkis *et al.*, 1989].

G.4 Adsorption isotherms

The adsorptive properties of the activated carbon is characterised by the porosity and surface area in the first stage [Byrne *et al.*, 1995], which can be obtained by the study of the adsorption isotherms. The adsorption isotherm is a method that can create the relationship between the amount adsorbed by a unit mass of activated carbon and the equilibrium pressure (P/P_0). This is the (*i.e.* relative pressure) at a known temperature, and the experimental adsorption isotherm is normally illustrated in graphic way [Rouquerol *et al.*, 1999].

Figure G.5 sets out the six major classes of isotherm shape that are obtained from adsorption experiments [Patrick, 1995].

Type I isotherms are concave to the axis of the relative pressure P/P_0 and the amount of adsorbate reaches a limiting value as approaches 1. This type of isotherm is a typical of microporous solids such as activated carbon and molecular sieves.

Type II isotherms describe physical adsorption of gases by non-porous solids, where monolayer coverage is succeeded by multilayer adsorption at higher P/P_0 values. Type II isotherms represent unrestricted monolayer-multilayer adsorption and can be obtained from carbons with mixed micro-and mesoporosity [Patrick, 1995].

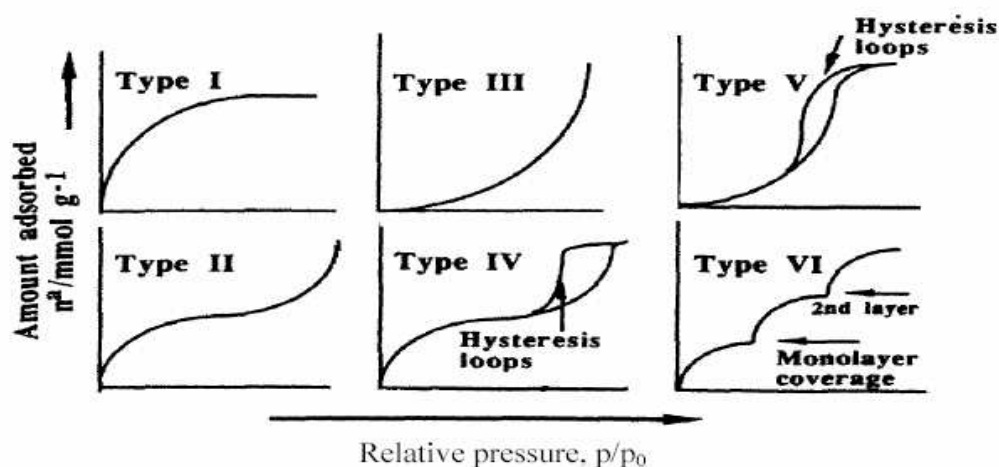


Figure G.5: Classification isotherms shape into six forms [Patrick, 1995].

Type III and Type V isotherms are convex towards the relative pressure axis. These isotherms are characteristic of weak gas-solid interaction and both of them are rarely developed. A well-known example of Type III isotherm is the adsorption of water vapour on nonporous carbons.

Type IV isotherms possess a hysteresis loop, whose shape varies from one adsorption system to another. Hysteresis loops are associated with capillary condensation in mesoporous solids indicated by the steep at higher relative pressures.

Type VI isotherms are stepwise isotherms and represent complete formation of successive monomolecular layers. An example is the adsorption at 90K of krypton on carbon black that has been graphitized at 3000K [Sing *et al.*, 1985 and Patrick, 1995].

